The Pennsylvania State University

The Graduate School

Department of Mechanical Engineering

PREDICTION OF PERFORMANCE MEASURES FOR BUSES:

A SYSTEM-BASED APPROACH

A Thesis in

Mechanical Engineering

by

Saravanan Muthiah

Submitted in Partial Fulfillment
of the Requirements
for the Degree of

Doctor of Philosophy

December 2006

The thesis of Saravanan Muthiah was reviewed and approved* by the following:

Thomas A. Litzinger
Professor of Mechanical Engineering
Thesis Advisor
Co-Chair of the Committee

Mirna Urquidi-Macdonald
Professor of Engineering Science and Mechanics
Co-Chair of the Committee

Timothy W. Simpson
Professor of Mechanical and Industrial Engineering

Sean N. Brennan
Assistant Professor of Mechanical Engineering

Shelley M. Stoffels
Associate Professor of Civil Engineering

Karen A. Thole
Professor of Mechanical Engineering
Head of the Department of Mechanical and Nuclear Engineering

*Signatures are on file in the Graduate School

ABSTRACT

Heavy vehicles transport people and freight in an efficient manner and form the backbone of any developed economy. Historically, heavy vehicle standards (called Design Based Standards-DBS) have relied primarily on placing limits on vehicle weights and dimensions. Ease of implementation and lack of complete understanding of the complex relationships between vehicle design parameters and vehicle performance are the primary reasons such standards have been in place for decades. However, recently there has been a realization that such indirect control of vehicle performance can lead to a wide gap between intended performance and actual performance. A concept called Performance Based Standards (PBS) that assigns numerical limits to performance measures but leaves open ways of achieving the performance has now gained attention. However, for an effective implementation of PBS and for an optimal design of vehicles capable of achieving such performance, it is imperative that vehicle designers, test engineers and regulatory authorities alike have a sound understanding of the complex relationships that exist between vehicle design parameters and vehicle performance.

The primary goal of this thesis was to establish and validate methods of analysis that can be used to investigate the relationships between vehicle design and performance. The other main goals include development of a reliable means of predicting the useful range of values for vehicle design parameters that would result in a vehicle with desired performance objectives (one or more) and evaluation of the effectiveness of PTI (Pennsylvania Transportation Institute) testing with an aim to suggest ways for further improvement. The thesis discusses four performance measures, namely fuel economy,

acceleration and gradeability, pass-by noise and vehicle reliability primarily because PTI data were readily available for these measures. However, as the methods developed in this thesis are very general in nature, they can be used for analyzing other vehicle performance measures as well, provided reliable and accurate data are available.

In this thesis, a two-stage system based model was implemented. In the first stage, functional relationships between vehicle design parameters and vehicle performance under laboratory/test track conditions were modeled using a vehicle transformation, *F*. In the second stage, the interdependence between test-track performance and real-life traffic performance was modeled using a traffic transformation, *G*. PTI data on fuel economy, acceleration and gradeability, pass-by noise and reliability for 124 diesel two-axle transit buses were used to model the vehicle transformation, *F*. On the other hand, the traffic transformation, *G,* was modeled using in-use data (at transit agencies) on fuel economy and reliability obtained from the National Transit Database (NTD).

Modeling was done using two artificial neural network (ANN) based methods – N2PFA/REFANN proposed by Setiono *et al.* and RF5 proposed by Saito and Nakano. Both approaches have built-in rule generation capabilities and an automatic means for selection of the number of hidden neurons. Hence the problem of ANN being a black box is alleviated with either approach. A two-step method of input selection was used in this study. Firstly, correlation coefficients were evaluated between all pairs of input variables. Based on the assumption that a low correlation coefficient (< 0.7) can be used as a measure of linear independence, inputs that are least correlated to other inputs were selected. In the second step, an information theory based approach was used to narrow

this input set down to a still smaller subset that contains most of the original information and is a good predictor of the output (vehicle performance measure) under study.

Often it is also of interest to know vehicle configurations that can achieve desired vehicle performance objectives. To this effect, a means for generating an inverse model based on non-linear programming is also presented. In this thesis, inversions were obtained starting from each known bus (the ANN training set) as a reference point. The final solution (inversion) selected was the one closest in terms of Euclidean distance to an existing bus. The main idea behind using such an objective function was ease of manufacture. However, one can easily modify the objective function as per one's requirement and achieve corresponding optimal solutions. Engineers often face the issue of determining a vehicle configuration that can simultaneously achieve more than one competing objectives. This study shows that Gembicki's Goal Attainment method for multi-objective optimization can be very effective for this purpose.

The results from the fuel economy and acceleration models validate the accuracy of the two ANN-based methods used in this study. This opens the way for use of these two methods for modeling other performance measures wherein knowledge may be inadequate. The two methods not only corroborate well with each other with respect to most relevant and least relevant inputs but also seem to perform better than two of the commonly used modeling methods, namely regression and decision tree. Further, unlike regression, the two methods make no assumption on the nature of the functional relationship being modeled.

The nonlinear effect of vehicle weight on fuel economy of a bus is clearly brought out in this study. This is in contrast with existing literature that suggests a linear

dependence. With regards to whole vehicle pass-by noise models, the methods used in this study were able to generate models that are very close in accuracies with the best such model ($\pm 1.1 dB(A)$) described in literature while using only 1.2% of the number of data samples. This study confirms the importance of vehicle weight in determining reliability and also brings forth the possible case for vehicle height as an important determining factor.

TABLE OF CONTENTS

LIST OF FIGURES

LIST OF TABLES

ACKNOWLEDGEMENTS

I would like to dedicate this thesis to the memory of my late advisor, Prof. Bohdan T. Kulakowski, who passed away in a tragic road accident in March 2006. Prof. Kulakowski not only gave me the opportunity to come to the United States in Aug. 2000 but also guided me through every aspect of my graduate study. I shall always be grateful for his help without which this thesis would not have been possible.

I would like to convey my sincere thanks to my present thesis co-chairs: Prof. Thomas Litzinger and Prof. Mirna Urquidi-MacDonald. Dr. Litzinger proof read the draft of this thesis and gave me his insightful comments which I think have made this thesis much better than the original draft. I would like to thank Dr. Macdonald for introducing me to the exciting topic of neural networks that I have used in this thesis and also for her invaluable guidance throughout the course of this work.

I gratefully acknowledge the invaluable help and support that I have received from my other committee members - Prof. Timothy Simpson, Prof. Sean Brennan and Prof. Shelley Stoffels. Dr. Simpson's thoroughness in proof reading my thesis draft amazes me. Dr. Brennan and his wonderful group of students have been a great pleasure to work with. I wish them the best of luck in their endeavors. I would like to extend my sincere thanks to Dr. Stoffels for agreeing to join my committee at such a late stage (after Dr. Kulakowski's death). Her meticulousness in helping me (Mechanical Engineering student) understand the basics of pavement design in her Civil Engineering class is something I shall always remember.

I would like acknowledge the help that I received from Mr. David Klinikowski, Director (Bus Testing Program) at PTI, during the course of my entire stay at Penn State. Dave and his crew (especially those at the test track) have been a pleasure to work with. Dave's help in collecting PTI test data was crucial to the timely completion of this work. Thanks are due to my friend, Nan Yu, for his help in various projects that we have worked on at PTI.

I would like to take this opportunity to thank all my teachers starting from my early school days in India. Without the basic building blocks that they helped me assimilate, none of this work would have been possible.

Finally, I would like to thank my family for their love and support. The successes of all my endeavors – past, present and future – are essentially theirs as nothing would have been possible without their unflinching support. My mom, dad and elder brother Siva have always ensured that I get the opportunities that they themselves did not have. Thanks for your love – Archana and Murali (brother's kids), and Usha (sister-in-law). My wife, Anuradha, underwent almost all of the joys and tribulations that were a part and parcel of this thesis work. Thank you, Anu, for all your love and care.

Chapter 1

Introduction

1.1 Motivation

Modern economies rely extensively on heavy vehicles for movement of people and freight in an efficient and cost effective manner. A feel for the magnitude of this reliance, in the United States (US) economy, can be obtained from the statistics given in the 57th edition of "Public Transportation Fact Book" published by the American Public Transportation Association (APTA) in April 2006 [1]. The fact book states that, in year 2004, the total vehicle revenue miles and passenger miles traveled by buses and trolleybuses in the United States were 3481 million kilometers (km) and 34,674 million km respectively. As is true for practically any technological means, the use of heavy vehicles is not devoid of the associated costs. These costs include, amongst others, expenses incurred in repair and maintenance of road and bridge infrastructure, negative impact on the environment and liability costs associated with the loss of human lives. Regulations are enacted primarily to minimize these costs associated with road use and to ensure protection of community interests [2].

Historically, the design of heavy vehicles has been governed by prescriptive or Design Based Standards (DBS) due to ease of implementation, lack of complete understanding of the complex relationships between vehicle performance and vehicle design parameters, difficulty in vehicle-performance evaluation and non-uniformity in

conditions of vehicle use. Prescriptive standards include regulations for vehicle configurations, vehicle and axle-group mass limits, and vehicle dimensions such as length, width, height and rear overhang amongst others. These regulations do not directly take into account the performance of the vehicle as such. In the last two decades, it has been widely recognized that the approach of prescriptive standards leads to situations wherein there are wide discrepancies between the actual performance of a vehicle and its intended performance [2]. A viable alternative to prescriptive standards is a situation where standards take into account the performance of a vehicle in a more direct manner. This concept was given an impetus by the report of Road Transport Association of Canada (RTAC) published in 1986 that recommended employing Performance Based Standards (PBS) [3]. A *Pure Performance Standard* is one that specifies the outcomes required of vehicle operations but leaves open the ways by which the outcomes are achieved. It assigns a numerical limit to a performance measure and thus defines a boundary between an acceptable performance and an unacceptable performance. Another approach is to indirectly regulate performance by formulating standards on parameters directly related to performance. Such standards are called *Parametric Performance Based Standards* [4]. For example, a pure performance standard can stipulate limits on dynamic tire forces while a parametric standard might regulate natural frequency and damping ratio of the suspension. The term Performance Based Standards (PBS) includes both *Pure Performance Standards* and *Parametric Performance Based Standards.*

The objective of PBS is to control vehicle size and weight by specifying vehicle performance requirements rather than through blanket limits for all vehicles regardless of their performance. The introduction of PBS is expected to encourage innovation, provide

a better match between vehicles and roads, increase regulatory transparency by providing a more consistent and rational regulatory approach and improve compliance to the regulations themselves [2].

1.2 Need for this Study

An effective implementation of PBS is possible only if there is a thorough understanding of the relationships between vehicle design parameters and vehicle performance, between vehicle use and road infrastructure costs, and between vehicle behavior and road safety for different road environments. After nearly a decade of development, Australia is the first country in the world to initiate a move towards implementation of PBS. Recent research in Australia indicates that the best method for completing the PBS assessment of a vehicle is a hybrid one that combines simulation and field testing [5]. Since tests can be expensive and cumbersome to conduct, simulation is preferred wherever possible. An effective simulation requires good knowledge of the complex relationships that exist between heavy vehicle design parameters and its performance, and detailed vehicle parametric data. Over the last few decades, numerous studies have tried to investigate how vehicle design parameters influence performance. A summary of such studies is given in the Chapter 2. The main problems that researchers in this area have faced include (a) lack of a complete theoretical understanding of the processes involved and (b) lack of computational resources. While one cannot claim that (a) has been effectively tackled due to the complex and in most cases highly nonlinear

nature of the problems, with the advent of computers, problem (b) has been mitigated to a fair extent.

Traditional modeling involves use of commercial simulation packages that require a lot of vehicle parametric data. In many cases, getting such detailed information is difficult. For example, in the absence of exact data, mass moment of inertia for a heavy vehicle is often guessed. Hence, there is a need for a method that can use commonly available vehicle parametric data such as those on weights and dimensions to accurately model vehicle performance. This study aims to come up with such a method and also compare its results with those available in literature.

Test agencies and manufacturers alike have over the years accumulated a good amount of test data that has hidden knowledge waiting to be discovered. It is a well recognized fact that empirical formulations from test data can not only give useful physical insights but also bring out some hereto unknown phenomenon for due consideration. Since its inception in 1989, the Federal Transit Administration's (FTA) Bus Testing Program at Pennsylvania Transportation Institute (PTI) has generated one such data set. Over 250 buses have been tested for maintainability, reliability, safety, performance, structural integrity, fuel economy and noise. The data collected at PTI have the following characteristics that give them a unique character:

1) The data collection period (1989 - date) is long, spanning well over a decade and a half.
2) Testing is done for new bus models and their variants. Hence it can reasonably be expected that the test data includes a major portion of the new bus designs introduced in the US since 1989. This makes the data fairly comprehensive.

3) Data are collected by trained personnel using well defined test procedures that have been applied uniformly. Hence, data are reliable. This is crucial to ensure that test errors and hence data noise are within acceptable limits.

The data available at PTI provide a valuable opportunity for modeling the performance of a bus under laboratory/test track conditions. Since PBS aims to regulate vehicle behavior on the road, it is also essential to investigate how vehicle performance in a laboratory/test track translates to actual performance in traffic conditions. Unfortunately, this area has been relatively unexplored. This study aims to develop methods that can be employed to generate models for such traffic transformations.

1.3 Approach Used in this Study

As mentioned in the previous section, PTI has collected performance data on transit buses for over 15 years. Data available for analysis include that related to fuel economy, acceleration and gradeability, pass-by noise and reliability. This study uses data on these four performance measures to model the relationship between vehicle design parameters and vehicle performance on a test track. Data pertaining to double lane change (DLC) tests conducted at PTI indicate that most buses were able to negotiate the maneuver at a maximum speed of 45 mph. Since there was not much variance in the values of the performance measure (maximum speed in DLC) amongst buses, it could not be used for modeling.

For analyzing the relationship between laboratory and real-life performances, performance data of buses operating at transit agencies were obtained from the National

Transit Database (NTD). Of the four performance measures analyzed using PTI data, only data pertaining to fuel economy and reliability were available at NTD. Hence, performance prediction models were generated only for fuel economy and reliability using NTD data. Using non-linear programming, the performance models were also inverted so as to provide automotive engineers with a tool to arrive at bus designs that can ensure a desired performance. Finally, multi-objective optimization was used to arrive at bus designs that can simultaneously achieve more than one performance goal.

1.4 Objectives and Potential Benefits

The following are the main objectives of this research:

a) To establish a unified method of analysis that can be employed to study the interrelationships that exist between vehicle design parameters and vehicle performance under laboratory/test track conditions, and between test track performance data and in-service performance data.

b) To explore the relevance and usefulness of different bus design parameters with respect to the performance measures under consideration.

c) To alleviate some of the shortcomings in the literature by comparing and validating the results of this study against those from previous such studies undertaken for buses and other vehicles.

d) To bring forth interdependencies between performance of a bus and its underlying design parameters.

e) To evaluate the effectiveness of PTI testing and suggest ways for improvement by investigating the relationship between performance data collected on buses at PTI and the data from transit agencies.

f) To develop a method that can help aid in drafting performance-based standards (PBS) by providing a reliable means of predicting the useful range of values for vehicle design parameters that would result in a vehicle with the desired performance characteristics

This research has the potential to help automotive engineers design better vehicles by enhancing their ability to predict vehicle performance at the design stage. Regulatory authorities should find the method of analysis (especially the inverse modeling) useful in drafting performance-based standards that are optimized to best benefit both society and vehicle manufacturers. Testing agencies can use the forward modeling approach as an alternative method for simulating vehicle performance. Further, they can investigate the modifications that are needed to design more effective testing procedures. Since the method of analysis developed in this thesis is very general in nature, it can be used in other fields of research, especially those that are data intensive and where potential exists for knowledge discovery from previously collected data.

1.5 Outline of this Thesis

The remainder of this thesis is organized as outlined in this section. Chapter 2 details the available literature on four performance aspects of a vehicle, namely fuel

economy, acceleration and gradeability, pass-by noise and reliability. The conclusions and shortcomings of previous studies have also been summarized.

Chapter 3 introduces the theoretical model that is proposed for modeling a vehicle-traffic system. Possible difficulties with this approach are also discussed. Details about data collection and salient statistics of the collected data are then presented.

Chapter 4 brings out the importance of data pre-processing and input selection. Practical means of implementing the proposed theoretical model are then introduced along with pros and cons of each alternative approach. Finally, techniques for model inversion and multi-objective optimization are covered.

Chapter 5 presents the results obtained from forward and inverse models that show the viability of the suggested approach. The results are compared with those available in literature. Results from a sample two-objective optimization problem, wherein bus design parameters capable of achieving more than one performance goal are sought, are also included. Finally, results from the two methods used in this study are compared with those from linear regression and decision (regression) tree.

Chapter 6 outlines the conclusions from this study and suggests avenues for future research.

Chapter 2

Literature Survey

2.1 Introduction

A study of literature in the field of vehicle modeling indicates that almost all the research that has been undertaken can be broadly classified into two categories. The categories are (a) Whole Vehicle or Macro Level modeling (b) Vehicle Systems or Micro Level modeling. Each approach has its own advantages and disadvantages.

Whole vehicle modeling encompasses the studies in which emphasis is laid on generating insight into the functioning of vehicle as a whole. Detailed analysis of individual vehicle systems like engine, transmission, exhaust system, traction control etc. is generally kept out of the purview of the study. However, salient features and important performance-related parameters of such systems are accounted for as found appropriate. Whole vehicle modeling is very useful in extracting knowledge in situations wherein detailed information on individual systems is not available. Detailed information may not be available for a number of reasons including proprietary nature of the information and difficulty and costs associated with collecting the data needed for extensive modeling. The obvious disadvantage of using whole vehicle approach is that sub-system level details are often excluded. There may occasionally be a situation, in which, the excluded parameters that were individually thought of as insignificant might collectively be found to be of greater importance.

In vehicle systems or micro level modeling, as the name suggests, individual systems are modeled in much greater detail. This helps in getting a much better design insight into the problem as the influence of each design detail can be simulated or studied on an individual basis. In a field like automotive engineering, where much of the information is proprietary due to the level of market competition, micro level modeling is mostly carried out by automotive companies. It would be ideal if macro and micro level modeling were amalgamated so as to allow the flexibility of selecting the level of detail that is desired. However, due to the complex nature of most automotive problems, such a venture would be prohibitively expensive both in terms of money and the time required.

The focus of this study is primarily at a macro or whole vehicle modeling level. As mentioned in Section **1.3**, PTI test data are available for four performance measures, namely fuel economy, acceleration and gradeability, pass-by noise and reliability. Hence only literature that pertains to macro modeling of these four performance measures is reviewed in detail here.

2.2 Fuel Economy

Fuel economy stands out as the most investigated aspect of vehicle performance. The reasons for this include the enormous impact that import of petroleum has on any developed economy, the continued stress on stringent emission norms starting with the 1970s and last but not the least the fact that mathematical analysis is possible as scientific theories exist on factors that influence fuel economy, such as road load.

It is well known that the road load, F_{wh}, on a vehicle moving at a speed, v, is given by

$$F_{wh} = F_{roll} + F_{aero} + F_{acc} + F_{grade} \qquad \textbf{2.1}$$

where, F_{roll}, F_{aero}, F_{acc} and F_{grade} are the rolling resistance, aerodynamic resistance, acceleration (inertial) resistance and grade resistance respectively [6,7,8,9,10]. Now let,

C_{r0} - speed-independent rolling resistance coefficient

C_{r1} - speed-dependent rolling resistance coefficient

M - mass of the vehicle

M_{eff} - effective mass of the vehicle (including rotational inertia effects)

K_m - mass correction factor = M_{eff}/M

g - acceleration due to gravity

W - weight of the vehicle (Mg)

ρ - density of air

C_d - air drag coefficient

A - projected frontal area of the vehicle

K - ratio A/W

v - vehicle speed

v_w - longitudinal component of wind speed

α - longitudinal inclination of the road

a - vehicle acceleration

V_f - volumetric fuel consumption rate

Q - heat of combustion per unit volume of fuel

η_e - brake thermal efficiency of the engine

η_t - transmission efficiency

P_e - engine power

P_w - power required at wheels

FE - fuel efficiency = v/V_f

V_d - engine displacement or size

N/v - speed ratio (engine revolutions per minute [rpm] to vehicle speed)

Then,

Rolling resistance, F_{roll} is

$$F_{roll} = (C_{r0} + C_{r1}v)Mg = (C_{r0} + C_{r1}v)W \qquad \textbf{2.2}$$

The net rolling resistance coefficient of a radial tire is largely independent of load but increases proportionally with decrease in inflation pressure at constant load [**11**]. On the other hand, for a cross-ply tire, rolling resistance coefficient decreases with load while the effect of inflation pressure remains similar to that for a radial tire. With regards to tire size, rolling resistance tends to increase as tire size is reduced.

Aerodynamic drag, F_{aero} , is given by

$$F_{aero} = 0.5\rho C_d A(v - v_w)^2 \qquad \textbf{2.3}$$

In evaluating acceleration resistance, ideally, the inertia term should include the influence of rotating parts even though this effect is not large (< 5%) [**9**]. Hence, F_{acc} can be evaluated as

$$F_{acc} = (M + \Delta m_{rotating})\mathrm{a} = M_{eff}\mathrm{a} \qquad \textbf{2.4}$$

Finally, the road grade resistance, F_{grade},

$$F_{grade} = Mg\sin(\alpha) = W\sin(\alpha) \quad \textbf{2.5}$$

Now, using Eqs. **2.1** - **2.5**, neglecting the effect of wind velocity and assuming a small grade ($\sin\alpha = \alpha$) yields

$$P_w = [(C_{r0} + C_{r1}v) + 0.5\rho C_d K v^2 + (K_m a / g) + \alpha]Wv \quad \textbf{2.6}$$

Brake engine power can be written as

$$P_e = V_f Q \eta_e \quad \textbf{2.7}$$

Neglecting the power needed to run accessories like engine fan, air-conditioning, alternator etc. and using transmission efficiency to correlate engine power and power at wheels,

$$P_w = \eta_t P_e = \eta_t \eta_e V_f Q \quad \textbf{2.8}$$

the expression for fuel economy, FE, can be now be written using Eq. **2.6** and Eq. **2.8** as

$$FE = \frac{\eta_e \eta_t Q}{[(C_{r0} + C_{r1}v) + 0.5\rho C_d K v^2 + (K_m a / g) + \alpha]W} \quad \textbf{2.9}$$

Eq. **2.9** indicates that fuel economy is directly proportional to engine efficiency and transmission efficiency and approximately inversely proportional to vehicle weight, W. Writing in a condensed form using a parameter λ_1

$$FE = \lambda_1 \frac{\eta_e \eta_t}{W} \quad \textbf{2.10}$$

In general, for a given vehicle weight, η_e decreases with V_d. Also, the transmission efficiency, η_t, decreases when the speed ratio (N/v) increases [8]. Bascunana postulates that the two relationships can be written as

$$\eta_e = \lambda_2 \frac{W^{\gamma}}{V_d^{\delta}} \qquad 2.11$$

$$\eta_t = \frac{\lambda_3}{(N/v)^{\tau}} \qquad 2.12$$

where λ_2, γ, δ, λ_3 and τ have constant values. For a given driving cycle, vehicle speed (V), acceleration (a) and road grade (α) do not vary with bus design and hence are fixed. Since Q, C_{r0}, C_{r1}, ρ, C_d, K and K_m are practically constant, substituting Eq. **2.11** and Eq. **2.12** in Eq. **2.9**

$$FE = \lambda \frac{W^{\gamma-1}}{V_d^{\delta}(N/v)^{\tau}} \qquad 2.13$$

where $\lambda = \lambda_1\lambda_2\lambda_3$ takes into account all the constants.

Over the last few decades, regression analysis seems to have been the tool of choice for studying the effect of various vehicle characteristics on fuel economy [8,12,13]. Recently, Gibbons and McDonald [14] have used constrained regression and Bayesian analysis to model the effects of technology on fuel economy. The main advantage of these two methods is that the analyst can incorporate any prior knowledge that he or she has of the relationships between the dependent and the independent variables.

Fuel economy is affected by both vehicle design factors and operational characteristics. Operational characteristics include ambient weather conditions, road conditions, quality of vehicle maintenance and driving cycle characteristics. Researchers

generally agree that the key vehicle design factors that influence fuel economy include vehicle weight, engine power, engine displacement, rear axle ratio, vehicle frontal area individually and in combinations [12,13,15]. This is in good agreement with the Bascunana's theoretical formulations given by Eq. 2.9 and Eq. 2.13.

Zub [16] concludes that increase in vehicle weight has nearly a linear effect (decrease) on the fuel economy of transit buses. Other studies on buses by Schubert *et al.* [15] and Gajendran and Clark [17] agree with this conclusion. The effect of *N/v* ratio on fuel economy depends on how a change in *N/v* ratio shifts the operating line on the brake-specific fuel consumption (BSFC) map [16]. Hence, fuel economy would depend on whether the new *N/v* ratio leads to operation of the engine in the regions of lower BSFC or not. For cars however, studies show that a numerical increase in *N/v* ratio normally leads to a decrease in fuel economy [8,13,18]. This is understandable as higher *N/v* ratios mean that for a given vehicle speed the corresponding engine rpm will be higher. Since a gasoline engine normally has higher BSFC at high speeds, the fuel economy decreases. Engine displacement has a significant effect on fuel economy if the driving cycle has a substantial amount of idling or standstill [19].

Driving cycle is another aspect that affects fuel economy. In vehicle testing, a driving cycle is a velocity time profile that a vehicle is to follow on a test track or on a chassis dynamometer. Central Business District (CBD) cycle, Arterial (ART) cycle and Commuter (COM) cycle are three of the most common driving cycles used for fuel economy testing of transit buses. CBD cycle consists of two miles (3.2 km) with seven stops per mile with a top speed of 20 miles per hour (32 km/hr). ART cycle is composed of two miles (3.2 km) with two stops per mile and a top speed of 40 mph (64 km/hr) and

COM cycle consists of a four-mile route (6.4 km) with a maximum speed of 55 mph (88 km/hr) and no stops in between. The COM cycle at Pennsylvania Transportation Institute is restricted to a maximum speed of 40 mph (64 km/hr) due to design restrictions of the track. Plots for CBD, ART and COM driving cycles are shown in Figures **2.1 - 2.3** [**20**]. The relative importance of vehicle weight (inertia), rolling resistance and aerodynamics on the fuel economy in different cycles varies depending on the driving cycle characteristics. Zub suggests that on a percent energy basis, almost 43% of the energy is spent on overcoming the effect of vehicle inertia (weight) in CBD and ART cycles. The rolling resistance and air drag components are 14% and 2% respectively for CBD and 16% and 8% for ART. In a COM cycle (unmodified), he estimates that vehicle weight (inertia), rolling resistance and air drag components are 13%, 23% and 25% respectively [**16**]. This clearly shows that at low speeds (below 64 km/hr) vehicle weight is the single most important factor while at higher speeds air drag and rolling resistance components are predominant.

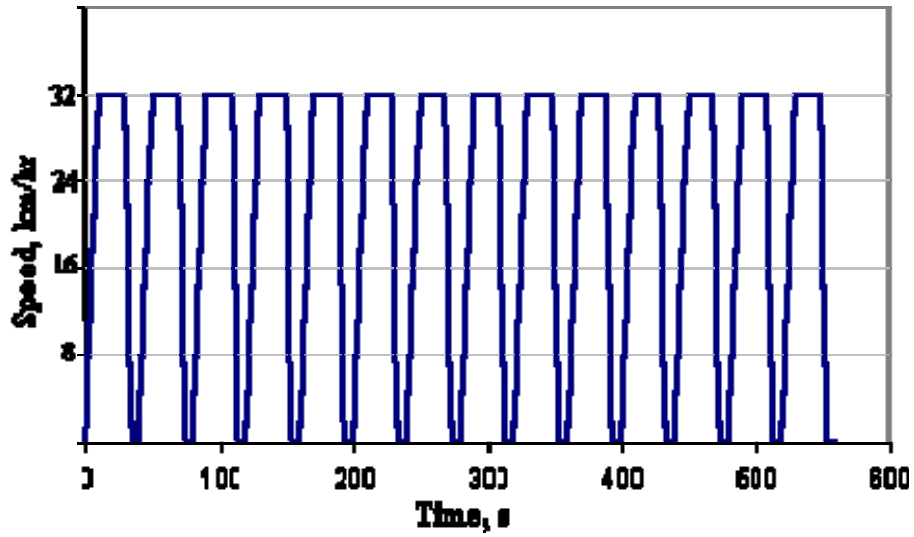

Figure 2.1: CBD driving cycle.

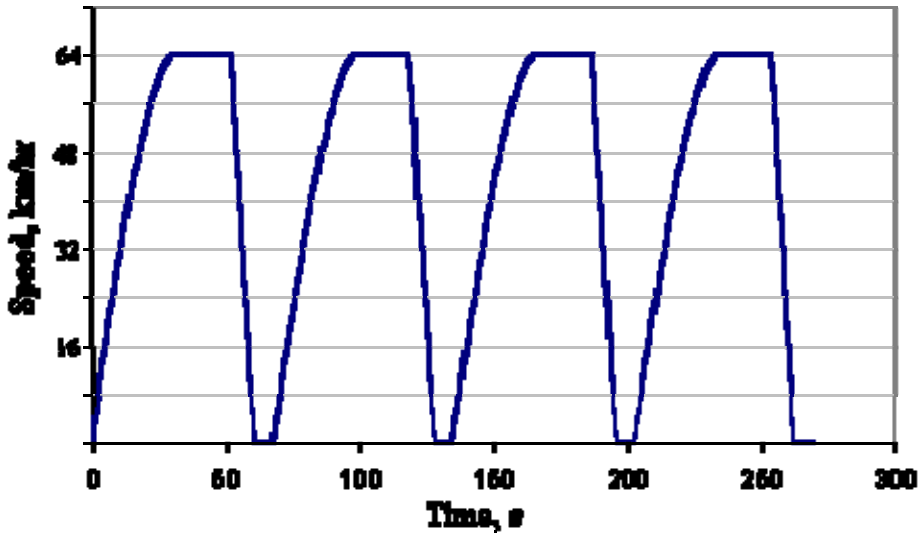

Figure 2.2: ART driving cycle.

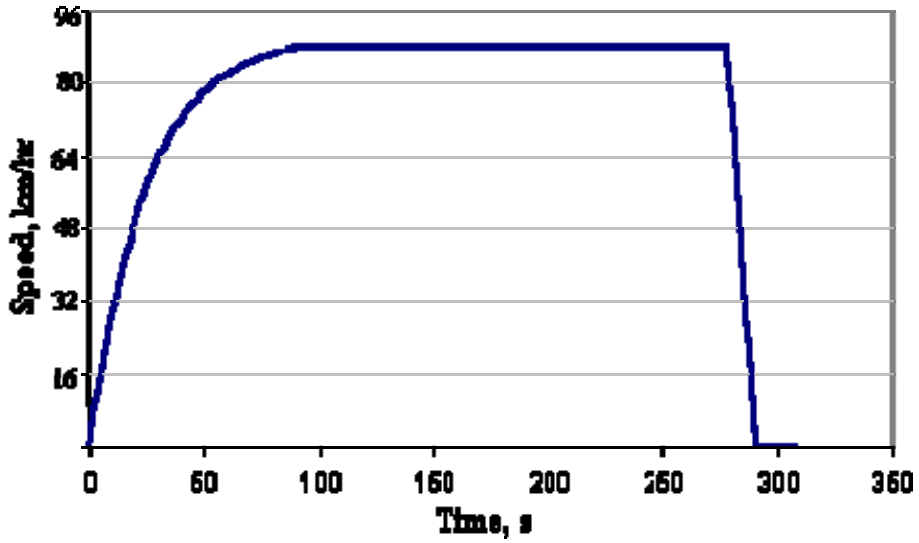

Figure 2.3: COM driving cycle.

2.3 Acceleration and Gradeability

In the United States (US), the primary measures used for evaluating vehicle performance are acceleration, gradeability and top speed. Acceleration capability of vehicle is generally measured in terms of the amount of time needed to accelerate to a given speed. Alternatively, instantaneous accelerations at given speeds are also used. Gradeability, on the other hand, is defined as the maximum grade that a vehicle can negotiate at a given speed. Acceleration and gradeability are directly related, except that gradeability is a steady state calculation and therefore the static weight of a vehicle is used rather than effective weight [18].

Under assumptions of zero tire slip and rolling resistance, zero air drag, zero grade, full engine power availability throughout the acceleration phase and no drive-train loss, Newton's Law of Motion dictates that acceleration time is proportional to the ratio

of vehicle weight to rated engine power [21]. To show this is true, consider a simple case of a vehicle accelerating from standstill on a level road at constant acceleration, a. If the time taken to reach a velocity, v, is given by t_f,

$$t_f = v/a \tag{2.14}$$

Using the nomenclature defined in Section 2.2

$$t_f = \frac{vM_{eff}}{F_{acc}} \tag{2.15}$$

Now, if P_{max} is the rated engine power

$$t_f = \frac{M_{eff}v^2}{P_{max}} \tag{2.16}$$

Neglecting the effect of rotational parts, and using $M_{eff}=M$

$$t_f = \frac{Mv^2}{P_{max}} = \left(\frac{W}{P_{max}}\right)\frac{v^2}{g} \tag{2.17}$$

For passenger cars, Malliaris *et al.* [13] conclude that the most simple and appropriate relationship for acceleration performance is given by

$$t_f = C\left(\frac{P_{max}}{W}\right)^{-n} \tag{2.18}$$

where 'C' and 'n' are empirical constants obtained by applying least-square fit on test data. While appreciating that a long series of factors apart from P_{max}/W ratio affect acceleration time, they state that engine power to vehicle weight ratio is overwhelmingly influential and allows by itself an adequate description of the acceleration performance. The other factors they mention include engine speed versus torque characteristics, drive train characteristics, human reaction times (applicable especially to manual transmission

vehicles) and test track conditions. Amann [21] lists the values of '*C*' and '*n*' that researchers over the years (1976-2000) have obtained for passenger cars. It is not surprising to note that both theoretical (Eq. 2.17) and empirical (Eq. 2.18) analyses arrive at similar conclusions, i.e., engine power to vehicle weight ratio is the most significant independent variable combination. Gillespie [22] confirms this by stating that the ratio of engine power to vehicle weight is the first-order determinant of acceleration performance. If the assumptions mentioned earlier are true, from Eq. 2.17 one can conclude that the acceleration capability of a vehicle decreases with increasing speed.

Gradeability can be calculated as

$$G = \left(\tan\left\{ \sin^{-1}\left(\frac{F_t - F_{wh}}{W} \right) \right\} \right) x100 \qquad 2.19$$

where G is in % and F_t is the tractive force. Even though gradeability and acceleration are identical measures of the net available engine torque used to either climb grades or to accelerate, vehicle design changes do not affect them in the same proportion. The reason for the same, as mentioned earlier, is that gradeability is a single steady-state calculation at one speed whereas acceleration time calculations include inertia effects which increase the kinetic energy of the tires, powertrain and other rotating components [16].

As expected, decrease in vehicle weight results in faster acceleration times and higher gradeability. This is due to the fact that with any reduction in the load on the engine, the engine has more available power to enhance vehicle performance. On the other hand, a decrease in the *N/v* ratio adversely affects acceleration performance and gradeability. It is interesting to note that, for passenger cars, Zub concludes that reduction in either aerodynamic drag or rolling resistance has no effect on acceleration and

gradeability performance. A plausible reason for this conclusion is that both air drag and rolling resistance become pronounced only at high speeds. At high speeds, there is very little extra power available with the engine to make a significant improvement in acceleration and gradeability performances.

2.4 Pass-by Noise

New vehicles all over the world face strict pass-by noise regulations. The actual pass-by noise level of a vehicle can be obtained only after a prototype has been built. While under-designing can result in a vehicle failing the pass-by noise standards, over-designing is wasteful and can adversely affect other vehicle performance characteristics. Hence, in a highly competitive automotive industry, it will immensely help vehicle designers if they had a means to predict pass-by noise given vehicle design parameters early in the design process [23]. However, this poses some severe challenges. Micro or component level noise modeling is generally done using Finite Element or Boundary Element Models. Extension of these models to the whole vehicle results in accumulation of errors. Further, such models are complex to build and difficult to maintain. The following statement by Fry and Jennings [24] in their paper in 2003 clearly brings out the severity of the problem.

> *Currently, there are no whole-vehicle analytical models that can predict pass-by noise, measured as a Sound Pressure Level, to better than about 3 dB(A).*

It is generally accepted that experienced engineers and acoustic specialists can predict pass-by noise results with an accuracy of ±3 dB(A) for new vehicle models and within ±1

dB(A) for variants of existing vehicle models. Consequently, analytical simulation approaches do not offer any significant advantage over noise-level predictions made by human experts as the error levels in both cases are comparable.

Fry *et al.* [23,24] list the four main noise sources on a vehicle as powertrain, intake system, exhaust system and tires. Their study uses artificial neural networks (ANN) to predict pass-by noise. The arguments put forth by them to justify the use of ANN include absence of an analytical solution for pass-by noise from a whole vehicle, existence of a causal relationship between vehicle design parameters and pass-by noise and easy availability of pass-by noise test data for most existing vehicles. The method of input selection for ANN, mentioned in their paper, consists of the following steps:

- Brainstorming by experts to come up with a list of candidate parameters
- Filtering of the list using some simple criteria
- Ranking of parameters according to the score received from experts
- Ensuring that the parameters cover all aspects of the vehicle
- Negotiation to make the final list practical and relevant

While they mention that a committee of 10 experts brainstormed a list of approximately 200 candidate parameters, due to confidentiality requirements, they do not divulge the full list of parameters that were finally selected for simulation. The only parameters mentioned are engine speed, relative positions of intake and exhaust systems with respect to the test microphones and engine fuel type. Fry and Jennings' ANN noise prediction model involves a two stage process - vehicle performance ANN and pass-by noise ANN. In the first stage, the vehicle performance ANN predicts acceleration performance. It has accuracies similar to other existing analytical models for acceleration. In the second

stage, the acceleration results along with other input data such as vehicle parameters and test conditions are passed on to the pass-by noise neural network. Fry and Jennings claim that their pass-by noise neural network outperforms analytical methods and the engineer's "guess" by predicting noise levels with an accuracy of ±1.4% which is equivalent to ±1.1 dB(A). Their model is however very data intensive. In all, it used 3500 samples for stage-1 and 5706 samples for stage-2.

Berge and Storeheier [25] studied the parameters influencing the noise levels from passenger cars in urban traffic. According to them, the primary parameters affecting noise emanating from a vehicle in traffic include engine speed, engine load and vehicle speed. These primary parameters are in turn controlled by a number of secondary parameters that can be classified into vehicle related, traffic related and driver related variables. The most important of the vehicle related parameters are ratio of engine power to vehicle weight ratio (P_{max}/W); ratio of engine power to engine displacement (P_{max}/V_d); and the gear ratios. While engine displacement alone is not correlated to any noise level, the ratio of engine power to engine displacement is correlated to the L_{95} level, exceeded by 5% of the cars. From their analysis of test results for cars accelerating from 50 km/hr (based on ISO 362 test procedure), Berge and Storeheier conclude that noise level strongly depends on approach engine speed at relatively short acceleration modes from moderate vehicle speeds. Curiously however, they say that power/weight ratio is correlated to the distribution of engine speed in urban traffic but is not correlated with noise levels measured during most of the type approval tests.

The total pass-by noise is the summation of engine related noise and tire noise. Engine related noise is predominant at lower vehicle speeds while tire noise is the major

noise source at high vehicle speeds. There are at least two well-known traffic noise prediction models - Federal Highway Administration's (FHWA) Traffic Noise Model (TNM) and the European Nordic Prediction Method. It is interesting to note that both methods include a simple one-parameter model wherein the A-weighted noise level (L_A) is linearly related to the logarithmic function of vehicle speed as given in Eq. **2.20**.

$$L_A = C.\log(v) + B \qquad \textbf{2.20}$$

C and B in Eq. **2.20** are constants that are calculated for each vehicle category (cars, buses etc.) using regression [**26**,**27**,**28**]. This corresponds well with the studies of Fry and Jennings [**24**] and Berge and Storeheier [**25**] who deduce that noise level is closely related to vehicle performance (acceleration and speed) characteristics. Using multiple regression analysis, Andersen and Bendtsen [**26**] also conclude that for heavy vehicles, the dependence of noise on engine displacement volume, V_d, is about 0.2-0.4 dB per liter. With regards to the commonly employed type approval test procedure for noise that involves full acceleration from a constant speed (50 km/hr), Bendtsen says that it covers an extreme driving situation where engine sound is the dominant source. The level of the road-tire noise, which is also very important, is underestimated in this test [**27**].

2.5 Reliability

Reliability of vehicles is a major consideration in the planning, design and operation of transit agencies. To the passenger, it means the ability of the transit system to meet route schedules while for the transit agency, it reflects the avoidance of penalties associated with unscheduled maintenance and inventory of spares [**29**]. Since vehicle

maintenance costs at a transit agency can be as much as 20 percent of the total expenditure, it is crucial for a transit agency to only employ reliable vehicles in transit service [1].

2.5.1 Reliability Theory

The origin of the mathematical theory of reliability dates back to World War II when German scientists introduced and applied basic chain links concept to improve the reliability of their rockets [30,31]. While in a qualitative sense, reliability has always been an important concern to engineers, the quantitative approach to reliability in non-military and non-aerospace applications is relatively recent. When reliability is quantified, it can be specified, designed for and measured. This enables the use of reliability as another parameter of design that needs to be optimized given its trade-offs with cost and performance. There is a growing awareness amongst design engineers that reliability needs to be built into a system at the development stage. Transit operators now specify numerical reliability targets to be demonstrated during the first year or so of the revenue operation [29].

The body of ideas, mathematical models and methods directed towards the problems of predicting or optimizing the mean life or life distribution of components and systems constitute reliability theory. The mathematics of reliability is based on probability theory because it is not possible to calculate the exact period for which a piece of equipment will work without failure. All that can be done is to calculate the probability of a piece of equipment working without failure for a particular period of time

[32]. Reliability is defined as the ability of an item to maintain the required function for a specified period of time (or mission time) under given operating conditions [33,34] .The time from the moment a component is put into use up to the moment of its failure obeys a probability distribution called the "failure law" of that component [35]. Typically used failure laws include exponential, normal, gamma, Weibull, modified extreme value distribution and the log-normal [31,36]. The exponential distribution has a constant failure rate, while gamma and Weibull distributions have increasing failure rates if the shape parameter has a value greater than 1. The modified extreme value distribution and the normal distribution have increasing failure rates. In the long-life range, log-normal distribution has a decreasing failure rate. Hence Barlow *et al.* [31] surmise that it appears doubtful for the log-normal distribution to be physically relevant to phenomenon such as fatigue in materials.

Mechanical failures can result due to a variety of reasons. These include defective design, wrong application, manufacturing defect, wear-out, incorrect installation, failure of other parts and gradual deterioration. For the truck industry, the product failures are due to manufacturing (12%), design (55%) and materials (33%) [32]. For most systems, the rate of failures follows what is commonly known as the "bath-tub curve" shown in Figure 2.4 [37]. The rate of failures is initially high due to manufacturing defects and compatibility issues between new components. It stabilizes to a practically constant value during the middle phase known as the "useful life". The useful life of a system lies between T_B (possible wear-in time) and T_W (start of wear-out time). Finally, when the system components wear down considerably, the failure rate again increases. This phase is called "wear out".

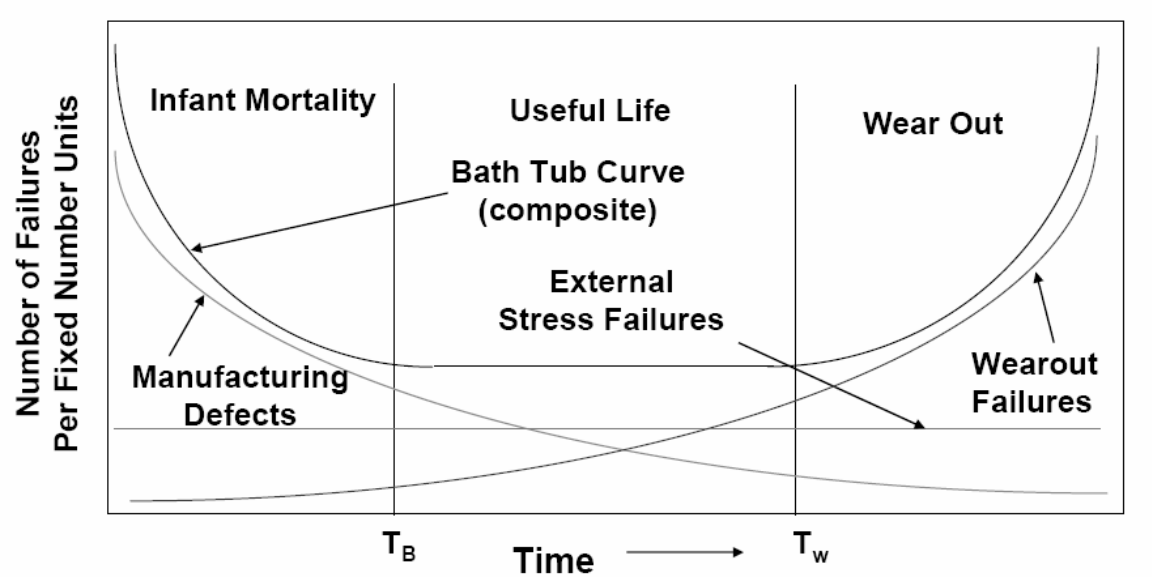

Figure 2.4: Bath-tub curve.

The average period a non-repairable item will function without failure is most often represented by the mean time to failure (MTTF). For a repairable item, the corresponding reliability measure is mean time between failures (MTBF). However, due to the multitude of reasons for failure and the complex nature of the problem, there is no certainty that it will not fail before the end of this period. The component might fail within a much shorter period, or perhaps run longer without failure. It is pertinent to note here that often in literature the abbreviation 'T' in the pseudonyms (MTBF & MTTF) is wrongly said to stand for "time", while it in fact represents "operating time" [33]. Transit agencies use a variety of reliability measures to determine and quantify performance. Of these, the most commonly used measure that is also of interest to a vehicle/maintenance engineer is mean distance between failures (MDBF). MDBF is the average distance in miles that a transit vehicle travels before failure of a vital component forces removal of that vehicle from service. A high MDBF indicates a more reliable vehicle. An alternative

measure of reliability that is also of relevance is road calls experienced per 1000 miles of operation [38].

Most methods of reliability analysis use the assumption of a Markov process. A deterioration law of a system is said to be Markovian if the future course of the system depends only on its state at the present time and not on its past history, i.e., an item's chance of failure in any operating period is not age dependent. MDBF (and MTBF – Mean Time Between Failures) calculation inherently uses Markov assumption. Barlow *et al.* [31] say that there are at least two good reasons for suggesting a Markov model to describe deterioration.

> *First of all, if each component has approximately an exponential failure law, the complete system can be described approximately by a Markov process. Secondly, the first order approximating description of many physical systems is that in which knowledge of the history of such systems contains no predictive value.*

Hence the calculation of MDBF is based on a failure law of exponential nature, i.e., constant failure rate is assumed. Under an exponential distribution assumption, the mean completely characterizes the distribution and is a sufficient metric. Critics of exponential law assumption say that if the underlying failure law is in reality not exponential, then the mean is not sufficient to describe the data and is hence a poor reliability metric [39].

Drenick is often quoted by the proponents of the exponential law assumption. In his seminal paper from 1960, he says [35]

> *Under some reasonably general conditions, the distribution of the time between failures tends to the exponential as the complexity and the time of operation increase: and somewhat less generally, so does the time up to first failure of the equipment.*

Drenick's statement seems to agree with engineering intuition. By their very nature, many systems (including transit buses) consist of thousands of parts. These parts can be old or new with many lying somewhere in between these extremes. Also, each part type will have a specific distribution of times to failure associated with it. The consequence of having parts of varying ages and distributions together in a complex system is that the system tends to exhibit a constant failure rate, i.e., the underlying statistical distribution of the time to failure is exponential [34].

At present, much of the research in the field of reliability concerns non-constant failure rate, i.e., distribution for which the time between failures does not follow an exponential distribution. For other distributions, one cannot talk of a failure rate. Instead, one should use the term hazard function which describes how the rate of failures varies with time. Interestingly however, most practical applications within the field of logistic-support assume constant failure rates [40].

2.5.2 Prediction of System Reliability

There are two basic methods for determining the failure rate (or hazard function) of a system or component [34]. These are:

1. Use the failure data for a comparable system or component already in use and assume that the principle of transferability is applicable.
2. Test the system or its components.

Although, theoretically the second method is better, it has two disadvantages. Firstly, reliability predictions are needed long before prototypes are available. Secondly, for

some highly reliable components, the cost of testing to measure reliability in a statistically valid manner would be prohibitive.

As per Kumar *et al.* [33], if times-to-failure for different components within the system are known and the items are non-repairable, then, reliability prediction will involve the following steps:

a) *Construct the reliability block diagram (RBD) of the system*
b) *Determine the operational profile of each block in the RBD*
c) *Derive the time-to-failure distribution of each block*
d) *Derive the life exchange rate matrix (LERM) for the different components within the system*
e) *Compute reliability function of each block*
f) *Compute the reliability function of the system*

For repairable items, an approach based on Markov models is normally used. The first step in calculating reliability using Markov modeling is to identify the system "up states" (states in which the system maintains the required function) and the system "down states". The state space of the Markov chain can then be partitioned into two mutually exclusive sets - one corresponding to system "up states" and the other to the "down or failed states". The state probabilities and time spent on each state can then be used to evaluate point availability and reliability of system using either differential equations or integral equations.

A reliability block diagram is a logical diagrammatic illustration of the system (hardware/software) in which each item within the system is represented by a block [33]. Depending on the item, an RBD can be represented by a series, parallel, series-parallel, r-out-of-n or complex configuration. In a series configuration, the failure of any one item of the system will cause failure of the system as whole. For example, if two components

A and B are connected in series as shown in Figure 2.5, the reliability of the system is given by $R_S = R_A \times R_B$ where R_A and R_B are the component reliabilities.

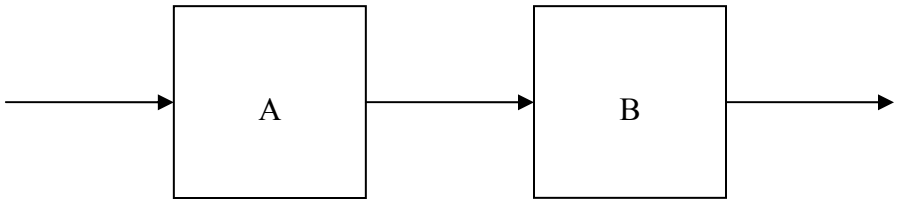

Figure 2.5: Series configuration.

Thus the reliability of a series configuration with n items is given by

$$R_S = \prod_{i=1}^{n} R_i \qquad 2.21$$

As evident from Eq. 2.21, the reliability for a series configuration is less than or equal to the minimum value of the reliability function of the constituting components.

In a parallel configuration the system fails only when all the items of the system fail. Thus the system has redundancy. Figure 2.6 shows two components A and B connected in parallel. The system reliability in this case is given by $R_P = 1 - [(1- R_A) \times (1- R_B)]$. For a system consisting of n components in parallel, the system reliability is given by

$$R_P = 1 - \prod_{i=1}^{n} (1 - R_i) \qquad 2.22$$

From Eq. 2.22, it is clear that by adding a component in parallel (i.e., redundancy) the reliability of the system improves. Two components in parallel (redundant) may either be always in operation (active redundancy) or one may be off and not in the "circuit" (standby redundancy).

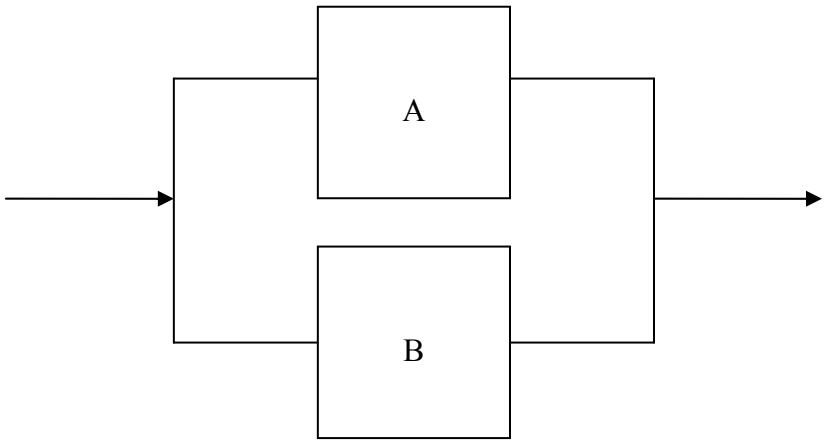

Figure 2.6: Parallel configuration.

2.5.3 Costs Associated with Reliability

An important aspect in procurement of any equipment is the cost. This cost includes not only the initial cost but also the costs incurred to keep the equipment in a satisfactory working condition after it has been purchased. On the production side, higher reliability normally means better quality and therefore more expensive parts. This is due to use of costlier materials, tighter tolerances and additional and more elaborate test and inspection facilities. Hence making a piece of equipment more reliable may mean increasing its initial cost. However, this increase can be more than offset by the repair and maintenance costs [32]. When an equipment fails there is not only a loss of production or service but also often of goodwill between the customer and the seller, both of which involve some form of direct or indirect financial loss.

Modern complex equipment like transit buses requires highly skilled technicians for repair work. Training such personnel can be a long and expensive process. More repair work entails more technicians, larger workshop installations and more pieces of equipment for carrying out the repairs. Another form of expense associated with maintenance is cost associated with keeping spares. Though such cost is immediately not obvious, unnecessarily large spare inventory could represent money lying idle which if invested could generate more revenue. The total cost of a piece of equipment is composed of 3 distinct costs - design and development, production, and maintenance and repair as shown in Figure 2.7.

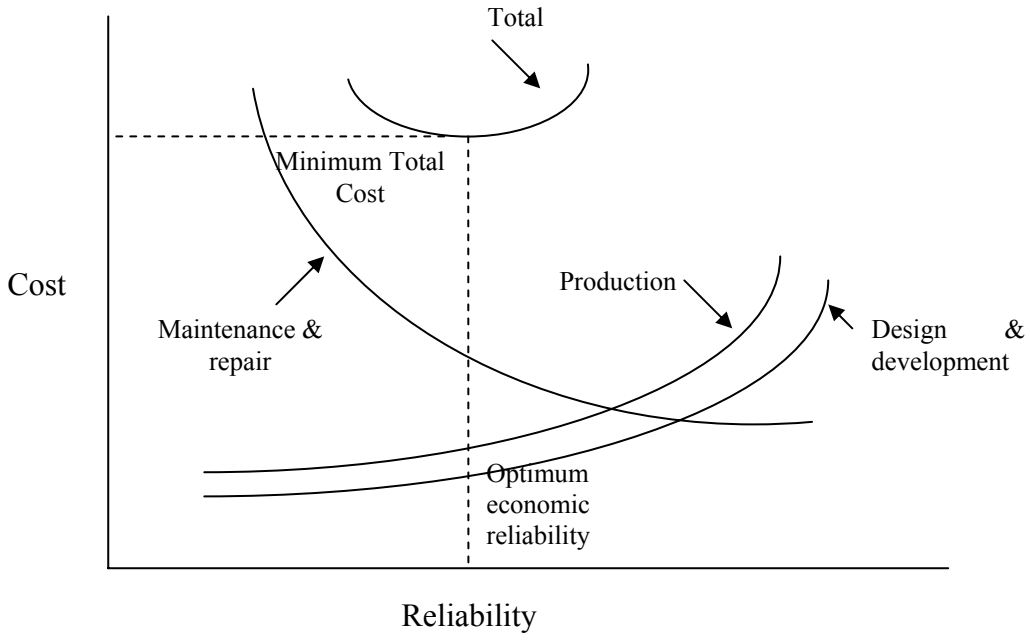

Figure 2.7: Variation of total cost with reliability.

Normally, as reliability increases, the design and production costs increase while maintenance and repair costs fall. Total cost first reduces and then increases. Optimum economic reliability is, however, very difficult to achieve in practice.

2.5.4 Measures of Reliability Used in Transit Industry

The two indices most commonly used to measure the capability of a system to provide high quality uninterrupted services are:

1. *Reliability*: It is defined as the probability that an item can perform its intended function for a specified interval under stated conditions [34].
2. *Availability*: It is defined as the percentage of time that a system is available to perform its functions. Availability is commonly calculated as

$$Availability = \left(\frac{Uptime}{Uptime + Downtime} \right) \qquad 2.23$$

Historically, industries such as electrical power, oil & gas, and communications have used availability as their measure of choice while transit industry has used reliability. One probable reason could be the fact that industries that use availability tend to run round the clock, i.e., 24 hours and hence uptime to downtime ratio is very critical. On the other hand, for transit bus industry, the frequency of repair (measure of reliability) has a more direct bearing on time schedule adherence and customer satisfaction.

The measures of reliability commonly used in the transit bus industry fall under two broad categories –

a) one that directly evaluates customer satisfaction and

b) one that evaluates the dependability of the bus itself

Adherence to schedule (on-time performance), service regularity and on-time departure are measures that directly affect service reliability and correspond well to customer satisfaction. Mean Distance Between Failures (MDBF) is the most commonly used reliability measure in the transit bus industry and falls under category (b). The popularity of MDBF as a reliability measure is possibly due to the fact that it evaluates the performance of the vehicle directly and helps transit agencies in planning their maintenance regimens and spares inventory.

2.5.5 Reliability Studies in the Field of Transportation

Reliability analysis has been widely used to study transportation systems. Dhillon developed five different Markov models to compute vehicle reliability, availability, mean time to failure and state probabilities [30]. Four of the models considered vehicles operating in changing weather conditions (normal and stormy) while the last model simulated vehicles used in a constant weather condition. Results show that vehicle availability decreases with increase in accident rate while mean time to failure decreases quite significantly due to increase in the occurrence of hostile weather conditions.

Singh and Kankam [29] collected failure data on 500 subway cars, 400 street cars and 1100 buses from the Toronto Transit Commission in an effort to create a database for reliability of transit vehicles and their components. They stress the need for availability of good data on the failure of transit vehicle components for successful application of quantitative reliability methods. For buses and their sub-systems, they found that the

probability distributions underlying the miles between defects appear to be exponential or Weibull with a shape parameter less than unity. Shape parameter of less than unity means a large number of early failures. This in turn indicates ineffectiveness of a maintenance task, problems induced by the repair process, and infant mortality of newer components replacing the older ones. With regards to influence of age of the buses, they found that older buses had lower reliability than newer buses.

Bedewy *et al.* [41] compared three different working designs of public transport buses operating in Cairo. They compared reliability and maintainability measures based on data collected over four years. It was assumed that the bus and its relevant subsystem generally fail according to normal distribution which in turn was approximated to a negative exponential distribution. The maintainability measures calculated include mean time to repair (MTTR), uptime ratio (UTR), probability of mission completion, and spare parts requirements.

Traditional methods of reliability prediction have concentrated on estimation using failure data gathered during trials or use. It has been increasingly recognized that predicting reliability earlier in the life cycle is important. Neil *et al.* [42] have used Bayesian belief networks (BNN) as a decision support tool to predict the reliability of military vehicles. Boessio *et al.* [43] developed a time domain approach to deal with fatigue effects due to pavement roughness on commercial vehicle structures. A computational code was formulated to estimate the vehicle lifetime and to alternatively determine the reliability index. Their preliminary tests have shown that significant variations in the lifetime exist amongst different samples.

Parker [44] developed a simulation model to analyze the reliability claims of manufacturers with regards to reliability of systems and sub-systems of combat vehicles. Smith *et al.* [45] have used neural networks to provide real time monitoring of an airport ground transportation vehicle with the objectives of improving availability and minimizing field failures by estimating the proper timing for condition-based maintenance. They used their method to predict degraded performance and anticipated failures for door systems. Marseguerra *et al.* [46] have also used artificial neural networks (ANN) to predict the reliability of automotive components and systems from experimental failure data. An ANN was implemented to predict the trend of the unreliability index and the number of faults per 100 vehicles at time t (number of months from production time) using information on the number of vehicles produced and sold and the predicted number of faults up to the previous time t-1.

Klinikowski *et al.* [47] investigated the relationship between in-service failures and failures during testing at PTI using failure data from two transit authorities for three different bus models. Each transit agency submitted data for ten buses of a specific model. The method of rank correlation coefficient was used to establish a correlation between in-service failures and test track failures. Their results indicated a good correlation between the two failures once questionable data pertaining to the suspension system for one bus model was excluded from analysis.

Very few studies, if at all, seem to have been conducted on analyzing the effects of different vehicle design parameters or operating conditions on reliability. In his article on reliability, Gaver [48] mentions that for trucks, tanks and other vehicles, the most

important factors influencing MDBF are terrain, vehicle speed and loading. However, no supporting data or mathematical models are presented.

2.6 Brief Note on Other Performance Measures

As mentioned in Section 1.3, this study focuses on four performance measures - fuel economy, acceleration and gradeability, pass-by noise and reliability - since data for these measures were readily available at PTI and at National Transit Database (NTD). Hence only literature pertaining to these four measures has been covered in this Chapter. However, as the methods developed in this study are very general in nature, they can easily be used for other performance measures as well.

PBS is approaching final stages of implementation in countries such as Australia, New Zealand and Canada. At present, the performance measures under consideration in these countries pertain mostly to vehicle dynamics since this aspect has long been neglected under existing heavy vehicle regulations. The list of PBS being considered for implementation in Australia is given in Table 2.1 [5]. Edgar *et al*. describe these standards and their test specifications in more detail [2].

Table 2.1: Australian Performance Based Standards

No.	Performance Standard
1	Startability
2	Gradeability
3	Acceleration Capability
4	*Overtaking Provision* (not finalized)
5	Tracking Ability of a Straight Path
6	*Ride Quality* (not finalized)
7	Low-speed swept path
8	Frontal Swing
9	Tail Swing
10	Steer-Tyre Friction Demand
11	Static Rollover Threshold
12	Rearward Amplification
13	High-Speed Transient Offtracking
14	Yaw Damping Coefficient
15	*Handling Quality* (not finalized)
16	*Stability Under Braking* (not finalized)

2.7 Summary of Available Literature

Multiple regression seems to have been the method of choice for studying vehicle performance. However, regression modeling means that the nature of the relationship has been pre-guessed. Recently, other methods such as constrained regression, Bayesian analysis and neural network have also been employed. Fuel economy is one of the most researched performance measures. For buses, researchers conclude that fuel economy decreases linearly with increase in weight. An important aspect that researchers agree upon is that, for most performance prediction performance models, only a few vehicle design parameters such as like weight and engine power amongst others count as the most influential. Inclusion of a larger number of inputs in the performance prediction

model only provides marginal improvements in accuracy. This conclusion seems to favor the use of macro-modeling.

Until recently, analytical models for pass-by noise were found to be only as accurate as human experts. In 2003, Fry and Jennings presented a two-stage pass-by noise model using ANN that had a better accuracy. However, their model is complex in terms of the network configuration and the number of samples required. Further due to proprietary restrictions, they do not give much detail with regards to the inputs that are important. Existing reliability studies have looked at the influence of weather and other operating conditions on mean distance between failures at transit agencies. However, very few efforts have been made to understand the relationship between the performance of a bus model on a test track and its performance at transit agencies. Practically no studies exist on the effect of vehicle design parameters on the reliability of buses.

2.8 Shortcomings in Available Literature

As is evident from Sections 2.2 - 2.5, researchers over the past few decades have spent a great deal of effort in trying to understand the factors that affect vehicle performance and have suggested various models. Although a good amount of progress has been made, there still are some shortcomings in the available literature. Those relevant to the research described in this thesis are:

1) Most of the studies use regression as the modeling approach. With regression, invariably, the nature of the relationship is pre-decided by the analyst. This is particularly problematic in cases where little is known in terms of the nature of

the relationship being modeled. Regression modeling may result in unreliable estimates due to multi-collinearity caused by high correlation between the vehicle parameters. Further, if the relationship between inputs and output is nonlinear, the results of linear regression analysis will under-estimate the true relationship and result in modeling errors.

2) Very few pass-by noise prediction models exist with predictive accuracies better than that of human experts (±3 dB(A)). Fry and Jennings [24] present a neural network based model that they claim to be the most accurate one (±1.1 dB(A)) available as of year 2003. Their presentation has a number of shortcomings. Firstly, little is mentioned in terms of the most relevant input variables due to the proprietary nature of their research. Secondly, the input selection methods used are cumbersome and are largely based on expert opinion. While this is advantageous under circumstances wherein one wants to incorporate prior knowledge, in cases where very little prior information is available on relevant inputs, such a method can lead to wrong conclusions. Thirdly, their models are complex and data intensive, both in terms of the number of inputs used and the number of samples needed.

3) A lot of research has been conducted on the effect of vehicle usage related parameters such as pavement roughness and weather on vehicle reliability. However, there appears to be a lack of studies on the effect of vehicle design parameters on vehicle reliability. This seems particularly odd if one considers the fact that almost 55% of the failures in the truck industry are due to design [32].

Gaver [48] mentions vehicle weight as an input, that is most relevant to reliability, but no mathematical model is presented.

4) With regards to fuel economy and reliability, practically no comprehensive studies (based on a large number of buses) have been undertaken to mathematically quantify the relationship (if it exists) between performance of a bus model on a test track and its in-service performances at various transit agencies. Klinikowksi *et al*. [47] used rank correlation coefficient to compare the number of failures encountered by the same bus model at PTI and at transit agencies and found that the two were highly correlated. It would be interesting to develop their analysis further by analyzing a much larger dataset and also by mathematically modeling the effects of other inputs pertaining to vehicle usage at a transit agency such as average operating speed, age of the vehicle and maintenance of the vehicle amongst others.

Chapter 3

Theoretical Model and Data Collection

3.1 Mathematical Approach

The method of analysis used in this thesis is based on the approach suggested by Kulakowski [49]. A block diagram of a simplified vehicle-traffic system is shown in Figure 3.1. In this diagram, a heavy vehicle is represented by a vector of design parameters, $\boldsymbol{\theta} = (\theta_1, \theta_2, \ldots\ldots\theta_p)$ that could include parameters such as length, width, height, wheel base, axle loads, engine power etc. The other two inputs to the vehicle block are driving vector, $\mathbf{u} = (u_1,u_2,\ldots\ldots u_r)$ and the road vector, $\mathbf{x} = (x_1,x_2,\ldots\ldots\ldots x_k)$. Driving vector includes actions of the driver such as steering, braking and acceleration, while road input vector comprises of road geometry, surface friction and pavement roughness amongst others.

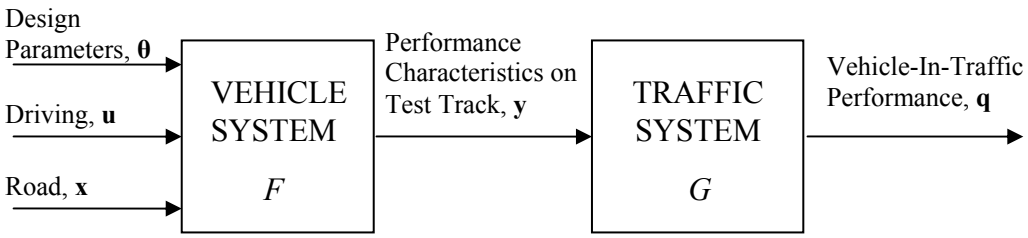

Figure 3.1: Block diagram of a vehicle-traffic system.

The output signal is a vector, $\mathbf{y} = (y_1, y_2, \ldots\ldots, y_n)$, that includes vehicle performance characteristics measured under laboratory or test track conditions. Examples of such performance characteristics include fuel efficiency, acceleration, roll stability and gradeability to name a few. Mathematically, the relationships can be written in vector form as

$$\mathbf{y} = F(\mathbf{u}, \mathbf{x}, \boldsymbol{\theta}) \qquad 3.1$$

The second block in Figure 3.1 represents a traffic system in which the vehicle is operating. The input for this block is the test-track performance characteristics vector, **y,** coming from the vehicle block while the output vector, **q**, represents vehicle behavior in an actual traffic environment. Some components of this vector that may be of interest are fuel economy in traffic, risk of traffic accidents, level of dynamic tire-pavement loads and pollution. Expressing the relationship in a compact form,

$$\mathbf{q} = G(\mathbf{y}) \qquad 3.2$$

The knowledge of the transformations F and G in Eqs. 3.1 and 3.2 is of great value in developing and implementing vehicle regulations since we can then predict, to a reasonable degree, the road performance of a vehicle given the regulatory standards to which it conforms. Also, if both F and G are known accurately, then we can apply reverse engineering concepts (assuming the inverse transform exists) to get corresponding vehicle design parameters that would result in a particular (desired) vehicle behavior in a traffic system. Mathematically, this can be expressed as

$$\mathbf{y}^* = G^{-1}(\mathbf{q}^*) \qquad 3.3$$

where, $\mathbf{q}^*$ represents one combination out of all acceptable measures of vehicle behavior in traffic and $\mathbf{y}^*$ represents a desired vector of vehicle performance characteristics on a test track. The final step in this reverse engineering process is to arrive at a vector of vehicle parameters, $\boldsymbol{\theta}^*$, that would ensure desired performance of a vehicle in a traffic system. If driver input, $\mathbf{u}$, and road input, $\mathbf{x}$, are assumed to be constant

$$\boldsymbol{\theta}^* = F^{-1}(\mathbf{y}^*) = F^{-1}\{G^{-1}(\mathbf{q}^*)\} \qquad \textbf{3.4}$$

The equations introduced so far can now be used to illustrate the prescriptive or design-based standards (DBS) and performance-based standards (PBS) approaches to vehicle regulations. If $\boldsymbol{\theta}_{\text{DBS}}$ and $\mathbf{y}_{\text{PBS}}$ represent vectors corresponding to desired performance, then the following relationships hold in general,

$$\mathbf{q}_{DBS} = G\{F(\boldsymbol{\theta}_{DBS})\} \qquad \textbf{3.5}$$

$$\mathbf{q}_{PBS} = G(\mathbf{y}_{PBS}) \qquad \textbf{3.6}$$

It is evident from the above equations that a vehicle designed to meet PBS would perform better than one designed to meet DBS since there is less uncertainty in Eq. **3.6** than in Eq. **3.5**. This is due to the fact that errors in estimating the transformations accumulate in Eq. **3.5** as it involves an additional transformation (F) when compared to Eq. **3.6**. One can express this succinctly as

$$||\mathbf{q}_{PBS} - \mathbf{q}^*|| \leq ||\mathbf{q}_{DBS} - \mathbf{q}^*|| \qquad \textbf{3.7}$$

3.2 Complexities in the Proposed Model

The theoretical approach introduced in Section 3.1 has some potential challenges. Two such problems are explained in the following sub-sections: the problem of inversion and the case involving additional inputs.

3.2.1 Problem of Inversion

As per Naylor and Sell [50],

> *A mapping Γ: $X \rightarrow Y$ is invertible if and only if it is one-to-one and Range(Γ) = Y.*

This means that for an inverse to exist, the mapping should be bijective, i.e., it should both be one-to-one (injective) and span the whole range (onto or surjective). The inverse transformations given in Eq. 3.3 and Eq. 3.4 can be ill-posed for the following reasons. Firstly, the given inverse transformations are in general one-to-many. For example, for a desired performance characteristics vector, $\mathbf{y}^*$, there could be innumerous combinations of design parameters, $\boldsymbol{\theta}^*$, that could satisfy Eq. 3.4. Secondly, there could be values of $\mathbf{y}^*$ for which there can be no physically realizable or practical $\boldsymbol{\theta}^*$. Hence, vehicle transformation, F, and traffic system transformation, G, are neither injective nor surjective. One way of circumventing this problem is to use constrained optimization.

3.2.2 Case with Additional Inputs

An additional complexity that may arise is a situation wherein there are other inputs into the traffic system apart from performance characteristics vector, $\mathbf{y}$. Study of

fuel economy at a transit agency is one such example. Apart from **y**, inputs could include the level and nature of vehicle maintenance, age/condition of the vehicle, number of stops in a trip and number of passengers amongst others. Using vector **w** to denote the extra inputs, the traffic system can be depicted as shown in Figure 3.2.

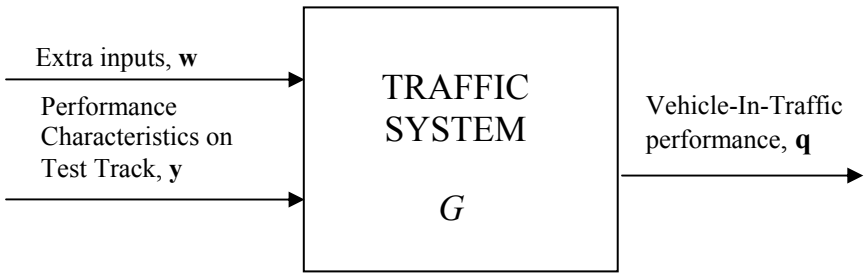

Figure 3.2: Traffic system with additional inputs.

In this case, the problem can be formulated as a two-stage inversion. In the first stage, using the technique described in Section 4.4, vectors **w*** and **y*** can be obtained from **q***. Mathematically, this can be written as

$$z^* = G^{-1}(q^*) \tag{3.8}$$

where

$$z^* = \begin{bmatrix} w^* \\ y^* \end{bmatrix} \tag{3.9}$$

Finally, one can use Eq. 3.4 to get the vehicle design parameters, **θ*** from **y***.

3.3 Data Collection

Using reliable and accurate data is crucial for developing a good simulation model. In this study, data from the Bus Testing Program at Pennsylvania Transportation Institute (PTI) were used to evaluate vehicle transformation, *F*, shown in Figure 3.1. For evaluating the traffic transformation, *G*, in-use field data from transit agencies were collected from the National Transit Database (NTD) [51].

3.3.1 PTI Test Track Data

Since its inception in 1989, the Bus Testing Program at Pennsylvania Transportation Institute (PTI) has been testing buses for maintainability, reliability, safety, performance, structural integrity, fuel economy and noise. Over the years, a substantial amount of reliable test data has been generated. For this study, test data were collected from PTI tests reports for four performance measures, namely, fuel economy, acceleration and gradeability, pass-by noise and reliability to evaluate the vehicle transformation, *F*. In order to avoid the complexities associated with grouping together vehicles running on different fuels and having markedly different configurations, only two-axle diesel powered transit buses were considered in study. Two-axle diesel powered buses constitute the majority of the buses tested at PTI. It should be noted, however, that if substantial data were available for alternative fuel buses and 3-axle buses, then, one could potentially use fuel type and axle configuration as input variables and develop one single model.

Data were collected from PTI test reports for a total of 124 diesel powered 2-axle transit buses. However, some bus models only undergo partial testing at PTI and hence not all data were available for the 124 buses under consideration. In all, fuel efficiency data (on CBD, ART and COM cycles) were available for 111 buses. Acceleration and pass-by noise data were available for 110 buses while reliability data (failure data) were available for a total of 108 buses. It should be noted that a majority of the buses were still common across the different datasets. With regards to reliability, there were two issues that needed to be resolved:

1. Selection of the reliability measure to use
2. Reconciliation of the differences between the data collection at PTI and that reported in NTD

As mentioned in Section **2.5.4**, availability is calculated from uptime and downtime. While uptime depends on reliability, downtime depends on maintainability of the vehicle. Maintainability is a function of design features, such as access to parts, interchangeability, standardization and modularity [**34**]. A system that is highly maintainable can be restored to full operation in minimum amount of time with minimum expenditure of resources. When only reliability and corrective maintenance effects are taken into account, one measures the "inherent availability" that is solely a function of the design characteristics of the vehicle. Comparison of inherent availabilities of the same bus model as measured under accelerated durability testing at Pennsylvania Transportation Institute (PTI) track and under real-life conditions at transit agencies is preferable. However, there are two potential issues. Firstly, availability is determined not only by reliability and repair but also by other factors related to preventive maintenance

and logistics. When these effects are included, one is talking in essence about "operational availability" which accounts for delays such as those caused when either spare parts or maintenance personnel are not readily at hand to accomplish a repair. It is hence problematic to get "inherent availability" from real-life "operational availability" related data that most transit agencies normally collect. Secondly, for a system (transit bus in our case) that does not run round the clock, uptime and downtime have to be calculated in terms of distance traveled instead of in time units. While such a conversion is readily available for uptime (distance traveled between failures, i.e., MDBF), such a conversion for downtime is difficult as the operating speeds are neither constant nor the same amongst different transit agencies. Hence, in this study, MDBF was chosen as the reliability measure.

At PTI, the Bus Testing Program staff categorizes malfunctions or failures into four different classes based on the severity. These are as follows:

> *Class 1 - Physical Safety: A failure that could lead directly to passenger or driver injury and represents a severe crash situation.*
>
> *Class 2 - Road Call: A failure resulting in an enroute interruption of revenue service. Service is discontinued until the bus is replaced or repaired at the point of failure.*
>
> *Class 3 - Bus Change: A failure that requires removal of the bus from service during its assignments. The bus is operable to a rendezvous point with a replacement bus.*
>
> *Class 4 - Bad Order: A failure that does not require removal of the bus from serviced during its assignments but does degrade coach operation. The failure shall be reported by driver, inspector, or hostler.*

On the other hand, since 2001, NTD only reports the following two categories of failures:

> *Major Mechanical Failure: A failure of some mechanical element of the revenue vehicle that prevents the vehicle from completing a scheduled*

revenue trip or from starting the next scheduled revenue trip because actual movement is limited or because of safety concerns. Major mechanical failures include breakdowns of air equipment, brakes, doors, engine cooling system, steering and front axle, rear axle and suspension and torque converters.

Other Mechanical Failure: A failure of some mechanical element of the revenue vehicle that because of local agency policy prevents the revenue vehicle from completing a scheduled revenue trip or from starting the next scheduled revenue trip even though the vehicle is physically able to continue in revenue service. Other mechanical failures include breakdown of fareboxes, wheelchair lifts, heating, ventilation and air conditioning (HVAC) systems and other problems not included as a major mechanical systems failure.

To reconcile the differences between the classifications used by PTI and NTD, reclassification of PTI failure data into "major" and "other" failures was done for all 124 buses as a part of this study. This is however not necessary for calculating MDBF since it is based on the number of total failures. An assumption was made that all failures encountered at PTI would have resulted in failure to complete a scheduled revenue trip or failure to start the next scheduled trip. This assumption helps one compare PTI and NTD failures on a one-to-one basis. However, differences may still be present due to the fact that failures such as those of fare-boxes and wheelchair lifts are not tested for at PTI.

Performance data were obtained for a total of 21 input variables and 11 outputs (3 for fuel economy, 4 for acceleration and 4 for pass-by noise). These are listed in Tables **3.1 - 3.3**. For reliability model, data were collected for a total of 23 inputs and one output (MDBF). The salient statistics of the data are included in Tables **3.4** and **3.5**. For some buses, engine power and displacement values were not available in the PTI test reports. Only engine model numbers were given. In such cases, the missing values were obtained from other sources such as marketing brochures and web-sites of engine/vehicle

manufacturers. Similarly, the effective tire diameters were obtained from tire data books based on the tire sizes given in PTI reports. Hence, presence of additional noise apart from ordinary measurement errors is expected for these input variables.

Table 3.1: List of input variables - PTI fuel economy model

Sr. No.	Input	Min.	Max.	Mean	Std. Dev.	Std. Dev. /Mean
1	Length (m)	6.17	12.54	9.99	1.75	0.18
2	Width (m)	2.16	2.69	2.49	0.09	0.03
3	Height (m)	2.56	3.50	3.06	0.17	0.05
4	Wheel Base (m)	3.10	7.59	5.43	1.22	0.22
5	Front Overhang (m)	0.68	3.04	1.68	0.69	0.41
6	Rear Overhang (m)	0.76	5.54	2.86	0.52	0.18
7	Ground Clearance (m)	0.08	0.34	0.22	0.05	0.21
8	Curb Weight - Front (kN)	14.02	46.06	30.44	8.65	0.28
9	Curb Weight - Rear (kN)	19.58	89.89	53.46	20.88	0.39
10	Curb Weight - Total (kN)	34.26	128.87	83.90	27.79	0.33
11	Seated Load Weight - Front (kN)	14.15	57.32	35.64	11.60	0.32
12	Seated Load Weight - Rear (kN)	24.59	109.96	68.94	22.57	0.33
13	Seated Load Weight - Total (kN)	41.16	158.24	104.54	32.66	0.31
14	Gross Vehicle Weight - Front (kN)	14.02	64.97	39.73	14.69	0.37
15	Gross Vehicle Weight - Rear (kN)	24.59	123.84	75.76	25.62	0.34
16	Gross Vehicle Weight - Total (kN)	41.61	192.95	115.54	39.44	0.34
17	Axle Ratio	2.90	6.60	4.40	0.70	0.16
18	Engine Power (kW)	123.1	223.8	166.00	25.11	0.15
19	Engine Displacement (cc)	4251	10831	7212	1363	0.19
20	Wheel Diameter (m)	0.41	0.57	0.53	0.06	0.11
21	Tire Diameter (m)	0.71	1.07	0.90	0.11	0.13

Table 3.2: List of input variables - PTI acceleration and pass-by noise models

Sr. No.	Input	Min.	Max.	Mean	Std. Dev.	Std. Dev. /Mean
1	Length (m)	6.17	12.54	9.99	1.76	0.18
2	Width (m)	2.16	2.69	2.49	0.09	0.03
3	Height (m)	2.56	3.50	3.06	0.17	0.06
4	Wheel Base (m)	3.10	7.59	5.44	1.22	0.22
5	Front Overhang (m)	0.69	3.04	1.67	0.69	0.41
6	Rear Overhang (m)	0.76	5.54	2.86	0.52	0.18
7	Ground Clearance (m)	0.08	0.34	0.22	0.05	0.21
8	Curb Weight - Front (kN)	14.02	46.06	30.47	8.69	0.28
9	Curb Weight - Rear (kN)	19.58	89.89	53.21	20.82	0.39
10	Curb Weight - Total (kN)	34.26	128.87	83.69	27.83	0.33
11	Seated Load Weight - Front (kN)	14.15	57.32	35.68	11.65	0.33
12	Seated Load Weight - Rear (kN)	24.59	109.96	68.72	22.55	0.33
13	Seated Load Weight - Total (kN)	41.16	158.24	104.35	32.75	0.31
14	Gross Vehicle Weight - Front (kN)	14.02	64.97	39.73	14.76	0.37
15	Gross Vehicle Weight - Rear (kN)	24.59	123.84	75.55	25.63	0.34
16	Gross Vehicle Weight - Total (kN)	41.61	192.95	115.33	39.55	0.34
17	Axle Ratio	2.90	6.60	4.40	0.70	0.16
18	Engine Power (kW)	123.1	223.8	165.9	25.22	0.15
19	Engine Displacement (cc)	4251	10831	7208	1368	0.19
20	Wheel Diameter (m)	0.41	0.57	0.53	0.06	0.11
21	Tire Diameter (m)	0.71	1.07	0.89	0.12	0.13

Table 3.3: List of output variables - PTI performance models

Sr. No.	Input	Min.	Max.	Mean	Std. Dev.	Std. Dev. /Mean
1	Fuel Economy- CBD cycle (km/L)	1.14	3.66	2.05	0.56	0.28
2	Fuel Economy- ART cycle (km/L)	1.33	4.24	2.25	0.58	0.26
3	Fuel Economy- COM cycle (km/L)	2.01	7.07	4.01	1.04	0.26
4	Acceleration at 16 km/hr (m/s^2)	0.70	2.19	1.31	0.34	0.26
5	Acceleration at 32 km/hr (m/s^2)	0.60	1.80	1.05	0.27	0.26
6	Acceleration at 48 km/hr (m/s^2)	0.46	1.52	0.81	0.22	0.28
7	Acceleration at 64 km/hr (m/s^2)	0.27	1.28	0.58	0.20	0.34
8	Pass-by Noise: Accelerating from Constant speed - Right Side (dBA)	67.6	86.8	75.8	3.05	0.04
9	Pass-by Noise: Accelerating from Constant speed - Left Side (dBA)	70.3	87.4	77.0	3.60	0.05
10	Pass-by Noise: Accelerating from Standstill - Right Side (dBA)	68.6	84.6	75.9	3.24	0.04
11	Pass-by Noise: Accelerating from Standstill - Left Side (dBA)	70.2	87.4	77.1	3.72	0.05

Table 3.4: List of input variables - PTI reliability model

Sr. No.	Input	Min.	Max.	Mean	Std. Dev.	Std. Dev. /Mean
1	Length (m)	6.17	12.55	9.91	1.69	0.17
2	Width (m)	2.16	2.69	2.49	0.08	0.03
3	Height (m)	2.56	3.50	3.06	0.17	0.06
4	Wheel Base (m)	3.10	7.58	5.36	1.22	0.21
5	Front Overhang (m)	0.69	3.04	1.64	0.70	0.42
6	Rear Overhang (m)	0.76	5.54	2.86	0.52	0.18
7	Ground Clearance (m)	0.08	0.34	0.22	0.05	0.21
8	Curb Weight - Front (kN)	14.02	46.06	30.14	8.54	0.28
9	Curb Weight - Rear (kN)	19.58	91.31	51.66	20.26	0.39
10	Curb Weight - Total (kN)	34.26	130.16	81.80	27.03	0.33
11	Seated Load Weight - Front (kN)	14.15	57.32	35.03	11.27	0.32
12	Seated Load Weight - Rear (kN)	24.59	111.25	67.37	21.98	0.33
13	Seated Load Weight - Total (kN)	41.16	158.24	102.35	31.78	0.31
14	Gross Vehicle Weight - Front (kN)	14.02	64.97	38.78	14.13	0.36
15	Gross Vehicle Weight - Rear (kN)	24.59	118.28	73.94	24.72	0.33
16	Gross Vehicle Weight - Total (kN)	41.61	192.95	112.79	38.01	0.34
17	Axle Ratio	2.92	6.57	4.43	0.71	0.16
18	Engine Power (kW)	123.1	238.7	164.6	25.91	0.16
19	Engine Displacement (cc)	5883	10831	7134	1311	0.18
20	Wheel Diameter (m)	0.41	0.57	0.53	0.06	0.11
21	Tire Diameter (m)	0.71	1.07	0.89	0.11	0.13
22	Durability Mileage (km)	4022	24701	12781	5762	0.45
23	Other Mileage (km)	1344	4626	3665	755	0.21

Table 3.5: Output variable - PTI reliability model

Sr. No.	Input	Min.	Max.	Mean	Std. Dev.	Std. Dev. /Mean
1	MDBF (km)	99.2	2014.9	594.5	389.2	0.65

3.3.2 National Transit Database (NTD) Data

In order to evaluate the traffic transformation, *G*, in-use data from transit agencies were collected from NTD for reporting years 1997-2004. Since data pertaining to acceleration and pass-by noise performances were not available, only data on fuel economy and reliability were collected. At present, NTD reports fuel economy and reliability data on a transit agency level and not at a bus model level. Hence, data pertaining to those transit agencies that employ only one diesel bus model were used in this study. The years of manufacture could, however, vary even though the bus model was the same. The input data collected from NTD can be broadly classified into the following categories:

1. Fleet size: The active fleet size reported in the NTD was used for this purpose.
2. Operating Area Characteristics: This included city elevation in meters, service area size in square kilometers and service area population. City elevation was obtained from web-sites that report weather.
3. Characteristics of Bus Plying Route: Average operating speed and average miles run per bus per annum constitute this category head.
4. Vehicle condition: Average mileage which is a measure of past histories of the buses was used for this purpose.
5. Maintenance related parameters: This included total labor hours on vehicle maintenance, maintenance labor hours per bus, total number of

maintenance facilities (directly owned and leased) and percentage of spare buses available for service.

Average operating speed for the buses was calculated as follows:

$$Average\ Speed = \frac{Total\ actual\ vehicle\ revenue\ miles}{Total\ actual\ vehicle\ revenue\ hours} \quad \textbf{3.10}$$

The output data collected include fuel economy (called as NTD-FE) and mean distance between failures (called as NTD-MDBF). Since NTD only reports the total amount of diesel fuel used by revenue vehicles and not the amount of fuel used by such vehicles while in revenue service, NTD-FE was calculated as below

$$NTD\ FE = \frac{Total\ actual\ vehicle\ miles}{Volume\ of\ diesel\ used} \quad \textbf{3.11}$$

For transit agencies that were using only one diesel bus model but simultaneously used other bus models running on either gasoline or alternative fuels, the vehicle miles used for NTD-FE calculation was the mileage pertaining only to diesel vehicles as given in NTD's revenue vehicle inventory form. NTD-MDBF was calculated as follows

$$NTD\ MDBF = \frac{Total\ actual\ vehicle\ miles}{(Major\ failures + Minor\ failures)} \quad \textbf{3.12}$$

In all, 30 and 14 sets of data were collected for NTD fuel economy and NTD reliability respectively. A short summary of the collected data is given in Table **3.6**. For fuel economy, data were obtained for 7 input variables and one output (NTD-FE). These are listed in Tables **3.7** and **3.8**. For reliability, data was collected for a total of 11 inputs and one output (NTD-MDBF). Their salient characteristics are included in Tables **3.9** and **3.10**.

Table 3.6: Summary of NTD data

Description	Fuel Economy	Reliability
Years	1997-2004	1997-2004
Data Sets	30	14
Transit Agencies	13	7
States	9	4
Bus Models	13	7
Total buses	1075	218

Table 3.7: List of additional input variables - NTD fuel economy model

Sr. No.	Input	Min.	Max.	Mean	Std. Dev.	Std. Dev. /Mean
1	Active Fleet	2	79	35.8	32.6	0.41
2	City Elevation (m)	6.1	1235.9	357.6	505.9	0.41
3	Service Area (sq. km)	5.2	4944.8	552.0	910.4	0.18
4	Service Population	9520	4.48E6	7.64E5	1.18E6	0.26
5	Average Speed (km/hr)	8.24	39.68	21.39	6.29	0.16
6	Average Miles Run per bus per annum (km)	1559	81915	53817	23540	0.29
7	Average Mileage (km)	4827	9.95E5	4.62E5	3.07E5	0.31

Table 3.8: Output variable - NTD fuel economy model

Sr. No.	Input	Min.	Max.	Mean	Std. Dev.	Std. Dev. /Mean
1	NTD Fuel Economy (km/L)	0.93	3.03	1.75	0.47	0.16

Table 3.9: List of additional input variables - NTD reliability model

Sr. No.	Input	Min.	Max.	Mean	Std. Dev.	Std. Dev. /Mean
1	Active Fleet	3	50	12.7	19.5	1.54
2	City Elevation (m)	6.1	186.5	32.7	64.1	1.96
3	Service Area (sq. km)	5.2	4944.8	327.5	1357.7	4.14
4	Service Population	9520	4.48E6	1.12E6	1.73E6	1.54
5	Average Speed (km/hr)	8.24	39.68	21.18	10.44	0.47
6	Average Miles Run per bus per annum (km)	20456	80995	46969	22016	0.47
7	Average Mileage (km)	69187	8.99E5	3.64E5	3.25E5	0.89
8	Total Labor Hours (hrs)	324	21839	7735.2	8981.8	1.16
9	Labor Hours Per Bus (hrs)	54	832	450	304.4	0.68
10	Number of Maintenance Facilities	0	1	0.69	0.45	0.66
11	Percentage Bus Spares (%)	0	50	17.7	20.2	1.14

Table 3.10: Output variable - NTD reliability model

Sr. No.	Input	Min.	Max.	Mean	Std. Dev.	Std. Dev. /Mean
1	NTD MDBF (km)	2400.3	73472.7	21273.3	22527.0	1.06

3.4 Summary

The mathematical approach used in this thesis consists of a two-stage implementation of a vehicle-traffic system. For modeling the first stage (vehicle transformation), data were collected from PTI test reports and other sources on four performance measures - fuel economy, acceleration, pass-by noise and reliability. The second stage consists of a traffic transformation. Data on fuel economy and reliability

were collected from the National Transit Database (NTD) for modeling this traffic transformation. Once the forward models have been obtained, model inversions need to be carried out to arrive at bus designs capable of achieving a desired performance. However, problems exist with such inversions.

Chapter 4

Model Implementation

4.1 Data Pre-processing

Kantardzic [52] observes that raw data are seldom the best for data analysis. The first step in any model generation process is to check the raw data for missing values, incorrectly recorded entities and anomalous or outlier values. Outliers are unusual data values that are not consistent with other observations. They normally result from measurement errors, recording errors and in some cases are natural but abnormal values. Since some modeling methods are very susceptible to outliers, it is important that such values be looked into carefully. Transformations may also be needed to produce more useful features (inputs) for data analysis. An example of such a transformation is normalization wherein the input is centered by subtracting the mean value and then the resulting value is divided by the standard deviation. This helps one make a direct comparison of the contribution of various inputs without taking into consideration their respective units of measurement, magnitude or relative accuracy of measurement.

One problem that analysts invariably face with regards to complex multi-dimensional design spaces is the difficulty in viewing all variables simultaneously due to the limitations of our three-dimensional world. Multi-dimensional data visualization methods alleviate this problem to some extent. Some commonly employed methods include scatter matrices, glyph plots, parallel co-ordinates and dimensional stacking. One

such software developed at the Applied Research Laboratory (ARL) at Penn State University is called the ARL Trade Space Visualizer (ATSV). The ATSV offers multi-dimensional visualizing techniques like glyph plots, histogram plots, parallel coordinate plots, scatter matrices, brushing and linked views [53]. In this study, histogram plots, scatter matrices and glyph plots were used to get a preliminary understanding of how the independent variables (inputs) are related to the dependent variable (output). Screenshots of ATSV program showing the histogram plots for the inputs and outputs, listed in Chapter 3, are given in Appendix A.

4.2 Input Selection

Input selection or feature selection is a crucial step in any function mapping process. Use of an unnecessarily large number of inputs (also referred to as attributes or features in literature) can result in the following disadvantages:

1) Increased expenditure in terms of computing time and resources
2) Decrease in predictive accuracy as irrelevant data may mislead the learning process and make it more complicated
3) Lack of simplicity in the final model leading to poor understanding
4) Failure to generate a model when the sample size is too small in relation to the number of inputs used

The last situation arises because the size of a data set yielding the same density of data points in an n-dimensional space increases exponentially with dimension [52]. For example, if ‘a’ is the number of points (samples) needed in 1-dimensional space to get a

desired density, then the number of points needed in an n-dimensional space to ensure similar density is a^n.

Proper selection of inputs involves a balance between two contradictory requirements. If the number of selected inputs is too low, then valuable information might be lost. On the contrary, if the number is too high, then, the noise due to irrelevant inputs might overshadow the information content in the relevant inputs. The marginal benefit resulting from the presence of an input in a given input set plays an important role. It should be noted that a given input might provide more information when present with other inputs than when it is considered by itself. Hence, a collection of best individual features may not necessarily constitute the best set of features. There exists a vast amount of literature on feature selection including books that specifically cover the topic [54,55,56].

Researchers have attempted feature selection through varied means such as statistical, geometrical, information theoretic measures and mathematical programming [54]. It is generally accepted that feature selection methods can be grouped into the following three classes [57]:

1) Embedded methods: those that embed the selection scheme within the basic induction algorithm
2) Filter methods: those that use feature selection to filter features passed to the induction algorithm
3) Wrapper methods: those that treat feature selection as a wrapper around the induction process

Embedded methods incorporate input selection as a part of the training process. Quinlan's ID3 and C4.5 and Breiman *et al.*'s CART that is based on decision tree are examples of such methods. Embedded methods are known to reach solutions quickly since they avoid re-running (re-training) of the model generation process for every input subset investigated [55]. However, while these methods work well in domains where there is little interaction among the relevant inputs, presence of interactions that lead a relevant input to look no more discriminating than an irrelevant one can cause significant problems.

Filter selection methods are independent of the induction algorithms that use their output and hence can be combined with any such algorithm. Kira and Rendell's RELIEF algorithm and Almuallim and Dietterich's FOCUS algorithm are examples of filter methods [57]. Principal Component Analysis (PCA) and Independent Component Analysis (ICA) comprise a class of filter methods that construct higher-order features from the original ones, order them in terms of the variances they explain and then select the best features. PCA generates linear combinations of features whose vectors are orthogonal in the original space while ICA insists that the new features be not only uncorrelated but also be statistically independent [58]. The difference between the two can be readily seen using a simple example. Suppose there are two variables, namely $x = \cos(z)$ and $y = \sin(z)$. The two are uncorrelated. However, this doesn't mean that information on y cannot be obtained from x since the sum of the squares of the two variables is 1. The main problem with PCA and ICA is that they generate combinations of the original inputs that have little physical meaning and are difficult to interpret.

Wrapper approach is a method of input selection that evaluates alternative input sets by running some induction algorithm on the training data and using the estimated accuracy of the algorithm as the metric. The main argument in favor of wrapper approach is that the induction method that will use the feature subset should provide a better estimate of accuracy than a separate measure that may have an entirely different inductive basis [57]. The major disadvantage of wrapper methods over filter methods is the former's computational cost which results from repeated calling of the induction algorithm for each input subset considered.

In this study, both filter and wrapper methods were used to select the relevant inputs. The two filter methods employed include correlation and the Information Theoretic Subset Selection (ITSS) method of Sridhar *et al.* [59]. These are explained in detail in Sub-sections 4.2.1 and 4.2.2. The wrapper approach used in the study was based on the N2PFA (Neural Network Pruning for Function Approximation) method proposed by Setiono *et al*. [60]. This method is explained in Sub-section 4.3.1.

4.2.1 Correlation Method

Correlation coefficient between two variables is a number between -1 and 1 which measures the degree to which the two variables are linearly related. It is defined as

$$R_{xy} = \frac{\sum_k (x_k - \bar{x})(y_k - \bar{y})}{\sqrt{\sum_k (x_k - \bar{x})^2 \sum_k (y_k - \bar{y})^2}} \qquad 4.1$$

where x and y are the two variables and $\bar{x}$ and $\bar{y}$ represent their mean values over k samples. In this study, as a first step, the correlation matrix was used to select those inputs that are least correlated with other inputs. The primary idea behind this approach was to select the inputs whose behavior could not be predicted by inclusion of other inputs. A cutoff value magnitude of 0.7 was chosen for the correlation coefficient. If the correlation coefficient between two inputs was below this cut-off value, then it was assumed that the two inputs are not correlated. The cut-off value of correlation coefficient was chosen as 0.7 because it implies that less than 50 % (since R^2 = 0.49) of the variations in the values of one input can be accounted for by a linear relationship with the second input. The main drawback of this approach of using correlation coefficients for selection of inputs is that the correlation coefficient works well only if the relationship that exists between two inputs is linear. The correlation coefficient matrices, for all inputs listed in Chapter 3 for different models, are given in Appendix B for reference.

4.2.2 Information Theoretic Subset Selection (ITSS) Method

The central idea behind ITSS is to use information theory to analyze the inter-dependence between inputs and outputs [59]. ITSS does not depend on the learning technique and is hence a filter method.

Shannon's information theory provides a means for quantifying the information content of any input vector **x**. Let **x** take on M discrete values $\mathbf{x_1}$, $\mathbf{x_2}$……$\mathbf{x_M}$. If N_i is the number of occurrences of the vector $\mathbf{x_i}$ in the data set and N is the total number of samples in the data set, then the probability that **x** takes a value $\mathbf{x_i}$ can be defined as

$$p_i = \frac{N_i}{N} \qquad \textbf{4.2}$$

The entropy or information presented by variable **x** can then be written as

$$H(\boldsymbol{x}) = -\sum_i p_i \ln(p_i) \qquad \textbf{4.3}$$

The joint entropy of two vectors **x** and **y** (output) can now be similarly defined as

$$H(\boldsymbol{x}, \boldsymbol{y}) = -\sum_{ij} p_{ij} \ln(p_{ij}) \qquad \textbf{4.4}$$

where p_{ij} is the probability that **x** will take on the value $\mathbf{x_i}$ and **y** will take on the value $\mathbf{y_j}$ simultaneously. The entropy of **y** given **x**, $H(\mathbf{y}|\mathbf{x})$, is a measure of the information in the vector **y** when **x** is known. It can be shown that

$$H(\boldsymbol{y} \mid \boldsymbol{x}) = H(\boldsymbol{x}, \boldsymbol{y}) - H(\boldsymbol{x}) \qquad \textbf{4.5}$$

Sridhar *et al*. then define an asymmetric dependency coefficient (ADC), $U(\mathbf{y}|\mathbf{x})$ that measures the dependency of **y** on **x**

$$U(\boldsymbol{y} \mid \boldsymbol{x}) = \frac{H(\boldsymbol{y}) - H(\boldsymbol{y} \mid \boldsymbol{x})}{H(\boldsymbol{y})} \qquad \textbf{4.6}$$

ADC measures the extent to which knowledge of **x** provides information about **y**. The numerator in Eq. **4.6** gives a measure of the amount of information in **y** that is known when **x** is known while the denominator denotes the total information content in **y**. Since the input variables in this study are continuous, the input domain was divided into a finite number of regions (called bins) within which $p(\mathbf{x})$ is assumed to be constant. By doing this, the methodology described above for discrete variables was made applicable to continuous variables. It is crucial not to use too many bins since random noise may be

considered as an important functional variation. Conversely, not using enough bins can result in a loss of accuracy.

The general methodology followed in ITSS is given below:

1) Calculate $U(\mathbf{y}|\mathbf{x})$
2) Generate a candidate input subset $\mathbf{x}_{sp}$ and determine $U(\mathbf{y}|\mathbf{x}_{sp})$
3) Check if the candidate subset is satisfactory using Eq. 4.7 where ε is an acceptable small loss of information in the input space with respect to predicting the output.

$$U(\boldsymbol{y} \mid \boldsymbol{x}_{sp}) - U(\boldsymbol{y} \mid \boldsymbol{x}) < \varepsilon \qquad 4.7$$

4) If candidate subset is satisfactory then stop, else go to step (2)

In this study, candidate subsets for step (2) were generated by forward selection process. The forward selection procedure generates a new candidate subset by adding one input variable at a time to the current subset. At each stage, the variable to be added is selected so that the new enlarged input vector maximizes $U(\mathbf{y}|\mathbf{x}_{sp})$. Input variable addition is terminated when Eq. 4.7 is satisfied.

4.3 Forward Model

In the context of this thesis, forward modeling refers to process of identifying the vehicle transformation, F, and the traffic transformation, G, as shown in Figure 3.1. Ordinary Regression and Decision (Regression) Tree are among the most commonly used methods for modeling the functional relationship between inputs and outputs. The primary reasons for their use include ease of modeling and ease in interpreting the results.

However, both methods have inherent deficiencies. Regression normally requires that the user define the form of the relationship before hand. This is particularly problematic when not much is known about the nature of the relationship itself. Standard multiple regression can only accurately estimate the relationship between dependent and independent variables if the relationship is linear in nature. If the relationship is nonlinear, the results of the regression analysis will under-estimate the true relationship. This under-estimation carries two risks: increase of a Type II error for that independent variable and in case of multiple regression, an increased risk of Type I errors (over-estimation) for other independent variables that share variance with that independent variable. Type I error or a "false positive" is the error of rejecting a null hypothesis that should have been accepted while a Type II error or a "false negative" is the error of accepting a null hypothesis that should have been rejected.

Decision trees (DT) do variable selection automatically and can be easily converted to a set of rules. They are also easy to understand. However, in some complex applications, typical decision trees can have lot of branches and too many nodes along one branch. In general, a decision tree generates axis-parallel hyperplanes to partition the data. This can result in very cumbersome trees for complex problems wherein oblique hyperplanes (involving linear combinations of inputs) are needed [**61**]. Another problem associated with classical decision tree algorithms is that the splitting tests towards the leaves (bottom of the tree) are selected using fewer instances (samples) than splitting tests toward the top of the tree [**62**].

In this study, Artificial Neural Network (ANN) was selected for forward modeling. The motivation for ANN is the complex but efficient functioning of the human

brain and its ability to learn from examples. Human brain consists of a large number (10^{11}) of highly interconnected elements called neurons. It is astonishing to note that even though biological neurons are slow (10^{-3} s) when compared to electrical circuits (10^{-9} s), the brain is still able to perform many tasks much faster than a computer due to its massive parallel structure. Each biological neuron has 3 principal components: cell body, axon and dendrites as shown in Figure **4.1** [**63**]. The point of contact between an axon of one neuron and the dendrite of another neuron is called synapse. The arrangement of neurons and the strength of synapses determine the functioning of a biological neural network.

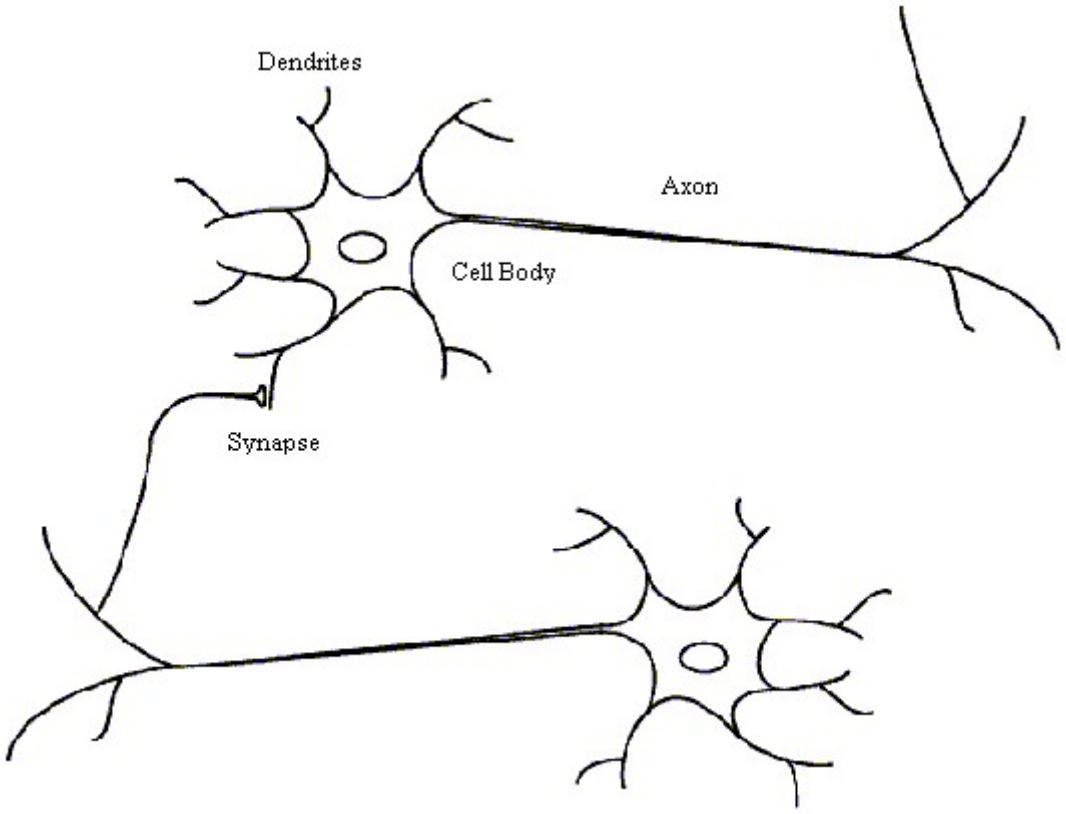

Figure **4.1**: Schematic diagram of biological neurons.

ANN is not as complex as a biological neural network in structure but still bears two close similarities, namely, building blocks of both networks are simple computational devices and both are highly interconnected structures with the strength of the interconnections determining how a network functions. The "artificial" neurons of an ANN weight, sum and threshold incoming signals to produce a net input. This is further modified by a transfer function to get the neuron output. An ANN can have many layers of neurons. Information is stored within the strengths of the interconnections or weights and the thresholds/biases. Knowledge is acquired through a learning process (training algorithm) that modifies the synaptic weights of the network in an orderly fashion to attain a desired objective. During learning, the network is presented pairs of input/output data and an attempt is made to search for a global minimum on the performance function (usually mean square error) surface over the space of the network parameters or weight values. Once trained, the ANN can then be used to predict outputs from new input data that the model has not previously seen. Figure **4.2** depicts the basic structure of a feed forward back-propagation network which is the most commonly used form of ANN [**63**]. The name is derived from the fact that the inputs propagate forward while the errors (difference between target outputs and ANN outputs) propagate backwards from the output layer to the input layer.

The advantages of ANN particularly relevant to modeling complex relationships are:

1) A feed-forward type of ANN with a single hidden layer can approximate any given continuous function on any compact set with arbitrary precision

provided there are sufficient hidden neurons [64,65]. Hence it is considered as a universal approximator.

2) It does not require a priori knowledge with regards to the nature of the functional relationships between inputs and output.
3) It is robust to noise and is easy to implement.
4) It can be parallelized where rapid computation is critical.

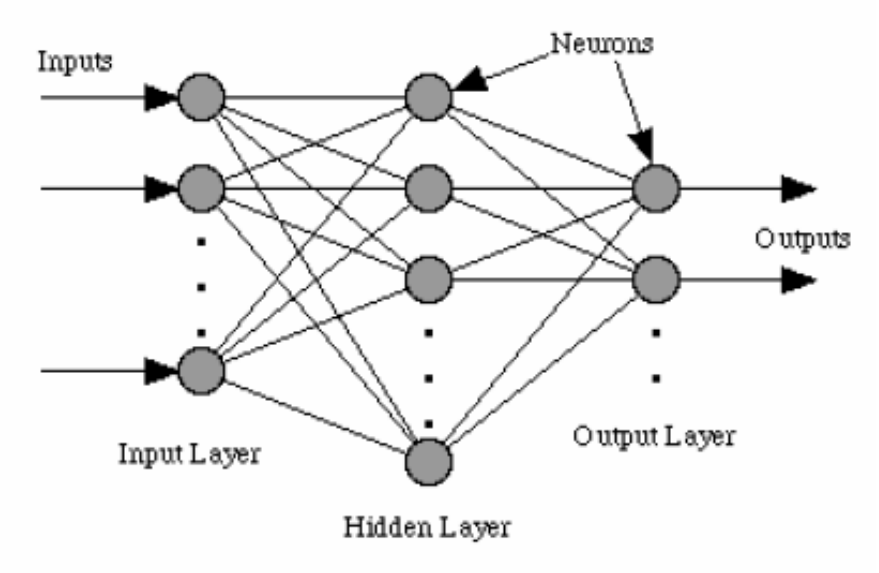

Figure 4.2: General structure of a feed-forward ANN.

For all the advantages they offer, ANNs have two serious detriments. Firstly, they are like black boxes and are not easy to comprehend. In particular, they afford an end user little or no insight into either the process by which they arrived at a given results or, in general, the totality of the "knowledge" embedded therein [66]. This is one of the reasons that they have historically been left out of consideration in the modeling of safety-critical applications. Secondly, there are no rigorous methods to find the exact

number of hidden neurons required for a particular problem. Recently, there has been a lot of effort put into extraction of comprehensible rules out of trained ANNs. A rule refers to the information stored in the ANN in the form of a mathematical or fuzzy logic expression. A comprehensive survey of such rule-generation studies is included in the papers by Tickle *et al.* [66] and Mitra and Hayashi [67]. With regards to the problem of finding the dimension of the hidden layer, there exist a lot of empirical rules that can serve as a starting point for ANN design [68]. However, their accuracies are debatable. Elisseeff and Paugam-Moisy [69] were able to analytically show that the number of hidden units, N_H, required for exactly learning all the real-valued examples is at most twice the number of examples, N_P, times the number of outputs N_S, divided by the sum of inputs and outputs $N_I + N_S$. However, they say that without a priori knowledge on the degree of redundancy in the learning set, exact learning is not the right goal in practical cases. Exact learning usually implies overfitting, especially if the examples are very noisy.

In this study, two ANN-based methods with built-in mechanisms for rule generation and determining the number of hidden neurons were employed. Thus the two main problems associated with ANN were alleviated. The two methods are described in the following two sub-sections.

4.3.1 Method-1: Based on Setiono's N2PFA and REFANN

In this method, a two layer (i.e., one hidden layer and one output layer) feed-forward backpropagation network was developed using Neural Network (NN) Toolbox

available in MATLAB. 'Tansig' (h(x) = tanh(x)) activation function was used for the hidden layer while the output layer had one linear neuron. The ANN was trained using 'Trainscg' algorithm that uses scaled conjugate gradient method. 'Trainlm', based on Levenberg-Marquardt algorithm, is much faster than 'Trainscg' but its memory requirement increases as the number of weights in the network increases since it needs to store the approximate Hessian matrix. On the other hand, 'Trainscg' performs well over a wide variety of problems, particularly for networks with a large number of weights [**70**]. Hence it was preferred in this method. Before modeling, both inputs and outputs were normalized by subtracting their mean values and then dividing the resulting values by the respective standard deviations. This was done to avoid an ill-conditioned error surface arising out of a vast difference in magnitude among the variables.

One of the problems that occur during neural network training is called overfitting. It refers to a case where the error on the training set is driven to a very small value, but when new data is presented to the network the error is large. The problem of overfitting can be mitigated to a great extent by:

a) Using a network that is just large enough to provide an adequate fit

b) Regularization

c) Early stopping

In this study, all three methods were simultaneously employed. The inputs and the output were first divided randomly into 3 subsets: the training set (80%), the cross-validation set (10%) and the test set (10%). Training set was used to generate the ANN model while the test set was used to check the accuracy of the developed model. The purpose of the validation set was to help decide the termination of the ANN training process so as to

prevent overfitting. This was accomplished by monitoring the error on the validation set during the training process. The validation error normally decreases during the initial phase of training, as does the training set error. However, when the network begins to overfit the data, the error on the validation set typically begins to rise. Training was stopped when the validation error increased for a pre-specified number of iterations.

For regularization, the performance function given by Setiono *et al.* [60] was used. Using the training data set, a network with *H* hidden units was trained, so as to minimize the sum of squared errors E(**w,v**) augmented with a penalty term $\phi(\mathbf{w},\mathbf{v})$. These are defined in Eq. 4.8 and Eq. 4.9

$$E(\mathbf{w},\mathbf{v}) = \sum_{P} (\tilde{y}_P - y_P)^2 + \phi(\mathbf{w},\mathbf{v}) \qquad \textbf{4.8}$$

$$\phi(w,v) = \varepsilon_1 \left(\sum_{i=1}^{H} \sum_{j=1}^{N} \frac{\beta w_{ij}^{\ 2}}{1+\beta w_{ij}^{\ 2}} + \sum_{i=1}^{H} \frac{\beta v_i^{\ 2}}{1+\beta v_i^{\ 2}} \right) + \varepsilon_2 \left(\sum_{i=1}^{H} \sum_{j=1}^{N} w_{ij}^{\ 2} + \sum_{i=1}^{H} v_i^{\ 2} \right) \qquad \textbf{4.9}$$

where ε_1, ε_2, β are positive penalty parameters, w_{ij} is the weight of the connection from input unit *j* to hidden unit *i* and v_i is the weight of the connection from the hidden unit *i* to the output unit. As per Setiono *et al.*, the penalty term $\phi(\mathbf{w},\mathbf{v})$ when minimized, pushes the weight values toward the origin of the weight space, and in practice results in many final weights taking values near or at zero. This enables removal of such network connections from the network without sacrificing network accuracy.

Once the network was trained, its hidden neurons and inputs were inspected as candidates for possible elimination by a network pruning algorithm. This network pruning algorithm is based on Setiono *et al.*'s N2PFA (Neural Network Pruning for

Function Approximation) algorithm [60]. N2PFA removes redundant and irrelevant units by computing and comparing the mean absolute error (MAE) of the network's prediction. In particular, MAEs on the training set and the validation set are used to determine when pruning should be terminated.

Setiono *et al.* also propose a method named REFANN (Rule Extraction from Function Approximating Neural Networks) for generating rules from a trained ANN that has already been pruned using N2PFA. REFANN is based on approximation of the Tansig (h(x) = tanh(x)) activation function by either a three-piece or a five-piece linear function. Figure 4.3 shows how tanh(x) can be approximated by a three-piece linear function for $x \in [0, x_m]$. If the same procedure is carried out for $x \in [0, -x_m]$ one will get a five piece approximation for domain since the two pieces at x=0 will be collinear due to symmetry.

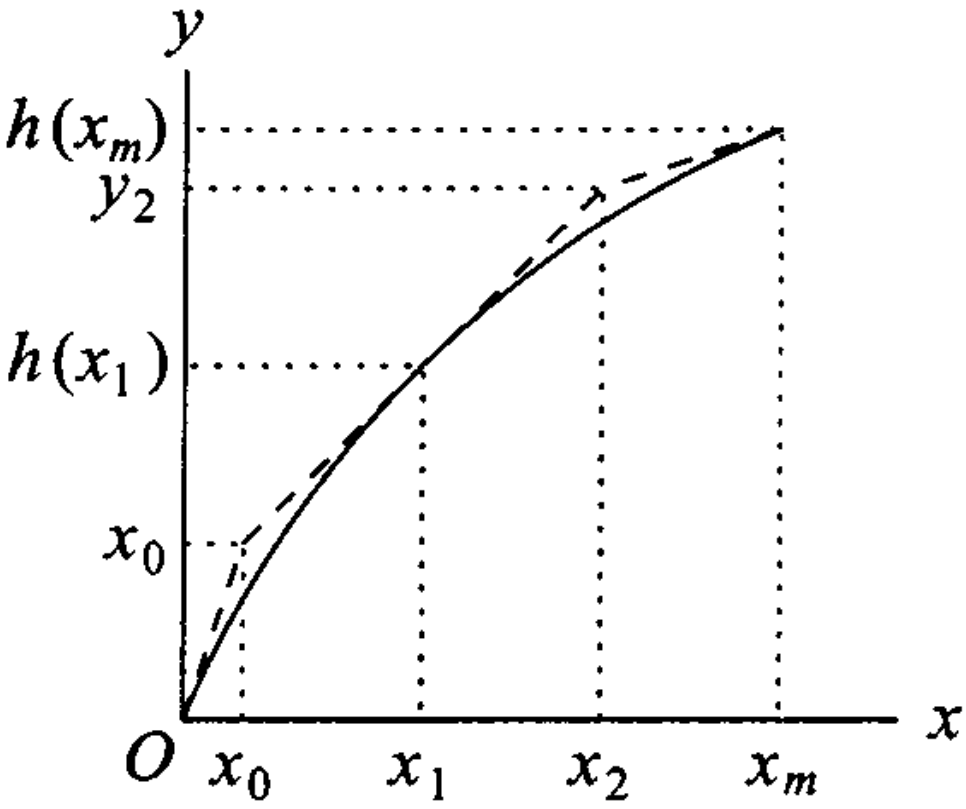

Figure 4.3: Approximation of tanh(x) function (solid curve) by 3-piece linear function.

In Figure 4.3, the three dashed lines are given by

$$L(x) = \begin{cases} x & 0 \le x \le x_0 \\ h'(x_1)(x - x_1) + h(x_1) & if \quad x_0 < x < x_2 \\ h'(x_m)(x - x_m) + h(x_m) & x \ge x_2 \end{cases} \qquad \textbf{4.10}$$

The underlying idea for this piece-wise linear approximation is to find the point x_1 that minimizes the total area A of the triangle and the two trapezoids. In Figure 4.3, area A is the area between the dashed lines and the x-axis. The Area, A, is given by

$$A = \frac{1}{2}[x_0^2 + (x_0 + y_2)(x_2 - x_0) + (y_2 + h(x_m))(x_m - x_2)] \qquad \textbf{4.11}$$

where x_0, x_2 and y_2 are expressed in terms of constant x_m and free parameter x_1 as

$$x_0 = \frac{h(x_1) - x_1 h'(x_1)}{1 - h'(x_1)} \quad \textbf{4.12}$$

$$x_2 = \frac{x_1 h'(x_1) - x_m h'(x_m) - h(x_1) + h(x_m)}{h'(x_1) - h'(x_m)} \quad \textbf{4.13}$$

$$y_2 = \frac{h'(x_1)h'(x_m)(x_1 - x_m) + h'(x_1)h(x_m) - h'(x_m)h(x_1)}{h'(x_1) - h'(x_m)} \quad \textbf{4.14}$$

The bisection method for one-dimensional optimization is employed to find the optimal value of x_1.

Setiono *et al*. claim that the extracted rules have better accuracies than multiple linear regression. However, there is one potential issue with this type of approach. The number of the generated rules (5^H for five-piece approximation) depends on the number of hidden neurons, *H*. For a complex ANN with many hidden neurons, this method could result in an unwieldy number of rules. Hence well-pruned networks are a key to fully utilizing the potential of REFANN.

4.3.2 Method-2: Based on Saito's RF5 Algorithm

RF5 (Rule extraction from Facts version 5) is a connectionist method proposed by Saito and Nakano [71] for numerical law discovery. It consists of a combination of 3 techniques:

1) Use of product unit networks for equation discovery
2) Employment of a second-order learning algorithm called BPQ for training
3) Adoption of Rissanen's Minimum Description Length (MDL) criterion for finding an adequate number of hidden neurons

Let **x** be an n-dimensional input vector and y be a target value corresponding to **x**. RF5 is capable of discovering a class of numeric laws that can be expressed as

$$y = c_0 + \sum_{i=1}^{H}\left(c_i \prod_{j=1}^{n} x_j^{w_{ij}} \right) \qquad \textbf{4.15}$$

where parameters c_0, c_i and w_{ij} are real numbers and H is an integer. Now if the range of inputs is positive, then Eq. **4.15** is equivalent to

$$y = c_0 + \sum_{i=1}^{H} c_i \, exp\left(\sum_{j=1}^{n} w_{ij} ln(x_j) \right) \qquad \textbf{4.16}$$

Here H, $\mathbf{w}_{ij}$ and c_i denote the number of hidden units (neurons), the weights between the input units j and hidden unit i, and the weights between the hidden units and the output unit respectively. Eq. **4.16** can be regarded as the feed-forward computation of a 3-layer (including input layer) neural network where the activation function of each hidden unit is exp(s) = e^s with no bias. The output layer has a single linear neuron that employs a bias, c_0. The 3-layer neural network realization is shown in Figure **4.4**.

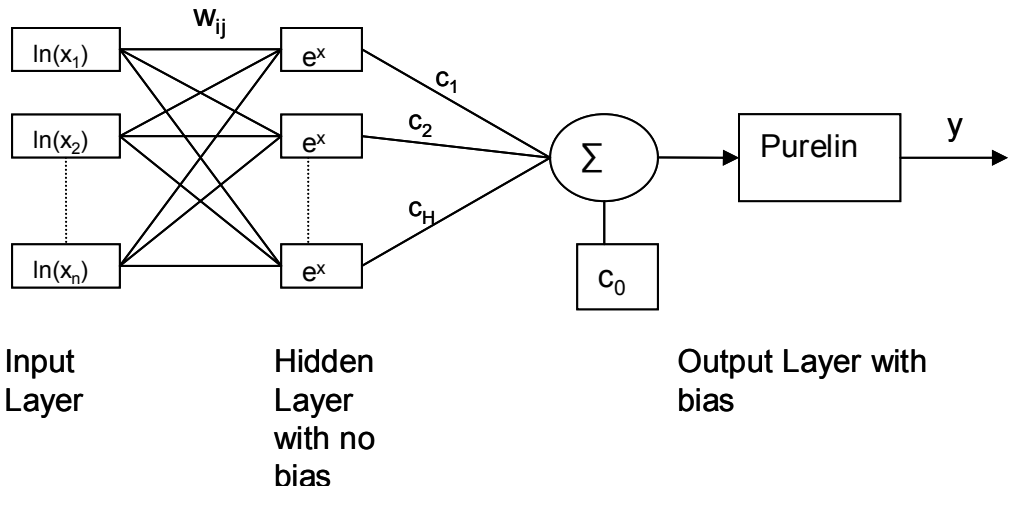

Figure **4.4**: Neural network realization of Saito's RF5 method.

RF5 employs a second-order learning algorithm called BPQ by adopting a quasi-Newton method as the basic framework. The descent direction is calculated on the basis of a partial BFGS (Broyden, Fletcher, Goldfarb and Shannon) update and a reasonably accurate step-length is efficiently calculated as the minimal point of a second-order approximation [71]. The problem of finding an adequate number of hidden units is formalized as a model selection problem of the maximum likelihood estimation problem [71]. MDL criterion is adopted for this purpose. The MDL fitness value is defined by

$$MDL = 0.5m\,log(MSE) + 0.5\widetilde{N}\,log(m) \qquad \textbf{4.17}$$

where m is the number of samples, MSE is the mean square error and $\widetilde{N}$ is the number of free parameters (weights and biases) in the ANN given by

$$\widetilde{N} = nH + H + 1 \qquad \textbf{4.18}$$

where n is the number of inputs and H is the number of hidden neurons. As is evident from Eq. **4.17**, the MDL criterion tries to select the neural network design that has a balance between accuracy of prediction (first term) and complexity of the network (second term).

The main advantage of RF5 is that most numerical law discovery methods are incapable of finding equations like Eq. **4.15** without preparing appropriate prototype functions before hand**.** Further, RF5 is resistant to presence of irrelevant variables and a small amount of noise. It is pertinent to note here that a two-layer (excluding input layer) neural network with exponential activation function in the hidden layer and a linear output layer can be shown (using Stone-Weierstrass theorem) to have the capability to

model any continuous function to any degree of accuracy on a bounded interval [64]. Weierstrass approximation theorem states that [72]

> *For any continuous f(x) on an interval J: $a \leq x \leq b$ and error bound $\beta > 0$, there is a polynomial $p_n(x)$ (of sufficiently high degree n) such that $| f(x) - p_n(x) | < \beta$ for all x on J.*

Polynomial functions comprise a small subset of the class of functions (as given in Eq. 4.15) that the RF5 algorithm can model. Hence, using RF5 algorithm, one can model any continuous function *f(x)* on an interval *J:* $a \leq x \leq b$ provided no constraint is placed on the number of hidden neurons or on the size of the weights.

One restriction with RF5 method is that the input vectors need to be restricted to non-zero positive values to prevent an output in the complex domain. Hence unlike Method-1 (N2PFA/REFANN), a different normalization procedure had to be used for Method-2 (RF5). Based on the recommendation by Oost [73], the inputs were normalized by their respective mean values so as to keep the normalized values positive. Outputs were only normalized if their magnitude was large (>10). RF5 was implemented with 'Trainlm' learning algorithm as suggested by Oost.

Since the results of RF5 method can be directly interpreted in an equation form, it is fairly straightforward to check its effectiveness. Before testing RF5 on the actual problem of predicting bus performance measures, RF5 was tested on two artificial problems:

1) Function with noisy inputs
2) Function with two missing inputs

The results from the two simulations are given in the following two sub-sections.

4.3.2.1 RF5 Function Mapping - Artificial Problem with Noisy Inputs

The first problem considered was function mapping under a situation involving noisy inputs. This is typical of most real life modeling problems. The actual function that was to be modeled is given in Eq. 4.19

$$f_1(\boldsymbol{x}) = 2.5x_1^{0.2}x_2^{-0.4}x_3^{-0.35}x_4^{1.8} \qquad 4.19$$

where **x** is the input vector comprising of variables x_1, x_2, x_3 and x_4. 60 samples were generated for all input variables using MATLAB's random number generating function called 'Rand'. The target output f_1 values were then calculated using these input values. For RF5 simulation, random noise was added to x_2 and x_4. Hence the resulting input vector used in RF5 had two pure and two noisy variables. Out of a total of 60 samples, 48 (80 percent) were used for ANN training and the remaining 12 were used for testing. Validation set was not used for this artificial problem. The ANN model was developed with only one hidden neuron and 'Trainlm' algorithm available in MATLAB. Upon convergence, RF5 gave the following simulated function which is very close in form to the original function

$$F_1(\boldsymbol{x}) = 2.529x_1^{0.20}x_2^{-0.39}x_3^{-0.33}x_4^{1.79} - 0.048 \qquad 4.20$$

The comparison plot between the actual output and the ANN output on the test set of 12 samples is given in Figure 4.5.

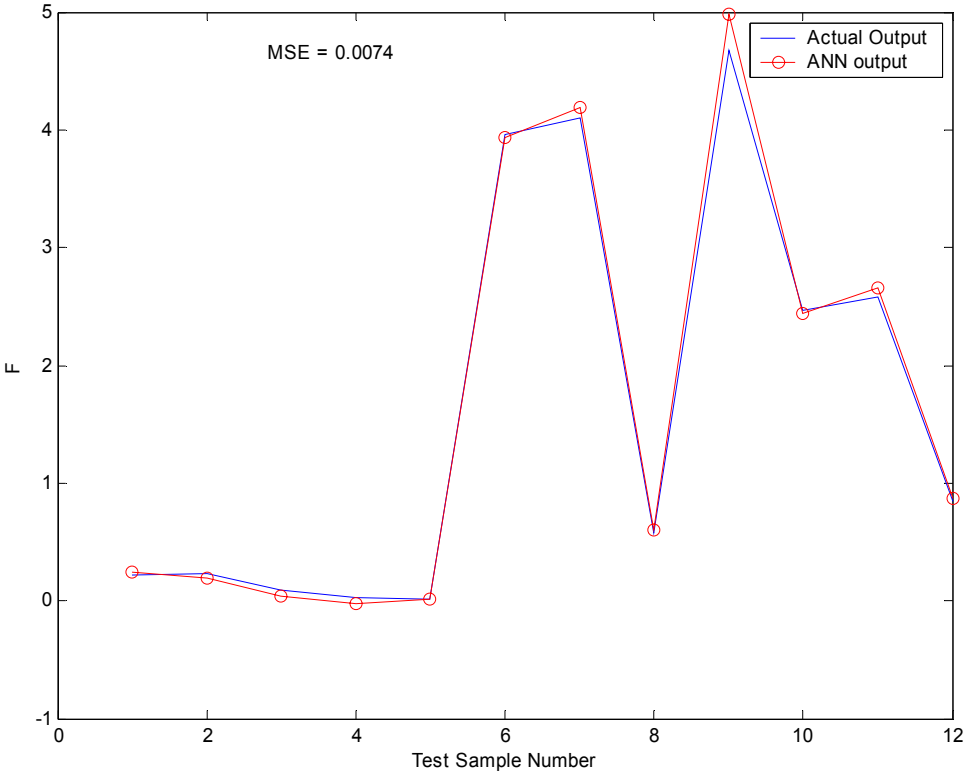

Figure 4.5: Comparison between actual and ANN outputs - noisy inputs case.

4.3.2.2 RF5 Function Mapping - Artificial Problem with Two Missing Inputs

The second problem tried out was that of mapping a function in the absence of two relevant inputs. It is felt that such a scenario might arise in this study since it might not always be possible to collect data pertaining to all inputs affecting a given performance measure. The 3-term function that was considered is given in Eq. 4.21.

$$f_2(\boldsymbol{x}) = 3.89 + 4.75x_1^{-0.37}x_2^{2.08}x_4x_5x_6 + 0.08x_3x_7 \qquad 4.21$$

Once again, 60 samples were generated for all variables using Rand function of MATLAB and the target values for ANN were calculated using Eq. **4.21**. Of the 60 samples, 48 were used for training. Only inputs x_1, x_2, x_4, x_5 and x_6 were given to RF5 and inputs x_3 and x_7 were not used. Using a network with two hidden neurons and 'Trainlm' training algorithm, RF5 came up with the following solution

$$F_2(\boldsymbol{x}) = 3.91 + 4.77x_1^{-0.37}x_2^{2.05}x_4^{1.00}x_5^{1.01}x_6^{0.99} - 0.01(.....) \qquad \textbf{4.22}$$

The comparison plot between the actual output and the ANN output on the test set is given in Figure **4.6**.

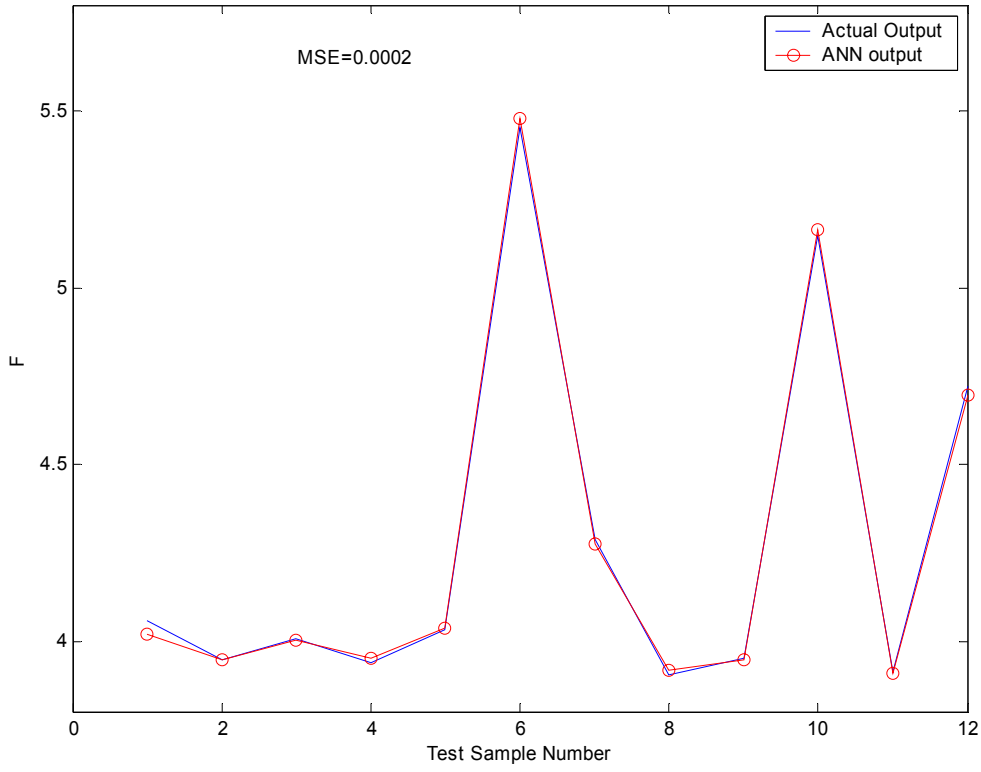

Figure **4.6**: Comparison between actual and ANN outputs - missing inputs case.

It is encouraging to note that the first two terms on the right hand sides of Eq. **4.21** and Eq. **4.22** are very similar and the third term on the right hand side of Eq. **4.22** is negligible. Hence, RF5 method seems robust to the absence of few of the relevant inputs. It may be noted that in the artificial problem considered here, the cumulative effect of x_3 and x_7 could be minimal due to the relatively small magnitude of the coefficient (0.08) in the third term.

4.4 Inverse Model

One of the goals of this study was to develop a method that can predict the input design parameters, of a diesel transit bus, needed to achieve a desired value of the output (say fuel economy). This requires the trained neural network (forward model) to be inverted. However, the inverse problem as given in Eq. **3.4** is an ill-posed problem since the inverse mapping is usually a one-to-many mapping. In general, the inverse problem is locally ill-posed in the sense that it has no unique solution and globally ill-posed because there are multiple solutions. One way of tackling this problem is to use nonlinear programming (NLP) techniques [74]. If we consider the problem of inverting the trained feed-forward network, $y = \boldsymbol{F(\theta)}$, the problem is to basically find an input vector $\boldsymbol{\theta}$ which yields a given output $\bar{y}$. To find various designated inversions for a given output, the inverse problem is formulated as below:

Minimize

$$P(\boldsymbol{\theta}) \qquad \textbf{4.23}$$

Subject to an equality constraint

$$F(W;\boldsymbol{\theta}) - \bar{y} = 0 \qquad \textbf{4.24}$$

And an inequality constraint

$$\boldsymbol{\rho} \leq \boldsymbol{\theta} \leq \boldsymbol{\gamma} \qquad \textbf{4.25}$$

where $P(\boldsymbol{\theta})$ is the objective function to be minimized, $\boldsymbol{\rho}$ and $\boldsymbol{\gamma}$ are the constant vectors representing the lower and upper bounds for the inputs, W is the weight matrix of the forward ANN and $\boldsymbol{\theta}$ is the input vector. The inequality constraint on the input vector is introduced to restrain the obtained inversions within a meaningful range of network inputs, i.e., design parameters that are expected to result in a transit bus.

The nature of the objective function determines the kind of inversions that are computed. In this study, the objective function was chosen as $P(\boldsymbol{\theta}) = \| \boldsymbol{\theta} - \boldsymbol{r} \|^2$, so as to result in an inversion that is nearest to the reference point $\mathbf{r}$. The reference point vector was sequentially selected as the input vector corresponding to each known bus. For example, one could use all buses in the training set used for forward ANN modeling and obtain an equal number of inversions. A bus manufacturer, on the other hand, could use the input vectors corresponding to the bus models currently in production and get the same number of inversions. After rejecting the solutions wherein the algorithm had not converged, the solution that was closest to a 'known' bus in terms of Euclidean distance was selected as the optimal solution. The Euclidean distance measure used in this study is in normalized input space and hence is not affected by the units in which the inputs are measured. It is felt that use of the Euclidean measure should result in a configuration that can give the desired performance (output) with only minimal changes being made to the

configuration of a 'previously known' bus. This feature is very desirable from the point of view of 'Mass Customization' of a standard product. Mass Customization refers to the ability of a manufacturer to customize an existing product for individual customers at a mass production price [75]. It is of particular significance in the automotive industry which is very dynamic and where the ability to customize can provide a manufacturer with a distinct competitive edge.

It should be noted that one could easily modify the objective function as per one's requirement to get other desired optimal solutions. An example of such a modified objective function is a weighted sum of inputs. The designer can select the weights based on the expected ease or difficulty in modifying different input variables.

4.5 Multi-objective Optimization

Real-world engineering design problems often involve concurrent optimization of several competing design objectives [76]. For example, with regards to this study, an improvement in acceleration performance might call for an increase in engine power which in turn could adversely affect fuel economy and noise. Multi-objective optimization (MOO) or Multi-criteria optimization (MCO) is concerned with minimization of a vector of objectives F(**x**) that can be subject to a number of constraints or bounds. Mathematically, it can be stated as

$$\begin{aligned} &\underset{x\in R^n}{Minimize} && F(x) && \\ &&& G_j(x) = 0 && j = 1,2....J \\ &Subject\ to && H_k(x) \le 0 && k = 1,2.....K \\ &&& x_l \le x \le x_u && \end{aligned} \qquad \textbf{4.26}$$

where **x** is design vector containing n components of design variables, F(**x**) is the objective function, G_j(**x**) is the equality constraint, H_k(**x**) is the inequality constraint, x_l is the lower bound and x_u is the upper bound. Since F(**x**) is a vector, if any of its components are competing, there is no unique solution to this problem. Instead, the concept of non-inferiority (also called as Pareto Optimality) must be used to characterize the objectives [77]. The definition of Pareto Optimal is given below [78]

> *Pareto Optimal: A point* $\boldsymbol{x}^* \in \boldsymbol{X}$*, is Pareto Optimal if and only if there does not exist another point,* $\boldsymbol{x} \in \boldsymbol{X}$*, such that* $F(\boldsymbol{x}) \le F(\boldsymbol{x}^*)$*, and* $F_i(\boldsymbol{x}) < F_i(\boldsymbol{x}^*)$ *for at least one function.*

Basically, it means that a non-inferior or Pareto solution is one in which an improvement in one objective requires a degradation of another.

The objective of MCO methods is to locate Pareto optima and from that generate a complete Pareto front. A large number of MCO methods have been developed till date and numerous ways of classifying the methods have been suggested as well [79]. Marler and Arora [78] give a comprehensive survey of multi-objective optimization methods used in engineering. Some prominent techniques include:

1) Weighted Sum Strategy
2) ε-Constraint Method
3) Goal Attainment Method

Brief descriptions of these three methods are given in subsequent sub-sections.

4.5.1 Weighted Sum Strategy

The weighted sum strategy converts the multi-objective problem of minimizing F(**x**) into a scalar problem by constructing a weighted sum of all the objectives.

$$U = \sum_{i-1}^{k} w_i F_i(x) \qquad 4.27$$

By perturbing the weights, w, each optimization process will produce a different Pareto optimum. The main problem with this method is that the weights do not necessarily correspond directly to the relative importance of the objectives or allow tradeoffs between the objectives to be expressed. Another serious drawback is that it cannot generate complete description of a Pareto front that is not convex [80].

4.5.2 ε-Constraint Method

This method involves minimizing the primary objective, F_p, and expressing the remaining objectives in the form of inequality constraints. Mathematically, this can be stated as

$$\begin{aligned} &\underset{x\in\Omega}{Minimize} && F_p(x) \\ &Subject\ to && F_i(x) \le \varepsilon_i \qquad i = 1,.....m \qquad i \neq p \end{aligned} \qquad 4.28$$

The ε-Constraint method can identify a number of non-inferior solutions on a non-convex boundary that are not obtainable using the weighted sum technique. The main drawback of this method is that, it is time consuming to make a suitable selection of ε_i to ensure a feasible solution especially as 'p' becomes larger. Another disadvantage arises from the

fact that the use of hard constraints is rarely adequate for expressing true design objectives [77].

4.5.3 Goal Attainment Method

The Goal Attainment method by Gembicki [81] provides a convenient intuitive interpretation of the design problem which can be solved using standard optimization procedures. It involves expressing a set of design goals $F = \{F_1^*, F_2^*, ..., F_m^*\}$ associated with a set of objectives $F = \{F_1(x), F_2(x), ..., F_m(x)\}$. It is assumed that the designer has sufficient intuitive understanding of the problem at hand to know the values of design goals to select [82]. The mathematical formulation for Goal Attainment method is

$$\begin{aligned} &\underset{\gamma\in\Re,\, x\in\Omega}{Minimize} && \gamma \\ &Subject\ to && F_i(x) - w_i\gamma \le F_i^* \qquad i = 1,.....m \end{aligned} \tag{4.29}$$

The term $w_i\gamma$ introduces an element of slackness into the problem which otherwise imposes that the goals be rigidly met. It is related to the degree of under or over attainment of the goal F_i^* with w_i being a weighting coefficient. This enables the designer to express a measure of the relative tradeoffs between the objectives. If one wishes to incorporate hard constraints into the design, one can set the relevant weighting factor to zero.

In this study, the Goal Attainment method was used to generate inversions (bus designs) of two forward ANN models corresponding to two performance measures. By

using this procedure one can get a bus design that can satisfy more than one competing goal to a pre-selected degree of accuracy (corresponding to over or under attainment).

4.6 Summary

Input selection is crucial to arrive at models that are accurate and simple. In this study, a two-stage input selection procedure based on input correlation and Information Theoretic Subset Selection (ITSS) has been proposed. Two ANN-based forward modeling methods, namely REFANN/N2PFA and RF5 were also introduced. N2PFA has its own pruning process for both hidden neurons and inputs. Both methods have an in-built way of arriving at the number of hidden neurons and their solutions can be expressed in a functional form. Hence, the two methods alleviate the black-box nature of neural networks. Non-linear programming has been suggested for obtaining model inversions. For multi-objective optimization, Gembicki's Goal Attainment method that can express a measure of relative tradeoffs between objectives has been used.

Chapter 5

Results and Discussion

This chapter presents the results obtained using the two ANN-based methods described in Chapter 4. In Method-1, inputs are selected using correlation and then a neural network model is developed using Setiono's N2PFA and REFANN algorithms. Sridhar's ITSS method of input selection is not used in this case as N2PFA has its own input pruning procedure. On the other hand, Method-2 utilizes a two stage input selection procedure based on correlation and ITSS. The selected inputs are then used in conjunction with Saito's RF5 algorithm for generating an ANN model that can be easily interpreted as an equation. A brief comparison of Methods-1 and 2 is given in Table 5.1.

Table 5.1: Comparison between the two ANN-based methods

	Method-1	**Method-2**
Input Selection	Correlation + Input Pruning	Correlation + ITSS
Neural Network Method	Setiono *et al.*'s N2PFA/REFANN	Saito and Nakano's RF5
ANN Configuration	Hidden Layer: Tansig Output Layer: Linear	Hidden Layer: Exponential Output Layer: Linear
Data Split	Training: 80% Validation: 10% Test: 10%	Training: 80% Validation: 10% Test: 10%
Data Normalization	MATLAB's Prestd	With mean values
Training Algorithm	Scaled Conjugate Gradient (Trainscg)	Levenberg-Marquardt (Trainlm)
Input Ranking	Based on input pruning	Based on magnitude of exponents
Type of rules generated	Linear combinations of input variables	Sum of product units
Number of rules	3^H or 5^H (H-Number of hidden neurons)	1

Results are presented for four bus performance measures - fuel economy, acceleration, pass-by noise and reliability. While PTI (test track) data were available for all four performance measures, NTD (transit) data were available only for fuel economy and reliability. Hence, only NTD fuel economy and reliability models are presented. With reference to Figure **3.1**, PTI models correspond to vehicle system transformation, F and NTD models correspond to traffic system transformation, G.

Section **5.2** includes results from the inverse model described in Section **4.4**. Results are presented for both one-stage (only F^{-1}) and two-stage (both F^{-1} and G^{-1}) inversions. Section **5.3** presents sample results from a two-objective optimization problem. Gembicki's Goal Attainment method, described in Sub-section **4.5.3**, was used to arrive at a bus design that can simultaneously achieve the two desired objectives - one for fuel economy and one for acceleration. The two goals were selected as they are expected to place contradictory demands on bus design parameters such as engine power. Section **5.4** compares the results obtained using Method-1 and Method-2 with those from two commonly used methods in the literature, namely linear regression and decision (regression) tree, and shows the effectiveness of the methods used in this study. Section **5.5** discusses the effect of linearization of 'Tansig' activation function under the REFANN procedure of Method-1. A sample comparison is also made between the performance of the pruned ANN and the linearized output of REFANN.

5.1 Forward Modeling

5.1.1 PTI Fuel Economy

As mentioned in Sub-section 3.3.1, PTI fuel economy data on CBD, ART and COM cycles were collected for a total of 111 two-axle diesel buses ranging from model years 1990 - 2004. These data were divided into 3 sets - training set (89 buses), validation set (11 buses) and test set (11 buses) - corresponding to a split of approximately 80%, 10% and 10%. The correlation coefficient matrix for all 21 inputs (listed in Table 3.1) in the PTI fuel economy model is given in Appendix B. Using a threshold value of 0.7 for the correlation coefficient, the number of inputs was reduced from 21 to 8. The selected inputs include width (W), height (H), rear overhang (RO), ground clearance (GC), seated load weight - total (SLW-T), axle ratio (AR), engine power (P) and engine displacement (D). The correlation matrix for these 8 inputs is given in Table 5.2. Since inputs (8) to (16), in Table 3.1, pertaining to vehicle weights are highly correlated, SLW-T was selected as fuel economy tests at PTI are carried out at SLW. Width has a correlation coefficient with SLW-T that is slightly greater than the threshold value of 0.7 but it was retained as it is not highly correlated with any of the other inputs that were selected.

Table 5.2: Correlation coefficient matrix for inputs - PTI fuel economy model

	W	H	RO	GC	SLW-T	AR	P	D
W	1.00	0.24	0.24	-0.34	0.72	0.32	0.53	0.42
H	0.24	1.00	0.46	0.28	0.31	0.14	0.05	-0.10
RO	0.24	0.46	1.00	0.23	0.32	0.11	0.23	-0.02
GC	-0.34	0.28	0.23	1.00	-0.15	-0.05	-0.10	-0.19
SLW-T	0.72	0.31	0.32	-0.15	1.00	0.41	0.63	0.57
AR	0.32	0.14	0.11	-0.05	0.41	1.00	0.42	0.20
P	0.53	0.05	0.23	-0.10	0.63	0.42	1.00	0.61
D	0.42	-0.10	-0.02	-0.19	0.57	0.20	0.61	1.00

In the second stage of input selection, the ITSS method was used to further reduce the number of inputs. As mentioned earlier, the ITSS method of input selection was used only with RF5 method and not with NP2FA/REFANN method. In this study, the value of ε in Eq. 4.7 was taken as 0.01. Since the number of discrete bins influences the number of selected inputs, it was varied from 5 to 20. The selected inputs in each case are listed in Table 5.3. It is seen that the number of selected inputs reduces when the number of discrete bins is increased. This happens because, in general, an increase in the number of bins corresponds to more variation in the inputs which in turn means that fewer inputs would be sufficient to accurately predict a given output. It is to be noted that in some rare cases, depending on the bin limits, an increase in bins may actually result in more inputs being selected. For this study, the number of bins used was five.

Table 5.3: Effect of number of discrete bins on selected inputs

CBD

No. of Bins	Selected Inputs						
5	SLW-T	GC	P	AR	W	H	RO
10	SLW-T	H	AR	P			
15	SLW-T	H	GC	AR			
20	SLW-T	H	GC				

ART

No. of Bins	Selected Inputs					
5	SLW-T	P	GC	AR	H	RO
10	SLW-T	GC	H	AR	P	
15	SLW-T	GC	H	D		
20	SLW-T	H	GC			

COM

No. of Bins	Selected Inputs					
5	SLW-T	P	AR	GC	H	RO
10	SLW-T	GC	H	AR	P	
15	SLW-T	H	GC	D		
20	P	H	AR			

For Method-1 based on N2PFA/REFANN, the inputs selected by the correlation method, as given in Table 5.2, were directly used for simulation. All data were normalized before use in the ANN simulation model. Normalization, i.e., centering by subtracting the mean value and dividing by the standard deviation, is a standard procedure used in neural networks to avoid an ill-conditioned surface arising out of a vast difference in magnitude among the variables. The initial number of neurons in the hidden layer was maintained at 5. Once a network was trained, it was pruned for both hidden neurons and inputs. Simulation was repeated a large number of times to enhance the chances of the training algorithm (Trainscg in this case) finding the global minimum on the error surface. Finally, the pruned network with the least mean square error (MSE) on the test set of 11 buses was selected as the optimal solution.

Table 5.4 shows the results of 10 sample runs done for fuel economy on the CBD cycle. The nomenclature used in the table is as follows:

1) HLN: number of neurons in the hidden layer after pruning
2) MSE: Mean square error on the test set
3) R-train: Correlation coefficient between actual outputs and ANN outputs on the training set
4) R-test: Correlation coefficient between actual outputs and ANN outputs on the test set
5) Mean % Error: Mean absolute percentage error on test set
6) MAE: Mean absolute error on test set

Figure 5.1 shows the comparison plots between actual fuel economy and the fuel economy predicted by optimal ANN (from run 1) on the training and test sets. The top two subplots correspond to results on the training set (89 buses) while the bottom two subplots are for test set (11 buses). Subplots on the left have the same information as subplots on the right, except that in the left subplots the actual and predicted outputs are plotted against the number of buses while in the right subplots they are directly plotted against each other. In the right subplots, the solid line indicates the best linear fit on the predicted output values while the dotted line corresponds to the perfect prediction model, i.e., ANN output, A = Target output, T. Correlation coefficients between the target outputs and ANN outputs are also included.

Table 5.5 and Figure 5.2 show similar results obtained for fuel economy on the ART cycle. Results for fuel economy on the COM cycle are given in Table 5.6 and Figure 5.3.

Table 5.4: Results for fuel economy on the CBD cycle: Method-1 (N2PFA)

Run No.	HLN	MSE $(km/L)^2$	R-train	R-test	Mean % Error	MAE (km/L)	W	H	RO	GC	SLW-T	AR	P	D
1	4	0.0377	0.8434	0.9518	8.94	0.1552	X	X	X	X	X	X	X	X
2	3	0.0405	0.8706	0.9456	9.05	0.1655		X			X			
3	2	0.0572	0.8551	0.9175	10.29	0.1887	X	X	X	X	X	X	X	
4	4	0.0530	0.8703	0.9296	10.78	0.1892		X			X		X	
5	3	0.0410	0.8467	0.9554	10.56	0.1865	X	X			X	X	X	X
6	2	0.0418	0.8413	0.9584	8.81	0.1663		X	X		X	X	X	X
7	4	0.0579	0.8582	0.9210	12.30	0.2212	X	X	X		X	X		X
8	2	0.0671	0.8668	0.8970	11.89	0.2298	X	X	X	X	X	X	X	X
9	3	0.0432	0.8642	0.9491	8.89	0.1675	X	X	X		X	X	X	X
10	1	0.0557	0.8716	0.9285	11.17	0.2021		X			X			

X Indicates selected input

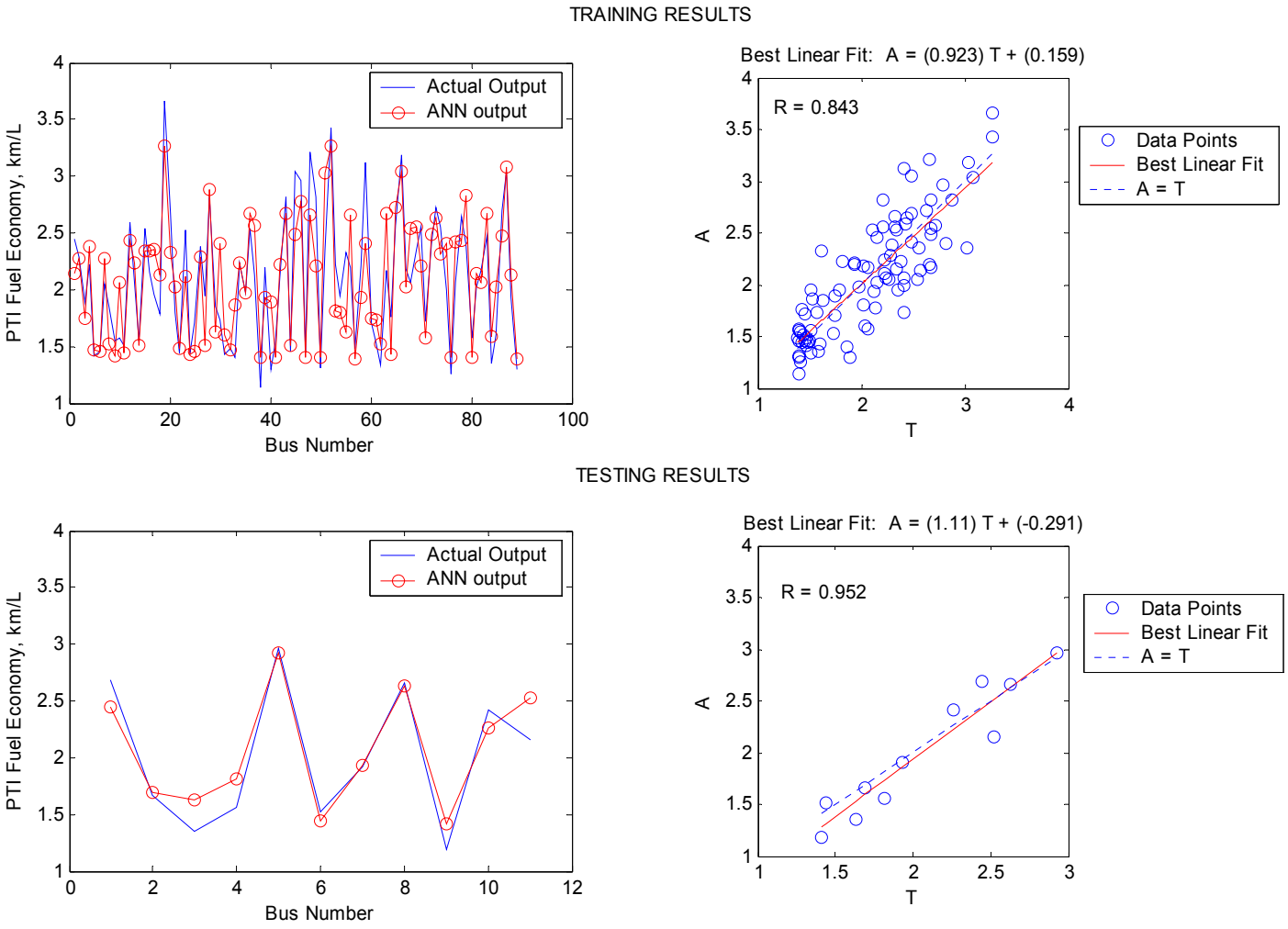

Figure **5.1**: Comparison plots for CBD fuel economy on training and test sets: Method-1 (N2PFA).

Table 5.5: Results for fuel economy on the ART cycle: Method-1 (N2PFA)

Run No.	HLN	MSE $(km/L)^2$	R-train	R-test	Mean % Error	MAE (km/L)	W	H	RO	GC	SLW-T	AR	P	D
1	4	0.0444	0.8651	0.9530	7.65	0.1630	X	X		X	X	X	X	X
2	1	0.0688	0.8453	0.9482	9.84	0.2102	X	X	X	X	X	X	X	X
3	4	0.0536	0.8753	0.9594	9.07	0.1812		X			X	X	X	
4	4	0.0809	0.7971	0.9302	10.35	0.2286	X	X			X			
5	3	0.0708	0.8920	0.9372	10.29	0.2186	X	X	X	X	X		X	X
6	4	0.0687	0.8965	0.9304	10.34	0.2237	X	X	X	X	X	X	X	X
7	4	0.0641	0.8892	0.9512	10.16	0.2161	X	X	X	X	X	X	X	X
8	2	0.0535	0.8815	0.9531	8.96	0.1911	X	X		X	X	X	X	X
9	4	0.0634	0.8838	0.9502	9.34	0.1932	X	X			X	X	X	
10	4	0.0739	0.8615	0.9358	10.38	0.2202	X	X	X	X	X	X	X	

X Indicates selected input

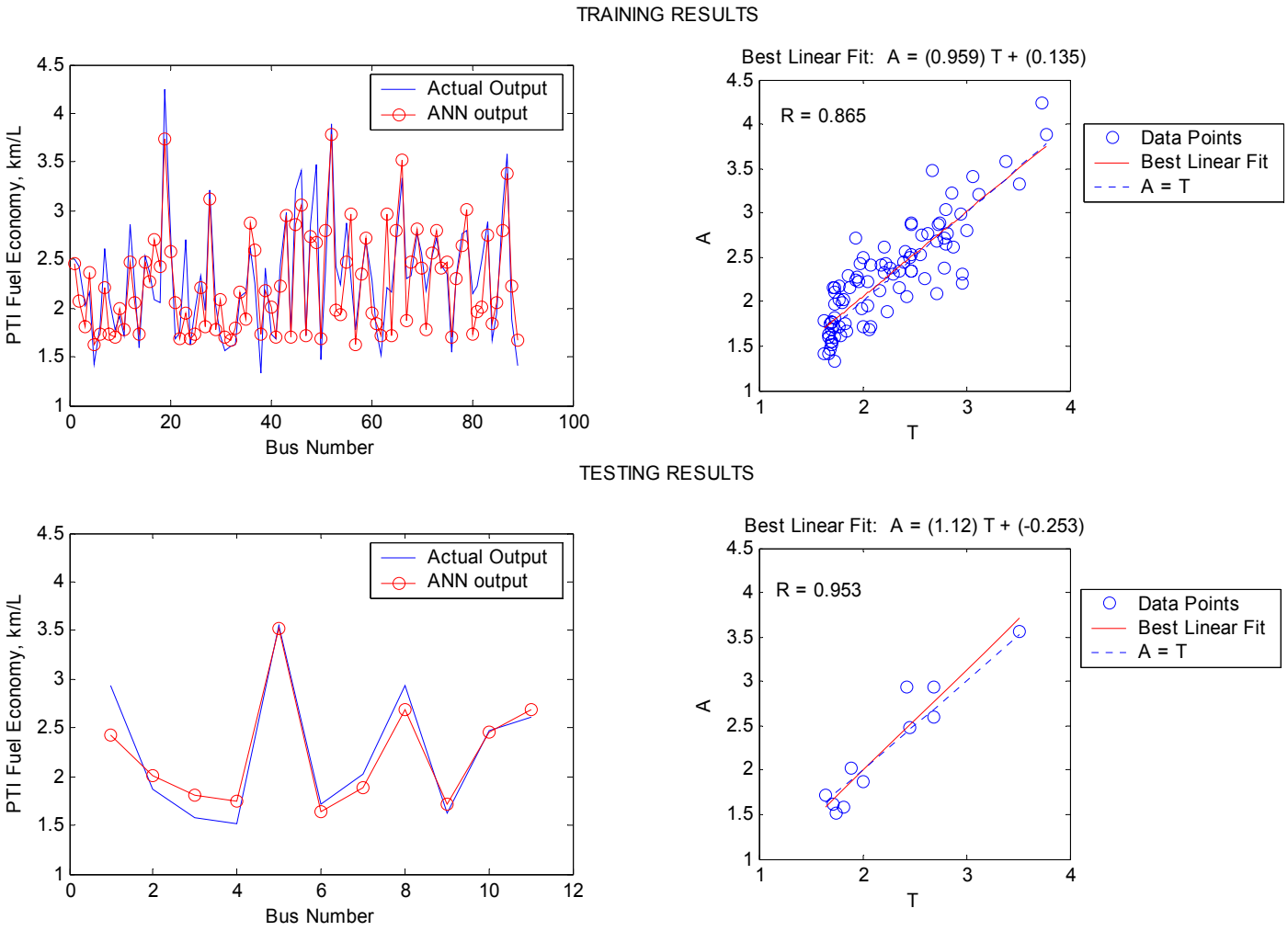

Figure **5.2**: Comparison plots for ART fuel economy on training and test sets: Method-1 (N2PFA).

Table 5.6: Results for fuel economy on the COM cycle: Method-1 (N2PFA)

Run No.	HLN	MSE $(km/L)^2$	R-train	R-test	Mean % Error	MAE (km/L)	W	H	RO	GC	SLW-T	AR	P	D
1	3	0.0631	0.8234	0.9727	5.68	0.2185		X		X	X	X	X	X
2	4	0.0447	0.7836	0.9802	4.43	0.1644	X	X	X	X	X	X	X	X
3	4	0.1201	0.8322	0.9601	7.07	0.2406		X			X		X	
4	1	0.0770	0.8085	0.9810	6.75	0.2536	X	X		X	X	X	X	X
5	1	0.0961	0.8113	0.9807	7.53	0.2745	X	X			X	X	X	X
6	4	0.1563	0.8341	0.9464	9.42	0.3233	X	X			X	X	X	
7	4	0.0831	0.8089	0.9612	6.89	0.2432	X	X	X	X	X	X	X	X
8	2	0.1141	0.8372	0.9608	7.93	0.2892	X	X	X	X	X	X	X	X
9	4	0.0953	0.7906	0.9847	5.91	0.2397	X	X	X	X	X	X	X	X
10	4	0.1181	0.8215	0.9432	7.23	0.2867	X	X		X	X	X	X	X

X Indicates selected input

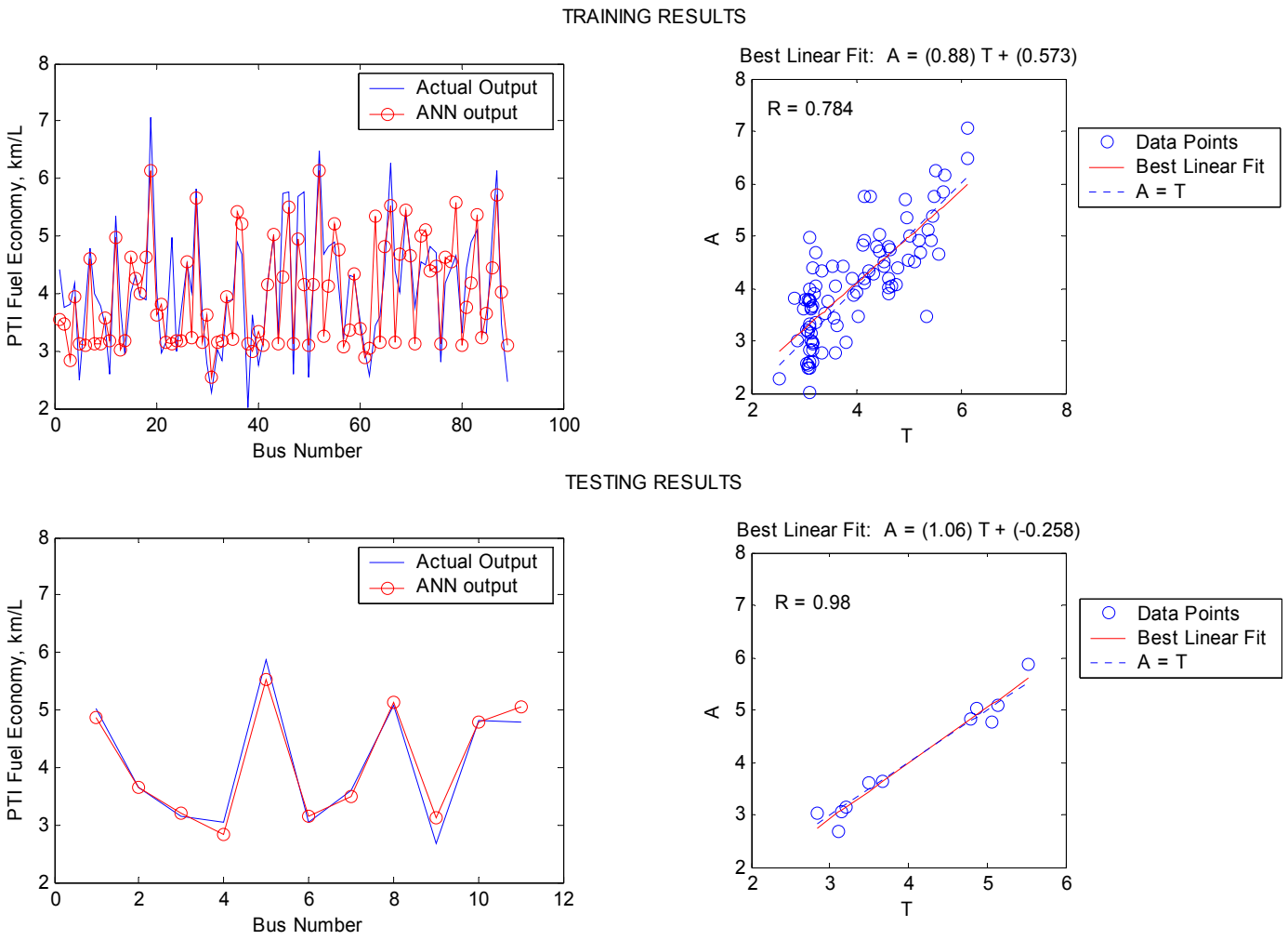

Figure **5.3**: Comparison plots for COM fuel economy on training and test sets: Method-1 (N2PFA).

In Method-2 (based on RF5), input selection consisted of two stages - one based on correlation and the other based on ITSS. The number of discrete bins used in ITSS was five. As seen from Table **5.3**, ITSS selected the same set of 6 inputs (although in different order) for ART and COM cycles. For CBD cycle, an additional input namely width was also selected. In order to make a one-to-one comparison of the effects of different input variables on fuel economies measured under the three driving cycles, all seven inputs were selected and ANN models were developed using RF5. As mentioned in Sub-section **4.3.2**, inputs were normalized with respect to their mean values before ANN modeling. Simulations were run by varying the number of hidden layer neurons from 1 to 5 and MDL criterion given in Eq. **4.17** was used to select the final configuration. It was found that in all three cases (CBD, ART and COM) the configuration with the least MDL value had only one hidden neuron. This means that the final equations as per Eq. **4.15** would consist of only two terms. The results obtained using the RF5 method for all three driving cycles are given in Table **5.7**. Based on the magnitude of the exponents, the relevant inputs for the three cycles in decreasing order are as below:

CBD: (i) SLW-T (ii) H (iii) P (iv) GC (v) AR (vi) RO (vii) W

ART: (i) H (ii) SLW-T (iii) W (iv) P (v) RO (vi) GC (vii) AR

COM: (i) H (ii) P (iii) SLW-T (iv) W (v) RO (vi) GC (vii) AR

It seems appealing to make a one-to-one comparison of the effects of the 7 input variables in the three driving cycles. In the case of a two-term functional expression for output, one can use the ratio of sensitivities of the output with various input variables as a means to understand the relative relevance of an input. A brief description of this

procedure is given in Appendix C. Also included in Table 5.7 are the ratio of the sensitivities of the output with respect to a given input and SLW-T.

It is interesting to note that for CBD cycle the RF5 method predicts that the fuel economy cannot be more that 6.64 km/L. While mathematically this means that the function obtained will not be able to predict correctly for buses having a higher fuel economy, in reality such a situation is highly unlikely since the maximum CBD fuel economy achieved by the 111 buses for which data were collected was only 3.66 km/L. However, in situations wherein the equation generated by RF5 method does not cover the entire range of the output, one can potentially neglect MDL criterion and go for more number of terms in the equation (i.e., more hidden neurons). Incorporation of more terms (some positive and some negative) in the equation ensures that one can model the whole range of the output. Comparison plots between actual fuel economy and the fuel economy predicted by the optimal ANN on the training and test sets for CBD, ART and COM driving cycles are given in Figures 5.4 - 5.6.

It would be helpful to see how results from Method-1 (N2PFA based) compare with those from Method-2 (RF5 based). For Method-1, a measure of the relevance of the inputs can be obtained by counting the number of times a given input has been rejected in the 10 sample simulation runs with low MSE values. One expects that an input of higher relevance would be pruned fewer number of times than an input with lesser relevance. For the CBD cycle, from Table 5.4 we see that the top two inputs as per Method-2, namely SLW-T and H, are never pruned in Method-1. Also, inputs such as W, RO, GC, and D that were ranked low by Method-2 are often pruned under Method-1.

Table 5.7: Results for fuel economy on the CBD, ART and COM cycles: Method-2 (RF5)

	c_0 (km/L)	c_i (km/L)	W	H	RO	GC	SLW-T	AR	P	MSE $(km/L)^2$	R-train	R-test	Mean % Error	MAE (km/L)
CBD	6.6401	-4.5944	-0.0022	0.2799	0.0022	-0.0319	0.2838	0.0085	0.0588	0.0673	0.8720	0.9092	13.05	0.2278
ART	0.0408	2.1472	-0.4108	-1.1050	0.1475	0.0812	-0.5041	0.0431	-0.2859	0.0802	0.8787	0.9274	11.47	0.2307
COM	0.6700	3.2227	-0.4058	-1.4155	0.2306	0.1865	-0.4729	-0.0334	-0.5795	0.1455	0.8325	0.9370	9.05	0.3381

Ratio of output sensitivities w.r.t. a given input and SLW-T

	W	H	RO	GC	SLW-T	AR	P
CBD	-0.0079	0.9864	0.0079	-0.1123	1.0000	0.0300	0.2073
ART	0.8149	2.1920	-0.2927	-0.1612	1.0000	-0.0854	0.5671
COM	0.8579	2.9930	-0.4876	-0.3943	1.0000	0.0706	1.2253

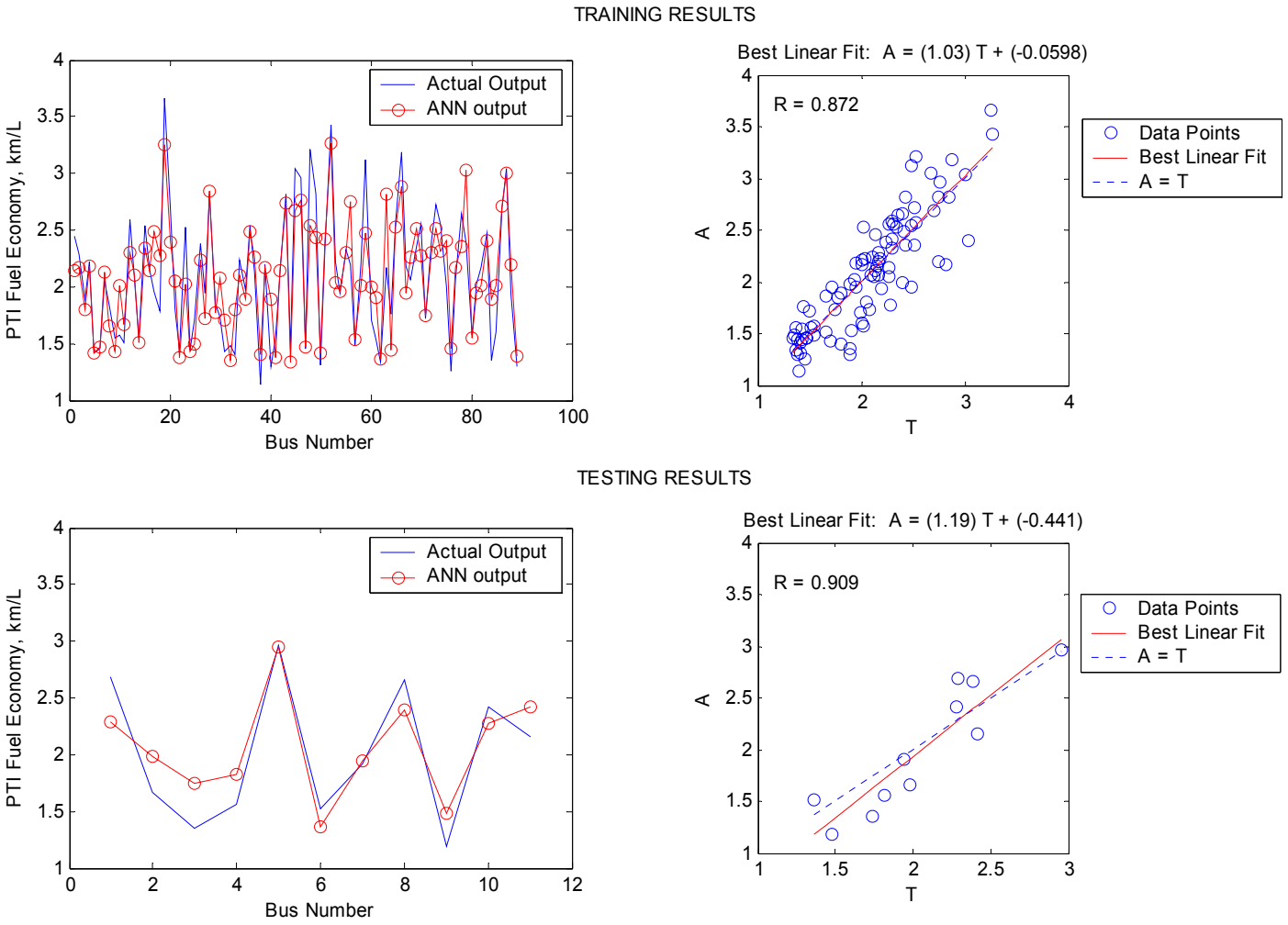

Figure **5.4**: Comparison plots for CBD fuel economy on training and test sets: Method-2 (RF5).

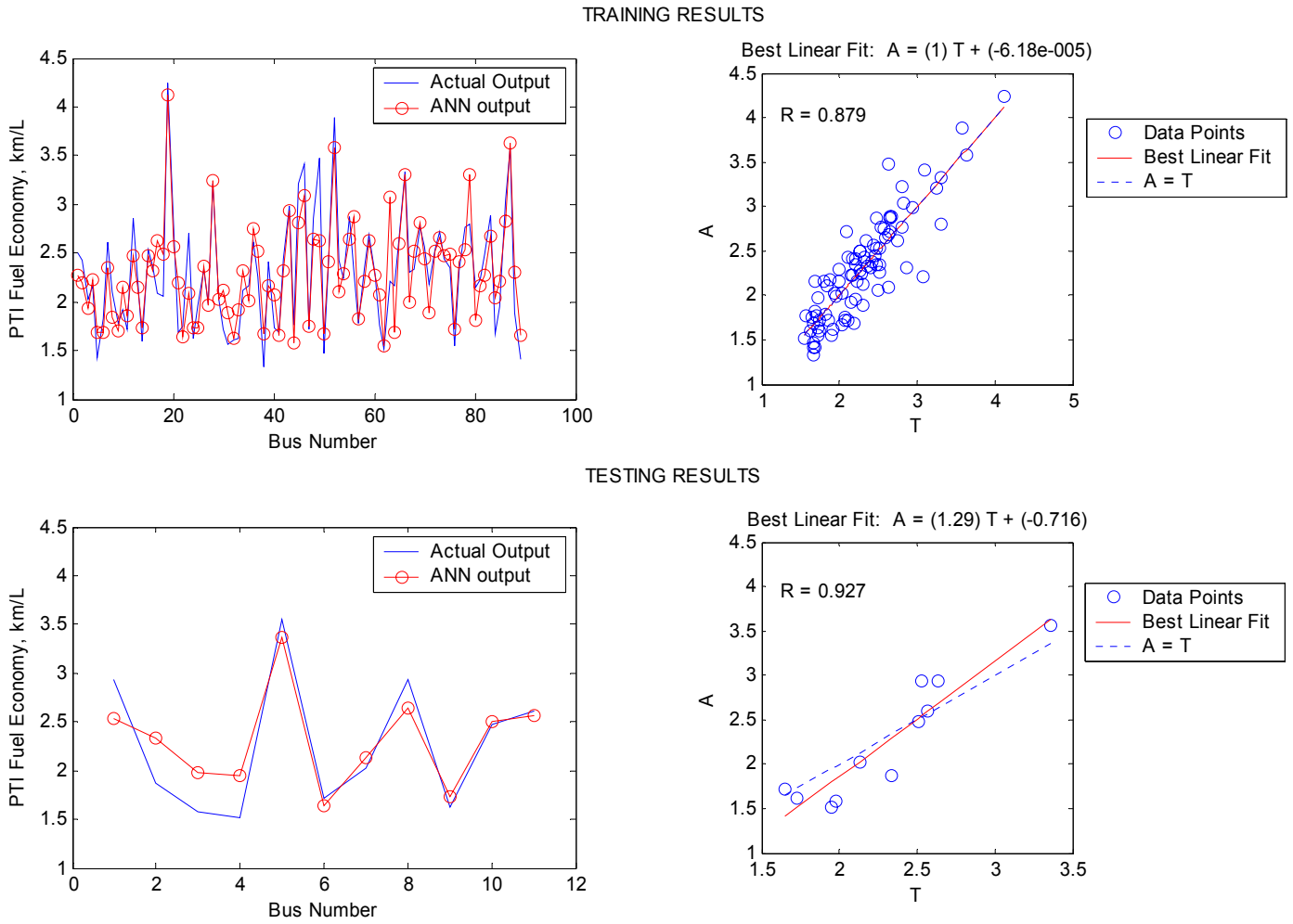

Figure **5.5**: Comparison plots for ART fuel economy on training and test sets: Method-2 (RF5).

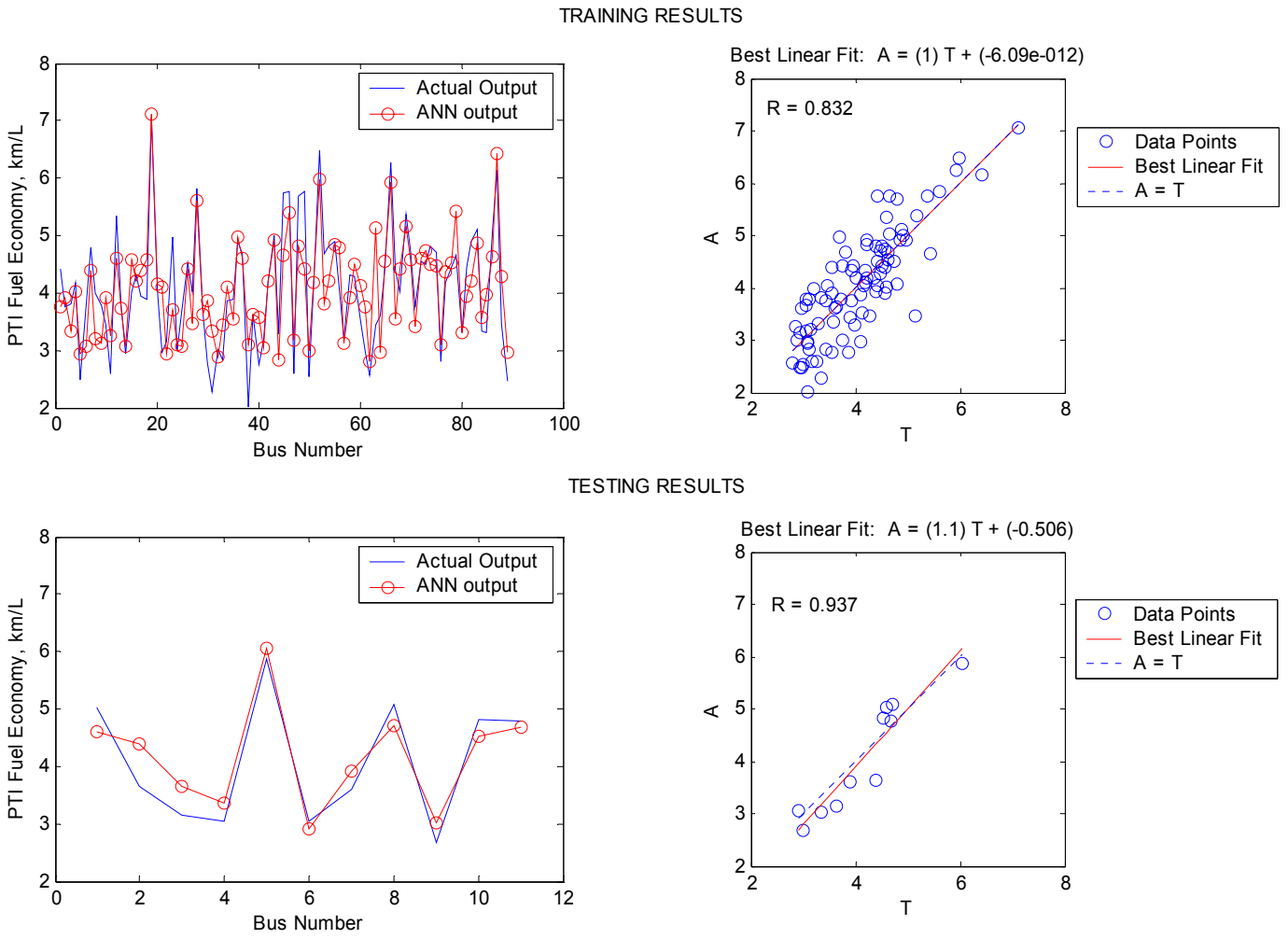

Figure **5.6**: Comparison plots for COM fuel economy on training and test sets: Method-2 (RF5).

A comparison of simulation results on ART cycle using the two methods show that the trends are similar. H and SLW-T are ranked as the top two inputs by Method-2 and these are never pruned out by Method-1. Inputs W and P are pruned only once and these are ranked 3 and 4 by Method-2. Further, RO, GC, D and AR retain their low rankings under both methods though their relative ranks are not the same. In COM cycle, input variables H, P and SLW-T are never pruned by Method-1 and these are ranked the highest by Method-2. Inputs W, RO, GC and D are rejected more often and this is commensurate with their low rankings under Method-2. However, the two methods seem to rate AR differently. While Method-1 seems to rate it as a relevant variable, Method-2 ranks it very low being just better than D that is rejected by ITSS.

From Table **5.7**, it is clear that an increase in vehicle weight will result in a decrease in fuel economy. This agrees well with engineering intuition and the results available in literature [**8**,**15**,**16**,**17**]. For transit buses, Zub [**16**] and Gajendran and Clark [**17**] found that the increase in vehicle weight causes a nearly linear decrease in fuel economy. The results obtained from Method-2 indicate that rate of decrease of fuel economy varies with vehicle weight. It is high at low vehicle weights and progressively decreases with increasing weight. If all input variables are kept constant at their mean values (i.e., normalized value of 1) and only SLW-T is allowed to vary, then partial differentiation of the fuel economy equations given by Table **5.7** yields the following equations for rate of change of fuel economy with SLW-T on CBD, ART and COM driving cycles.

$$\frac{\partial F.E.}{\partial SLW} = \begin{cases} -1.303(SLW)^{-0.716} & for\ CBD \\ -1.082(SLW)^{-1.504} & for\ ART \\ -1.524(SLW)^{-1.473} & for\ COM \end{cases} \qquad \textbf{5.1}$$

Figure **5.7** shows the plots for fuel economy versus normalized SLW-T on CBD, ART and COM driving cycles.

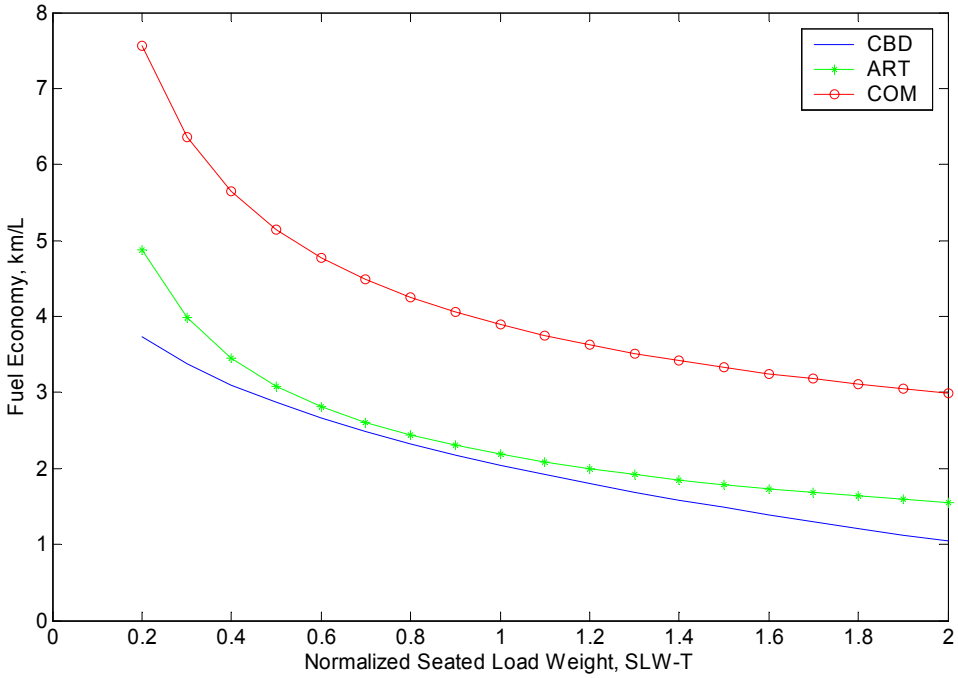

Figure **5.7**: Change of fuel economy with normalized SLW-T.

It is evident from Figure **5.7** that if one changes the normalized SLW-T from say 1.3 to 2, the behavior is approximately linear. In their tests, Zub [**16**] changed SLW-T for six buses by only 8.3% while Gajendran and Clark [**17**] modified the gross vehicle weight (GVW) by about 30%. Hence their results are accurate representations of the behavior over a small region. One cannot extend their results to a case wherein the weight of the vehicle is subjected to a very large change. In such cases, the results from this study

indicate that the behavior is clearly nonlinear. In this study, it was found that vehicle weight (inertia) has the biggest effect on CBD fuel economy while aerodynamic effects (i.e., effect of W and H) become very significant in high speed driving cycles such as ART and COM. This is consistent with the results obtained by Zub.

5.1.2 NTD Fuel Economy

NTD reports fuel usage data at a transit agency level and not at a model level. Hence, only data from those transit agencies that employed a single bus model could be used for analysis. In all, 30 sets of data from a total of 13 transit agencies were available. The data were split into training, validation and test sets as per the 80%, 10% and 10% distribution mentioned earlier. Of the three fuel economy values available, fuel economy on ART cycle was selected for use as an input (corresponding to **y** in Figure 3.1) into the traffic transformation, *G*, since it had the highest correlation values with the other two. In addition, the 7 inputs listed in Table 3.7 were used in input selection using the correlation method (refer Appendix B). Correlation rejected active fleet (ACT-FL) which refers to the number of buses available for operation in revenue service. The seven variables that were selected include city elevation (ELEV), service area (SERV-MIL), service population (SERV-POP), average operating speed (AVG-SP), average miles per bus per annum (MIL-PER-BUS), average mileage (AVG-MIL) and fuel economy in ART cycle (PTI-ART). In the second stage of input selection, the ITSS method was used to reduce this list to four inputs: AVG-SP, MIL-PER-BUS, AVG-MIL and PTI-ART. The results from 10 sample runs using the 7 inputs (selected by correlation) in Method-1 (N2PFA)

are given in Table **5.8**. Comparison plots of the actual NTD fuel economy and the fuel economy predicted by the optimal neural network (from run 6) on training and test sets are shown in Figure **5.8**.

Table 5.8: Results for NTD fuel economy: Method-1 (N2PFA)

Run N.	HLN	MSE $(km/L)^2$	R-train	R-test	Mean % Errr	MAE (km/L)	ELEV	SERV-MIL	SERV-POP	AVG-SP	MIL-PER-BUS	AVG-MIL	PTI-ART
1	3	0.0400	0.9022	0.9585	9.66	0.1755				X		X	X
2	3	0.0162	0.7643	0.9994	6.72	0.1110				X	X		X
3	2	0.0541	0.8330	0.9363	10.77	0.1955			X	X	X	X	X
4	3	0.0199	0.8669	0.9846	7.66	0.1343	X	X	X	X	X	X	X
5	2	0.0354	0.8299	0.9392	8.60	0.1534	X	X		X	X	X	
6	2	0.0115	0.9394	0.9405	4.72	0.0852		X		X	X	X	X
7	2	0.0507	0.8243	0.9561	11.23	0.2021		X	X	X		X	X
8	4	0.0341	0.9154	0.8639	8.14	0.1507		X	X	X	X	X	X
9	3	0.0338	0.8486	0.9967	9.50	0.1757					X	X	
10	3	0.0466	0.8258	0.9399	10.38	0.1837		X	X	X		X	X

X Indicates selected input

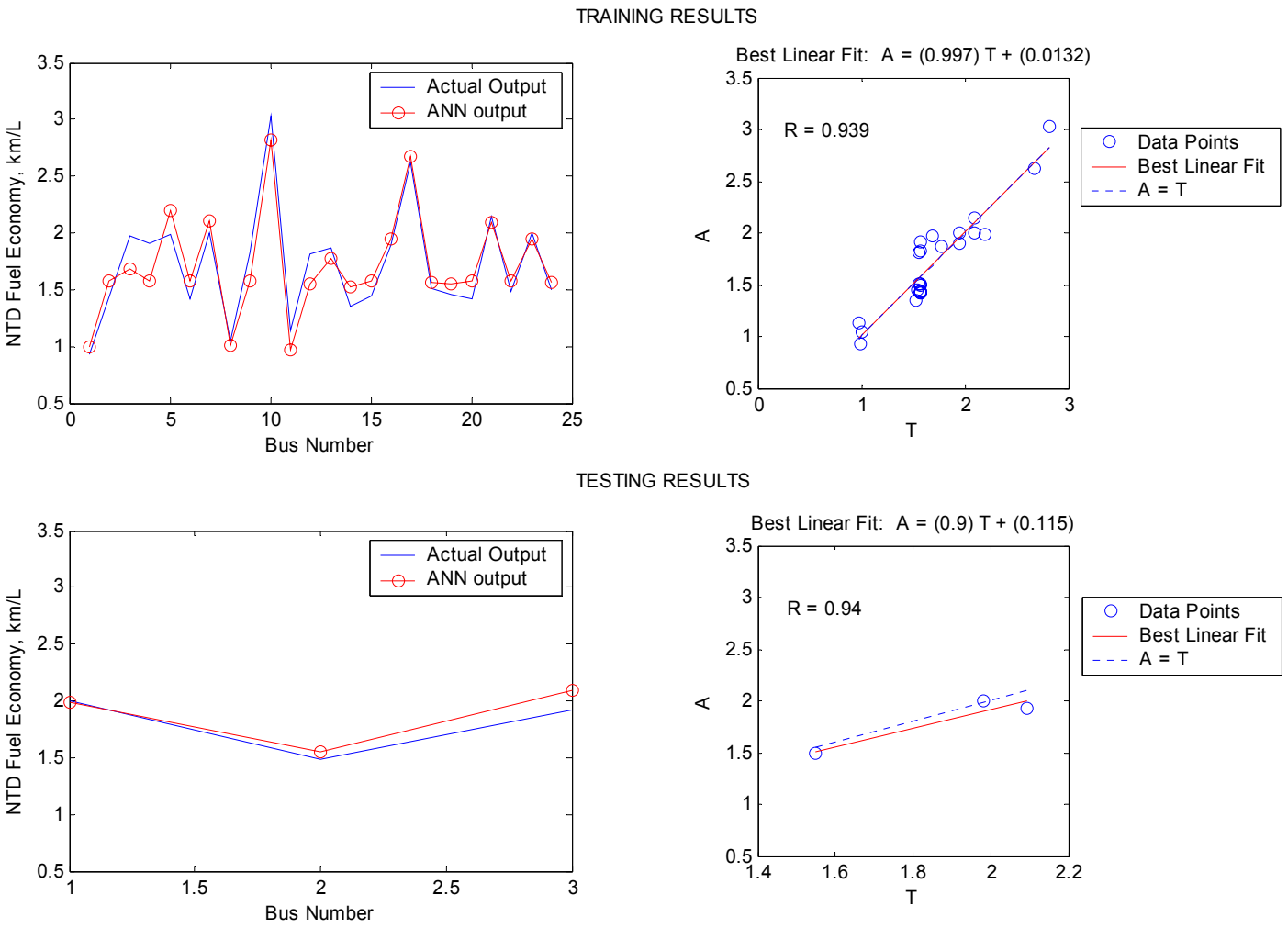

Figure **5.8**: Comparison plots for NTD fuel economy on training and test sets: Method-1 (N2PFA).

In Method-2 (RF5), the four input variables selected by ITSS were used. The optimal network required 5 hidden neurons. Simulation results are given in Table **5.9** and comparison plots of the actual NTD fuel economy and the fuel economy predicted by the ANN model are shown in Figure **5.9**. It is seen from Table **5.9** that the exponent corresponding to PTI-ART is the highest in magnitude in all 5 terms. This indicates that of the four inputs, PTI-ART is the most relevant variable in predicting NTD fuel economy and hence gives credibility to PTI testing. Unlike in Sub-section **5.1.1**, ranking of other variables is not that straightforward.

A comparison between the results obtained from Methods-1 and 2 shows that the variables rejected by ITSS such as ELEV, SERV-MIL and SERV-POP are rejected most often by Method-1. AVG-SP and AVG-MIL are pruned only once while PTI-ART is rejected twice in Method-1. This may seem at odds with the conclusion from Method-2. However, if we look at the two predominant terms (i.e., terms 1 and 3 that have the largest absolute c_i) we see that for AVG-SP and AVG-MIL the exponents are of the same sign while for ART this is not the case. Appendix D includes a calculation that shows that both terms are significant even though there is approximately a nine-order difference between the exponents for PTI-ART in the two terms. Hence, there appears to be a possibility that in some cases AVG-SP and AVG-MIL may be of more relevance. One such case would be a very high mileage bus that is plying well beyond its useful life. Under such circumstances, the age of the vehicle as measured by AVG-MIL may be more relevant than the fuel economy at PTI test track which is measured for new buses.

Unfortunately, it is difficult to compare the results from this section with those from other such studies. There appears to be a dearth of literature on comparison of

vehicle fuel economy under test track conditions with those from in-service conditions. It is relevant to note that the results on in-service transit bus fuel economy models presented here seem to make engineering sense. This section of the study used a fairly large dataset. In total, data pertaining to 13 bus models and 1075 buses from a total of 13 transit agencies were used. Data from the same transit agency but for different revenue years were also included. It is the understanding of the author that this study may be one of the first such large scale studies undertaken that not only compared fuel economies of the buses on a test track with those from in-traffic values (at transit agencies) but also generated mathematical prediction models.

Table 5.9: Results for NTD fuel economy: Method-2 (RF5)

c_0 (km/L)	c_i (km/L)	AVG-SP	MIL-PER-BUS	AVG-MIL	PTI-ART	MSE $(km/L)^2$	R-train	R-test	Mean % Error	MAE (km/L)
1.8842	-0.0584	-0.4452	-0.5280	0.6571	-9.0451	0.0068	0.9978	0.9900	4.05	0.0744
	0.0014	1.2781	0.6733	-1.8578	-18.6320					
	-0.0062	-9.7793	6.1662	4.8838	18.2700					
	0.0000	-7.5469	-0.0831	3.7800	-28.7470					
	0.0003	-0.6738	5.2733	-0.4178	27.4550					

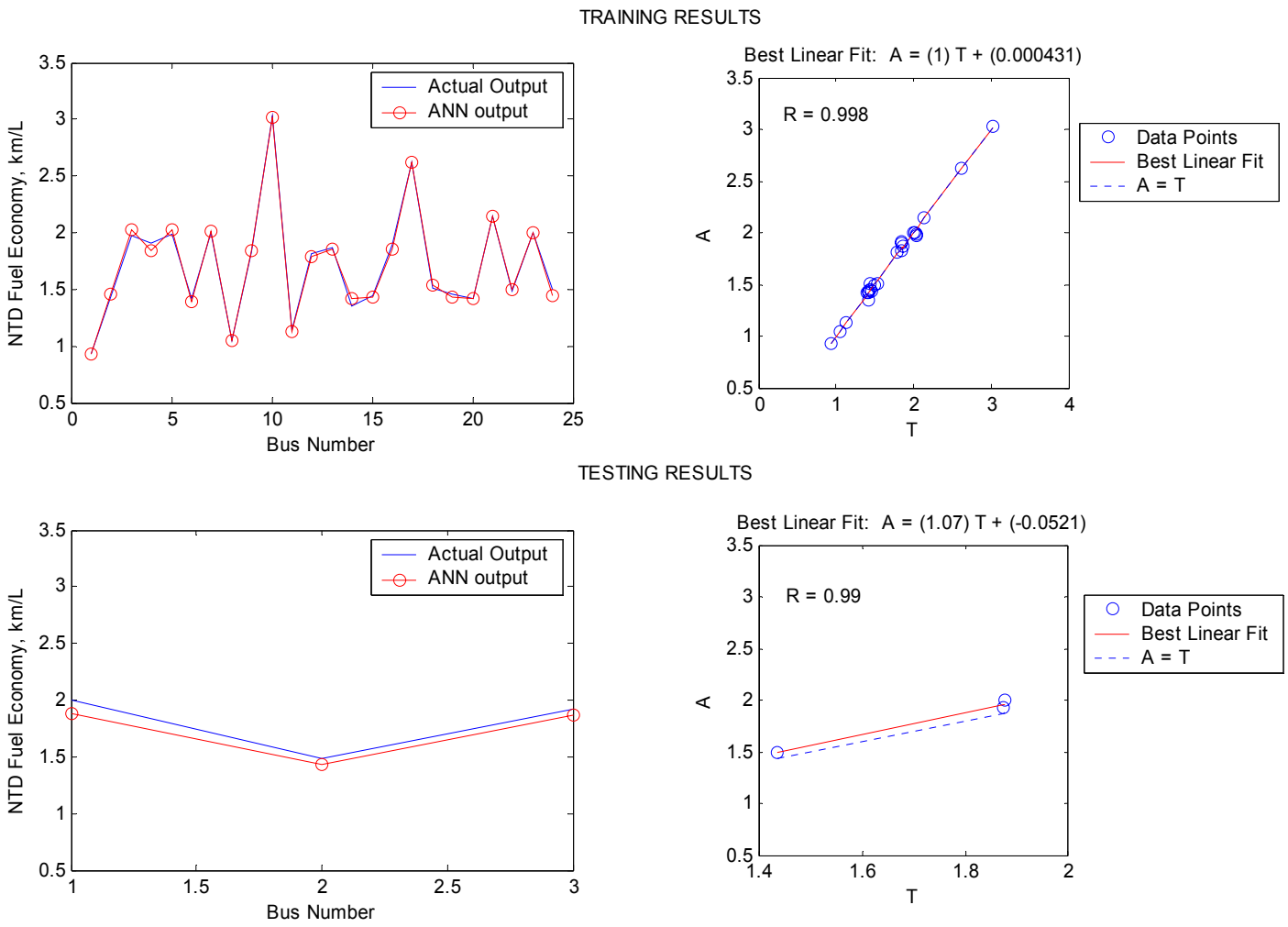

Figure **5.9**: Comparison plots for NTD fuel economy on training and test sets: Method-2 (RF5).

5.1.3 Acceleration

In this part of the study, PTI acceleration-test data on 110 two-axle diesel transit buses were used to generate the ANN models. Separate models were developed for instantaneous accelerations at 16 km/hr (ACC-16), 32 km/hr (ACC-32), 48 km/hr (ACC-48) and 64 km/hr (ACC-64). The data set was first partitioned into training set (88 buses), validation set (11 buses) and test set (11 buses). Using correlation (refer Appendix B), the original list of 21 inputs was reduced to 9 variables. These included weight (W), height (H), wheelbase (WB), rear overhang (RO), ground clearance (GC), seated load weight – total (SLW-T), axle ratio (AR), engine power (P) and engine displacement (D). This list was further narrowed down to 7 inputs using the ITSS method. The two variables eliminated at this stage include W and RO. Tables **5.10** - **5.13** give the results on 10 sample runs obtained using Method-1 (N2PFA) and the 9 inputs selected by correlation. The corresponding comparison plots between actual acceleration values and the values predicted by the neural network models are given in Figures **5.10** - **5.13**.

In Method-2 (RF5), the seven inputs selected using correlation and ITSS were used to generate the four acceleration models. In all 4 cases, MDL criterion resulted in neural networks with only one hidden neuron. This means that for each case, a simple two term function would suffice. The results from Method-2 are tabulated in Table **5.14**. Comparison plots showing the performance of the ANN models on training and test sets are given in Figures **5.14** - **5.17**.

Table 5.10: Results for acceleration at 16 km/hr: Method-1 (N2PFA)

Run N.	HLN	MSE $(m/s^2)^2$	R-train	R-test	Mean % Errr	MAE (m/s^2)	W	H	WB	RO	GC	SLW-T	AR	P	D
1	3	0.0221	0.8865	0.9659	11.59	0.1172			X		X	X	X	X	X
2	4	0.0182	0.8992	0.9731	10.89	0.1039	X	X	X	X	X	X	X	X	X
3	3	0.0235	0.8102	0.9557	11.50	0.1161	X	X				X		X	
4	4	0.0216	0.8933	0.9568	11.55	0.1256	X	X			X	X	X	X	
5	2	0.0223	0.8605	0.9559	11.26	0.1156	X		X	X	X	X	X	X	X
6	4	0.0187	0.8756	0.9665	10.81	0.1177	X	X	X	X	X	X	X	X	X
7	4	0.0215	0.8777	0.9640	10.80	0.1055			X		X	X	X		X
8	4	0.0167	0.8521	0.9665	9.66	0.1028	X	X	X	X	X	X	X	X	X
9	3	0.0220	0.8449	0.9763	11.55	0.1151	X	X	X		X	X		X	X
10	3	0.0235	0.8793	0.9616	11.51	0.1128	X	X	X	X	X	X	X	X	

X Indicates selected input

Table 5.11: Results for acceleration at 32 km/hr: Method-1 (N2PFA)

Run No.	HLN	MSE $(m/s^2)^2$	R-train	R-test	Mean % Error	MAE (m/s^2)	W	H	WB	RO	GC	SLW-T	AR	P	D
1	4	0.0098	0.9153	0.9738	9.60	0.0813	X	X	X	X	X	X	X	X	
2	3	0.0110	0.8862	0.9697	9.40	0.0790	X	X	X		X	X	X		X
3	3	0.0105	0.8855	0.9770	9.75	0.0841		X	X	X	X	X	X		
4	4	0.0113	0.8966	0.9719	10.29	0.0808			X	X	X	X	X		
5	3	0.0098	0.8979	0.9752	10.05	0.0860	X	X			X	X		X	X
6	4	0.0075	0.8595	0.9810	6.11	0.0610		X			X	X			X
7	4	0.0070	0.8931	0.9858	8.29	0.0704	X	X	X		X	X	X	X	X
8	4	0.0135	0.8937	0.9641	11.14	0.0907		X				X		X	
9	3	0.0102	0.8725	0.9708	8.75	0.0889	X	X		X	X	X	X	X	X
10	3	0.0111	0.8915	0.9752	10.16	0.0897		X	X		X	X	X	X	

X Indicates selected input

Table 5.12: Results for acceleration at 48 km/hr: Method-1 (N2PFA)

Run No.	HLN	MSE $(m/s^2)^2$	R-train	R-test	Mean % Error	MAE (m/s^2)	W	H	WB	RO	GC	SLW-T	AR	P	D
1	3	0.0065	0.8676	0.9812	9.74	0.0629		X	X	X	X	X			X
2	4	0.0052	0.8771	0.9838	8.83	0.0608		X			X	X			X
3	4	0.0067	0.8874	0.9785	10.31	0.0651	X	X	X	X	X	X		X	X
4	4	0.0072	0.8818	0.9683	8.86	0.0641	X			X	X	X	X	X	X
5	4	0.0063	0.8945	0.9790	10.10	0.0698	X	X		X	X	X		X	X
6	3	0.0076	0.8633	0.9756	11.54	0.0736		X	X		X	X			X
7	4	0.0064	0.9020	0.9778	10.52	0.0774	X	X	X	X	X	X	X	X	X
8	2	0.0069	0.8522	0.9775	10.85	0.0673	X	X	X		X	X	X		X
9	4	0.0071	0.8938	0.9746	10.36	0.0698		X	X		X	X		X	X
10	4	0.0047	0.8485	0.9831	8.94	0.0639	X	X	X	X	X	X			X

X Indicates selected input

Table 5.13: Results for acceleration at 64 km/hr: Method-1 (N2PFA)

Run No.	HLN	MSE $(m/s^2)^2$	R-train	R-test	Mean % Error	MAE (m/s^2)	W	H	WB	RO	GC	SLW-T	AR	P	D
1	4	0.0053	0.8942	0.9769	14.35	0.0647	X	X	X	X	X	X	X	X	X
2	4	0.0044	0.8584	0.9879	13.08	0.0525		X	X		X	X	X		
3	3	0.0060	0.8380	0.9824	15.85	0.0646	X	X	X		X	X	X		
4	3	0.0064	0.8860	0.9776	15.48	0.0692		X	X	X	X	X	X	X	X
5	4	0.0071	0.8463	0.9811	17.18	0.0740		X		X	X	X	X		
6	4	0.0048	0.8402	0.9856	14.11	0.0536	X	X	X		X	X	X		X
7	4	0.0043	0.8929	0.9820	11.94	0.0574	X	X	X	X	X	X	X	X	X
8	4	0.0066	0.8419	0.9805	16.76	0.0709	X	X	X		X	X	X		
9	4	0.0033	0.8204	0.9851	10.46	0.0504	X	X	X	X	X	X	X		X
10	4	0.0052	0.8257	0.9756	13.62	0.0542		X		X	X	X			

X Indicates selected input

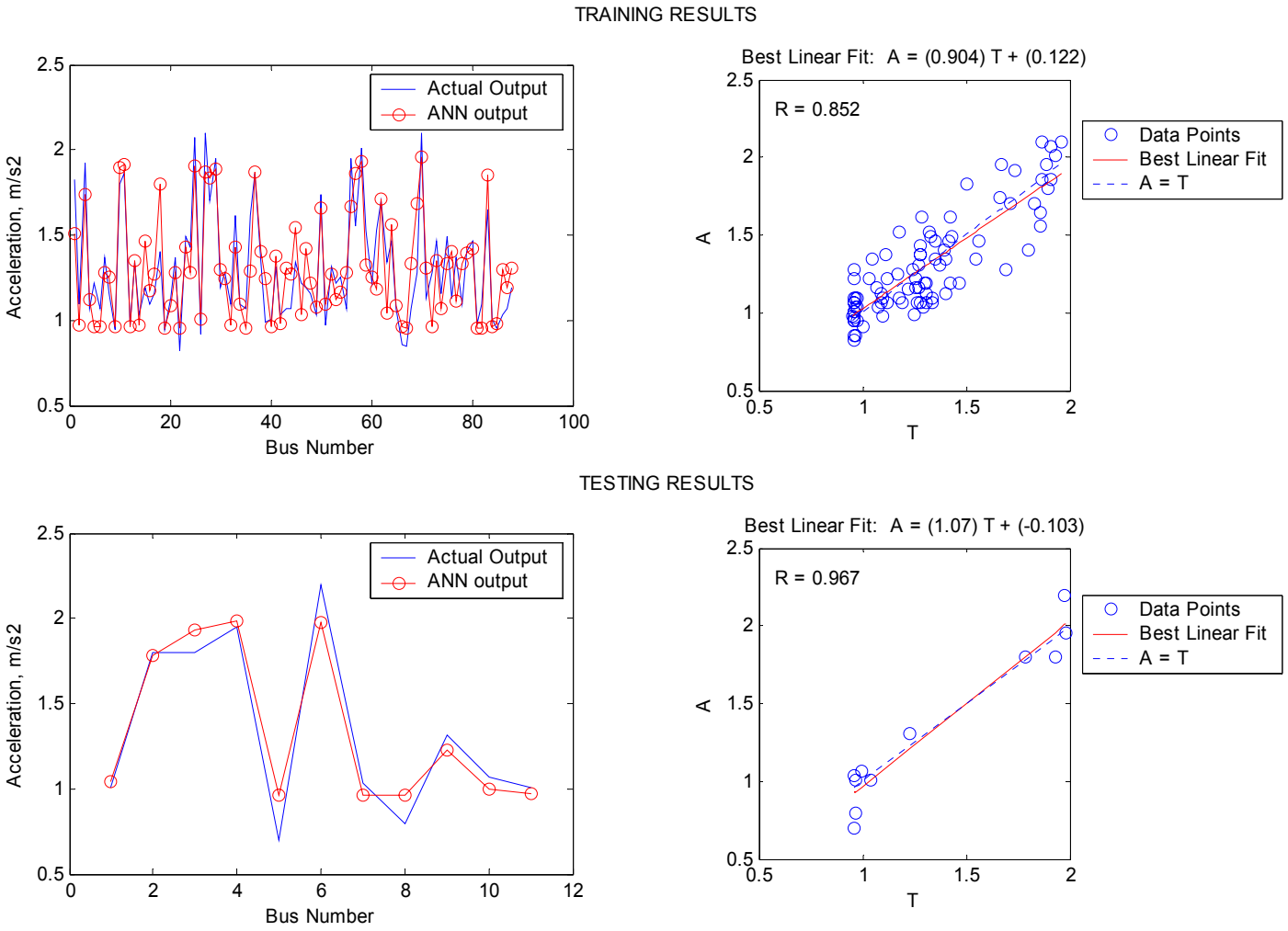

Figure **5.10**: Comparison plots for acceleration at 16 km/hr on training and test sets: Method-1 (N2PFA).

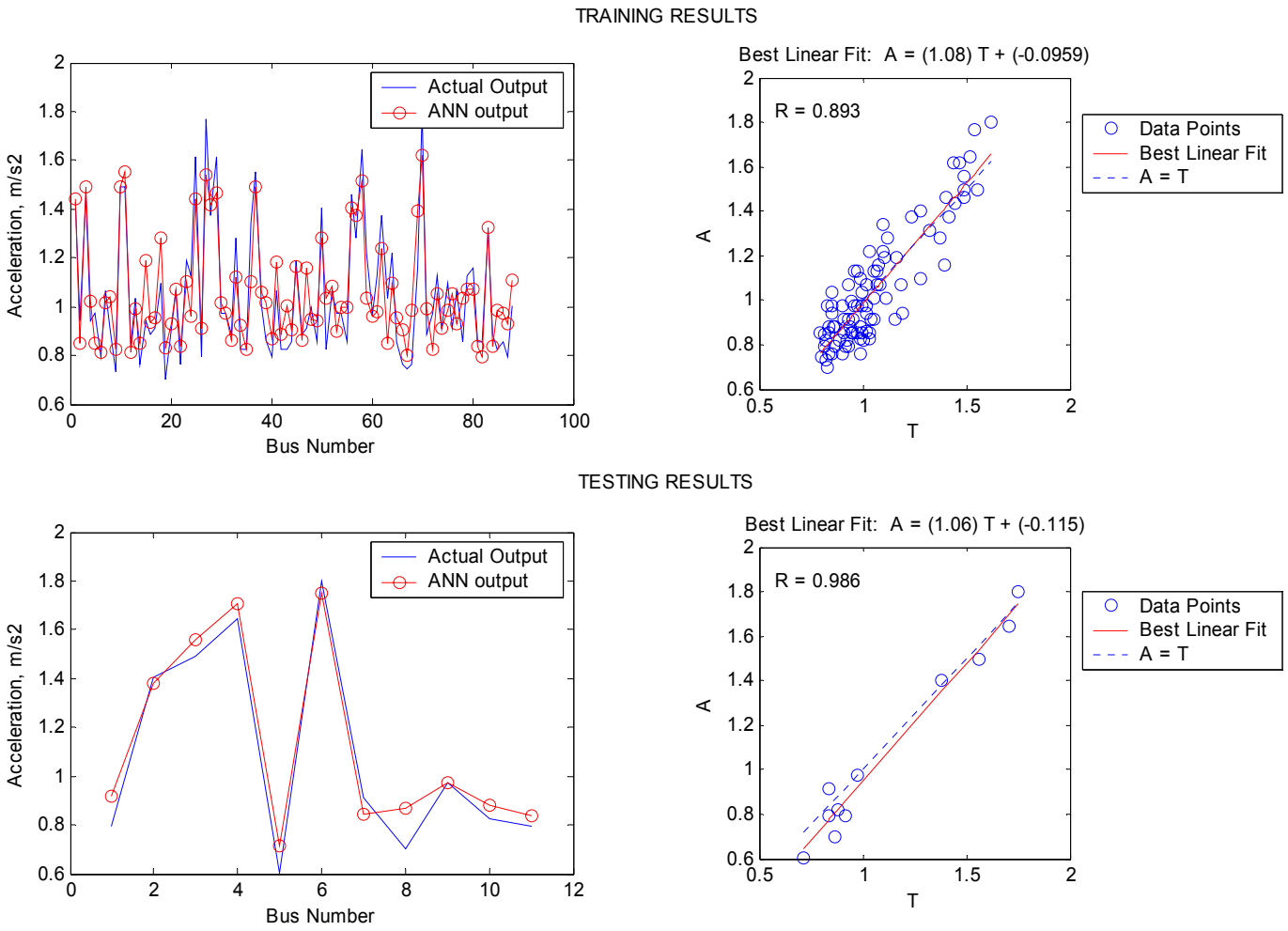

Figure **5.11**: Comparison plots for acceleration at 32 km/hr on training and test sets: Method-1 (N2PFA).

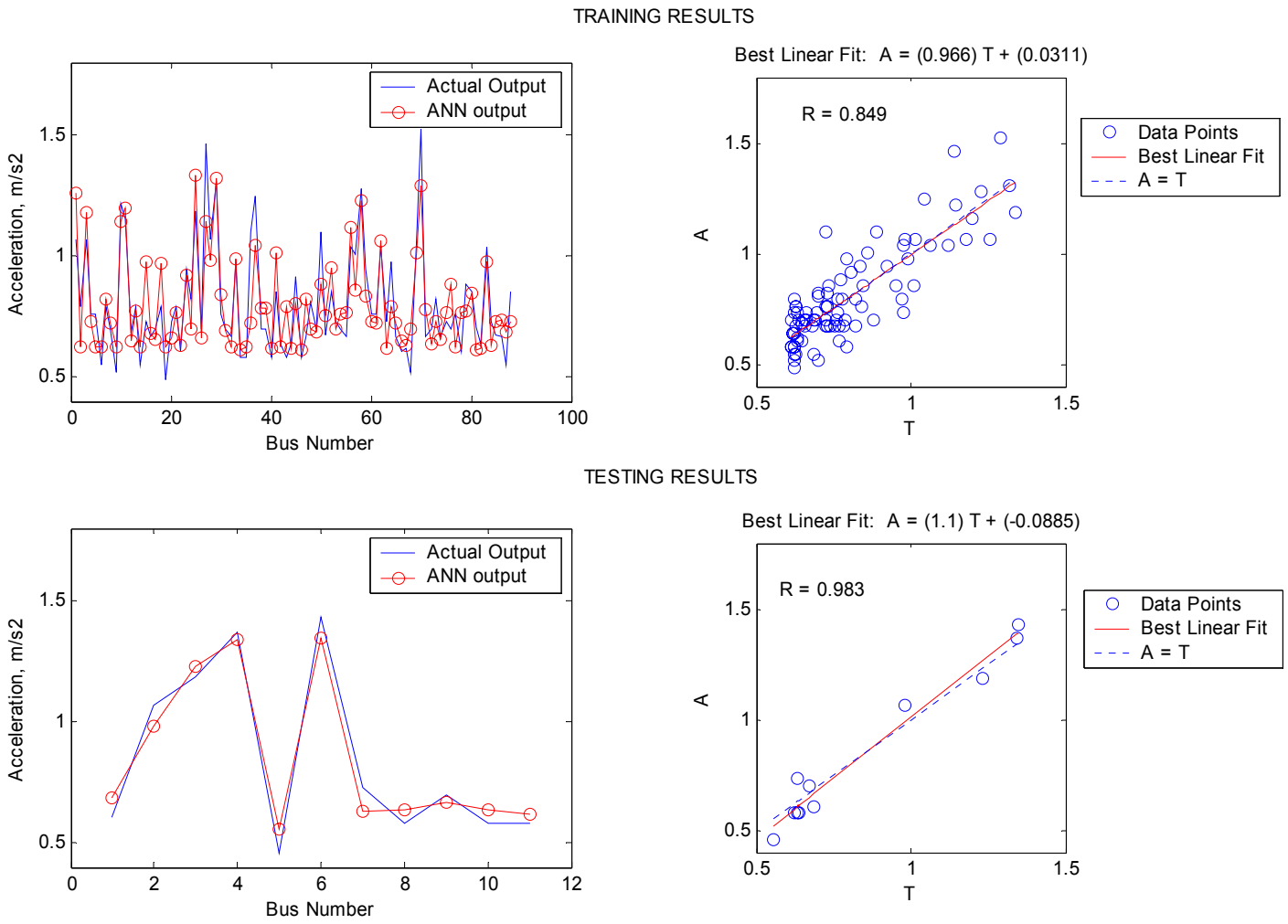

Figure **5.12**: Comparison plots for acceleration at 48 km/hr on training and test sets: Method-1 (N2PFA).

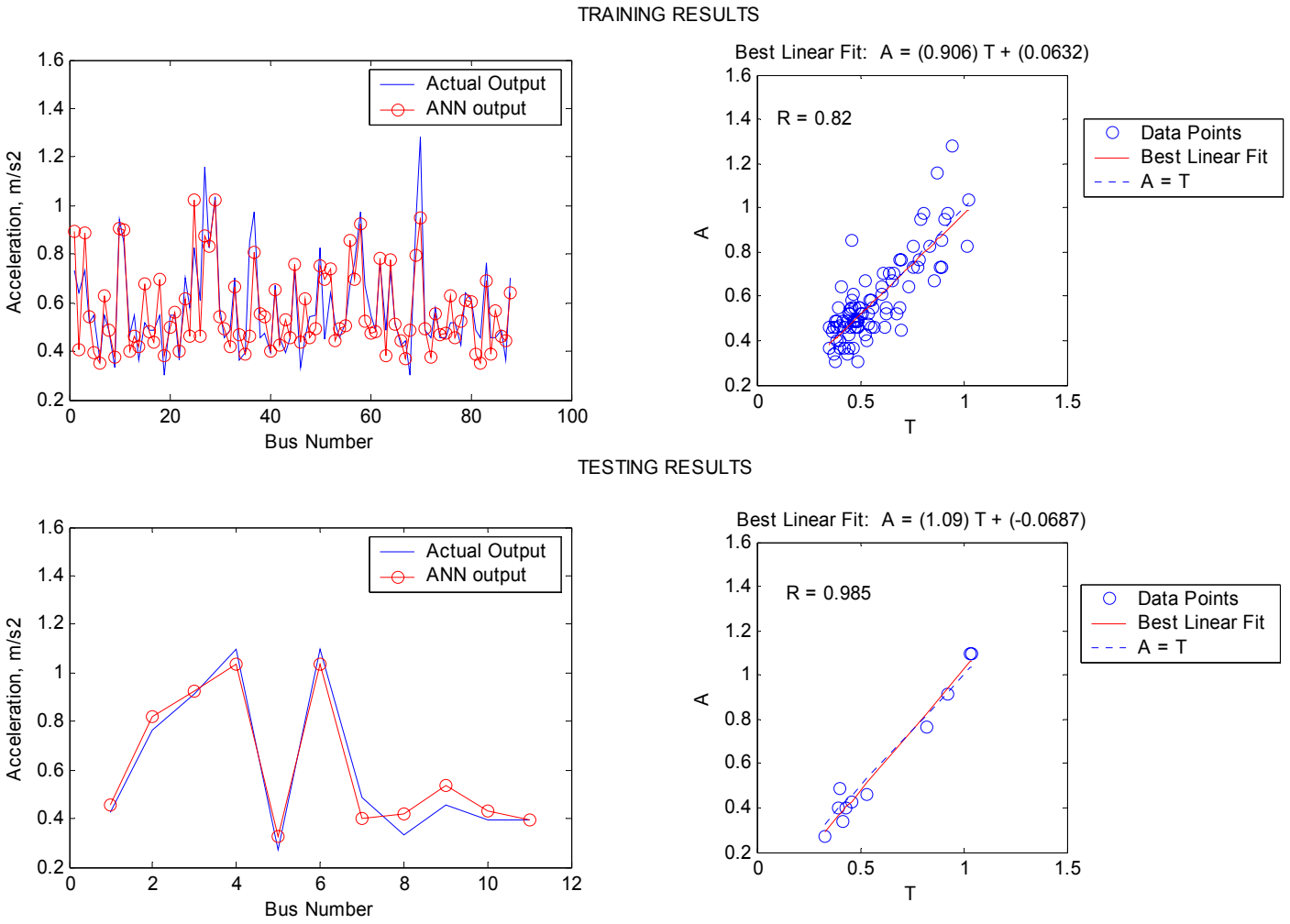

Figure **5.13**: Comparison plots for acceleration at 64 km/hr on training and test sets: Method-1 (N2PFA).

Table 5.14: Results for acceleration: Method-2 (RF5)

	c_0 (m/s^2)	c_i (m/s^2)	H	WB	GC	SLW-T	AR	P	D	MSE (m/s^2)^2	R-train	R-test	Mean % Error	MAE (m/s^2)
ACC-16	0.6714	0.5544	0.2258	0.4276	0.2363	-1.6224	0.5956	0.3471	-0.0555	0.0478	0.8914	0.9394	14.79	0.1720
ACC-32	0.5454	0.4388	-0.1398	0.3926	0.2248	-1.6382	0.5959	0.5115	0.0396	0.0243	0.9101	0.9637	12.96	0.1258
ACC-48	0.3619	0.3939	-0.7036	0.2446	0.2194	-1.4556	0.4392	0.7930	0.1196	0.0119	0.9018	0.9782	12.79	0.0948
ACC-64	0.1962	0.3429	-1.1377	0.1245	0.2707	-1.3497	0.3165	1.0978	0.1033	0.0087	0.8850	0.9855	17.91	0.0856

Ratio of output sensitivities w.r.t. a given input and SLW-T

	H	WB	GC	SLW-T	AR	P	D
ACC-16	-0.1391	-0.2636	-0.1456	1.0000	-0.3671	-0.2140	0.0342
ACC-32	0.0854	-0.2397	-0.1372	1.0000	-0.3637	-0.3122	-0.0242
ACC-48	0.4834	-0.1680	-0.1507	1.0000	-0.3017	-0.5448	-0.0822
ACC-64	0.8429	-0.0923	-0.2006	1.0000	-0.2345	-0.8134	-0.0765

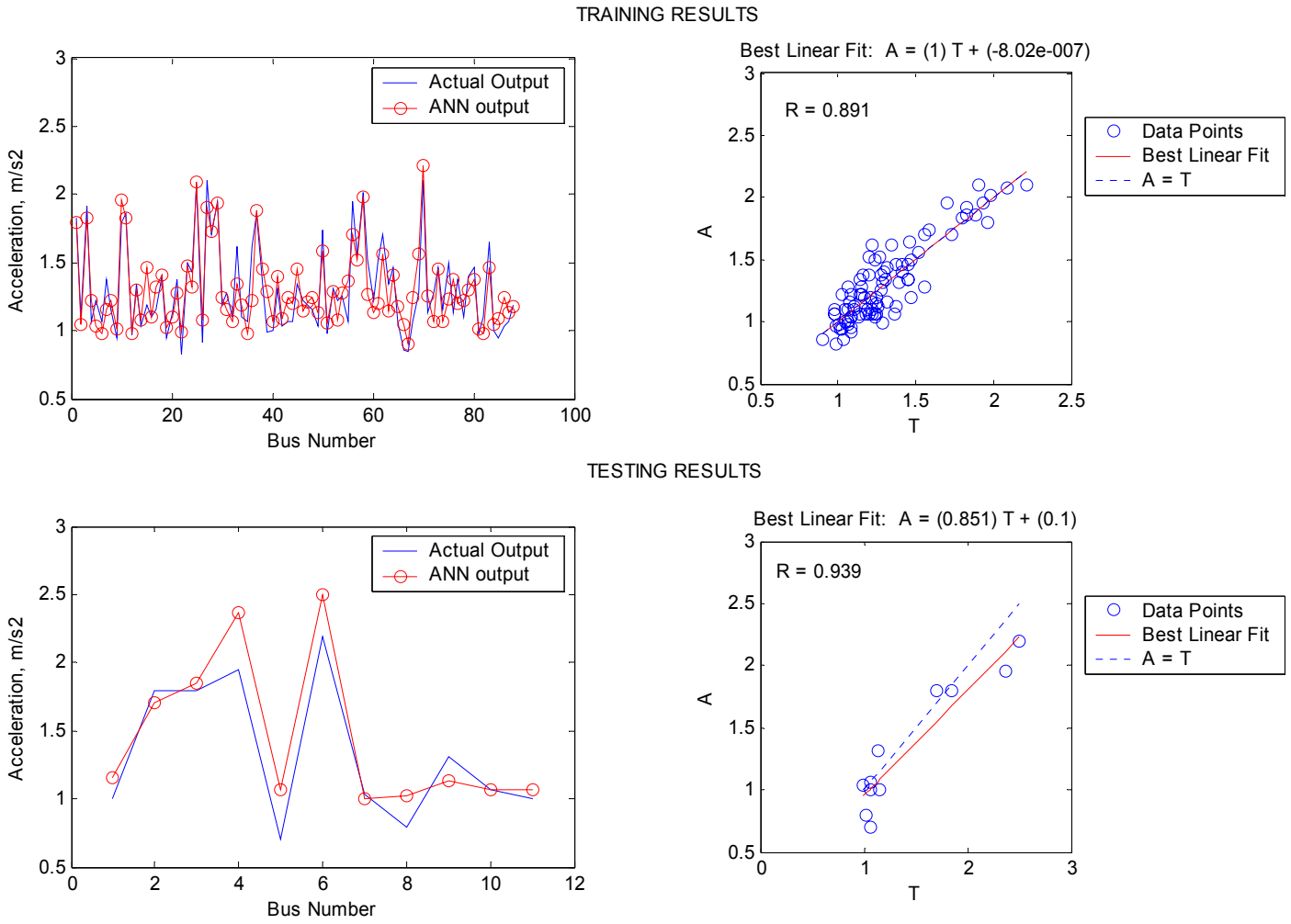

Figure **5.14**: Comparison plots for acceleration at 16 km/hr on training and test sets: Method-2 (RF5).

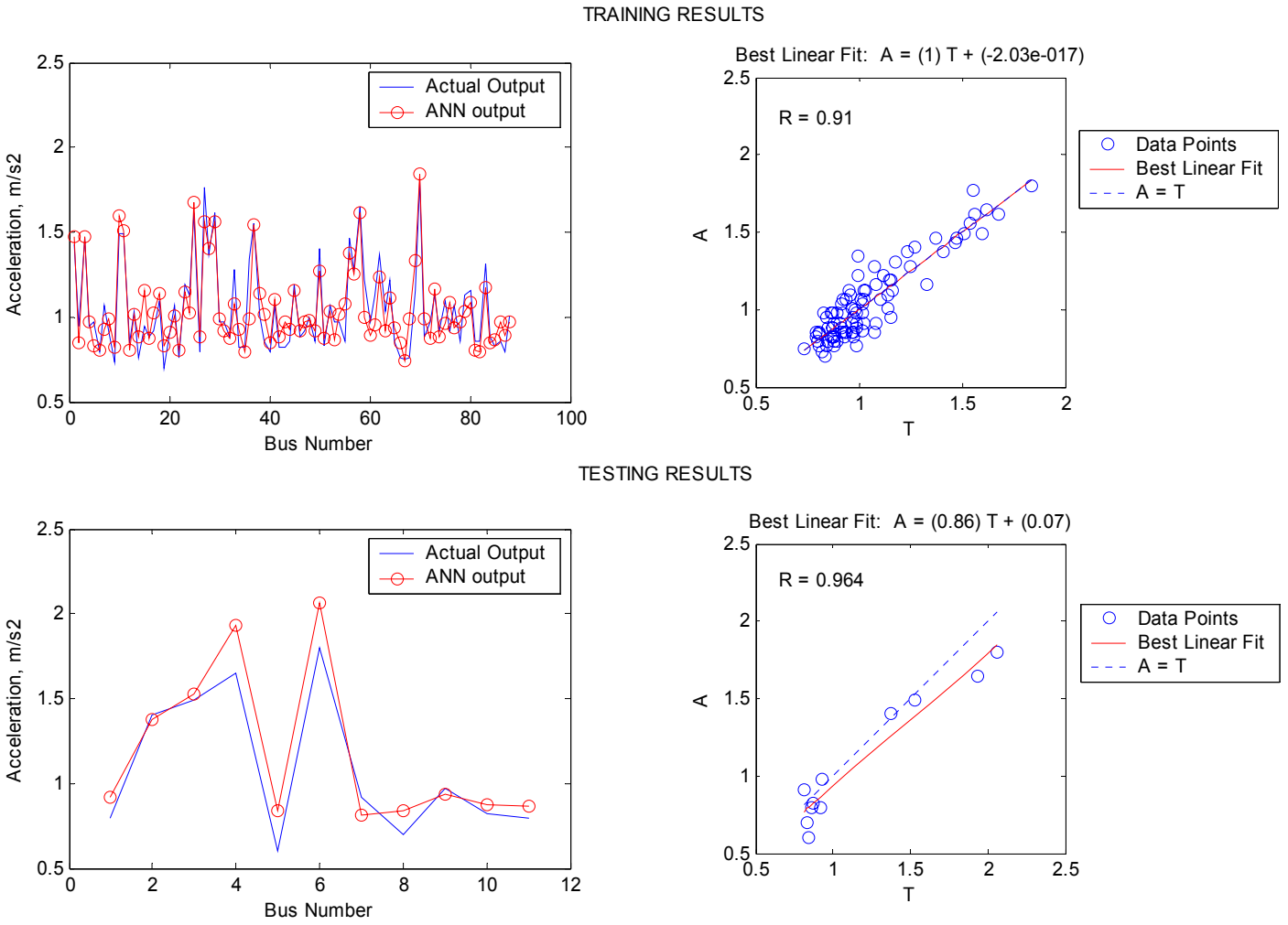

Figure **5.15**: Comparison plots for acceleration at 32 km/hr on training and test sets: Method-2 (RF5).

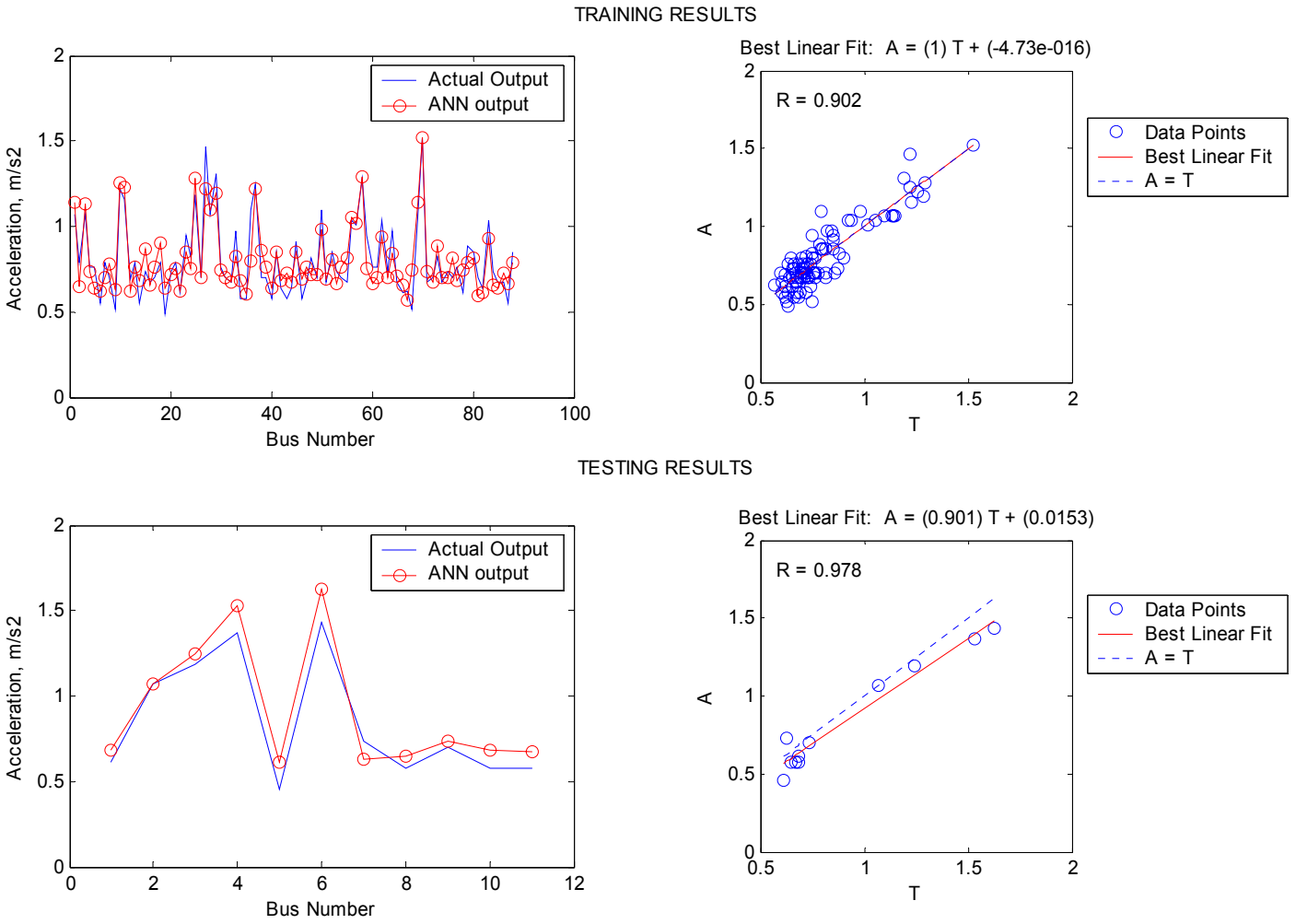

Figure **5.16**: Comparison plots for acceleration at 48 km/hr on training and test sets: Method-2 (RF5).

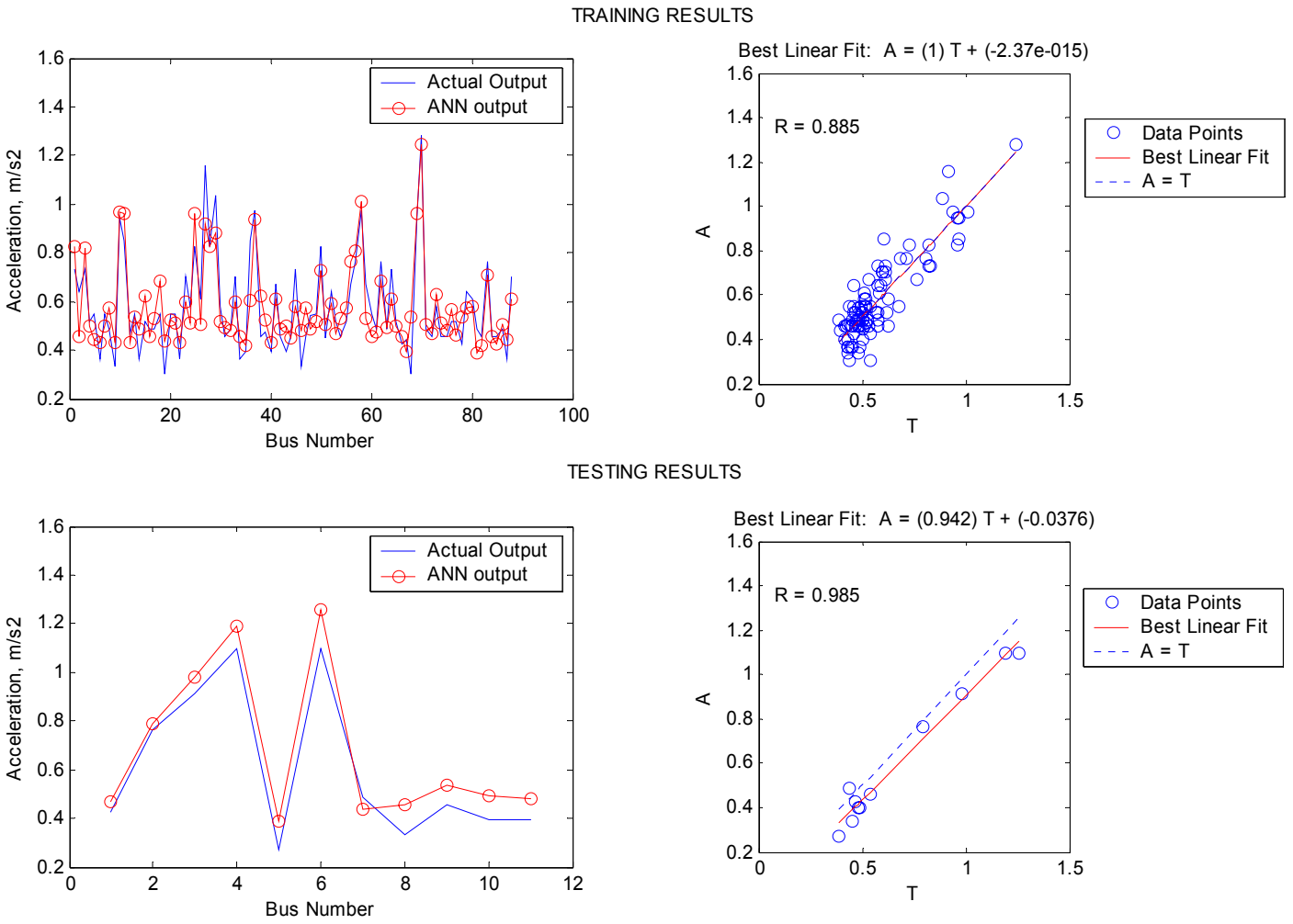

Figure **5.17**: Comparison plots for acceleration at 64 km/hr on training and test sets: Method-2 (RF5).

Using Table **5.14**, one can rank the inputs in the order of decreasing importance as follows based on the magnitude of the exponents:

ACC-16: (i) SLW-T (ii) AR (iii) WB (iv) P (v) GC (vi) H (vii) D

ACC-32: (i) SLW-T (ii) AR (iii) P (iv) WB (v) GC (vi) H (vii) D

ACC-48: (i) SLW-T (ii) P (iii) H (iv) AR (v) WB (vi) GC (vii) D

ACC-64: (i) SLW-T (ii) H (iii) P (iv) AR (v) GC (vi) WB (vii) D

Additionally, the following observations can be made:

1) SLW-T stands out as the most important variable in all four cases and its exponent is negative as expected indicating that acceleration capability decreases with increasing weight.
2) Ground clearance and engine displacement seem to have little impact on acceleration capabilities of a bus. The fact that engine displacement is not highly ranked seems to be counter-intuitive. However, one needs to understand it in light of the fact that engine displacement is not very highly correlated (R=0.61) with engine power. In the presence of engine power as an input, the effect of engine displacement is marginal.
3) The influence of vehicle height on acceleration values increases with speed. This is due to the fact that aerodynamic drag force, which is dependent on vehicle frontal area, is negligible at low speeds and increases with speed.
4) The exponent for wheelbase decreases with increasing speed. This probably results from the fact that longitudinal load transfer plays a more important role at high acceleration values which occur at lower gears, i.e., lower vehicle speeds.

5) The value of the exponent for axle ratio decreases with increasing speed. Axle ratio has a two fold effect on net tractive force. Firstly, it magnifies the torque coming from the engine to the wheels. Secondly, it plays a major part in determining the loss of tractive force due to inertia of rotating components (engine and drive-train). Since higher speed corresponds to a lower acceleration value, which in turn means a smaller axle ratio, the results seem consistent with known theory.

6) Engine power becomes a dominant factor as the speed increases. It is interesting to note that the ratio of the exponents for seated load weight and power approaches -1 as speed increases, i.e., acceleration becomes proportional to power to weight (P/W) ratio. The P/W ratio is commonly used to denote acceleration capability [13,21,22].

Comparison of the results presented in Tables 5.10 - 5.14 provides a direct means of comparing the performances of Methods-1 and 2. In all four cases, namely ACC-16, ACC-32, ACC-48 and ACC-64, we see that SLW-T is never pruned out. This matches well with the number one status of the input under Method-2 (RF5). Except for ACC-48, in all other instances we see that the two variables - RO and D - ranked the lowest by Method-2 are pruned often. For inputs that are ranked in between (as per Method-2), it is seen that the two methods have a tendency to treat them differently. This seems to be the case especially for P and GC, wherein Method-1 places more emphasis on GC while Method-2 seems to prefer P. In terms of predictive accuracies as measured from MSE values, it is clear that Method-1 performs better. However, Method-2 results in much simpler ANN configurations.

One of the first steps that need to be undertaken by any vehicle engineer (or analyst) before using a new simulation method is to check its validity on known problems. The results obtained using Methods-1 and 2 on acceleration and on fuel economy (Sub-sections 5.1.1 - 5.1.3) clearly show that the two procedures perform very well with regards to accuracies of prediction and follow the results either already given in literature or as perceived by engineering intuition. Hence, it is felt that one can successfully apply the two methods presented in this thesis to other vehicle performance measures provided reliable and accurate data are available on the relevant inputs and outputs.

5.1.4 Pass-by Noise

At PTI, pass-by noise tests are conducted as per SAE standard J366 - "Exterior Sound Level for Heavy Trucks and Buses". In this study, pass-by noise data for 110 diesel buses were collected from PTI bus reports and used to generate ANN-based predictive models. Separate models were generated for two output variables, namely pass-by noise measured on the right hand side (curb side) of the bus when accelerating from constant speed (called as CON-NOISE-R) and pass-by noise measured on the right hand side of bus when accelerating from a standstill position (called as ST-NOISE-R). The right hand side was selected since it more directly affects pedestrians on the curb. However, similar models can be developed for left hand side as well. Data were split into 80%, 10% and 10% for training, validation and testing respectively. The test set hence had data for 11 buses. As the first step in input selection, correlation was used to reduce

the initial 21 inputs (Appendix B). A total of 9 inputs were selected at this stage. These include width (W), height (H), wheelbase (WB), rear overhang (RO), ground clearance (GC), seated load weight-total (SLW-T), axle ratio (AR), engine power (P) and engine displacement (D). In the next stage, ITSS was used to reduce the number on inputs as follows:

CON-NOISE-R: H, WB, RO, GC, SLW-T, AR, P and D (8 inputs)

ST-NOISE-R: W, WB, GC, SLW-T, AR, P and D (7 inputs)

Method-1 (N2PFA) used all nine inputs selected using correlation method. The results obtained from 10 sample runs are shown in Tables **5.15** and **5.16** for CON-NOISE-R and ST-NOISE-R respectively. Optimal solutions were found to require 2 hidden neurons in the case of the former and 4 hidden neurons in case of the latter. Comparison plots between actual outputs and those predicted by Method-1 are shown in Figures **5.18** and **5.19**.

Table 5.15: Results for CON-NOISE-R: Method-1 (N2PFA)

Run No.	HLN	MSE $(dB(A))^2$	R-train	R-test	Mean % Error	MAE dB(A)	W	H	WB	RO	GC	SLW-T	AR	P	D
1	2	3.48	0.3249	0.5909	1.80	1.36	X	X		X		X	X	X	X
2	3	4.78	0.2342	0.4699	2.31	1.73	X			X		X		X	X
3	4	3.92	0.5789	0.5693	1.93	1.45	X		X	X	X	X	X	X	X
4	4	4.39	0.3528	0.5177	2.25	1.70	X	X				X	X	X	X
5	3	4.61	0.5135	0.6187	2.26	1.69	X	X	X	X	X	X	X	X	X
6	1	5.80	0.4680	0.4931	2.51	1.88		X	X	X	X	X	X	X	X
7	4	4.02	0.4506	0.5653	2.10	1.57	X	X		X	X		X	X	X
8	3	3.90	0.4060	0.6195	1.96	1.47			X						X
9	3	3.50	0.6268	0.6640	2.04	1.54	X	X		X	X		X	X	X
10	4	3.64	0.6148	0.6654	1.94	1.45	X		X	X	X	X	X	X	X

X Indicates selected input

Table 5.16: Results for ST-NOISE-R: Method-1 (N2PFA)

Run No.	HLN	MSE $(dB(A))^2$	R-train	R-test	Mean % Error	MAE dB(A)	W	H	WB	RO	GC	SLW-T	AR	P	D
1	1	6.04	0.6584	0.5105	2.25	1.75				X		X			X
2	2	5.85	0.6262	0.5233	2.26	1.75						X			X
3	3	5.74	0.6569	0.5435	2.09	1.62	X			X	X	X		X	X
4	4	5.71	0.6259	0.5342	1.70	1.70						X			X
5	3	5.48	0.6454	0.5644	2.32	1.79	X		X	X	X	X	X	X	X
6	3	5.01	0.6855	0.5997	2.24	1.74	X	X	X	X	X	X	X	X	X
7	3	5.96	0.7080	0.5001	2.12	1.65	X		X	X	X	X	X	X	X
8	2	5.70	0.4366	0.7272	2.10	1.65	X	X	X	X	X	X	X	X	X
9	4	5.16	0.6536	0.5905	2.23	1.72	X		X		X	X		X	X
10	4	4.30	0.6690	0.6770	2.08	1.62	X		X	X	X	X		X	X

X Indicates selected input

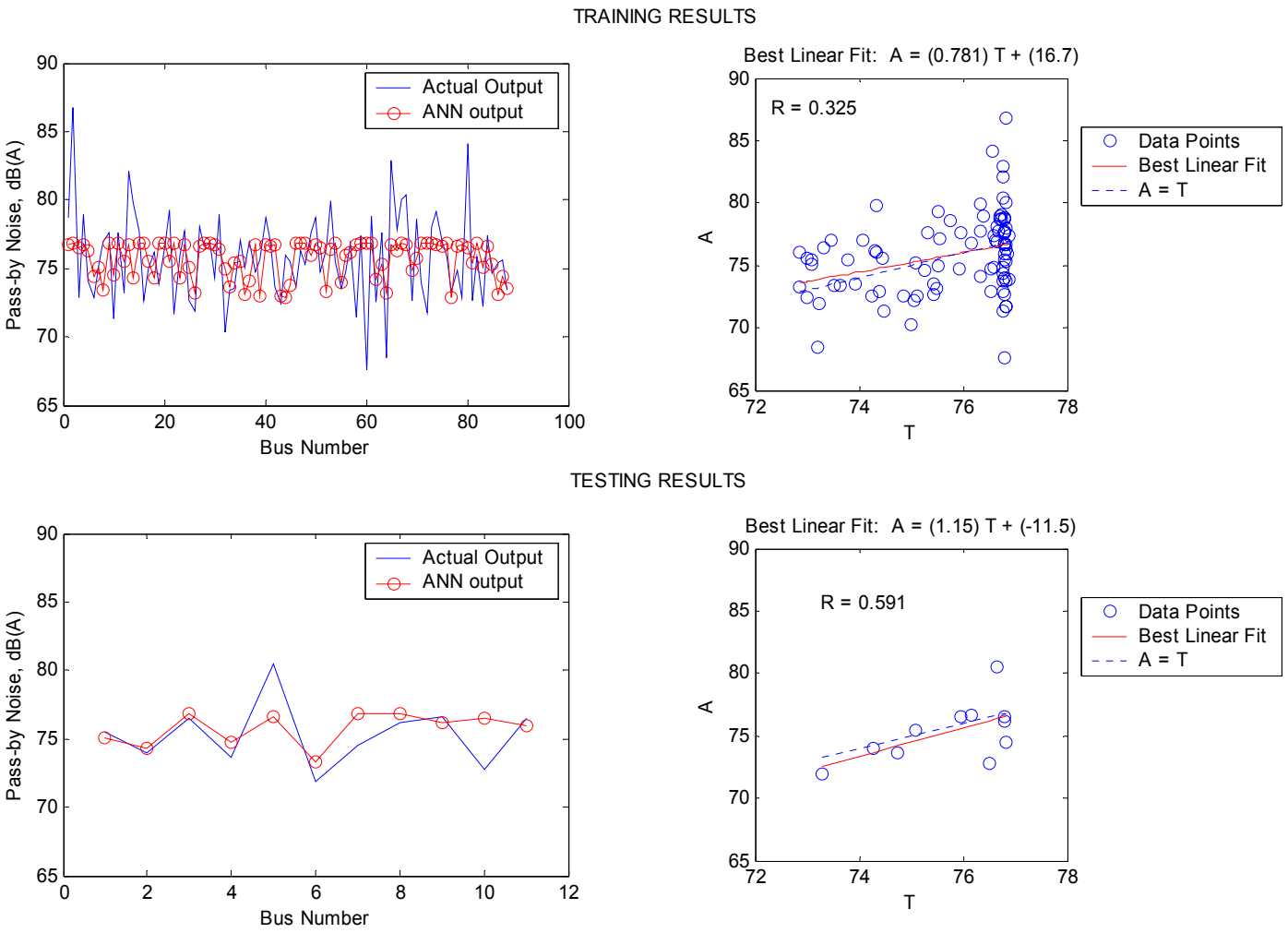

Figure **5.18**: Comparison plots for CON-NOISE-R on training and test sets: Method-1 (N2PFA).

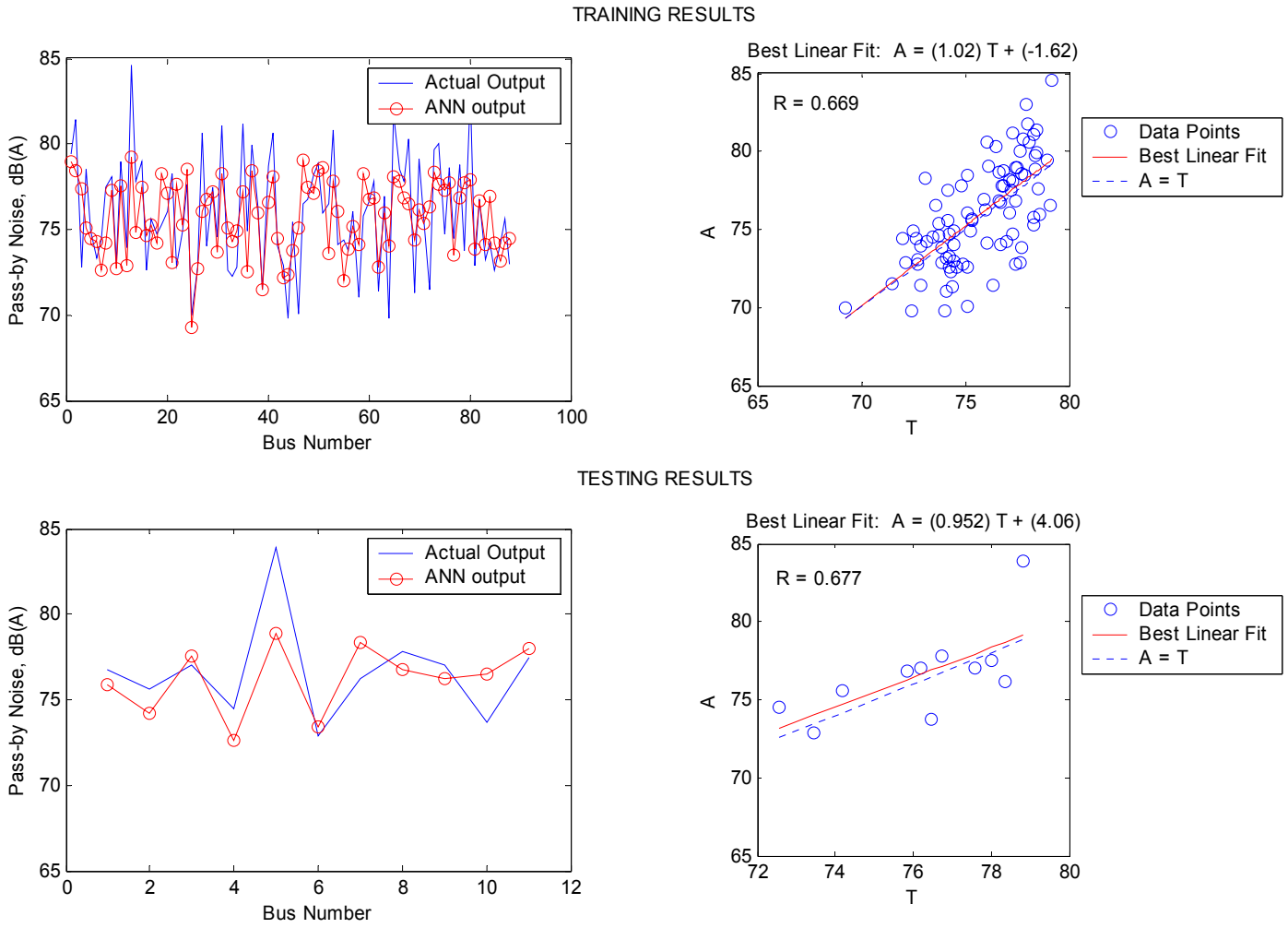

Figure **5.19**: Comparison plots for ST-NOISE-R on training and test sets: Method-1 (N2PFA).

In Method-2 (RF5), models were generated using the inputs selected by ITSS. The results for CON-NOISE-R and ST-NOISE-R are given in Table **5.17**. Based on the magnitude of the exponents of the input variables, the following is the list of variables in the decreasing order of relevance:

CON-NOISE-R: (i) D (ii) H (iii) P (iv) SLW-T (v) RO (vi) GC (vii) WB (viii) AR

ST-NOISE-R: (i) D (ii) SLW-T (iii) P (iv) W (v) AR (vi) WB (vii) GC

Comparison plots between actual outputs and the output values predicted by Method-2 on the test set are included in Figures **5.20** and **5.21**. From Table **5.17**, it is seen that the maximum value that can be predicted using this method for CON-NOISE-R is 79.47 dB(A) since c_i is negative. As suggested earlier in Sub-section **5.1.1** for the CBD fuel economy model, if the expected CON-NOISE-R values are greater than this limit, one can neglect MDL criterion and go in for more terms in the equation, i.e., more number of hidden neurons.

Comparison of the results from Methods-1 and 2 shows encouraging results. For CON-NOISE-R, top ranking inputs such as D and P under Method-2 do not get pruned that often in Method-1 whereas lowly ranked inputs such as WB and GC do get rejected consistently. The two methods seem to rate H differently. However, for the best performing model (with lowest MSE) only WB and GC were rejected. For ST-NOISE-R, the top two variables under Method-2, namely D and SLW-T, are never pruned by Method-1. Variables such as AR and WB that are ranked low under Method-2 are rejected often under Method-1 as well. H that was rejected by ITSS is pruned in eight out of ten cases. The two methods however appear to rate GC differently.

Table 5.17: Results for Pass-by Noise: Method-2 (RF5)

	c_0 db(A)	c_i db(A)	H	WB	RO	GC	SLW-T	AR	P	D	MSE $(db(A))^2$	R-train	R-test	Mean % Error	MAE db(A)
CON-NOISE-R	79.4740	-3.4955	-1.5012	0.2205	0.5400	0.3139	-0.5665	-0.1734	-1.4540	2.0280	3.4738	0.4265	0.6333	1.74	1.3161

	c_0 db(A)	c_i db(A)	W	WB	GC	SLW-T	AR	P	D	MSE $(db(A))^2$	R-train	R-test	Mean % Error	MAE db(A)
ST-NOISE-R	72.2230	3.3314	0.6965	-0.4885	0.2966	1.9115	-0.4959	1.4808	-2.8397	3.9119	0.5849	0.7068	1.75	1.3640

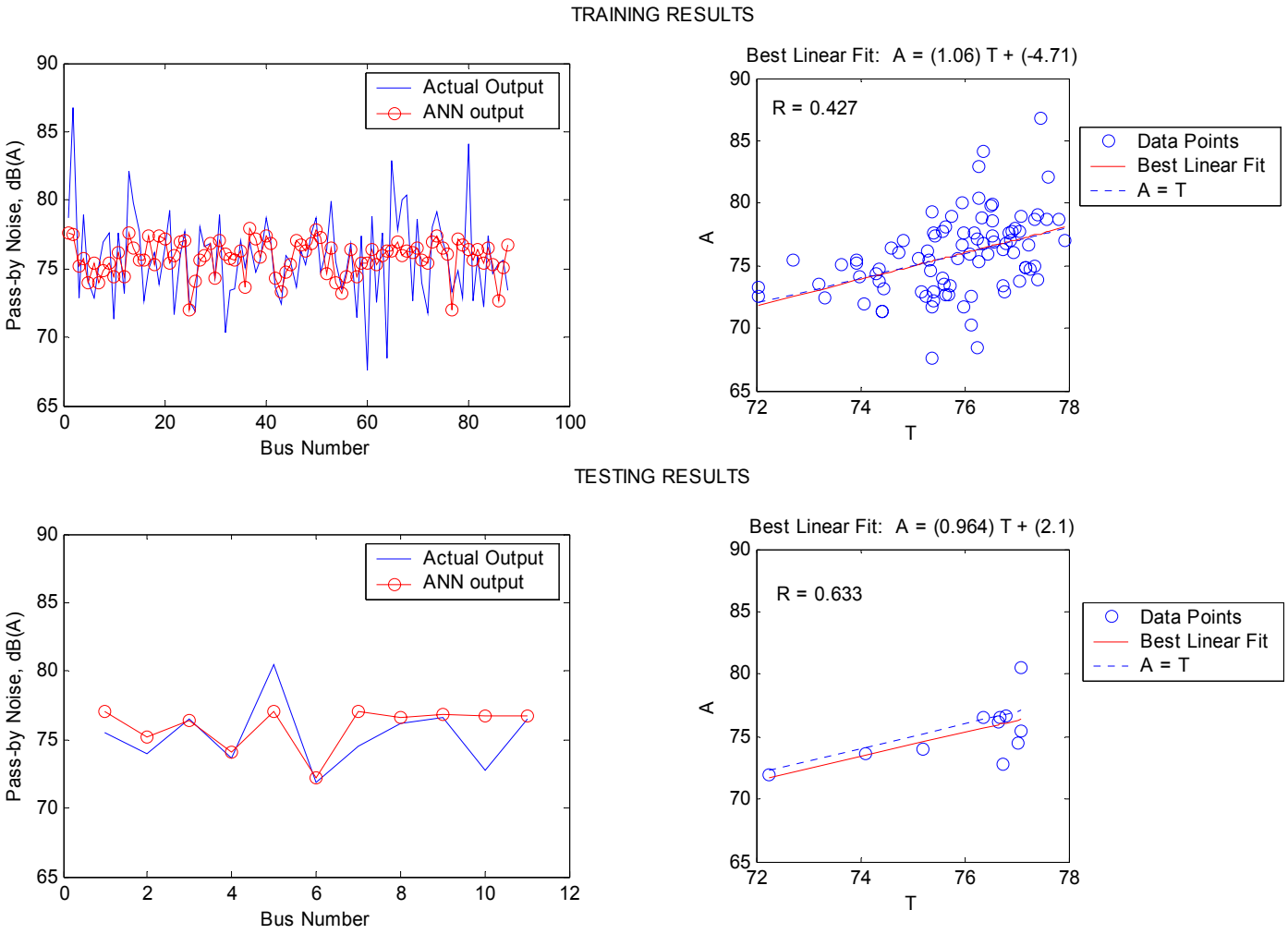

Figure **5.20**: Comparison plots for CON-NOISE-R on training and test sets: Method-2 (RF5).

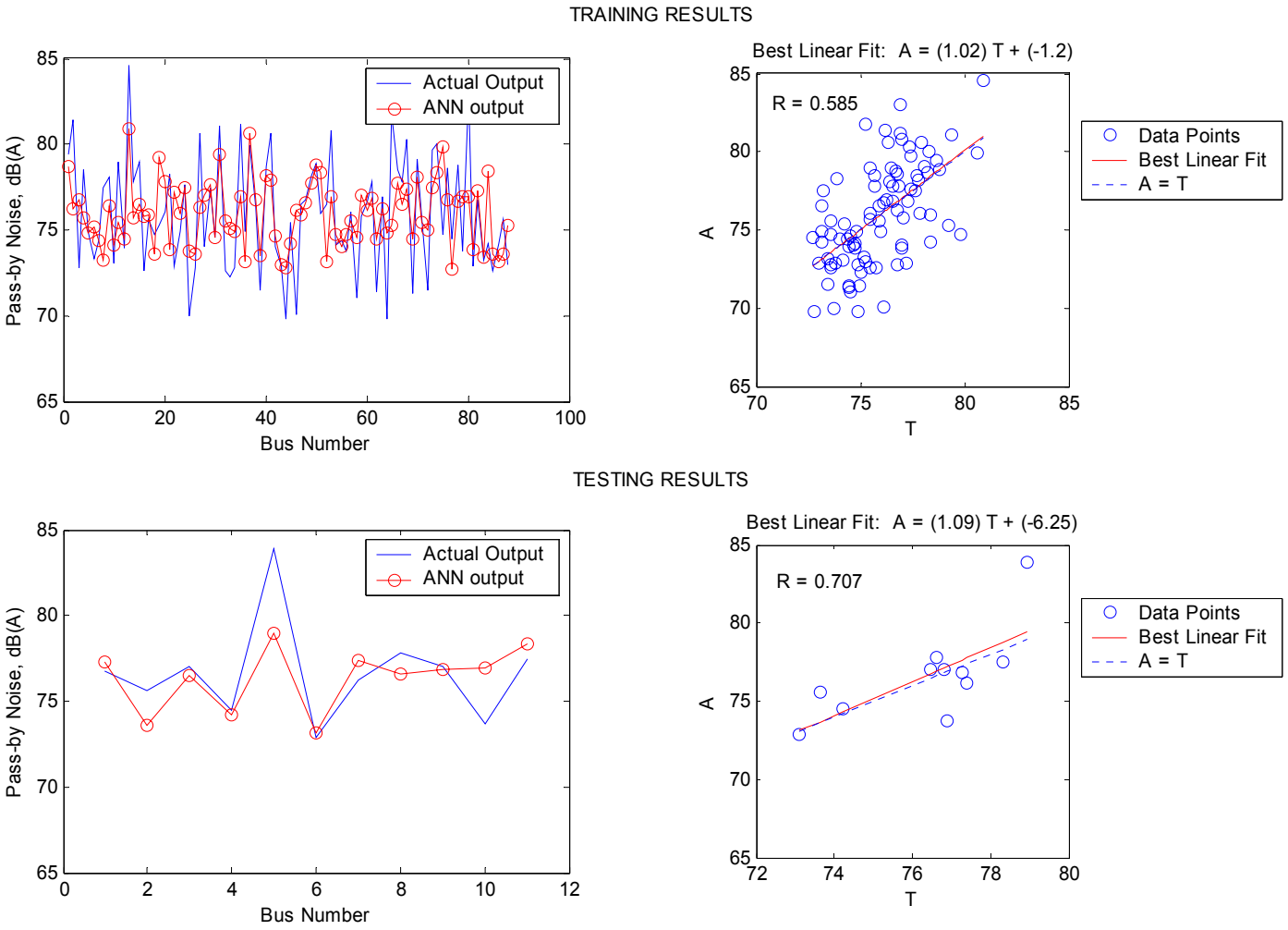

Figure **5.21**: Comparison plots for ST-NOISE-R on training and test sets: Method-2 (RF5).

The results presented for pass-by noise in this section don't seem to have high correlation coefficients between the actual outputs and the ANN predicted outputs. Pass-by noise depends on a lot factors pertaining to the powertrain, air intake system, exhaust system, tires and noise mitigation strategies employed in the engine compartment. In this study, such inputs could not be included as historical data were not available. However, one can get a good estimate of the capability of the two methods (N2PFA and RF5 based) presented in this study by comparing the results with other such studies available in the literature. Fry and Jennings [24] claim that as of year 2003, there were no whole-vehicle analytical models that could predict pass-by noise better than $\pm$ 3 dB(A) and this was only about as accurate as the prediction by human experts. They present a two-stage model with an accuracy of $\pm$ 1.1 dB(A). Table 5.18 compares the salient characteristics of the optimal models found in this study with that of Fry and Jennings' model.

Table 5.18: Comparison with Fry and Jennings' Noise Model

Characteristic	Fry's Model	Method -1	Method - 2
Stages	2	1	1
Inputs	25 (Stage-1) 58 (Stage-2)	7 (CON-NOISE-R) 7 (ST-NOISE-R)	8 (CON-NOISE-R) 7 (ST-NOISE-R)
Hidden Neurons	15 (Stage-1) 19 (Stage-2)	2 (CON-NOISE-R) 4 (ST-NOISE-R)	1 (CON-NOISE-R) 1 (ST-NOISE-R)
Training Samples	2503 (Stage-1) 4282 (Stage-2)	88	88
Test Samples	997 (Stage-1) 1424 (Stage-2)	11	11
Vehicles	24 + 13 (Stage -1) 21 + 7 (Stage - 2)	110	110
Mean % Error	$\pm$ 1.4	$\pm$ 1.80 (CON-NOISE-R) $\pm$ 2.08 (ST-NOISE-R)	$\pm$ 1.74 (CON-NOISE-R) $\pm$ 1.75 (ST-NOISE-R)
MAE (dB (A))	$\pm$ 1.1	$\pm$ 1.36 (CON-NOISE-R) $\pm$ 1.62 (ST-NOISE-R)	$\pm$ 1.32 (CON-NOISE-R) $\pm$ 1.36 (ST-NOISE-R)

It is evident from Table 5.18 that the two methods, presented in this study, generate models that are much simpler than Fry and Jennings' model even though the problem they are trying to solve is much more complex due to fewer data samples and a much higher number of vehicles being modeled. With regards to accuracies, Methods-1 and 2 are able to give performances comparable to Fry and Jennings' model. Unlike their model, the methods presented in this study do not necessitate any prior knowledge of the problem in terms of expert opinion. Another important aspect is that the two models presented in this study are transparent as they can be interpreted in the form of mathematical expressions.

5.1.5 PTI Reliability

Reliability data were collected for a total of 108 two-axle diesel buses from PTI test reports. Data were divided into training set (86 buses), validation set (11 buses) and test set (11 buses). As mentioned in Sub-section 3.3.1, mean distance between failures (MDBF) was used as the performance measure in this study. Since the use of MDBF as a measure hinges on the assumption of constant failure rate, as a first step, cumulative number of failures over the period of PTI testing was plotted for 5 sample buses. The plot is shown in Figure 5.22 in which each line corresponds to a different bus model. Since the lines seem to have more or less constant slope it seems that the assumption of a constant failure rate (i.e., exponential distribution) is valid. An extended analysis on 28 bus models yielded a similar result.

The correlation method (Appendix B) resulted in selection of 11 input variables namely width (W), height (H), wheelbase (WB), rear overhang (RO), ground clearance (GC), seated load weight-total (SLW-T), axle ratio (AR), engine power (P), engine displacement (D), durability miles (D-MIL) and other miles (O-MIL) on PTI test track. Using ITSS, this list was reduced to a total of 8 inputs. The eliminated variables include W, RO and AR. The results from Method-1 on ten sample runs using the 11 inputs selected by correlation are given in Table **5.19**. Comparison plots between actual outputs and the ANN predicted outputs on training and test sets are shown in Figure **5.23**. The results obtained using Method-2 are given in Table **5.20** and the comparison plots between outputs are shown in Figure **5.24**. Since the magnitude of the output variable (PTI-MDBF) was large, it was normalized with respect to its mean value in a manner similar to that for inputs. This was done to help the training algorithm reach an optimal solution quickly.

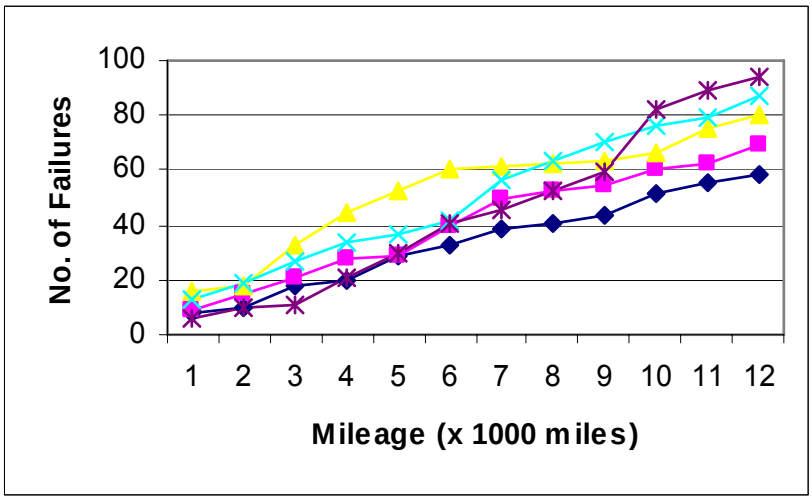

Figure **5.22**: Plot of cumulative failures versus durability miles for five buses.

Table 5.19: Results for PTI reliability: Method-1 (N2PFA)

Run No.	HLN	MSE (km^2)	R-train	R-test	Mean % Error	MAE (km)	W	H	WB	RO	GC	SLW-T	AR	P	D	D-MIL	O-MIL
1	4	1.39E+05	0.4958	0.7228	35.3	265.3	X	X	X	X	X	X	X	X	X	X	X
2	1	1.35E+05	0.5088	0.7067	45.4	286.0		X				X		X	X	X	
3	4	1.40E+05	0.6987	0.7440	36.9	263.4	X	X	X	X	X	X	X	X	X	X	
4	3	1.64E+05	0.5135	0.5557	55.4	348.7	X	X	X	X	X	X	X	X	X	X	X
5	2	1.55E+05	0.4305	0.5715	53.4	261.4				X		X	X	X	X	X	X
6	2	1.13E+05	0.6053	0.8494	34.5	251.7	X	X	X	X		X	X	X	X	X	X
7	4	1.66E+05	0.5339	0.6840	44.0	308.5	X	X	X	X	X	X	X	X	X	X	X
8	4	1.56E+05	0.5041	0.5897	58.9	307.0	X	X	X	X	X	X	X	X	X	X	X
9	2	1.60E+05	0.7418	0.6493	23.7	226.7	X	X	X	X		X	X	X	X	X	X
10	2	1.60E+05	0.4901	0.5409	67.1	320.2	X	X	X	X	X	X	X	X	X	X	X

X Indicates selected input

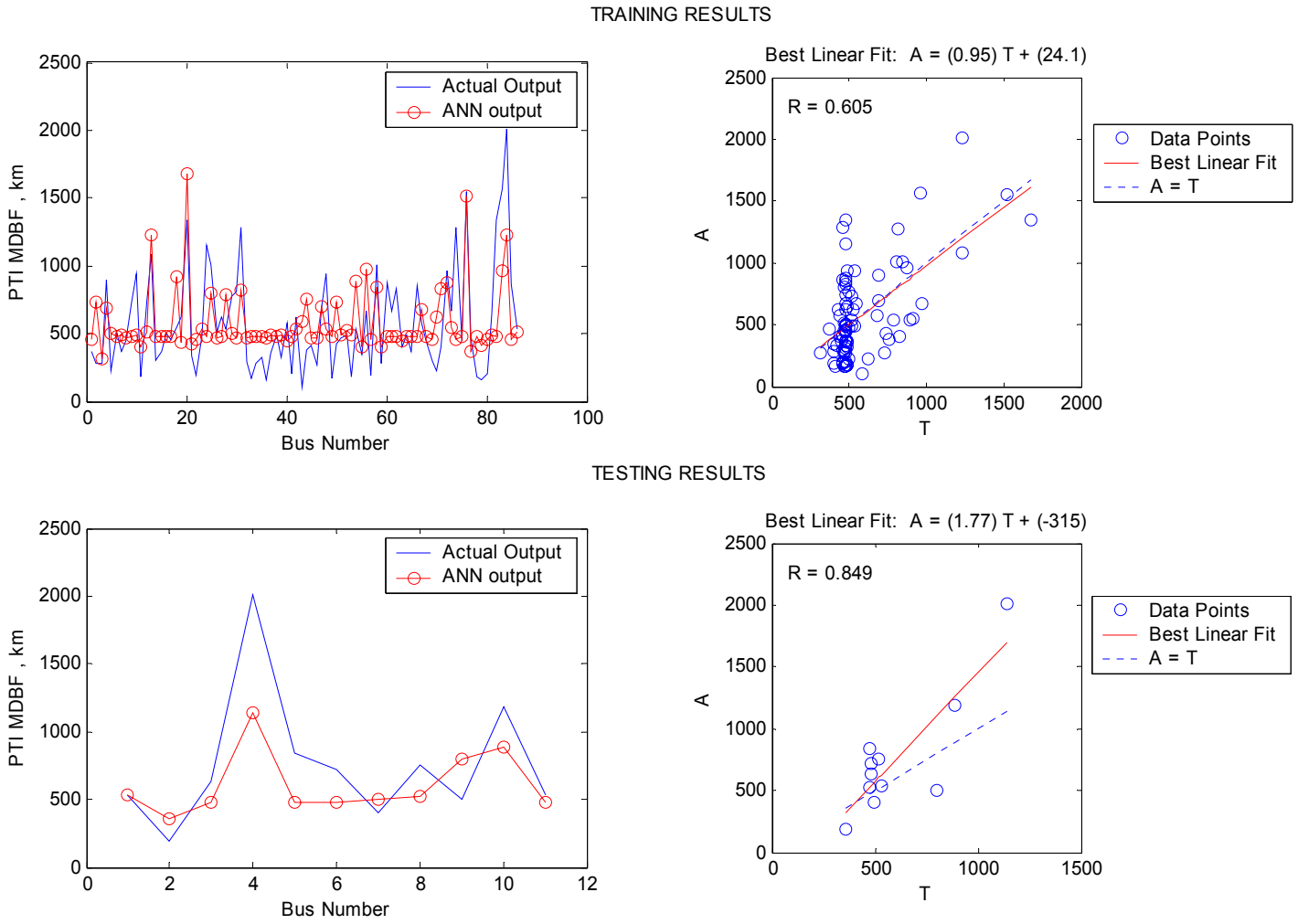

Figure **5.23**: Comparison plots for PTI-MDBF on training and test sets: Method-1 (N2PFA).

Table 5.20: Results for PTI reliability: Method-2 (RF5)

c_0 (km)	c_i (km)	H	WB	GC	SLW-T	P	D	D-MIL	O-MIL	MSE (km^2)	R-train	R-test	Mean % Error	MAE (km)
499.4468	0.6076	25.3080	-3.0745	-2.2831	-16.6700	11.8180	-16.6130	3.5650	2.2047	7.197E+04	0.5783	0.8535	41.05	225.32

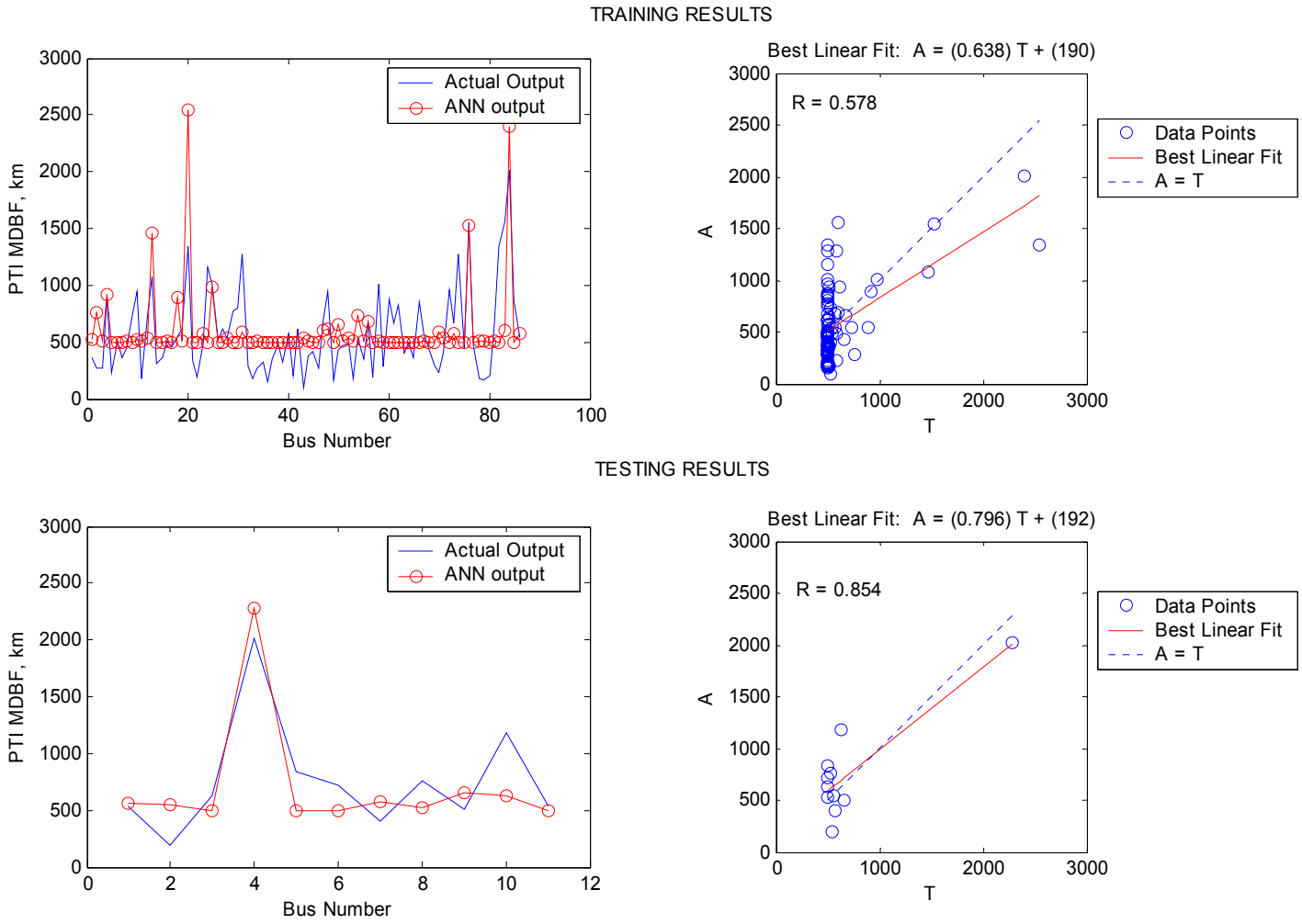

Figure **5.24**: Comparison plots for PTI-MDBF on training and test sets: Method-2 (RF5).

From the results of Method-2 (RF5), given in Table **5.20**, the ranking of the inputs as per decreasing order of relevance is H, SLW-T, D, P, D-MIL, WB, GC and O-MIL. Comparing this list with results from Method-1 (N2PFA), we find that variables that rank highly in Method-2, such as SLW-T, D, P and D-MIL, are not pruned at all while H is rejected only once. Variables that rank low in Method-2 such as GC, O-MIL and WB are deleted more often. Input W that was rejected by ITSS is also pruned twice. Overall, it is seen that both methods give comparable performance though Method-2 based ANN is simpler in configuration.

Reliability depends a lot on the quality of manufacturing and material used and not just on design features of a product. For the truck industry, the influence of these two factors on failures can be as high as 45% [**32**]. Inputs that give a measure of the manufacturing quality of buses were not available and hence could not be used in this analysis. It is felt that inclusion of such inputs has the potential to further improve the PTI-MDBF prediction models. As mentioned in Sub-section **2.5.5**, not many studies have been conducted on analyzing the influence of vehicle design parameters on reliability and this makes comparison of the results obtained in this study very difficult. In this study, SLW-T stands out as one of the important variables affecting PTI-MDBF and it matches well with the predictions by Gaver [**48**]. Further, engineering intuition tells us that inputs such as SLW-T, D and P can influence reliability by affecting the vibration that a bus encounters on PTI durability track. The importance of H is not that self-evident. One possible reason could be the fact that a larger H could mean a high center of gravity. Such a vehicle is normally expected to be equipped with a stiffer stabilizer bar that can help suppress body roll on one-wheel bumps seen on durability tracks.

5.1.6 NTD Reliability

This part of the study was affected by lack of transit data on reliability. Since NTD classifies data on a transit agency basis and not on a bus model basis, only 14 sets of data were available. These pertained to a total of 7 transit agencies and 7 bus models in four different states. Even though the data set was fairly small, the analysis procedure was kept the same to test its effectiveness. The whole data set was divided into 3 sub-sets: training set (10 samples), validation set (2 samples) and test set (2 samples). Since only two samples were used for testing, using R-test as an evaluation criterion can be misleading.

Using correlation, a list of 10 inputs was selected (Appendix B). These include active fleet (ACT-FL), city elevation (ELEV), service area (SERV-MIL), service population (SERV-POP), average operating speed (AVG-SP), maintenance (labor) hours per bus (LHPB), total number of maintenance facilities (T-FAC), bus spare ratio in percentage (PER-SP), average mileage (AVG-MIL) and MDBF at PTI (PTI-MDBF). ITSS reduced this further to five inputs namely AVG-SP, LHPB, PER-SP, AVG-MIL and PTI-MDBF. The results obtained from Method-1, using the 10 inputs selected by correlation method, are given in Table 5.21. Comparison plots between actual NTD-MDBF and the MDBF predicted by the ANN are shown in Figure 5.25. Since the magnitudes of NTD-MDBF are large (mean = 21273 km), they were normalized using their mean value in a manner similar to that carried out for inputs before being used in Method-2. This aids the training algorithm in reaching an optimal solution. Results

obtained from Method-2 are given in Table 5.22 and comparison plots for outputs (predicted and actual) are shown in Figure 5.26.

The results of Method-2 (RF5), given in Table 5.22, provide a means to evaluate the influences of the different inputs on NTD-MDBF. Neglecting the third term for which c_i is very small, PTI-MDBF has the highest exponent of all five input variables. It means that PTI-MDBF is the most relevant input variable for predicting MDBF at transit agencies (NTD-MDBF). This clearly brings forth the utility of PTI's reliability testing for both bus manufacturers and transit agencies. The results of Method-1 compare well with those from obtained using Method-2. PTI-MDBF was never pruned by Method-1. Variables such as ELEV, SERV-MIL and SERV-POP are rejected by Method-1 very often. This compares well with ITSS that rejected these three inputs as well. However, Method-1 never rejects ACTV-FL that was rejected by ITSS but rejects LHPB that was selected by ITSS. One possible reason could be the fact that the correlation coefficient between PTI-MDBF and ACTV-FL is 0.61 in the data set used for developing the model.

Singh and Kankam [29] found that probability distributions underlying the miles between defects for buses appear to be exponential or Weibull with a shape parameter less than unity. This agrees well Figure 5.22 that indicates a constant failure rate, i.e., exponential distribution. As per Singh and Kankam [29], older buses had lower reliability than newer buses. The two dominant terms (largest c_i) in the expression for NTD-MDBF given in Table 5.22 have negative exponents for AVG-MIL. This shows that, as expected, older buses (with higher AVG-MIL) are less reliable than newer buses as their NTD-MDBF values will be lower.

Table 5.21: Results for NTD reliability: Method-1 (N2PFA)

Run No.	HLN	MSE (km^2)	R_train	R_test	Mean % Error	MAE (km)	ACT-FL	ELEV	SERV-MIL	SERV-POP	AVG-SP	LHPB	TOT-FAC	PER-SP	AVG-MIL	PTI-MDBF
1	3	4.03E+05	0.9420	1.0000	2.66	580.3	X	X	X	X	X	X	X	X	X	X
2	4	8.94E+05	0.8877	1.0000	7.10	824.0	X	X	X	X	X	X	X	X	X	X
3	1	1.18E+06	0.8224	1.0000	3.38	908.1	X	X			X		X		X	X
4	4	4.11E+06	0.8270	1.0000	10.71	1973.1	X	X		X	X		X	X	X	X
5	3	3.50E+06	0.9470	1.0000	13.78	1358.7	X	X	X	X	X	X		X	X	X
6	4	4.81E+05	0.9687	1.0000	4.54	692.5	X	X	X	X	X	X	X	X	X	X
7	3	9.76E+05	0.9783	1.0000	2.91	811.5	X	X	X	X	X		X		X	X
8	4	1.02E+06	0.9150	1.0000	6.73	1009.0	X	X	X	X	X	X	X	X	X	X
9	4	1.08E+07	0.8683	1.0000	24.57	2900.6	X				X	X	X			X
10	4	1.03E+07	0.9038	1.0000	9.75	2657.9	X			X	X		X	X	X	X

X Indicates selected input

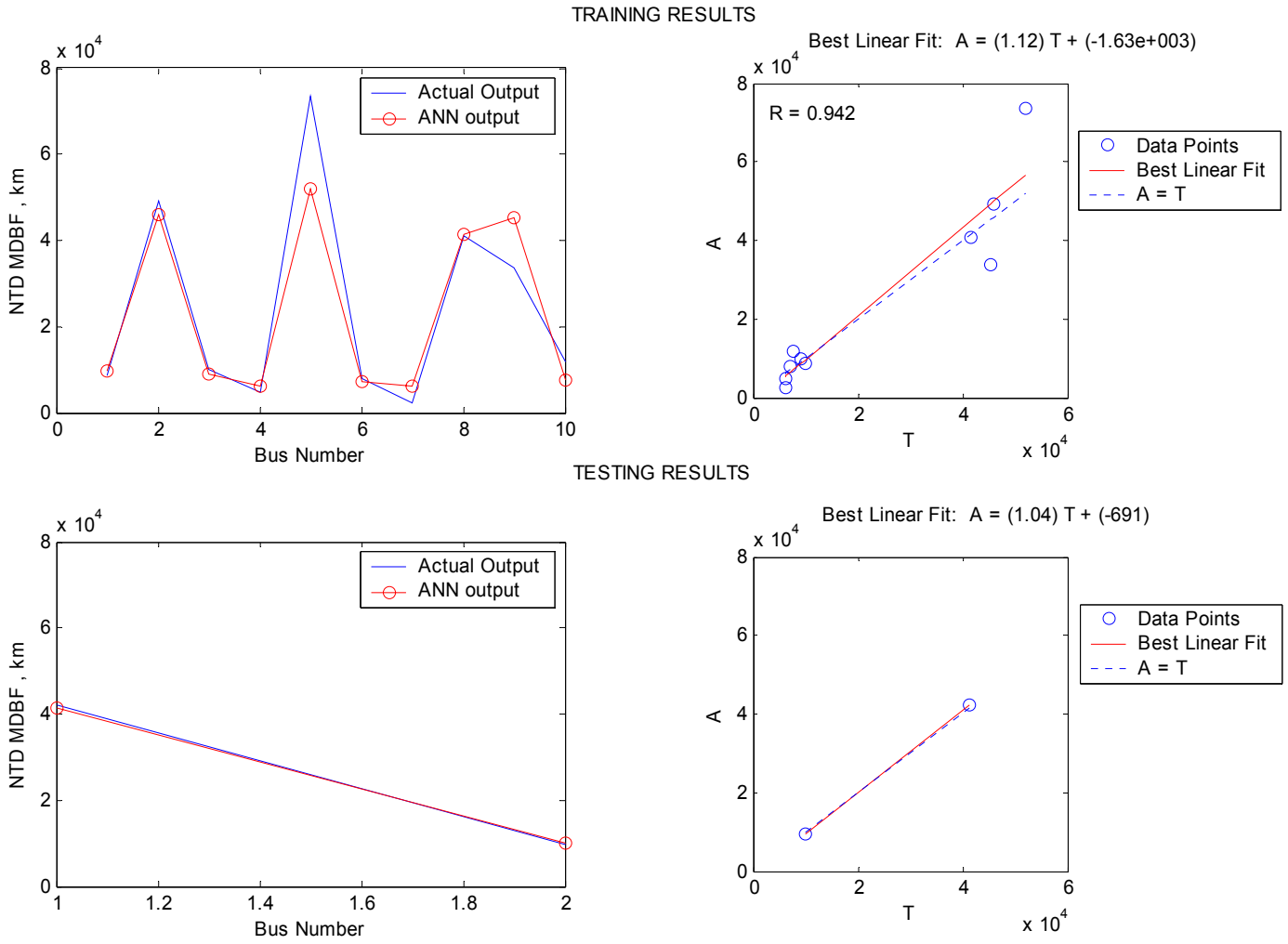

Figure **5.25**: Comparison plots for NTD-MDBF on training and test sets: Method-1 (N2PFA).

Table 5.22: Results for NTD reliability: Method-2 (RF5)

c_0 (km)	c_i (km)	AVG_SP	LHPB	PER_SP	AVG_MIL	PTI-MDBF	MSE (km^2)	R-train	R-test	Mean % Error	MAE (km)
664.1000	946.3793	0.5471	2.2734	1.1447	-4.1747	4.9770	9.498E+05	0.99998	1.0000	7.26	748.44
	317.5209	-0.5442	3.3002	-0.0505	-0.0076	7.1583					
	0.0502	5.5297	4.8009	-0.3995	-3.2026	-2.2570					
	118.2431	-4.4185	-1.7351	1.8199	3.7946	-6.7146					

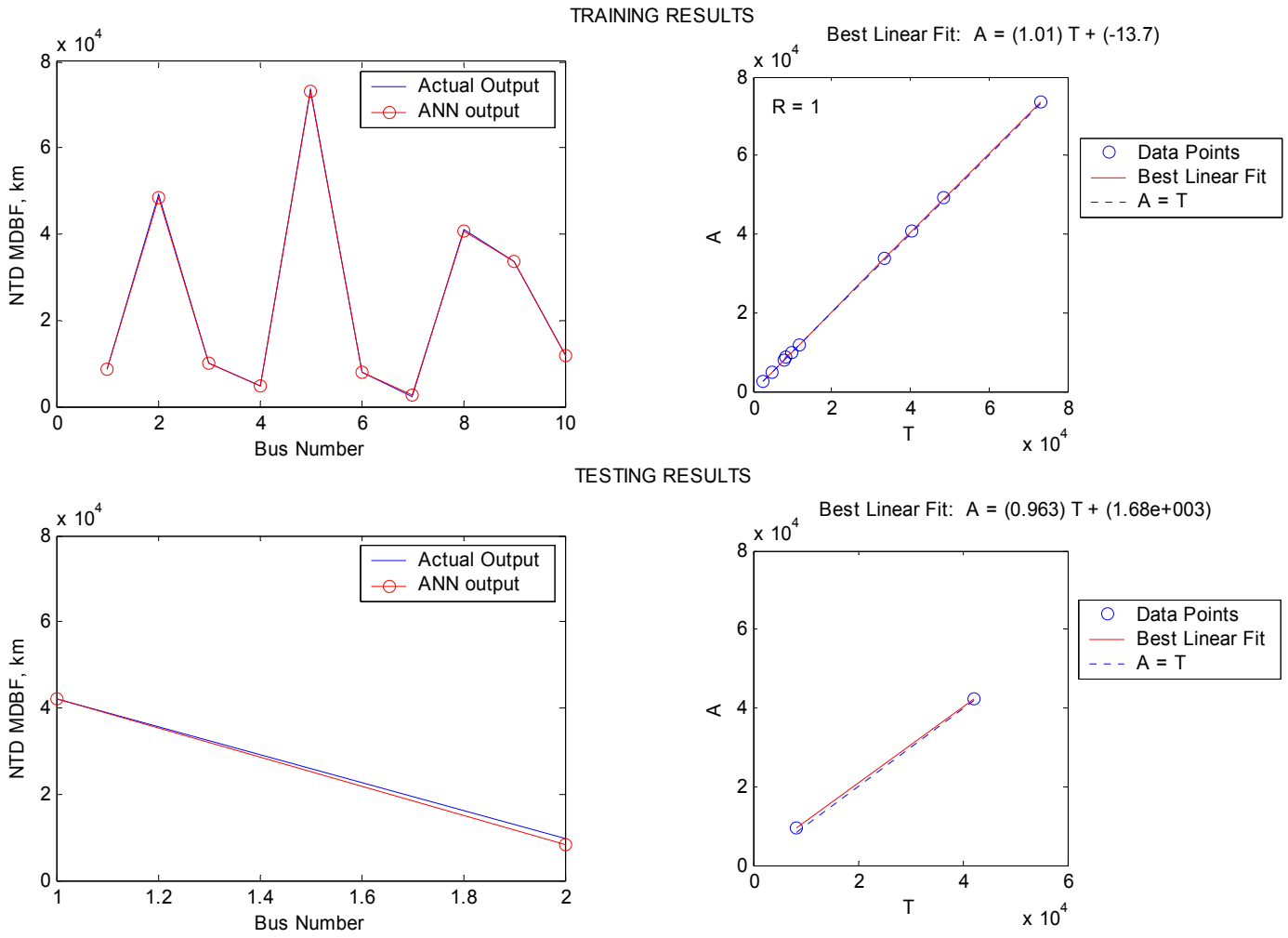

Figure **5.26**: Comparison plots for NTD-MDBF on training and test sets: Method-2 (RF5).

This study extends the results obtained by Klinikowski *et al.* [47] on the relationship between in-service failures and failures at PTI test track for different bus models. In their analysis, they used failure data from two transit agencies for three different bus models with each transit agency submitting data for ten buses of a specific model. The present study is based on a much larger sample - 7 transit agencies, 7 bus models and a total of 218 buses. While both studies reached the same conclusion that there is a good correlation between in-service failures (NTD) and test track failures (PTI), this study additionally developed a mathematical prediction model for NTD-MDBF that included not only PTI-MDBF but also other transit agency related input variables such as AVG-SP, LHPB, PER-SP and AVG-MIL.

5.2 Inverse Modeling

Design engineers and regulatory authorities are often interested in finding bus designs that can achieve a desired on-road performance objective. A straight-forward means of achieving this goal is to invert the forward models developed in Section 5.1 using the method described in Section 4.4. This section discusses the results obtained from two such sample inversions - single stage inversion (only F^{-1}) using fuel economy on the ART cycle (PTI-ART) as the performance measure and a two-stage inversion (both F^{-1} and G^{-1}) using fuel economy as the performance measure. In both cases, forward models obtained from Method-2 (RF5) were inverted. However, similar inversions can be done with Method-1 (N2PFA) models as well.

5.2.1 Single-stage Inversion

A hypothetical situation was considered wherein a bus manufacturer has two bus designs in production that have a fuel economy on the ART cycle of 2.30 km/L (Bus-1) and 2.34 km/L (Bus-2) respectively. The manufacturer intends to arrive at a bus design that can provide a 10% increase in fuel economy than what is achieved by Bus-2. Since the fuel economy values of the two buses are very close to each other, it may not be readily apparent to the bus manufacturer as to which original design offers more promise. A sample simulation was hence carried out to search for a bus configuration that would give a desired ART fuel economy of 2.57 km/L (10% increase). As mentioned in Section 4.4, inversions were obtained starting from each known bus which for this case was two in number. Finally, the inversion that was closest to a known bus in terms of Euclidean distance was selected based on ease of manufacturing. The final results obtained by inverting the forward model obtained in Sub-section 5.1.1 are as follows:

Table 5.23: Optimal bus configuration for a desired fuel economy performance

Parameter	Original Configuration: Bus-1	Inversion Obtained from Bus-1	Original Configuration: Bus-2	Inversion Obtained from Bus-2
Width (m)	2.59	2.44	2.44	2.43
Height (m)	3.33	2.83	2.84	2.81
Rear Overhang (m)	3.12	3.19	2.37	2.38
Ground Clearance (m)	0.24	0.24	0.14	0.14
SLW Total (kN)	101.10	93.87	90.78	90.20
Axle Ratio	4.33	4.36	4.88	4.88
Engine Power (kW)	167.85	160.93	134.28	133.79
ART Fuel Economy (km/L)	2.30	2.57	2.34	2.57

As seen from the above table, both inversions are capable of achieving the desired fuel economy of 2.57 km/L. However, in terms of the Euclidean distance (in normalized input space) between original bus configurations and the obtained inversions, the values were 0.0381 and 0.0003 respectively for Bus-1 and Bus-2. The inversion results clearly show that the bus manufacturer would probably find it more convenient to modify Bus-2 to achieve the desired fuel economy goal. Since changes in most of the other inputs are negligible, the results seem to indicate that the easiest way of achieving the desired fuel economy is to modify the seated load weight and engine power of Bus-2. It needs to be noted here that the objective function used in this study (minimum Euclidean distance) is one out of many such desirable objective functions. Vehicle designers can easily adapt the inversion method presented in this thesis to other objective functions.

5.2.2 Two-stage Inversion

In this simulation, the objective was to get a bus design that can give an on-road fuel economy of 2.44 km/L (equivalent to 5.75 miles per gallon). This was achieved through a two-stage inversion. In the first stage, NTD fuel economy model obtained in Sub-section **5.1.2** was inverted resulting in a value for PTI fuel economy on the ART cycle (PTI-ART). Starting from a known sample from the training set used to develop the NTD fuel economy model, the following inversion was obtained.

Table 5.24: Inversion of NTD fuel economy model

Parameter	Inverted Configuration	Existing Sample
Average Speed (m/s)	13.16	13.18
Mileage per annum (km)	1559.10	1559.10
Average Mileage (km)	4834.00	4827.00
PTI-ART (km/L)	1.78	1.76
NTD Fuel Economy (km/L)	2.44	2.62

In the second stage, PTI fuel economy model on ART cycle given in Sub-section 5.1.1 was inverted to give a bus design capable of achieving 1.78 km/L. The resulting bus configuration and the closest existing bus configuration in terms of Euclidean distance are given below.

Table 5.25: Inversion of PTI fuel economy model – ART cycle

Parameter	Optimal Bus Configuration	Closest Existing Bus
Width (m)	2.60	2.59
Height (m)	3.04	3.02
Rear Overhang (m)	2.99	3.00
Ground Clearance (m)	0.23	0.23
SLW Total (kN)	146.30	145.87
Axle Ratio	4.56	4.56
Engine Power (kW)	179.33	179.04
ART Fuel Economy (km/L)	1.78	2.15

The closest bus configuration had a PTI-ART fuel economy of 2.15 km/L. Hence, if the values of the bus design parameters are maintained as per the optimal configuration given in Table 5.25 and the inputs pertaining to the operation of the bus at the transit agency are

as per the inverted configuration given in Table 5.24, then, one can realize the desired on-road fuel economy of 2.44 km/L. If specific values for the inputs that characterize operation at transit agency are desired, then, appropriate constraints on those inputs can be placed while doing the first-stage inversion (NTD model inversion). Two-stage inversions presented in this sub-section can be useful for transit agencies in determining the type of bus models to procure. Bus manufacturers can use the same information to design buses that can achieve a desired on-road performance.

5.3 Multi-objective Optimization

Vehicle design engineers are often confronted with problems which require a design that can simultaneously achieve two or more objectives. In many cases, the objectives place conflicting requirements on vehicle design parameters. In this study, forward models were generated for four performance measures, namely fuel economy, acceleration, pass-by noise and reliability. However, as the models for pass-by noise and reliability were not highly accurate, simultaneous inversion of only two forward models - fuel economy and acceleration - was carried out. While this in essence rendered the example considered here as a two-objective optimization, it needs to be noted that inversion using Gembicki's Goal Attainment method can handle any number of objectives provided forward models are available for each objective.

The problem considered here was to generate a bus design that can achieve a given acceleration performance while achieving or surpassing another requirement placed on fuel economy. A sample simulation was carried out in this study wherein two

objectives - one on ACC-16 and one on PTI-ART - were placed and a bus design meeting these objectives was sought. Simulation was done as per Gembicki's Goal Attainment method explained in Sub-section **4.5.3**. The goals were selected as a fuel economy of 3.4 km/L on ART cycle and an acceleration capability of 1.70 m/s^2 at a speed of 16 km/hr, i.e., ACC-16.

Inversion of the two forward ANN models - Acceleration at 16 km/hr and PTI fuel economy on ART cycle- simultaneously by Gembicki's method resulted in the bus design given in Table **5.26**. Models developed using Method-2 (RF5) were used in this simulation. However, a similar simulation can be easily carried out for models generated using Method-1 (N2PFA) by using the appropriate neural networks. Of the nine inputs listed in the Table **5.26**, five inputs - H, GC, SLW-T, AR and P - were common to both forward models, W and RO were specific to fuel economy model while D and WB were specific to the acceleration model. In the process of carrying out this inversion, all 9 input variables were allowed to be modified.

Goal attainment method was able to achieve both the objectives, namely a fuel economy of 3.40 km/L on ART cycle and an ACC-16 of 1.70 m/s^2. Comparing the results given in Table **5.26** with the range of input values given in Tables **3.1** and **3.2**, it is evident that the optimal design obtained is realistic. As expected, the design indicates that for the achieving the relatively high values of desired fuel economy and acceleration, a bus with a small frontal area and weight with high engine power and a low numerical gear ratio would be needed.

Table 5.26: Results from multi-objective optimization

Parameter	Optimal Bus Configuration
Width (m)	2.19
Height (m)	2.59
Wheelbase (m)	4.95
Rear Overhang (m)	3.79
Ground Clearance (m)	0.23
SLW Total (kN)	62.30
Axle Ratio	3.06
Engine Power (kW)	207.67
Engine Displacement (cm^3)	7531
ART Fuel Economy (km/L)	3.40
ACC-16 (m/s^2)	1.70

5.4 Comparison with Other Methods

The term 'residual' refers to the difference between actual output and the predicted (ANN) output. The residual plots for the models developed in Section 5.1 are given in Appendix E for both training and test sets. Since most of the residual plots do not exhibit any evident pattern, it seems that the models are adequate representations of the underlying datasets. A summary of all model relationships obtained in Section 5.1 using Method-2 is given in Appendix F.

Linear regression and Decision (Regression) Tree are two of the commonly used methods in literature for modeling functional relationships. Hence, it is useful to compare the two methods used in this study with these methods. Noise was selected as the

performance measure for comparison since it presented probably the most challenging problem. While one could potentially use all 21 inputs listed in Table **3.2** to generate noise models using linear regression and decision tree (DT), such a procedure would not provide the means for a uniform comparison amongst all four methods. Hence, the nine inputs selected by the correlation method were used to develop noise models. The inputs include width (W), height (H), wheelbase (WB), rear overhang (RO), ground clearance (GC), seated load weight - total (SLW-T), axle ratio (AR), engine power (P) and engine displacement (D). Inputs and outputs were normalized in a manner similar to that used in Method-1 (N2PFA) wherein all inputs were centered with respect to their mean values and then divided by their respective standard deviations. Linear regression and decision tree models were developed using the Statistical Toolbox available in MATLAB. The decision trees were not pruned and the minimum number of observations needed for splitting at impure nodes was kept as 3. The results from all four methods on CON-NOISE-R and ST-NOISE-R performance measures are given in Table **5.27** for the same test set of 11 buses used in Sub-section **5.1.4**.

The results show that the two methods used in this study perform better than both linear regression and decision tree on all four measures of performance given in Table **5.27**. For ST-NOISE-R, the MSE values obtained using regression and DT are almost twice as high as those from Methods-1 and 2. This is particularly important as decibel scale is logarithmic and not linear. The case is similar for CON-NOISE-R, where both Methods-1 and 2 perform much better than DT. However, in this case regression seems to perform better than in ST-NOISE-R.

Table 5.27: Performance comparison of regression and DT with Methods-1 and 2

	CON-NOISE-R				ST-NOISE-R			
	Regression	DT	Method-1	Method-2	Regression	DT	Method-1	Method-2
MSE $(db(A))^2$	4.5384	7.7739	3.4781	3.4738	7.1706	7.7841	4.3020	3.9119
R-test	0.5823	0.5043	0.5909	0.6333	0.4902	0.5303	0.6770	0.7068
Mean % Error	2.2351	3.3111	1.8020	1.7446	2.5846	2.8187	2.0802	1.7463
MAE (db(A))	1.6835	2.4864	1.3595	1.3161	2.0054	2.1727	1.6162	1.3640

5.5 Rule Extraction from Method-1

The rule extraction methodology in Method-1 (N2PFA) is based on piece-wise linearization of the 'Tansig' activation function. If 'Tansig' is approximated by a 5-piece linear function, then the number of rules generated is given by 5^H where H is the number of neurons in the hidden layer. In this study, the minimum number of hidden neurons was found to be two for three cases. The include NTD fuel economy, CON-NOISE-R and PTI reliability models. However, even in these cases the number of rules generated would be twenty-five. The number of rules tends to be unwieldy as the ANN model becomes more complex and has more hidden neurons.

Setiono *et al.* [60] claim that the accuracy of the five-piece approximation is practically identical to the accuracy of the pruned networks. To check the validity of their claim with respect to the models generated in this study, a sample comparison was made on the model for acceleration at 16 km/hr (ACC-16). Figure 5.27 shows the comparison plots on the test set of 11 buses. The statistics after REFANN linearization are given below:

MSE $(m/s^2)^2$: 0.0229

MAE (m/s^2): 0.1120

These results compare very well with results from run number-8 given in Table 5.10 and hence confirm the assertion made by Setiono *et al*.

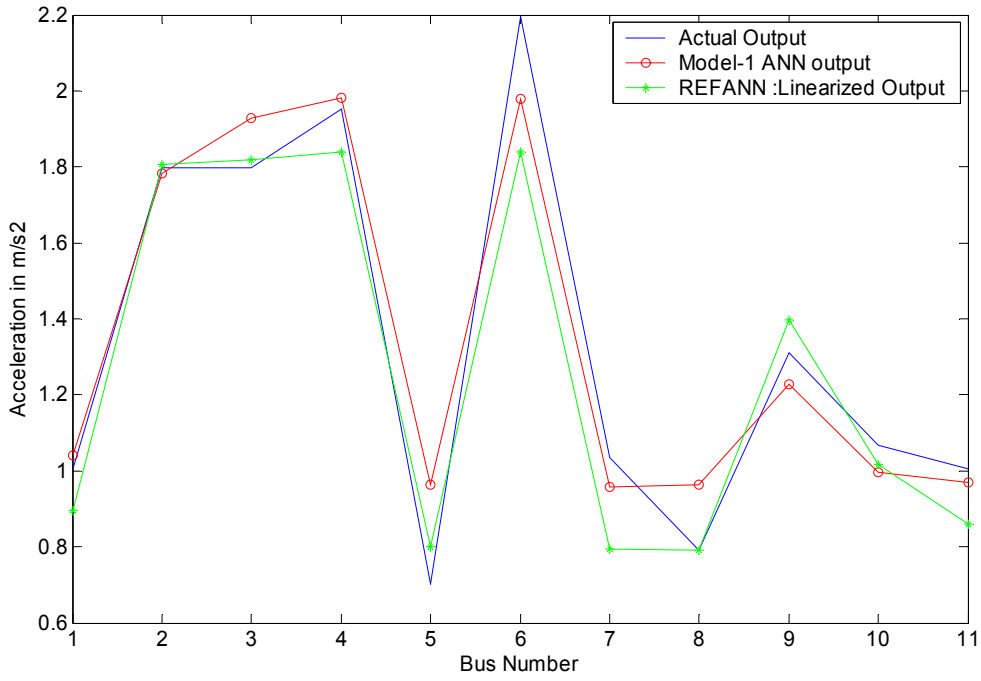

Figure **5.27**: Effect of 5-piece linearization of Tansig under REFANN.

5.6 Summary

In this study, two ANN-based methods were used to generate models for four performance measures - fuel economy, acceleration, pass-by noise and reliability. PTI models were developed for all 4 measures while NTD models were developed for fuel economy and reliability. The results from the two methods compare well with each other especially with regards to the accuracies of the models and rankings of the most relevant and the least relevant input variables. However, with regards to inputs with intermediate relevance the two methods sometimes differ. One reason for the same could be the fact that Method-1 (based on N2PFA/REFANN) has an in-built method for selecting inputs

while Method-2 uses the ITSS method for selecting inputs. ITSS method is a filter approach that is independent of RF5 algorithm. Another possible reason for the seeming difference in the ranking of the inputs is that one needs to be a bit cautious while using the number of times an input is rejected as a criterion for deciding relevance in Method-1. Despite the fact that simulation was carried out a large number of times and only the best ten simulations were used, there is still a small possibility the original initialization (random) may play some part in the solution reached by Method-1.

Results from inversion modeling indicate that the methods presented in this study are able to achieve the desired performance goals with a high degree of accuracy. A comparison with two of the commonly used methods - linear regression and decision tree - in literature shows the promise offered by the two methods presented in this thesis. Appendix F lists all model equations developed in this study using Method-2.

Chapter 6

Conclusions and Suggestions for Future Work

Heavy vehicles play a major part in any modern economy. Historically, heavy vehicles have been governed through prescriptive or Design Based standards (DBS) that regulate vehicle performance by placing limits on vehicle weights and dimensions. Since such an indirect control of vehicle performance has some major disadvantages, efforts are ongoing in various parts of the world to develop Performance Based Standards (PBS) that directly place limits on vehicle performance measures. However, to do this successfully, vehicle design engineers and regulatory authorities require an in-depth knowledge of the nature of the relationships between vehicle design parameters and vehicle performance on a test track and between vehicle performance in traffic and vehicle performance on a test track.

Over the last few decades, researchers have spent a lot of effort investigating the influence of vehicle design parameters on performance. However, there still are a number of shortcomings that need to be addressed:

1) Regression and decision trees have been the most commonly used modeling methods. The former makes an assumption on the nature of the functional relationship while the latter can result in highly complex trees when axis-parallel hyperplanes (i.e., splits based on one input variable) are unsuitable.
2) Artificial Neural Network (ANN) has seen some limited use in vehicle performance modeling. However, in the absence of in-built rule-generation

mechanisms and a rigorous method to determine the number of hidden neurons required, ANN models are like black-boxes. This means that their usage in safety critical applications is severely hampered.

3) Very little work has been done on understanding the relationships between vehicle performance on a test-track and vehicle performance under traffic conditions.
4) Practically no studies exist on the influence of bus design parameters on reliability performance.
5) The best whole-vehicle pass-by noise model (Fry and Jennings) in literature, as of year 2003, is data intensive and complex. Moreover, it gives out very few details on the relevant parameters that were selected largely based on expert opinion.

Based on the above background, the main goals of this study were:

1) To develop and validate modeling methods that could help understand the complex relationships between vehicle design and performance both under laboratory conditions and in use at transit agencies.
2) To alleviate the shortcomings in the literature as mentioned above and to compare the results of this study with those already available.
3) To investigate the utility of PTI testing and to make recommendations on improving its effectiveness.
4) To develop methods that can be used to arrive at vehicle designs that are capable of achieving the desired performance objectives.

In this study, two ANN-based methods were used to develop mathematical models for four performance measures, namely fuel economy, acceleration, pass-by noise and reliability using the two stage approach discussed in Section 3.1. Data from PTI were used to generate the vehicle system models while NTD data were used for traffic system models. NTD data were available only for fuel economy and reliability. Since vehicle designers are often interested in knowing designs that can achieve a given set of objectives, inversion models based on non-linear programming and Gembicki's Goal Attainment method were also developed. The following sections discuss the main conclusions of this research and some suggestions for extending this work further.

6.1 Conclusions

6.1.1 Modeling Methods Used in this Study

1) The two ANN-based models - Method-1 (N2PFA/REFANN) and Method-2 (RF5) - presented in this study give results that either match the results given in literature or closely follow engineering intuition. This is especially true for fuel economy and acceleration wherein the models are accurate (Sub-sections 5.1.1 and 5.1.3). Based on the models results for fuel economy and acceleration, one can confidently validate the accuracy of the two methods presented in this thesis. This opens the way for application of these two methods to modeling other performance measures wherein existing knowledge may be inadequate.

2) Both methods have in-built mechanisms for arriving at the required number of hidden neurons and can be interpreted in the form of rules. This alleviates the black-box nature of neural networks and makes the methods suitable for modeling safety related performance measures.

3) The rankings of various input variables as per their relevance show that Methods-1 and 2 are very similar with regards to the variables at either extreme. The two, however, sometimes differ in their evaluation of inputs with intermediate relevance. The author feels that this may be due to three factors. Firstly, the two methods differ in the way the inputs are selected. Method-1 uses a single-stage filter method based on correlation and a wrapper method (N2PFA) that is in-built into the ANN algorithm. On the other hand, Method-2 uses a two-stage input selection procedure based on correlation and ITSS. Secondly, using the number of times a variable is rejected as a measure of its lack of relevance has its limitation. Even if the simulation is carried out a large number of times and only the ten best simulation results are used, there is still a small possibility that the original initialization (random) may influence the solution reached by Method-1. Lastly, the inputs used in this study are not totally independent of each other even though the correlation method of input selection ensures that they are not highly correlated.

4) The performance capabilities of Methods-1 and 2 appear to be better than the two commonly used modeling methods - linear regression and decision (regression) tree (Section **5.4**). Unlike regression that assumes the nature of

the functional relationships, ANN-based methods do not need to make any such assumption.

5) Testing agencies can use the forward modeling approach explained in this study as an alternative method for simulating vehicle performance. Further, they can investigate the modifications that are needed to design more effective testing procedures. One possible way of doing this would be to make the testing methods more focused on the input variables of high relevance. Vehicle test engineers at bus manufacturing facilities can accrue similar benefits.

6) The inversion models developed in this study were able to successfully arrive at bus designs capable of achieving one or two objectives (Sections **5.2** and **5.3**). Extension to the multi-objective optimization case is relatively straight forward. The inversion method presented here provides vehicle designers with a useful tool for evaluating alternative bus designs at the design stage. Regulatory authorities can use inverse modeling in drafting performance-based standards that are optimized to best benefit both society and vehicle manufacturers.

6.1.2 Results Obtained on the Four Performance Measures

1) The effect of vehicle weight (SLW-T) on fuel economy under test track conditions is nonlinear (Sub-section **5.1.1**). Zub [**16**] and Gajendran and Clark [**17**] conclude that fuel economy of buses decreases linearly with vehicle

weight. However, their results are only valid when vehicle weight is changed by a small amount.

2) PTI-ART fuel economy stands out as the most important input for predicting NTD fuel economy (Sub-section **5.1.2**). This part of the study used data from 13 transit agencies and covered a total of 13 bus models and 1075 buses. The author, to the best of his knowledge, understands that this research is the first such large scale study undertaken that not only compared fuel economies of buses on a test track (PTI) and at transit agencies but also generated mathematical prediction models. Results also indicate that for older buses with high mileage, the average operating speed (AVG-SP) and average mileage (AVG-MIL) may be more relevant than PTI-ART. This is expected for vehicles that may be close to the end of their useful life span.

3) This study confirms that vehicle weight is the most important factor influencing acceleration performance of buses. At high speeds (64 km/hr), it is seen that acceleration is proportional to the ratio of engine power to vehicle weight (Sub-section **5.1.3**). P/W ratio is very commonly used as first order determinant of acceleration performance. However, results from this study show that it is mainly true at high speeds when the assumption of full engine power availability throughout the acceleration phase is more valid as vehicle speed and hence engine speed do not change appreciably.

4) Most analytical whole vehicle pass-by noise models are only as accurate as human experts ($\pm$3 dB(A)). Fry and Jennings' pass-by noise model, claimed to be the most accurate as of year 2003, has an accuracy of $\pm$1.4% and $\pm$1.1

dB(A). The two methods used in this study, namely Method-1 (N2PFA) and Method-2 (RF5), result in models that achieve comparable accuracies with approximately 1.2% of the number of data samples used to develop Fry and Jennings' model. The models developed in this study are much simpler (Sub-section **5.1.4**) in terms of number of model-stages, number of inputs used and number of hidden neurons employed. Further, unlike Fry and Jennings' model, Methods-1 and 2 are not black-box models.

5) Though the models developed for PTI reliability were not very accurate, both Method-1 (N2PFA) and Method-2 (RF5) were able to mathematically confirm Gaver's assertion that vehicle weight is one of the most important vehicle design parameters affecting reliability (Sub-section **5.1.5**). Additionally, they bring out an interesting result that vehicle height (H) is the most important input variable influencing PTI-MDBF.

6) Methods-1 and 2 were able to develop accurate prediction models for in-service reliability even with the small data set obtained from NTD (Sub-section **5.1.6**). This study confirmed Klinikowski *et al.*'s conclusion, that failures at PTI and in-service failures for a given bus model are highly correlated, on a much larger data set (218 buses from seven transit agencies). Further, this study generated mathematical prediction models for NTD-MDBF which show that PTI-MDBF is the most relevant variable for predicting NTD-MDBF.

6.1.3 The Utility of PTI testing

The results from the NTD models on fuel economy and reliability show that in both cases the inputs variables relevant to PTI testing, namely PTI-ART and PTI-MDBF, stand out as the most relevant variables. This confirms the utility of PTI testing for both transit agencies and bus manufacturers.

6.2 Suggestions for Future Work

In light of the conclusions of this research, the following are some suggestions that the author feels would help in extending this research further.

6.2.1 Recommendations on Modeling Methods

1) After generating the neural network models, the neural networks can be interpreted as oblique decision trees. Oblique decision trees use combination of the input variables (non axis-parallel hyper-planes) as the splitting criterion at each node instead of basing it on just one input variable. This can result in much simpler decision trees for some complex problems [61]. Further, such a step has the potential to combine the best capabilities of two different methods, namely ANN and decision tree.
2) Models that incorporate driver and road inputs can be developed using appropriate performance measures.

6.2.2 Recommendations for Improving Accuracy of the Results

1) More data from transit agencies need to be collected. A larger data set would make the NTD fuel economy and NTD reliability models more accurate. In this regard, PTI efforts are currently underway to obtain data directly from transit agencies [83].
2) Reliability data from transit agencies can be collected at a sub-system level such as engine, transmission, body, electrical system and suspension instead of at a vehicle level. This would greatly enhance the understanding of the correlation between PTI and NTD reliabilities.
3) A much more accurate pass-by noise model can be developed by using input parameters pertaining to power-train, air intake system, exhaust system, engine compartment noise mitigation strategies and tires.

6.2.3 Recommendations for PTI

1) Sub-section 5.1.2 indicates that PTI-ART is the most relevant input variable affecting NTD fuel economy. However, it is also seen that under certain circumstances such as a vehicle towards the end of its useful lifespan, variables such as average operating speed (AVG-SP) and average mileage (AVG-MIL) may be more relevant that PTI-ART. At present, PTI fuel economy tests are conducted at a very early stage in the durability testing. If an additional fuel economy test is conducted at the end of the accelerated durability test, then it would generate very good data that can be used to study

the effect of average mileage of the bus on fuel economy. The author believes that models that mathematically correlate PTI fuel economy with both bus design parameters and the age of a bus (in terms of mileage) would be very useful for transit agencies in making their purchase decisions on available bus models.

2) This study compared PTI-MDBF with NTD-MDBF. MDBF is calculated based on all failures (major and minor). It would be interesting to compare the two values of MDBF for minor and major failures. However, this poses some challenges. Firstly, PTI collects data on four classes of failures while NTD collects data on two classes -major and minor failures- that need to be reported only when they affect the schedule of a bus. Secondly, there is a distinct difference in the way major failures are defined at PTI and at NTD. While the former bases the evaluation on severity of the problem, the latter focuses on the influence of the failure on bus operation under revenue service. For example, a problem with the door system is a major failure under NTD while it may not necessarily be the case under PTI testing. Lastly, some systems such as fare-boxes and wheel chair lifts, that are very important in revenue service, do not get severely tested under PTI system of accelerated testing that focuses mainly on vehicle body and suspension. Hence, it is recommended that PTI try to align its reliability data collection procedure with that presently used by NTD. This would help transit agencies compare the two on a one-to-one basis (Sub-section **3.3.1**).

Bibliography

1. American Public Transportation Association (APTA), "Public Transportation Fact Book", 57th Edition, Published by APTA, Washington DC, USA, April 2006.

2. J. Edgar, F. Calvert and H. Prem, "Performance Standards for Heavy Vehicles in Australia", National Road Transport Commission, Melbourne, Australia, September 2001.

3. Road Transportation Association of Canada (RTAC), "Vehicle Weights and Dimensions Study: Technical Steering Committee Report", Canroad Transportation Research Corporation, Ottawa, Canada, December 1986.

4. J. York and T.H. Maze, "Applicability of Performance-Based Standards for U.S. Truck Size and Weight Regulations", Proceedings of Semisesquicentennial Transportation Conference, Session-5, Center for Transportation Research and Education (CTRE), Iowa State University, Ames, Iowa, May 1996.

5. A. Germanchev and L. Bruzsa, "Hybrid Testing Method to Prove the Compliance of Heavy Vehicle", Proceedings of the 9th International Symposium on Heavy Vehicle Weights and Dimnesions (9ISHVWD), pp. 200-208, Penn State University, State College, PA, June 2006.

6. L. Pelkmans, D.D. Keukeleere, H. Bruneel and G. Lenears, "Influence of Vehicle Test Cycle Characteristics on Fuel Consumption and Emission of City Buses", 01FL-308, Society of Automotive Engineers (SAE), USA, 2001.

7. G. Genta, "Motor Vehicle Dynamics - Modeling and Simulation", Series on Advances in Mathematics for Applied Sciences - Vol. 43, World Scientific Publishing Co. Pte. Ltd., Singapore, 1999.

8. J.L. Bascunana, "Derivation and Discussion of a Regression Model for Estimating the Fuel Economy of Automobiles", SAE Paper 790654, Society of Automotive Engineers (SAE), USA, 1979.

9. G. Sovran and M.S. Bohn, "Formulae for the Tractive-Energy Requirements of Vehicles Driving the EPA Schedules", SAE Paper 810184, Society of Automotive Engineers, USA, 1981.

10. A.C. Malliaris, E. Withjack and H. Gould, "Simulated Sensitivities of Auto Fuel Economy, Performance and Emissions", SAE Paper 760157, Society of Automotive Engineers, USA, 1976.

11. J. Ramshaw and T. Williams, "The rolling Resistance of Commercial Vehicle Tyres", Supplementary Report 701, Transport and Road Research Laboratory, Crowthorne, Berkshire, UK.

12. J.D. Murrell, "Factors Affecting Fuel Economy", SAE Paper 750958, Society of Automotive Engineers, USA, 1975.

13. A.C. Malliaris, H. Hsia and H. Gould, "Concise Description of Auto Fuel Economy and Performance in Recent Model Years", SAE Paper 760045, Society of Automotive Engineers, USA, 1976.

14. D.I. Gibbons and G.C. McDonald, "Constrained Regression Estimates of Technology Effects on Fuel Economy", Journal of Quality Technology, Vol. 31, No. 2, pp. 235-245, April 1999.

15. K. Schubert, H. Drewitz and P. von Korff, "Optimization of the Drive Train of City Buses", International Journal of Vehicle Design, Vol. 9, No. 1, pp. 67-84, 1988.

16. R.W. Zub, "Transit Bus Fuel Economy and Performance Simulation", SAE Paper 841691, Society of Automotive Engineers, USA, 1984.

17. P. Gajendran and N.N. Clark, "Effect of Truck Operating Weight on Heavy-Duty Diesel Emissions", Environmental Science & Technology, Vol. 37, No. 18, pp. 4309-4317, 2003.

18. R.W. Zub and R.G. Colello, "Effect of Vehicle Design Variables on Top Sped, Performance, and Fuel Economy", SAE Paper 800215, Society of Automotive Engineers, USA, 1980.

19. D.C. Biggs and R. Akcelik, "Estimating Effect of Vehicle Characteristics on Fuel Consumption", Journal of Transportation Engineering, Vol. 113, No.1, pp. 101-106, January 1987.

20. Web-site: www.dieselnet.com (Accessed on July 1, 2005)

21. C.A. Amann, "Passenger-car Fuel Consumption Versus Performance in Retrospect", Paper No. 2001-ICE-411, ICE-Vol. 37, No. 2, 2001 Fall Technical Conference, ASME, USA, 2001.

22. T.D. Gillespie, "Fundamentals of Vehicle Dynamics", Society of Automotive Engineers, Warrendale, PA, USA, 1992.

23. J. Fry, P. Jennings, N. Taylor and P. Jackson, "Vehicle Drive-By Noise Prediction: A Neural Networks Approach", SAE Paper 1999-01-1740, Society of Automotive Engineers, USA, 1999.

24. J. Fry and P. Jennings, "Using Multi-layer Perceptrons to Predict Vehicle Pass-By Noise", Neural Computing and Applications, Vol. 11, pp. 161-167, Springer Verlag London Limited, 2003.

25. T. Berge and S.A. Storeheier, "Parameters Influencing the Noise Emission Levels from Passenger Cars in Urban Traffic", SAE Paper 861286, Society of Automotive Engineers, USA, 1986.

26. B. Andersen and H. Bendtsen, "Noise Emission from 4000 Vehicle Pass-Bys – An Inter-Noise 2004 Presentation", Danish Road Institute, Report 134, 2004.

27. H. Bendtsen, "The Nordic Prediction Method for Road Traffic Noise", The Science of the Total Environment, Vol. 235, pp. 331-338, Elsevier Science, 1999.

28. C.S.Y. Lee and G.G. Fleming, "Measurement of Highway-Related Noise", US DOT/FHWA Report, FHWA-PD-96-046, DOT-VNTSC-FHWA-96-5, Final Report, May 1996.

29. C. Singh and M.D. Kankam, "Failure Data Analysis of Transit Vehicles", Proceedings of 1979 Annual Reliability and Maintainability Symposium, pp. 308-313, IEEE, 1979.

30. B.S. Dhillon, "RAM Analysis of Vehicles in Changing Weather", 1984 Proceedings of Annual Reliability and Maintainability Symposium, pp. 48-53, IEEE, 1984.

31. R.E. Barlow, F. Proschan and L.C. Hunter, "Mathematical Theory of Reliability", John Wiley & Sons Inc., New York, USA, 1965.

32. G.W.A. Dummer, M.H. Tooley and R.C. Winton, "An Elementary Guide to Reliability", 5th Edition, Butterworth-Heinemann, Oxford, Great Britain, 1997.

33. U.D. Kumar, J. Crocker, J. Knezevic and M. El-Haram, "Reliability, Maintenance and Logistic Support - A Life Cycle Approach", Kluwer Academic Publishers, Norwell, Massachusetts, USA, 2000.

34. Headquarters, Department of Army, TM 5-698-1, "Reliability/Availability of Electrical & Mechanical Systems for Command, Control, Communications, Computer, Intelligence, Surveillance, and Reconnaissance (C4ISR) Facilities", March 2003.

35. R.F. Drenick, "The Failure Law of Complex Equipment", Journal of the Society of Industrial and Applied Mathematics, Vol. 8, No. 4, pp. 680-690, December 1960.

36. R.F. Drenick, "Mathematical Aspects of the Reliability Problem", Journal of the Society of Industrial and Applied Mathematics", Vol. 8, No. 1, pp. 125-149, March 1960.

37. P. T. Hetherington, "Mechanical Design Reliability', Course by The Reliability Analysis Center, Rome, New York, USA, 2005.

38. K. Chandler, N. Clark, K. Kelly, R. Motta, P. Norton and L. Schumacher, "Alternative Fuel Transit Buses – Final Results from the National Renewable Energy Laboratory (NREL) Vehicle Evaluation Program", October 1996.

39. Reliasoft web-site: www.Reliasoft.com (Accessed on July 1, 2005)

40. P. Alfredsson and O. Waak, "Constant vs. Non-Constant Failure Rates; Some Misconceptions with Respect to Practical Applications", White Paper, Systecon AB, Stockholm, Sweden, 2001.

41. M.K. Bedewy, M.A. Radwan and H. Hammam, "A Comparative Study on the Reliability and Maintanability of Public Transport Vehicles", Reliability Engineering and Systems Safety, Vol. 26, pp. 271-277, 1989.

42. M. Neil, N. Fenton, S. Forey and R. Harris, "Using Bayesian Belief Networks to Predict Reliability of Military Vehicles", Computing & Control Engineering Journal, pp. 11-20, February 2001.

43. M.L. Boessio, I.B. Morsch and AM.M. Awruch, "Fatigue Lifetime Estimation of Commercial Vehicles", Journal of Sound and Vibration, Vol. 291, pp. 169-191, 2006.

44. S.R. Parker, "Combat Vehicle Reliability Assessment Simulation Model (CVRASM)", Proceedings of the 1991 Winter Simulation Conference, Editors – B.L. Nelson, W.D. Kelton and G.M. Clark, pp. 491-498, 1991.

45. A.E. Smith, D.W. Coit and C.W. McCullers, "Reliability Improvement of Airport Ground Transportation Vehicles Using Neural Networks to Anticipate System Failure", 2002 Proceedings of Annual Reliability and Maintainability Symposium, pp. 74-79, IEEE, 2002.

46. M. Marseguerra, E. Zio, M. Ammaturo and V. Fontana, "Predicting Reliability Via Neural Networks", 2003 Proceedings of Annual Reliability and Maintainability Symposium, pp. 196-2001, IEEE, 2003.

47. D.J. Klinikowski, B.J. Gilmore and B.T. Kulakowski, "Transit Bus Durability Track Assessment and Validation", Heavy Vehicle Systems, International Journal of Vehicle Design, Vol. 6, Nos. 1-4, pp. 273-286, 1999.

48. D.P. Gaver Jr.,"Reliability - Detailed Overview", Naval Postgraduate School, Montery, California, 2005.

49. B.T. Kulakowski, "Performance-Based Standards - The time has come!", Performance-Based Standards 2003 International Seminar, Melbourne, Australia, February 2003.

50. A.W. Naylor and G.R. Sell, "Linear Operator Theory in Engineering and Science", Springer-Verlag, New York, 1982.

51. Nattional Transit Database (NTD) Web-site: www.ntdprogram.com (accessed on May 1, 2006)

52. M. Kantardzic, "Data Mining – Concepts, Models, Methods, and Algorithms", IEEE Press, Wiley-Interscience, Piscataway, New Jersey, USA, 2003.

53. G.M. Stump, M.A. Yukish, J.D. Martin and T.W. Simpson, "The ARL Trade Space Visualizer: An Engineering Decision-Making Tool", AIAA-2004-4483, 10th AIAA/ISSMO Multidisciplinary Analysis and Optimization Conference, pp. 2976-2986, Albany, New York, 2004.

54. S. Piramuthu, "Evaluating Feature Selection Methods for Learning in Data Mining Applications", European Journal of Operational Research, Vol. 156, pp. 483-494, 2004.

55. I. Guyon and A. Elisseeff, "An Introduction to Variable and Feature Selection" Journal of Machine Learning Research, Vol. 3, pp. 1157-1182, 2003.

56. H. Liu and H. Motoda, "Feature Extraction, Construction and Selection: A Data Mining Perspective", Kluwer Academic Publishers, Norwell, Massachusetts, USA, 1998.

57. A. Blum and P. Langley, "Selection of Relevant Features and Examples in Machine Learning", Artificial Intelligence, Vol. 97, Nos. 1-2, pp. 245-271, December 1997.

58. J.V. Stone, "Independent Component Analysis: An Introduction", TRENDS in Cognitive Sciences, Vol. 6, No.2, February 2002.

59. D.V. Sridhar, E.B. Bartlett and R.C. Seagrave, "Information Theoretic Subset Selection for Neural Network Models", Computers in Chemical Engineering Vol. 22, No. 4/5, pp. 613-626, 1998.

60. R. Setiono, W.K. Leow and J.M. Zurada, "Extraction of Rules from Artificial Neural Networks for Nonlinear Regression", IEEE Transactions on Neural Networks, Vol. 13, No. 3, pp. 564-577, May 2002.

61. R. Setiono and H. Liu, "A Connectionist Approach to Generating Oblique Decision Trees", IEEE Transactions on System, Man and Cybernetics – Part B: Cybernetics, Vol. 29, No.3, pp. 440-444, June 1999.

62. O. Boz, "Extracting Decision Trees From Trained Neural Networks", SIGKDD' 02, Edmonton, Alberta, Canada, July 2002.

63. M.T. Hagan, H.B. Demuth and M. Beale, "Neural Network Design", First Reprint, Thomson Asia Pte. Ltd., Singapore, 2002.

64. G. Cybenko, "Approximation by Superpositions of a Sigmoidal Function", Mathematics of Control, Signals, and Systems, Vol. 2, pp. 303-314, Springer-Verlag New York, 1989.

65. R. Setiono and A. Azcarraga, "An Effective Method for Generating Multiple Linear Regression Rules from Artificial Neural Networks", Proceedings of the 13th International Conference on Tools with Artificial Intelligence, pp. 171-178, November 2001.

66. A.B. Tickle, R. Andrews, M. Golea and J. Diederich, "The Truth Will Come to Light: Directions and Challenges in Extracting the Knowledge Embedded Within Trained Artificial Neural Networks", IEEE Transactions on Neural Networks, Vol. 9, No. 6, pp. 1057-1067, November 1998.

67. S. Mitra and Y. Hayashi, "Neuro-Fuzzy Rule Generation: Survey in Soft Computing Framework", IEEE Transactions on Neural Networks, Vol. 11, No. 3, pp. 748-768, May 2000.

68. J.C. Principe, N.R. Euliano and W.C. Lefebvre, "Neural and Adaptive Systems: Fundamentals through Simulations", John Wiley & Sons, Inc., 1999.

69. A. Elisseeff and H. Paugam-Moisy, "Size of Multilayer Networks for Exact Learning: Analytic Approach", NeuroCOLT Technical Report Series NC-TR-97-002, February 1997.

70. Mathworks, Inc., "MATLAB Neural Network Toolbox – Documentation", 2005.

71. K. Saito and R. Nakano, "Law Discovery Using Neural Networks", Proceedings of the 15th International Joint Conference on Artificial Intelligence, pp. 1078-1093, Nagoya, Japan, 1997.

72. E. Kreyszig, "Advanced Engineering Mathematics", 8th Edition, John Wiley & Sons (Asia) Pte. Ltd., Singapore, 1999.

73. E. Oost, "Opening Pandora's Box, Bottom Side Uo", Master's Thesis, University of Amsterdam IAS Group, The Netherlands, August 2002.

74. B. Lu, H. Kita and Y. Nishikawa, "Inverting Feedforward Neural Networks Using Linear and Nonlinear Programming", IEEE Transactions on Neural Networks, Vol. 10, No. 6, pp. 1271-1290, November 1999.

75. B.J. Pine II, "Mass Customization: The New Frontier in Business Competition", Harvard Business School Press, Boston, Massachusetts, USA, 1993.

76. J. Wu and S. Azarm, "Metrics for Quality Assessment of a Multiobjective Design Optimization Solution Set", Journal of Mechanical Design, Transactions of the ASME, Vol. 123, pp. 18-25, 2001.

77. Mathworks, Inc., "MATLAB Optimization Toolbox – Documentation", 2005.

78. R.T. Marler and J.S. Arora, "Survey of Multi-objective Optimization Methods for Engineering", Structural and Multidisciplinary Optimization, Vol. 26, pp. 369-395, 2004.

79. J. Lewe, "A Spotlight Search Method for Multi-criteria Optimization Problems" 9th AIAA/ISSMO Symposium on Multidisciplinary Analysis and Optimization, AIAA 2002-5432, Atlanta, Georgia, September 2002.

80. J. Koski, "Defectiveness of Weighting Method in Multicriterion Optimization of Structures ", Communications in Applied Numerical Methods, Vol. 1, No. 6, pp. 333-337, Nov. 1985.

81. F. Gembicki, "Performance and Sensitivity Optimization: A Vector Index Approach", Ph.D. Thesis, Department of Systems Engineering, Case Western Reserve University, Cleveland, Ohio, USA, 1974.

82. F. Gembicki and Y.Y. Haimes, "Approach to Performance and Sensitivity Multiobjectove Optimization: The Goal Attainment Method", Short Paper, IEEE Transactions on Automatic Control, Vol. 20, Issue 6, pp. 769-771, December 1975.

83. B.T. Kulakowski, S. Brennan, D.J. Klinikowski and S. Muthiah, "Study of the Relationship between Results of the Bus Testing Program and In-service Performance of Buses", PTI proposal submitted to The Federal Transit Administration (FTA), February 2005.

Appendix A

Histogram Plots Obtained Using ATSV

The ARL Trade Space Visualizer (ATSV), developed at Penn State's Applied Research Laboratory, offers multi-dimensional data visualization techniques such as glyph plots, histogram plots, parallel co-ordinate plots and scatter matrices. In this thesis, ATSV was used to plot histograms for input and output variables. Figures **A.1 - A.6** show screenshots of the ATSV program with histograms for the input and output variables listed in Tables **3.1** - **3.10**. A total of 10 bins were used to generate the histograms, except for the NTD reliability model wherein five bins were used due to lower number of data samples. Histograms reveal the underlying distribution of the inputs and outputs. The following nomenclature is used is the histogram plots.

L	: Length
W	: Width
H	: Height
WB	: Wheelbase
FO	: Front Overhang
RO	: Rear Overhang
GC	: Ground Clearance
CW-F	: Curb Weight - Front
CW-R	: Curb Weight - Rear
CW-T	: Curb Weight - Total

SLW-F : Seated Load Weight - Front

SLW-R : Seated Load Weight - Rear

SLW-T : Seated Load Weight - Total

GVW-F : Gross Vehicle Weight - Front

GVW-R : Gross Vehicle Weight - Rear

GVW-T : Gross Vehicle Weight - Total

AR : Axle Ratio

P : Engine Power

D : Engine Displacement

WD : Wheel Diameter

TD : Tire Diameter

D-MIL : Durability Mileage

O-MIL : Other Mileage

ACT-FL : Active Fleet

ELEV : City Elevation

SERV-MIL : Service Area

SERV-POP : Service Population

AVG-SP : Average Operating Speed

MIL-PER-BUS : Average Miles per Bus per Annum

AVG-MIL : Average Mileage

TLH : Total Labor Hours

LHPB : Labor Hours per Bus

T-FAC : Total Number of Maintenance Facilities

PER-SP	: Bus Spare Ratio in Percentage
CBD	: Fuel Economy on CBD Driving Cycle
ART	: Fuel Economy on ART Driving Cycle
COM	: Fuel Economy on COM Driving Cycle
NTD-FE	: NTD Fuel Economy
ACC-16	: Acceleration at 16 km/hr
ACC-32	: Acceleration at 32 km/hr
ACC-48	: Acceleration at 48 km/hr
ACC-64	: Acceleration at 64 km/hr
CON-NOISE-R	: Pass-by Noise: Accelerating from Constant Speed - Right
CON-NOISE-L	: Pass-by Noise: Accelerating from Constant Speed - Left
ST-NOISE-R	: Pass-by Noise: Accelerating from Standstill - Right
ST-NOISE-L	: Pass-by Noise: Accelerating from Standstill - Left
PTI-MDBF	: Mean Distance Between Failures at PTI
NTD-MDBF	: Mean Distance Between Failures at NTD

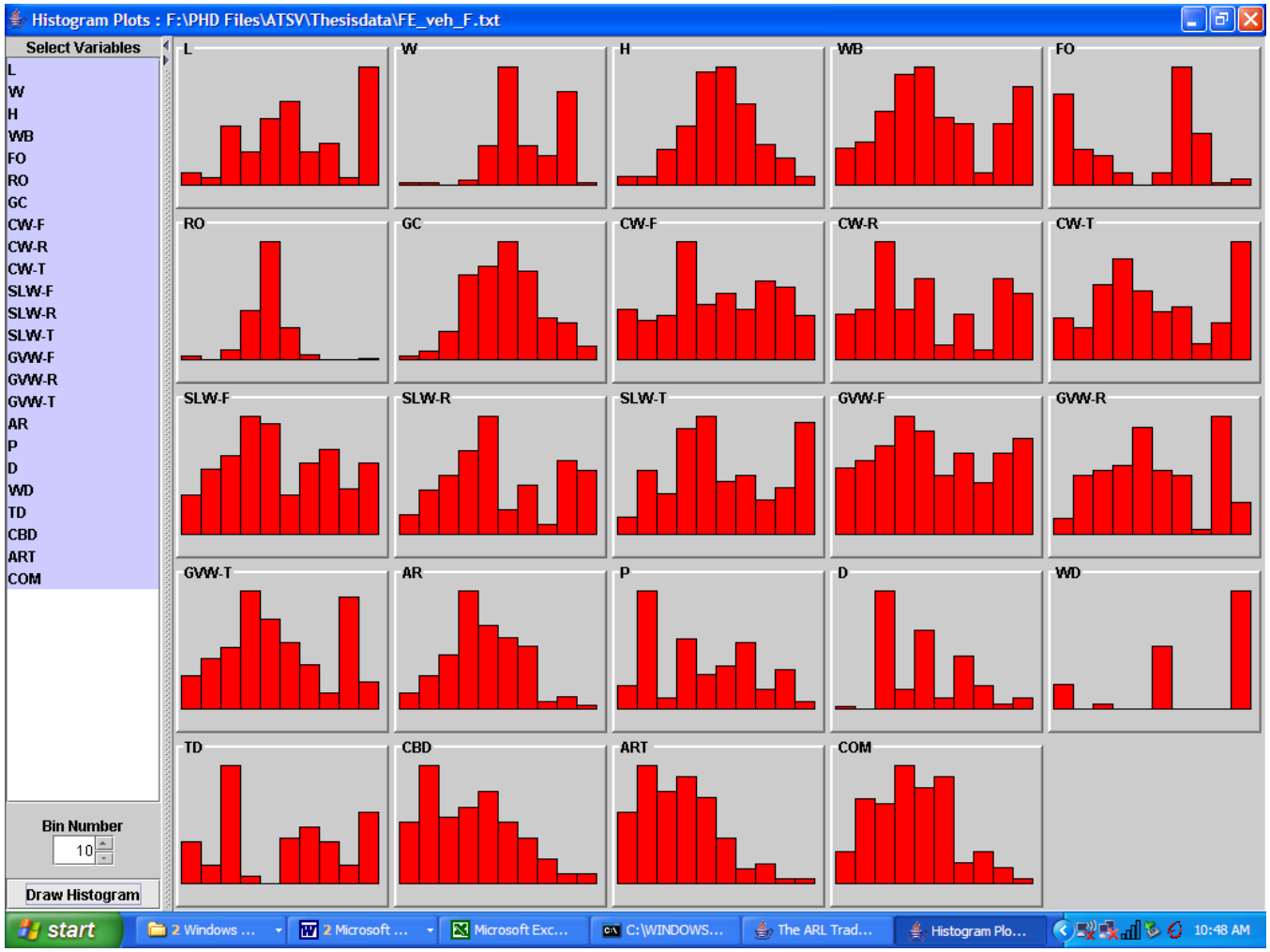

Figure A.1: Screenshot of ATSV with histograms for inputs and outputs - PTI fuel economy model.

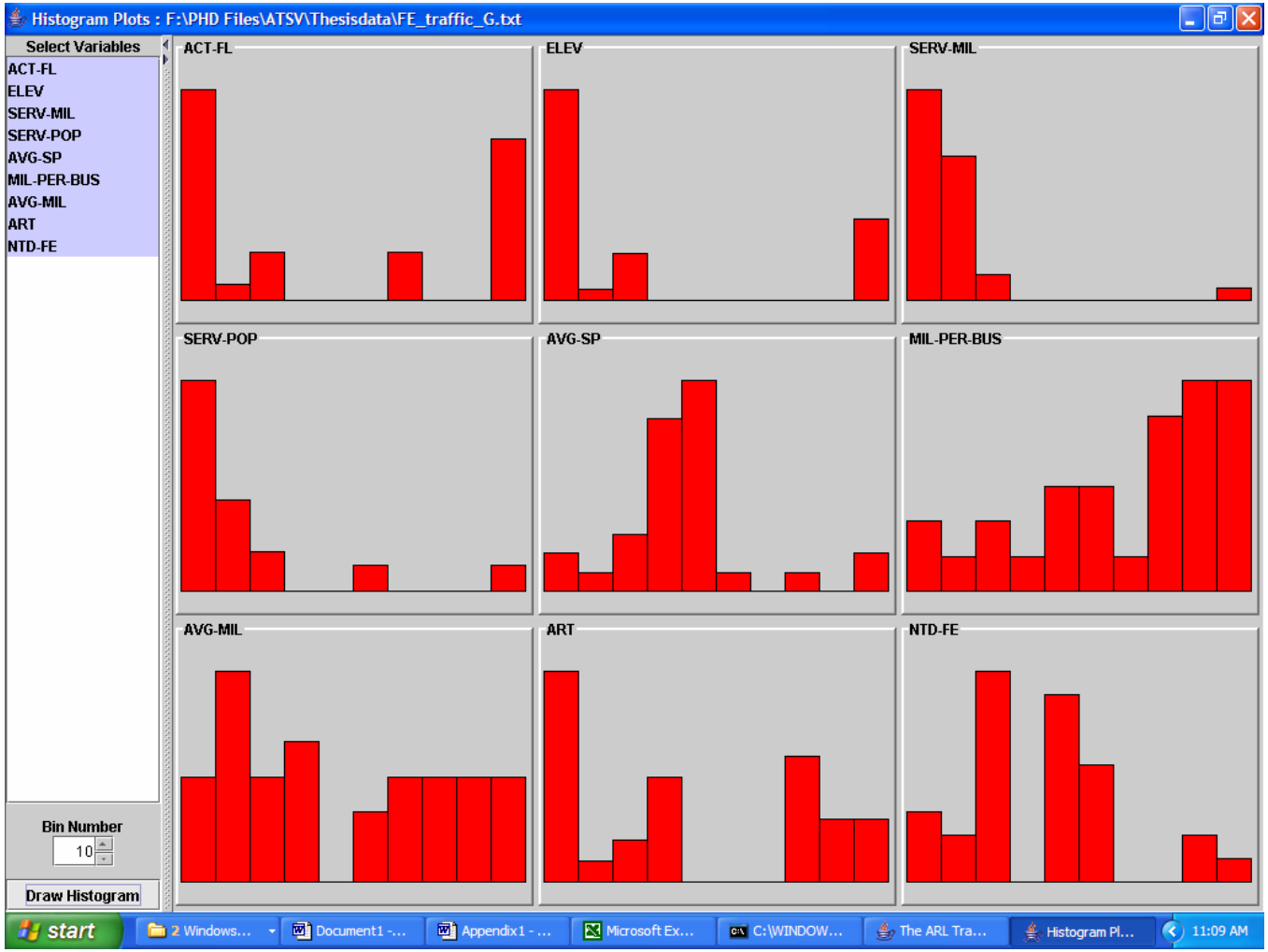

Figure A.2: Screenshot of ATSV with histograms for inputs and outputs - NTD fuel economy model.

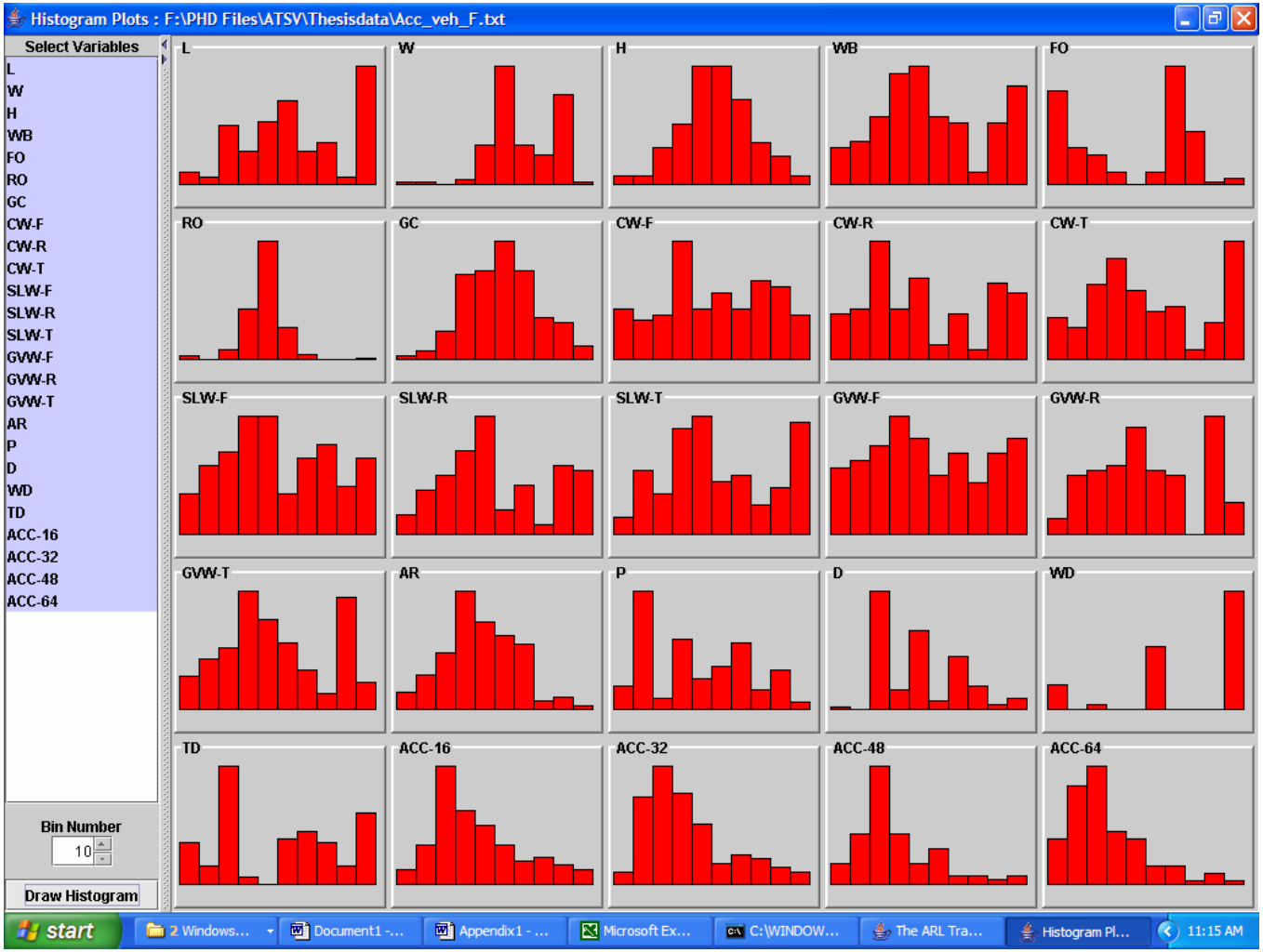

Figure **A.3**: Screenshot of ATSV with histograms for inputs and outputs - Acceleration model.

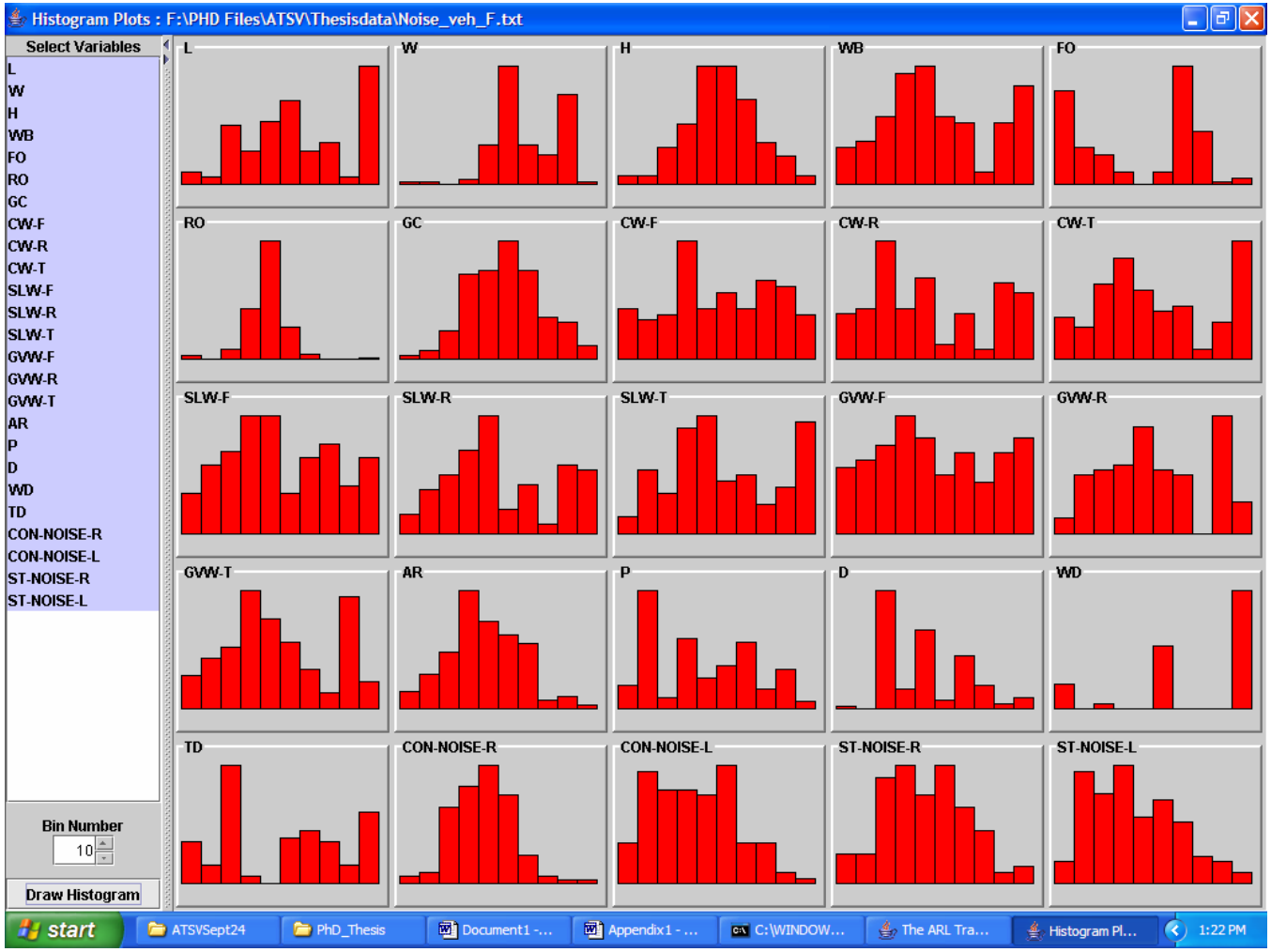

Figure A.4: Screenshot of ATSV with histograms for inputs and outputs - Pass-by noise model.

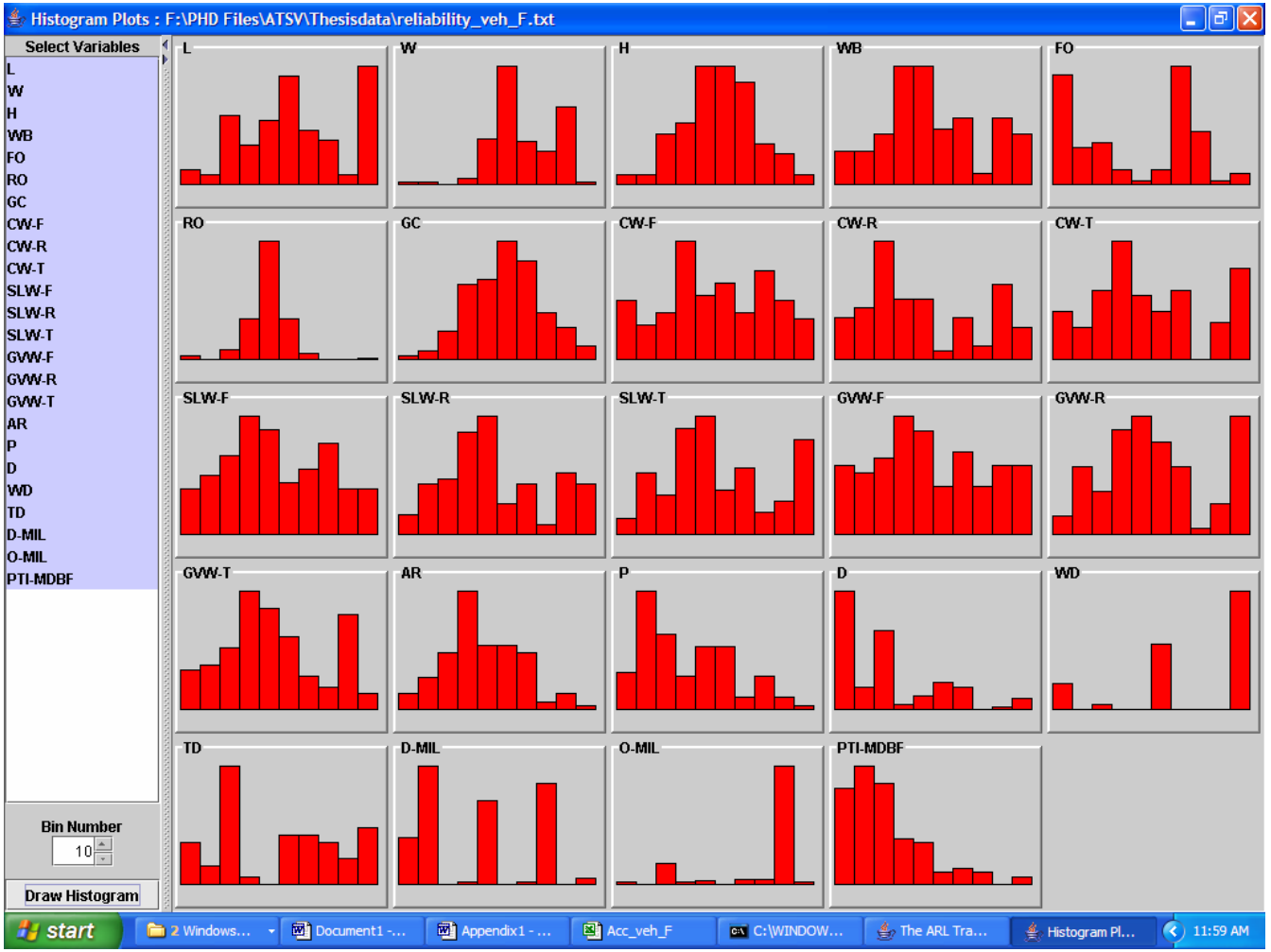

Figure A.5: Screenshot of ATSV with histograms for inputs and outputs - PTI reliability model.

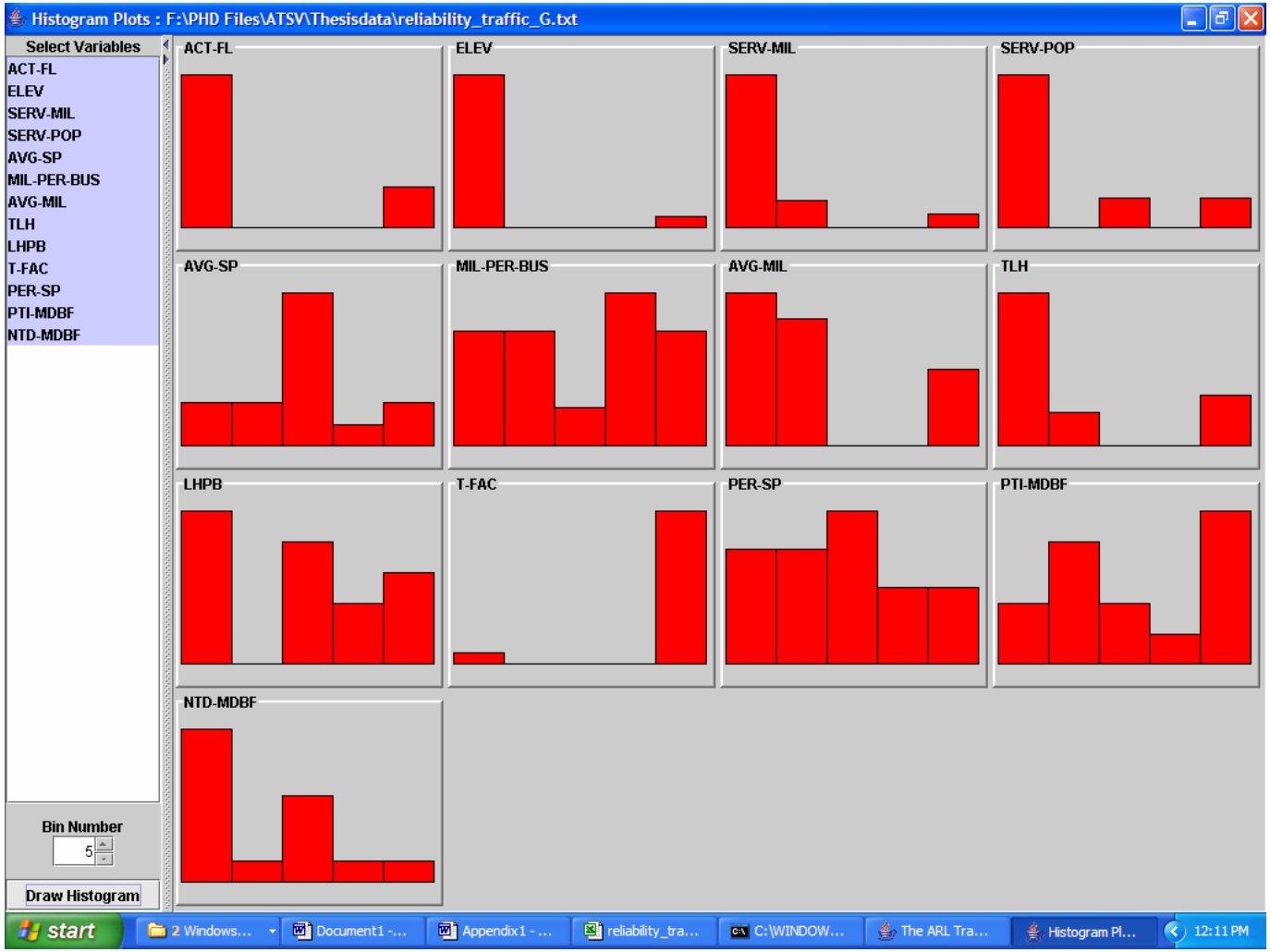

Figure A.6: Screenshot of ATSV with histograms for inputs and outputs - NTD reliability model.

It is evident from the above figures that many of the variables are not normally distributed. Lilliefors test is a modification of Kolmogorov-Smirnov test that can be used to determine if the null hypothesis of composite normality is a reasonable assumption. In this study, MATLAB function called 'Lillietest' that can perform Lilliefors test was used to check if the variables were normally distributed. For example, results from the Lilliefors test showed that amongst the 21 inputs given in Figure **A.1**, except for height (H), ground clearance (GC) and seated load weight - front (SLW-FR), the null hypothesis was rejected at a significance level of 0.05 for all other input variables. With regards to the outputs, the null hypothesis was rejected for fuel economy on the CBD driving cycle.

Appendix B

Correlation Coefficient Matrices for Model Inputs

In this study, as a first step in the input selection process, correlation matrix was used to select inputs that are least correlated with other inputs. A cutoff value of 0.7 was chosen, since it implies that less than 50% of the variations in one input can be explained for by a linear relationship with the second input. The following tables show the correlation coefficient matrices obtained using all inputs for the models described in Sub-sections **5.1.1** - **5.1.6**.

Table **B.1**: Input correlation matrix: PTI fuel economy model

	L	W	H	WB	FO	RO	GC	CW-F	CW-R	CW-T	SLW-F	SLW-R	SLW-T	GVW-F	GVW-R	GVW-T	AR	P	D	WD	TD
L	1.00	0.66	0.34	0.87	0.72	0.47	-0.04	0.78	0.87	0.89	0.83	0.91	0.92	0.86	0.91	0.91	0.34	0.62	0.46	0.69	0.78
W	0.66	1.00	0.24	0.61	0.51	0.24	-0.34	0.61	0.72	0.72	0.63	0.72	0.72	0.66	0.72	0.71	0.32	0.53	0.42	0.56	0.59
H	0.34	0.24	1.00	0.17	0.24	0.46	0.28	0.36	0.23	0.29	0.32	0.28	0.31	0.31	0.33	0.33	0.14	0.05	-0.10	0.40	0.33
WB	0.87	0.61	0.17	1.00	0.41	0.15	-0.16	0.65	0.73	0.75	0.69	0.77	0.78	0.73	0.77	0.78	0.20	0.58	0.54	0.47	0.62
FO	0.72	0.51	0.24	0.41	1.00	0.24	-0.01	0.70	0.80	0.81	0.78	0.76	0.80	0.81	0.75	0.79	0.45	0.43	0.28	0.74	0.77
RO	0.47	0.24	0.46	0.15	0.24	1.00	0.23	0.25	0.27	0.28	0.22	0.34	0.32	0.21	0.36	0.31	0.11	0.23	-0.02	0.32	0.23
GC	-0.04	-0.34	0.28	-0.16	-0.01	0.23	1.00	-0.10	-0.21	-0.19	-0.10	-0.17	-0.15	-0.13	-0.17	-0.15	-0.05	-0.10	-0.19	-0.01	-0.04
CW-F	0.78	0.61	0.36	0.65	0.70	0.25	-0.10	1.00	0.74	0.86	0.97	0.76	0.87	0.93	0.79	0.86	0.43	0.41	0.36	0.82	0.88
CW-R	0.87	0.72	0.23	0.73	0.80	0.27	-0.21	0.74	1.00	0.98	0.82	0.99	0.97	0.87	0.97	0.96	0.39	0.67	0.62	0.72	0.82
CW-T	0.89	0.72	0.29	0.75	0.81	0.28	-0.19	0.86	0.98	1.00	0.91	0.97	0.99	0.94	0.97	0.99	0.42	0.63	0.58	0.80	0.88
SLW-F	0.83	0.63	0.32	0.69	0.78	0.22	-0.10	0.97	0.82	0.91	1.00	0.82	0.92	0.97	0.84	0.91	0.41	0.45	0.42	0.82	0.91
SLW-R	0.91	0.72	0.28	0.77	0.76	0.34	-0.17	0.76	0.99	0.97	0.82	1.00	0.98	0.87	0.99	0.97	0.37	0.67	0.61	0.72	0.81
SLW-T	0.92	0.72	0.31	0.78	0.80	0.32	-0.15	0.87	0.97	0.99	0.92	0.98	1.00	0.95	0.98	0.99	0.41	0.63	0.57	0.79	0.89
GVW-F	0.86	0.66	0.31	0.73	0.81	0.21	-0.13	0.93	0.87	0.94	0.97	0.87	0.95	1.00	0.90	0.96	0.47	0.53	0.49	0.80	0.91
GVW-R	0.91	0.72	0.33	0.77	0.75	0.36	-0.17	0.79	0.97	0.97	0.84	0.99	0.98	0.90	1.00	0.99	0.38	0.66	0.60	0.74	0.83
GVW-T	0.91	0.71	0.33	0.78	0.79	0.31	-0.15	0.86	0.96	0.99	0.91	0.97	0.99	0.96	0.99	1.00	0.43	0.62	0.57	0.78	0.88
AR	0.34	0.32	0.14	0.20	0.45	0.11	-0.05	0.43	0.39	0.42	0.41	0.37	0.41	0.47	0.38	0.43	1.00	0.42	0.20	0.41	0.43
P	0.62	0.53	0.05	0.58	0.43	0.23	-0.10	0.41	0.67	0.63	0.45	0.67	0.63	0.53	0.66	0.62	0.42	1.00	0.61	0.35	0.47
D	0.46	0.42	-0.10	0.54	0.28	-0.02	-0.19	0.36	0.62	0.58	0.42	0.61	0.57	0.49	0.60	0.57	0.20	0.61	1.00	0.22	0.44
WD	0.69	0.56	0.40	0.47	0.74	0.32	-0.01	0.82	0.72	0.80	0.82	0.72	0.79	0.80	0.74	0.78	0.41	0.35	0.22	1.00	0.89
TD	0.78	0.59	0.33	0.62	0.77	0.23	-0.04	0.88	0.82	0.88	0.91	0.81	0.89	0.91	0.83	0.88	0.43	0.47	0.44	0.89	1.00

Table **B.2**: Input correlation matrix: NTD fuel economy model

	ACT-FL	ELEV	SERV-MIL	SERV-POP	AVG-SP	MIL-PER-BUS	AVG-MIL	CBD	ART	COM
ACT-FL	1.00	0.75	0.28	-0.06	-0.12	0.62	0.55	-0.73	-0.77	-0.73
ELEV	0.75	1.00	0.02	-0.09	-0.11	0.63	0.49	-0.54	-0.62	-0.69
SERV-MIL	0.28	0.02	1.00	0.14	-0.03	0.13	0.01	-0.24	-0.18	-0.07
SERV-POP	-0.06	-0.09	0.14	1.00	-0.37	-0.26	0.22	0.32	0.18	0.17
AVG-SP	-0.12	-0.11	-0.03	-0.37	1.00	0.44	0.15	0.00	0.01	-0.04
MIL-PER-BUS	0.62	0.63	0.13	-0.26	0.44	1.00	0.41	-0.39	-0.35	-0.40
AVG-MIL	0.55	0.49	0.01	0.22	0.15	0.41	1.00	-0.31	-0.52	-0.63
CBD	-0.73	-0.54	-0.24	0.32	0.00	-0.39	-0.31	1.00	0.94	0.87
ART	-0.77	-0.62	-0.18	0.18	0.01	-0.35	-0.52	0.94	1.00	0.95
COM	-0.73	-0.69	-0.07	0.17	-0.04	-0.40	-0.63	0.87	0.95	1.00

Table **B.3**: Input correlation matrix: Acceleration model

	L	W	H	WB	FO	RO	GC	CW-F	CW-R	CW-T	SLW-F	SLW-R	SLW-T	GVW-F	GVW-R	GVW-T	AR	P	D	WD	TD
L	1.00	0.61	0.30	0.85	0.68	0.41	-0.03	0.75	0.85	0.87	0.81	0.89	0.90	0.84	0.89	0.90	0.27	0.60	0.46	0.65	0.76
W	0.61	1.00	0.11	0.59	0.45	0.03	-0.32	0.53	0.69	0.69	0.57	0.68	0.67	0.62	0.67	0.67	0.33	0.55	0.49	0.44	0.54
H	0.30	0.11	1.00	0.12	0.21	0.40	0.34	0.34	0.19	0.25	0.30	0.24	0.27	0.29	0.29	0.30	0.12	0.05	-0.09	0.35	0.31
WB	0.85	0.59	0.12	1.00	0.32	0.06	-0.13	0.60	0.67	0.69	0.64	0.72	0.73	0.67	0.72	0.72	0.09	0.54	0.51	0.40	0.56
FO	0.68	0.45	0.21	0.32	1.00	0.19	-0.06	0.65	0.78	0.79	0.75	0.74	0.78	0.79	0.73	0.77	0.46	0.41	0.27	0.70	0.74
RO	0.41	0.03	0.40	0.06	0.19	1.00	0.32	0.18	0.20	0.21	0.16	0.28	0.25	0.15	0.29	0.25	0.04	0.19	-0.01	0.25	0.20
GC	-0.03	-0.32	0.34	-0.13	-0.06	0.32	1.00	-0.08	-0.26	-0.22	-0.09	-0.22	-0.18	-0.15	-0.20	-0.19	-0.08	-0.13	-0.25	0.03	-0.03
CW-F	0.75	0.53	0.34	0.60	0.65	0.18	-0.08	1.00	0.70	0.85	0.97	0.73	0.85	0.93	0.76	0.84	0.40	0.41	0.36	0.81	0.86
CW-R	0.85	0.69	0.19	0.67	0.78	0.20	-0.26	0.70	1.00	0.97	0.80	0.98	0.96	0.86	0.97	0.95	0.39	0.64	0.63	0.68	0.80
CW-T	0.87	0.69	0.25	0.69	0.79	0.21	-0.22	0.85	0.97	1.00	0.90	0.97	0.99	0.94	0.97	0.98	0.42	0.61	0.58	0.77	0.87
SLW-F	0.81	0.57	0.30	0.64	0.75	0.16	-0.09	0.97	0.80	0.90	1.00	0.80	0.91	0.97	0.82	0.90	0.39	0.46	0.43	0.82	0.91
SLW-R	0.89	0.68	0.24	0.72	0.74	0.28	-0.22	0.73	0.98	0.97	0.80	1.00	0.98	0.86	0.99	0.97	0.36	0.64	0.61	0.69	0.80
SLW-T	0.90	0.67	0.27	0.73	0.78	0.25	-0.18	0.85	0.96	0.99	0.91	0.98	1.00	0.94	0.97	0.99	0.39	0.61	0.58	0.77	0.88
GVW-F	0.84	0.62	0.29	0.67	0.79	0.15	-0.15	0.93	0.86	0.94	0.97	0.86	0.94	1.00	0.88	0.95	0.45	0.52	0.49	0.78	0.89
GVW-R	0.89	0.67	0.29	0.72	0.73	0.29	-0.20	0.76	0.97	0.97	0.82	0.99	0.97	0.88	1.00	0.98	0.37	0.63	0.60	0.71	0.81
GVW-T	0.90	0.67	0.30	0.72	0.77	0.25	-0.19	0.84	0.95	0.98	0.90	0.97	0.99	0.95	0.98	1.00	0.41	0.60	0.57	0.75	0.87
AR	0.27	0.33	0.12	0.09	0.46	0.04	-0.08	0.40	0.39	0.42	0.39	0.36	0.39	0.45	0.37	0.41	1.00	0.37	0.18	0.38	0.41
P	0.60	0.55	0.05	0.54	0.41	0.19	-0.13	0.41	0.64	0.61	0.46	0.64	0.61	0.52	0.63	0.60	0.37	1.00	0.58	0.34	0.46
D	0.46	0.49	-0.09	0.51	0.27	-0.01	-0.25	0.36	0.63	0.58	0.43	0.61	0.58	0.49	0.60	0.57	0.18	0.58	1.00	0.25	0.45
WD	0.65	0.44	0.35	0.40	0.70	0.25	0.03	0.81	0.68	0.77	0.82	0.69	0.77	0.78	0.71	0.75	0.38	0.34	0.25	1.00	0.89
TD	0.76	0.54	0.31	0.56	0.74	0.20	-0.03	0.86	0.80	0.87	0.91	0.80	0.88	0.89	0.81	0.87	0.41	0.46	0.45	0.89	1.00

Table **B.4**: Input correlation matrix: Pass-by noise model

	L	W	H	WB	FO	RO	GC	CW-F	CW-R	CW-T	SLW-F	SLW-R	SLW-T	GVW-F	GVW-R	GVW-T	AR	P	D	WD	TD
L	1.00	0.66	0.35	0.87	0.72	0.49	0.03	0.77	0.86	0.89	0.83	0.91	0.92	0.87	0.91	0.91	0.32	0.62	0.47	0.69	0.79
W	0.66	1.00	0.28	0.60	0.52	0.25	-0.31	0.63	0.69	0.71	0.64	0.70	0.71	0.67	0.70	0.70	0.34	0.53	0.39	0.56	0.60
H	0.35	0.28	1.00	0.17	0.21	0.50	0.28	0.33	0.24	0.28	0.29	0.30	0.31	0.29	0.34	0.33	0.21	0.09	-0.08	0.39	0.31
WB	0.87	0.60	0.17	1.00	0.41	0.17	-0.04	0.64	0.70	0.72	0.68	0.76	0.76	0.73	0.76	0.77	0.16	0.57	0.52	0.48	0.63
FO	0.72	0.52	0.21	0.41	1.00	0.24	-0.05	0.67	0.82	0.82	0.76	0.79	0.81	0.80	0.77	0.80	0.47	0.46	0.35	0.70	0.75
RO	0.49	0.25	0.50	0.17	0.24	1.00	0.24	0.28	0.28	0.30	0.26	0.36	0.34	0.23	0.38	0.33	0.11	0.24	0.01	0.34	0.27
GC	0.03	-0.31	0.28	-0.04	-0.05	0.24	1.00	-0.09	-0.16	-0.15	-0.07	-0.12	-0.11	-0.11	-0.12	-0.12	-0.07	-0.02	-0.13	0.02	-0.02
CW-F	0.77	0.63	0.33	0.64	0.67	0.28	-0.09	1.00	0.74	0.86	0.97	0.77	0.87	0.93	0.79	0.86	0.43	0.43	0.38	0.83	0.87
CW-R	0.86	0.69	0.24	0.70	0.82	0.28	-0.16	0.74	1.00	0.98	0.82	0.99	0.97	0.89	0.97	0.96	0.42	0.66	0.63	0.71	0.82
CW-T	0.89	0.71	0.28	0.72	0.82	0.30	-0.15	0.86	0.98	1.00	0.92	0.98	0.99	0.95	0.97	0.99	0.45	0.63	0.59	0.79	0.89
SLW-F	0.83	0.64	0.29	0.68	0.76	0.26	-0.07	0.97	0.82	0.92	1.00	0.83	0.92	0.97	0.84	0.91	0.41	0.47	0.46	0.83	0.91
SLW-R	0.91	0.70	0.30	0.76	0.79	0.36	-0.12	0.77	0.99	0.98	0.83	1.00	0.98	0.89	0.99	0.98	0.41	0.67	0.61	0.72	0.82
SLW-T	0.92	0.71	0.31	0.76	0.81	0.34	-0.11	0.87	0.97	0.99	0.92	0.98	1.00	0.95	0.98	0.99	0.42	0.63	0.58	0.79	0.89
GVW-F	0.87	0.67	0.29	0.73	0.80	0.23	-0.11	0.93	0.89	0.95	0.97	0.89	0.95	1.00	0.91	0.96	0.47	0.55	0.52	0.79	0.90
GVW-R	0.91	0.70	0.34	0.76	0.77	0.38	-0.12	0.79	0.97	0.97	0.84	0.99	0.98	0.91	1.00	0.99	0.41	0.65	0.60	0.73	0.83
GVW-T	0.91	0.70	0.33	0.77	0.80	0.33	-0.12	0.86	0.96	0.99	0.91	0.98	0.99	0.96	0.99	1.00	0.44	0.63	0.58	0.77	0.87
AR	0.32	0.34	0.21	0.16	0.47	0.11	-0.07	0.43	0.42	0.45	0.41	0.41	0.42	0.47	0.41	0.44	1.00	0.41	0.21	0.41	0.42
P	0.62	0.53	0.09	0.57	0.46	0.24	-0.02	0.43	0.66	0.63	0.47	0.67	0.63	0.55	0.65	0.63	0.41	1.00	0.60	0.38	0.50
D	0.47	0.39	-0.08	0.52	0.35	0.01	-0.13	0.38	0.63	0.59	0.46	0.61	0.58	0.52	0.60	0.58	0.21	0.60	1.00	0.28	0.51
WD	0.69	0.56	0.39	0.48	0.70	0.34	0.02	0.83	0.71	0.79	0.83	0.72	0.79	0.79	0.73	0.77	0.41	0.38	0.28	1.00	0.89
TD	0.79	0.60	0.31	0.63	0.75	0.27	-0.02	0.87	0.82	0.89	0.91	0.82	0.89	0.90	0.83	0.87	0.42	0.50	0.51	0.89	1.00

Table **B.5**: Input correlation matrix: PTI reliability model

	L	W	H	WB	FO	RO	GC	CW-F	CW-R	CW-T	SLW-F	SLW-R	SLW-T	GVW-F	GVW-R	GVW-T	AR	P	D	WD	TD	D-MIL	O-MIL
L	1.00	0.57	0.34	0.84	0.70	0.48	-0.01	0.75	0.83	0.87	0.81	0.88	0.90	0.84	0.88	0.89	0.33	0.67	0.41	0.65	0.74	0.70	0.49
W	0.57	1.00	0.19	0.54	0.41	0.12	-0.30	0.51	0.59	0.61	0.53	0.59	0.60	0.57	0.60	0.61	0.27	0.47	0.37	0.37	0.42	0.55	0.24
H	0.34	0.19	1.00	0.13	0.24	0.43	0.23	0.37	0.25	0.30	0.34	0.29	0.32	0.31	0.34	0.34	0.20	0.18	-0.11	0.43	0.39	0.28	0.34
WB	0.84	0.54	0.13	1.00	0.33	0.13	-0.11	0.59	0.64	0.67	0.62	0.70	0.71	0.66	0.70	0.71	0.13	0.59	0.47	0.39	0.51	0.54	0.36
FO	0.70	0.41	0.24	0.33	1.00	0.22	-0.02	0.65	0.79	0.80	0.76	0.75	0.79	0.80	0.74	0.78	0.52	0.50	0.28	0.70	0.77	0.70	0.37
RO	0.48	0.12	0.43	0.13	0.22	1.00	0.27	0.24	0.26	0.27	0.23	0.34	0.31	0.21	0.36	0.31	0.04	0.22	-0.03	0.30	0.26	0.17	0.32
GC	-0.01	-0.30	0.23	-0.11	-0.02	0.27	1.00	-0.10	-0.23	-0.20	-0.09	-0.20	-0.17	-0.14	-0.19	-0.17	-0.06	-0.08	-0.22	0.01	-0.03	-0.19	0.13
CW-F	0.75	0.51	0.37	0.59	0.65	0.24	-0.10	1.00	0.69	0.84	0.96	0.72	0.84	0.92	0.75	0.84	0.42	0.47	0.30	0.81	0.84	0.68	0.35
CW-R	0.83	0.59	0.25	0.64	0.79	0.26	-0.23	0.69	1.00	0.97	0.79	0.98	0.96	0.85	0.96	0.95	0.46	0.69	0.60	0.68	0.80	0.82	0.42
CW-T	0.87	0.61	0.30	0.67	0.80	0.27	-0.20	0.84	0.97	1.00	0.90	0.97	0.99	0.94	0.97	0.98	0.48	0.67	0.55	0.77	0.87	0.84	0.43
SLW-F	0.81	0.53	0.34	0.62	0.76	0.23	-0.09	0.96	0.79	0.90	1.00	0.80	0.91	0.96	0.82	0.90	0.43	0.53	0.39	0.82	0.89	0.73	0.36
SLW-R	0.88	0.59	0.29	0.70	0.75	0.34	-0.20	0.72	0.98	0.97	0.80	1.00	0.98	0.86	0.98	0.97	0.42	0.71	0.58	0.69	0.80	0.82	0.46
SLW-T	0.90	0.60	0.32	0.71	0.79	0.31	-0.17	0.84	0.96	0.99	0.91	0.98	1.00	0.94	0.97	0.99	0.45	0.68	0.54	0.77	0.87	0.83	0.45
GVW-F	0.84	0.57	0.31	0.66	0.80	0.21	-0.14	0.92	0.85	0.94	0.96	0.86	0.94	1.00	0.88	0.95	0.51	0.59	0.44	0.79	0.88	0.79	0.39
GVW-R	0.88	0.60	0.34	0.70	0.74	0.36	-0.19	0.75	0.96	0.97	0.82	0.98	0.97	0.88	1.00	0.98	0.42	0.68	0.56	0.72	0.81	0.83	0.48
GVW-T	0.89	0.61	0.34	0.71	0.78	0.31	-0.17	0.84	0.95	0.98	0.90	0.97	0.99	0.95	0.98	1.00	0.46	0.67	0.53	0.76	0.86	0.83	0.46
AR	0.33	0.27	0.20	0.13	0.52	0.04	-0.06	0.42	0.46	0.48	0.43	0.42	0.45	0.51	0.42	0.46	1.00	0.39	0.18	0.44	0.48	0.47	0.14
P	0.67	0.47	0.18	0.59	0.50	0.22	-0.08	0.47	0.69	0.67	0.53	0.71	0.68	0.59	0.68	0.67	0.39	1.00	0.59	0.38	0.51	0.58	0.22
D	0.41	0.37	-0.11	0.47	0.28	-0.03	-0.22	0.30	0.60	0.55	0.39	0.58	0.54	0.44	0.56	0.53	0.18	0.59	1.00	0.20	0.40	0.43	0.05
WD	0.65	0.37	0.43	0.39	0.70	0.30	0.01	0.81	0.68	0.77	0.82	0.69	0.77	0.79	0.72	0.76	0.44	0.38	0.20	1.00	0.90	0.60	0.41
TD	0.74	0.42	0.39	0.51	0.77	0.26	-0.03	0.84	0.80	0.87	0.89	0.80	0.87	0.88	0.81	0.86	0.48	0.51	0.40	0.90	1.00	0.71	0.42
D-MIL	0.70	0.55	0.28	0.54	0.70	0.17	-0.19	0.68	0.82	0.84	0.73	0.82	0.83	0.79	0.83	0.83	0.47	0.58	0.43	0.60	0.71	1.00	0.52
O-MIL	0.49	0.24	0.34	0.36	0.37	0.32	0.13	0.35	0.42	0.43	0.36	0.46	0.45	0.39	0.48	0.46	0.14	0.22	0.05	0.41	0.42	0.52	1.00

Table **B.6**: Input correlation matrix: NTD reliability model

	ACT-FL	ELEV	SERV-MIL	SERV-POP	AVG-SP	MIL-PER-BUS	TLH	LHPB	T-FAC	PER-SP	AVG-MIL	PTI-MDBF
ACT-FL	1.00	0.07	0.62	-0.19	-0.05	0.39	0.96	-0.07	0.10	0.06	-0.05	0.61
ELEV	0.07	1.00	0.12	-0.13	0.47	0.60	0.07	0.00	0.05	-0.36	0.48	0.31
SERV-MIL	0.62	0.12	1.00	0.12	-0.18	0.09	0.58	-0.21	0.13	0.17	-0.17	0.32
SERV-POP	-0.19	-0.13	0.12	1.00	-0.66	-0.61	-0.29	-0.33	-0.22	0.20	0.05	-0.01
AVG-SP	-0.05	0.47	-0.18	-0.66	1.00	0.76	0.08	0.38	0.00	-0.23	0.39	0.22
MIL-PER-BUS	0.39	0.60	0.09	-0.61	0.76	1.00	0.45	0.17	0.09	-0.32	0.33	0.56
TLH	0.96	0.07	0.58	-0.29	0.08	0.45	1.00	0.20	0.03	-0.04	0.13	0.70
LHPB	-0.07	0.00	-0.21	-0.33	0.38	0.17	0.20	1.00	-0.17	-0.55	0.58	0.30
T-FAC	0.10	0.05	0.13	-0.22	0.00	0.09	0.03	-0.17	1.00	-0.27	-0.54	-0.37
PER-SP	0.06	-0.36	0.17	0.20	-0.23	-0.32	-0.04	-0.55	-0.27	1.00	-0.20	-0.11
AVG-MIL	-0.05	0.48	-0.17	0.05	0.39	0.33	0.13	0.58	-0.54	-0.20	1.00	0.67
PTI-MDBF	0.61	0.31	0.32	-0.01	0.22	0.56	0.70	0.30	-0.37	-0.11	0.67	1.00

Appendix C

Comparison of the Effect of Various Inputs

Consider the case wherein Method-2 results in a two term functional expression for output as given below

$$y = c_0 + c_1 p^a q^b r^c \qquad \text{C.1}$$

where

y is the output

p, q and r are inputs

a, b and c are the corresponding exponents

The sensitivity of the output, y, with respect to input p is given by

$$\frac{\partial y}{\partial p} = c_1 a p^{a-1} q^b r^c \qquad \text{C.2}$$

Similarly, the sensitivity of the output, y, with respect to input q is given by

$$\frac{\partial y}{\partial q} = c_1 b p^a q^{b-1} r^c \qquad \text{C.3}$$

Now taking the ratio of the two sensitivities given above

$$\frac{\partial y}{\partial p} \Big/ \frac{\partial y}{\partial q} = \frac{a}{b}\left(\frac{q}{p}\right) \qquad \text{C.4}$$

Eq. C.4 provides a means for making a one-to-one comparison of the relative relevance of inputs p and q for two similar outputs (say fuel economies on CBD and ART cycles). For a known operating point (given values of p and q), one can directly compare the

values of the ratio $\frac{a}{b}$ in the two instances (CBD and ART) as a means of understanding the relative importance of input p with respect to input q. It is relevant to note here that the above analysis would not be so straightforward if the functional expression for output y involves more than two terms. In such cases, one may need to evaluate the expressions for the sensitivities.

Appendix D

Effect of PTI-ART on NTD Fuel Economy

If we take into account only the top two terms with the largest c_i (in terms of absolute magnitude) we get the following equation

$$NTD\_FE = 1.88 - 0.058\ s^{-0.44} m^{-0.53} a^{0.66} p^{-9.04} - 0.006\ s^{-9.78} m^{6.17} a^{4.88} p^{18.27} \qquad \textbf{D.1}$$

where for ease of representation the following nomenclature has been used

NTD_FE	=	NTD Fuel Economy (achieved at transit agency)
s	=	normalized average speed (AVG-SP)
m	=	normalized average miles per bus per annum (MIL-PER-BUS)
a	=	normalized average mileage (AVG-MIL)
p	=	normalized PTI fuel economy on ART cycle (PTI-ART)

It is clear from the above equation that an increase in 's' tends to increase fuel economy and an increase in 'a' tends to decrease the NTD fuel economy. For 'p' however, the first term tends to increase NTD fuel economy while the second term tends to decrease NTD fuel economy. Differentiating Eq. **D.1** partially with respect to p

$$\frac{\partial NTD\_FE}{\partial p} = 0.5243\ s^{-0.44} m^{-0.53} a^{0.66} p^{-10.04} - 0.1096\ s^{-9.78} m^{6.17} a^{4.88} p^{17.27} \qquad \textbf{D.2}$$

Now, if we hold the other variables at 1 (i.e., mean values) we find that that the first term is greater than the second term for all $p < 1.06$. In absolute terms, this means a fuel economy of 1.06*Mean Fuel economy = 2.38 km/L since the mean fuel economy is 2.25

km/L on ART. From the histogram for ART fuel economy, shown in Figure **D.1**, we see that this would mean well over half the buses since the plot is skewed to the left.

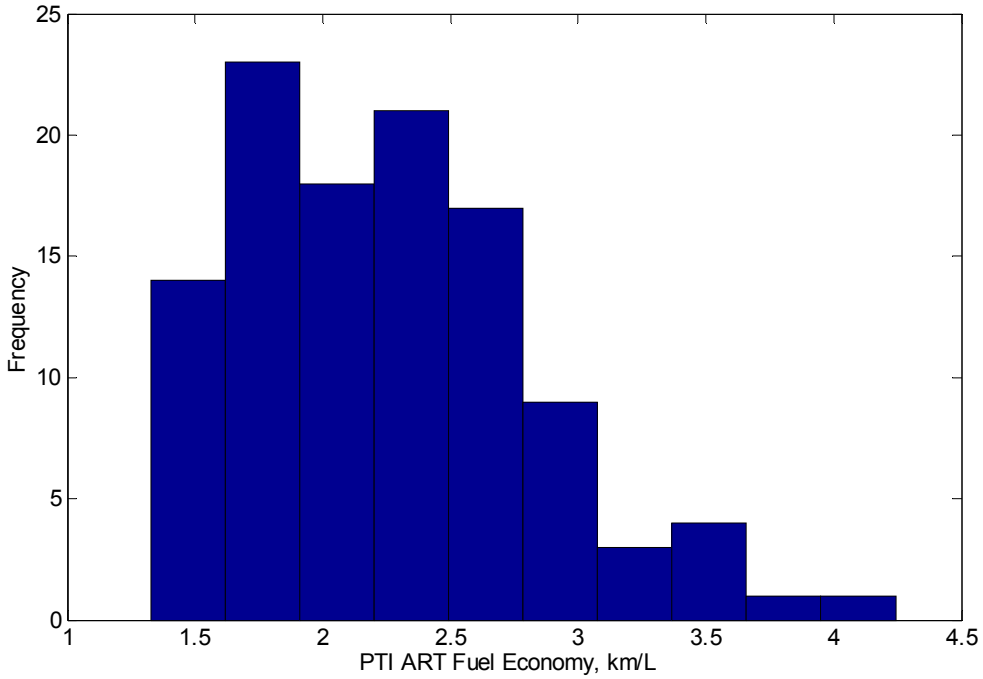

Figure **D.1**: Histogram for PTI-ART fuel economy.

Appendix E

Residual Plots

The term 'residual' refers to the difference between actual output and the predicted (ANN) output. If a model is an adequate representation of a given dataset, then, the residuals should not exhibit any evident pattern. The following figures plot the residuals against the predicted value (ANN output) for both training and test sets. The results are presented in the same sequence as in Chapter 5.

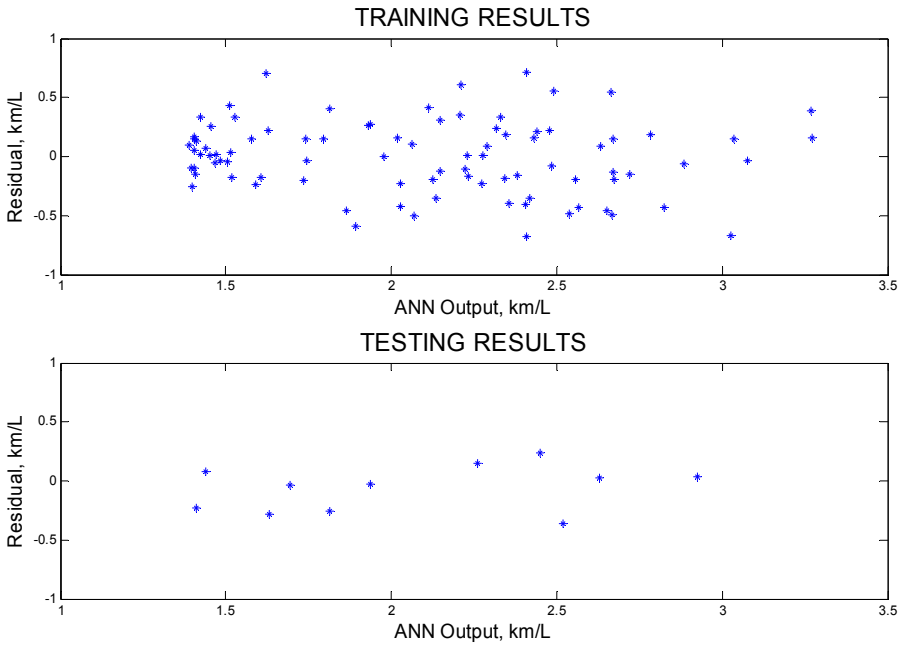

Figure **E.1**: Residual plots for CBD fuel economy: Method-1 (N2PFA).

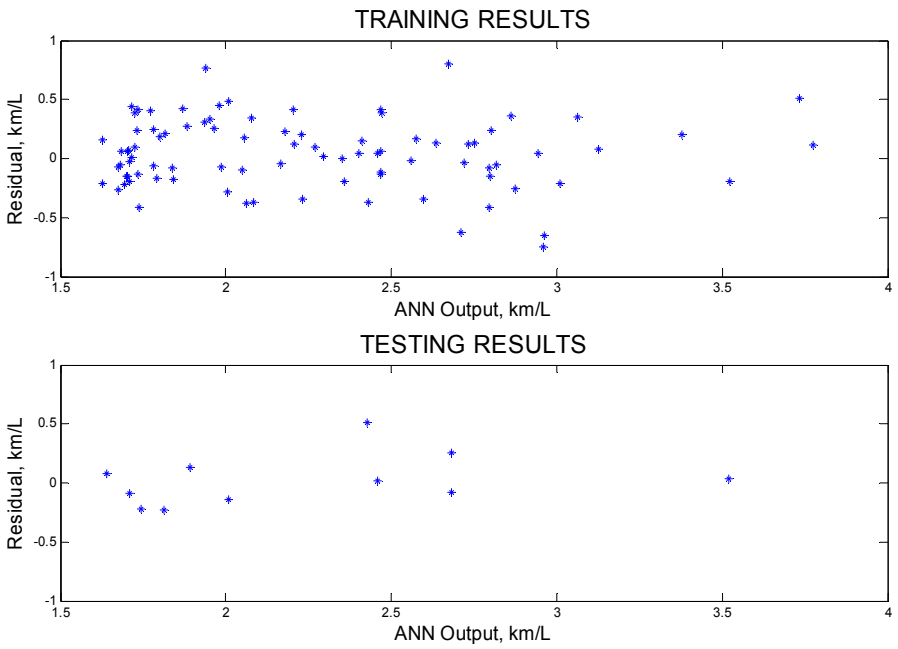

Figure **E.2**: Residual plots for ART fuel economy: Method-1 (N2PFA).

Figure **E.3**: Residual plots for COM fuel economy: Method-1 (N2PFA).

Figure **E.4**: Residual plots for CBD fuel economy: Method-2 (RF5).

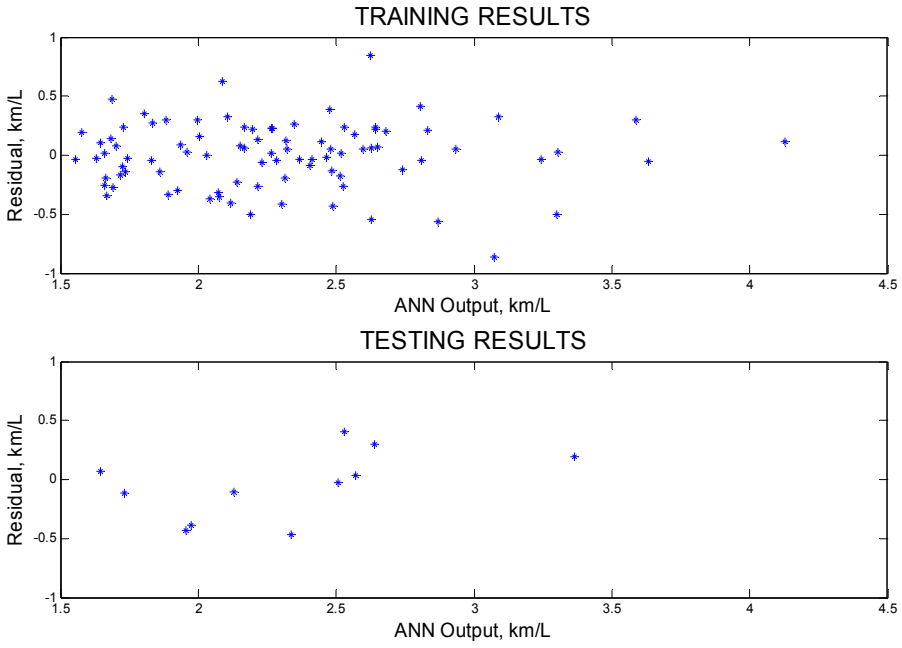

Figure **E.5**: Residual plots for ART fuel economy: Method-2 (RF5).

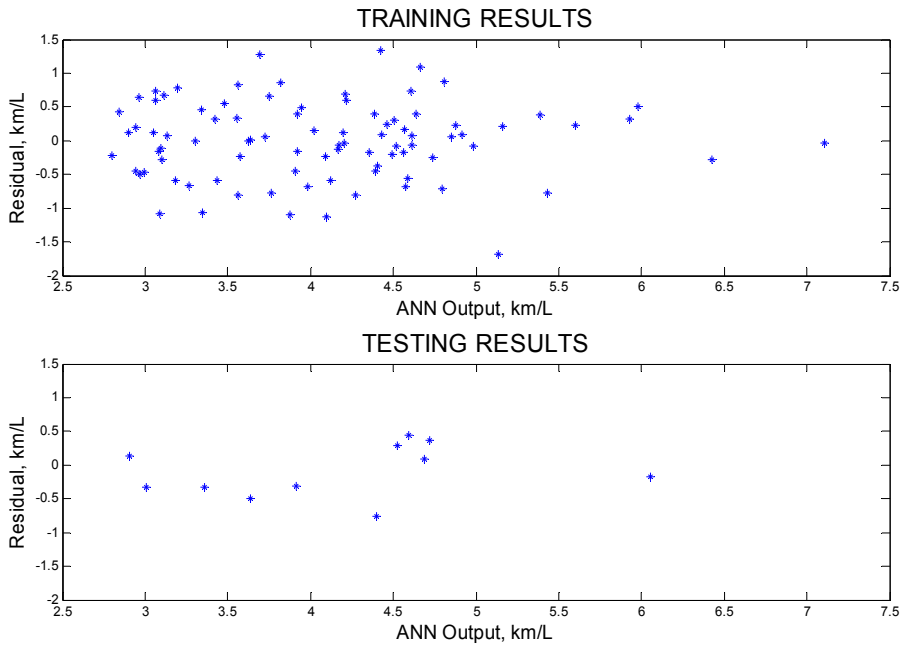

Figure **E.6**: Residual plots for COM fuel economy: Method-2 (RF5).

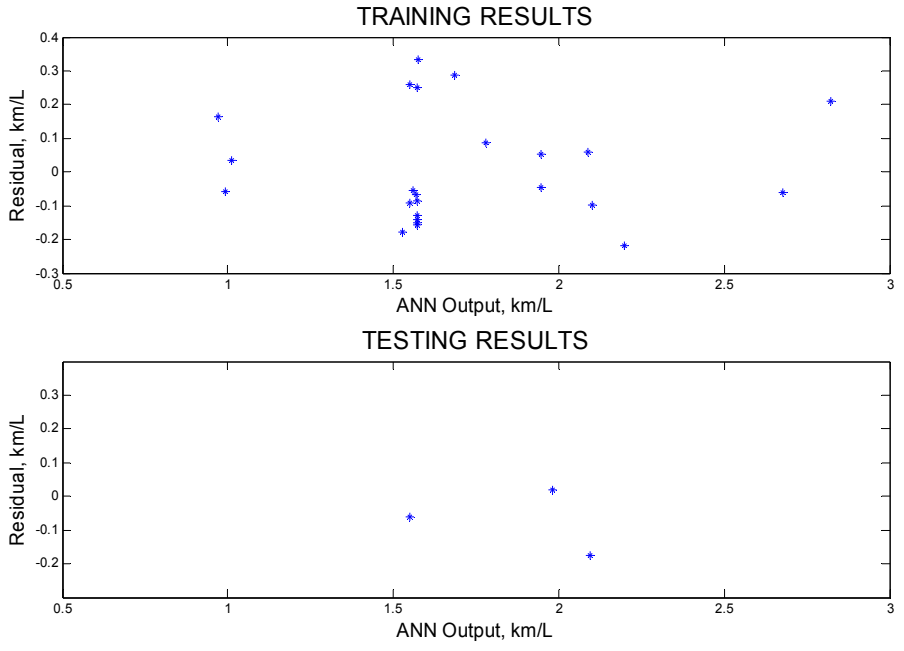

Figure **E.7**: Residual plots for NTD fuel economy: Method-1 (N2PFA).

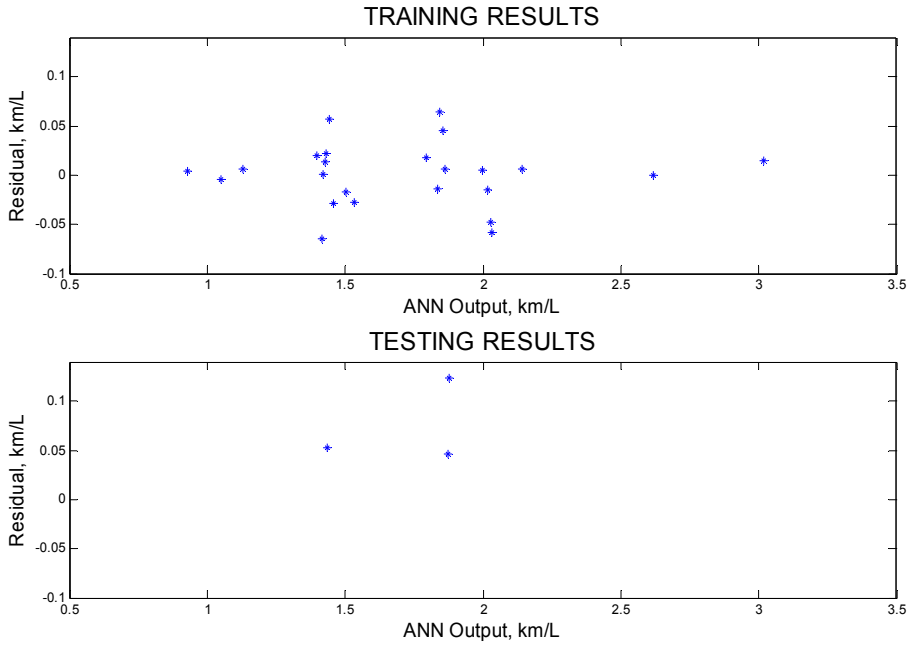

Figure **E.8**: Residual plots for NTD fuel economy: Method-2 (RF5).

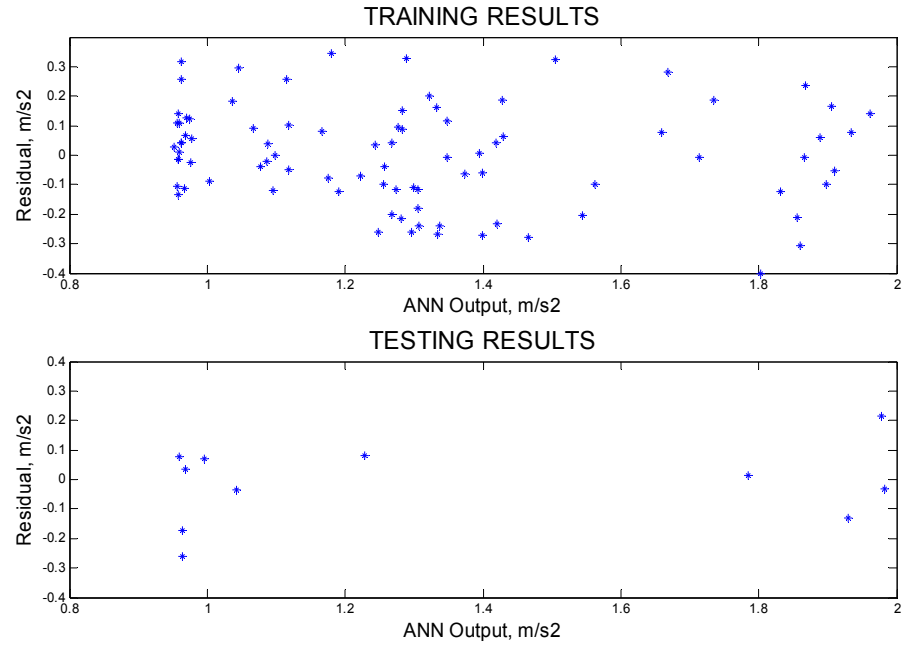

Figure **E.9**: Residual plots for acceleration at 16 km/hr: Method-1 (N2PFA).

Figure **E.10**: Residual plots for acceleration at 32 km/hr: Method-1 (N2PFA).

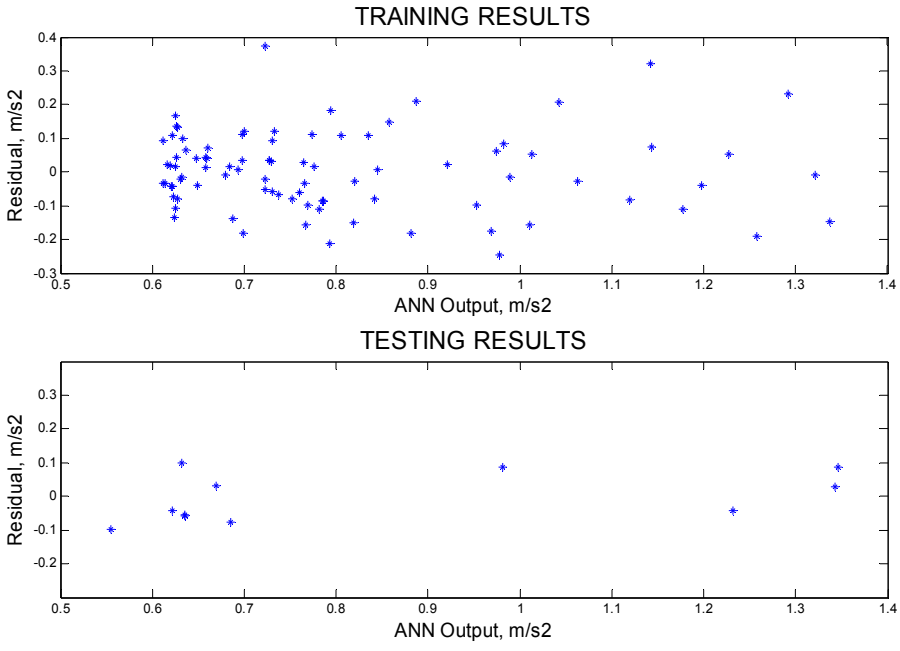

Figure **E.11**: Residual plots for acceleration at 48 km/hr: Method-1 (N2PFA).

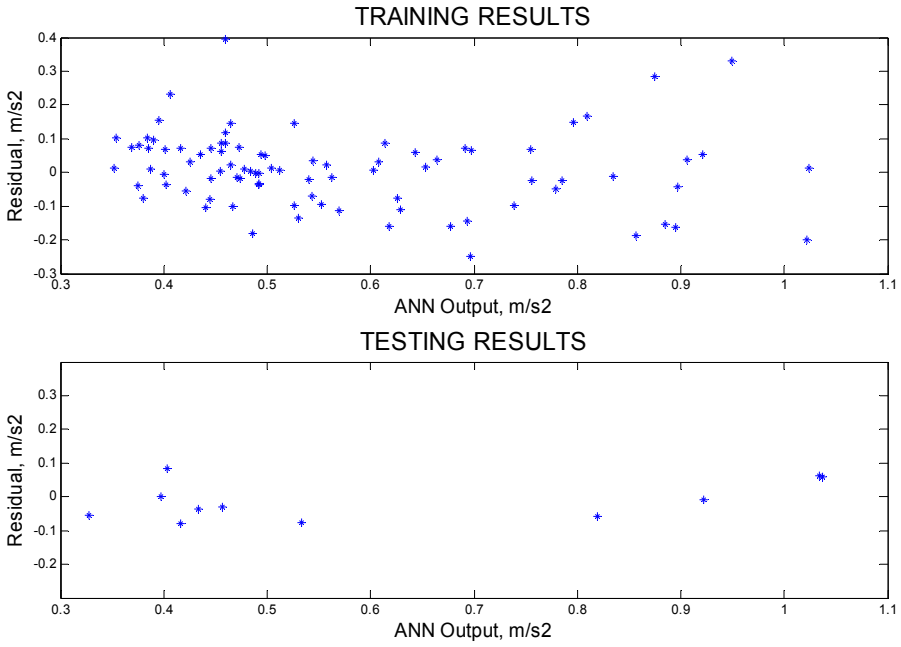

Figure **E.12**: Residual plots for acceleration at 64 km/hr: Method-1 (N2PFA).

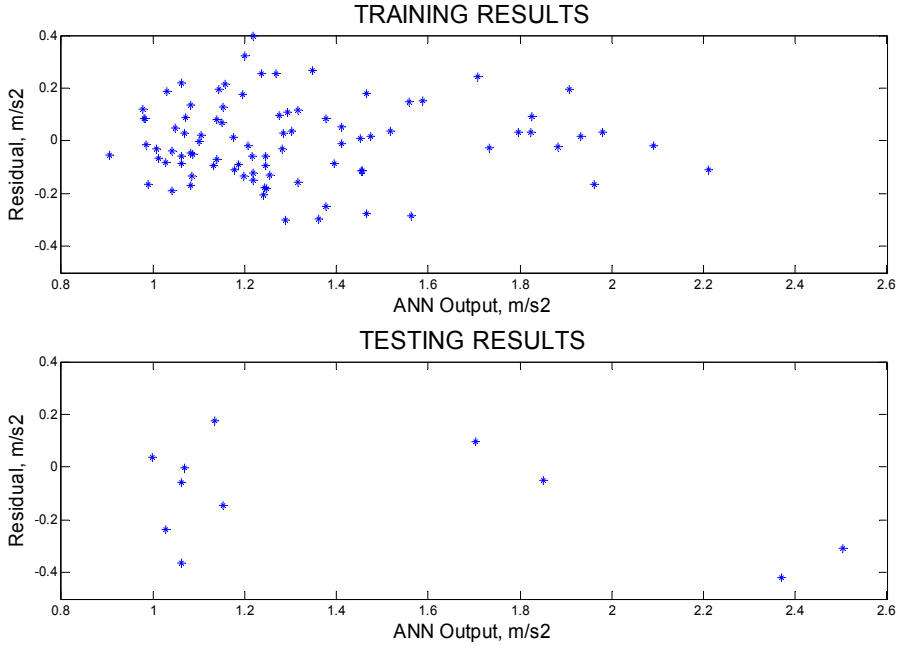

Figure **E.13**: Residual plots for acceleration at 16 km/hr: Method-2 (RF5).

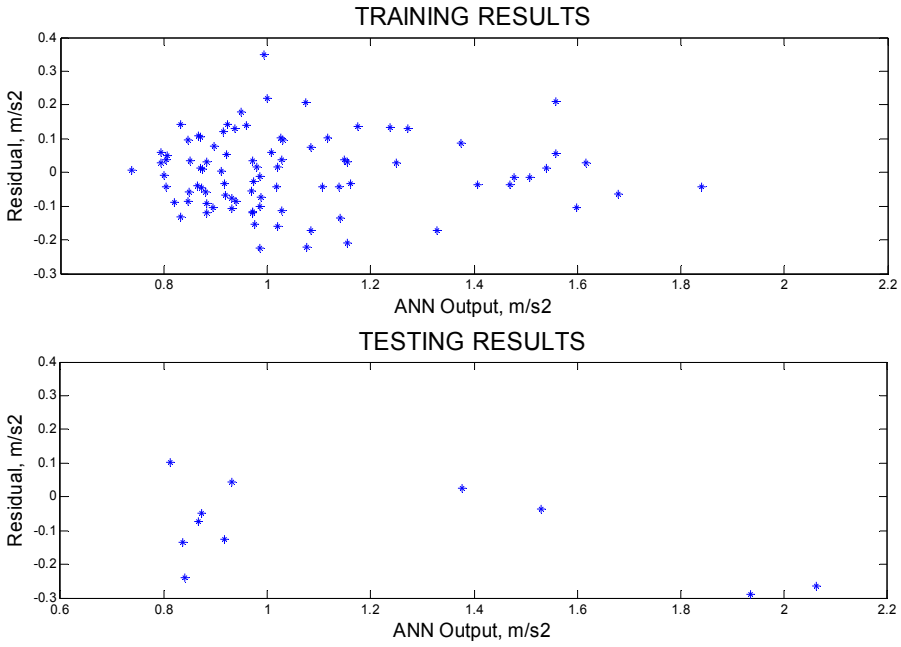

Figure **E.14**: Residual plots for acceleration at 32 km/hr: Method-2 (RF5).

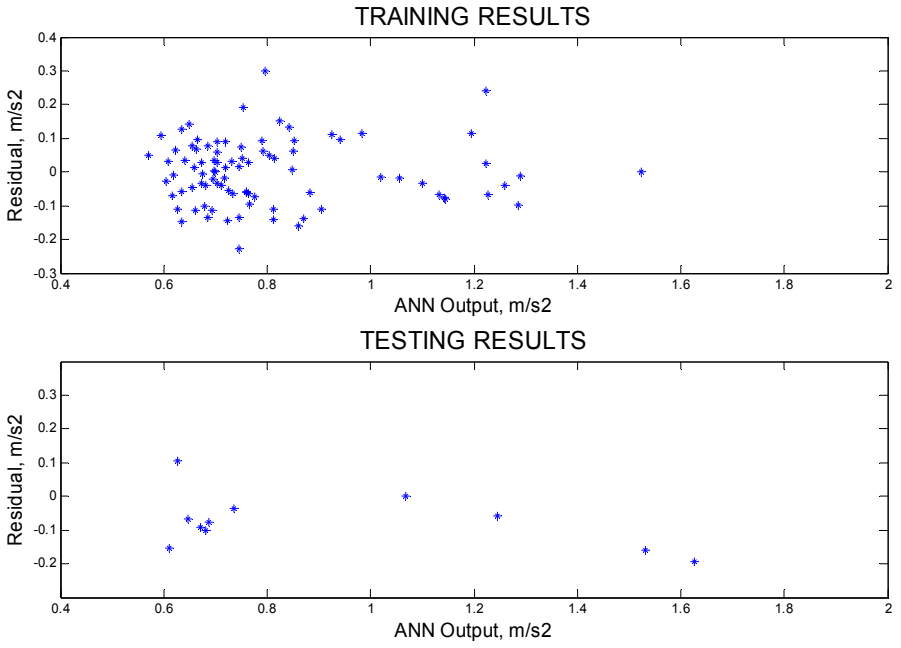

Figure **E.15**: Residual plots for acceleration at 48 km/hr: Method-2 (RF5).

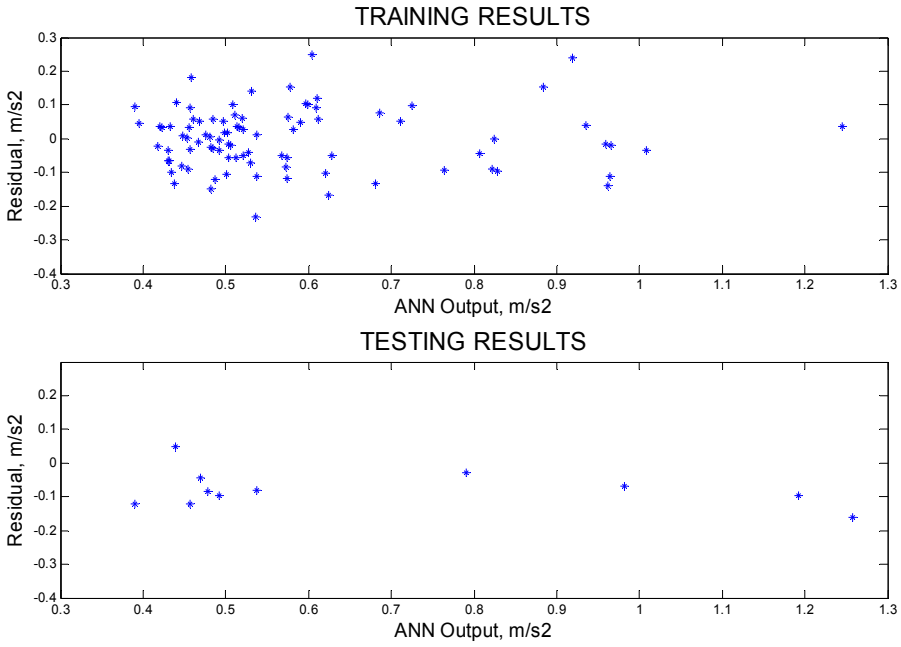

Figure **E.16**: Residual plots for acceleration at 64 km/hr: Method-2 (RF5).

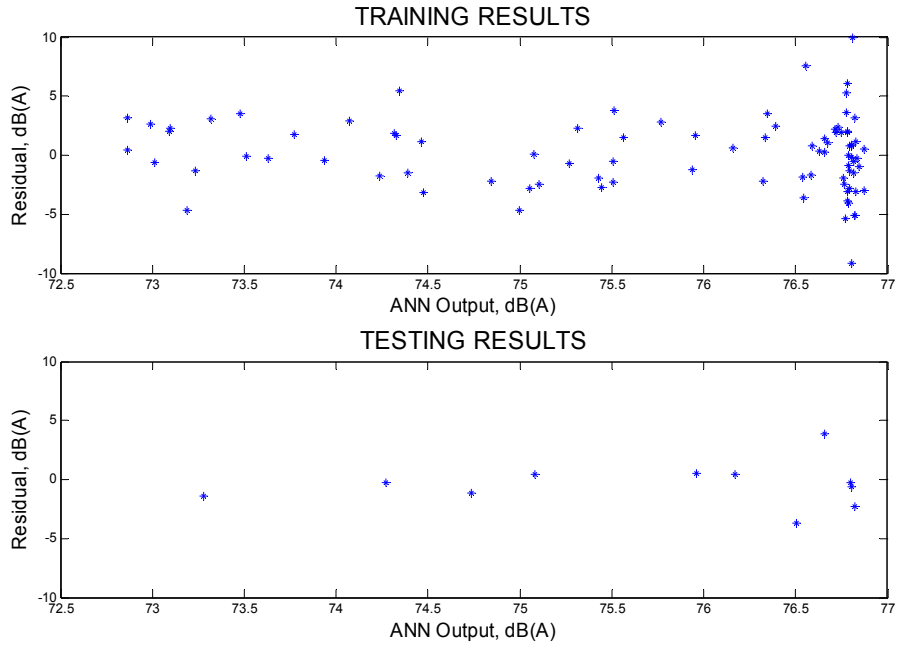

Figure **E.17**: Residual plots for CON-NOISE-R: Method-1 (N2PFA).

Figure **E.18**: Residual plots for ST-NOISE-R: Method-1 (N2PFA).

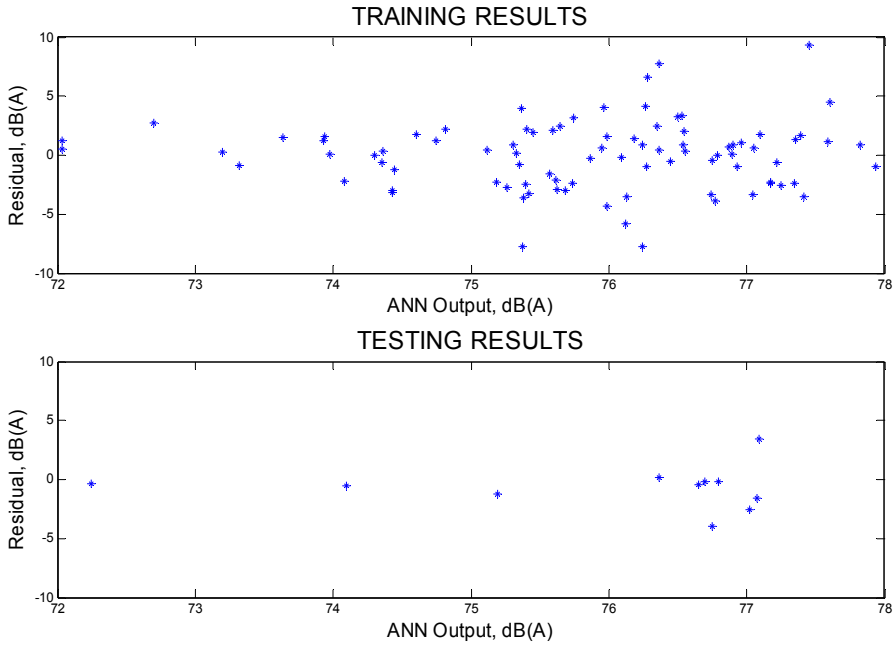

Figure **E.19**: Residual plots for CON-NOISE-R: Method-2 (RF5).

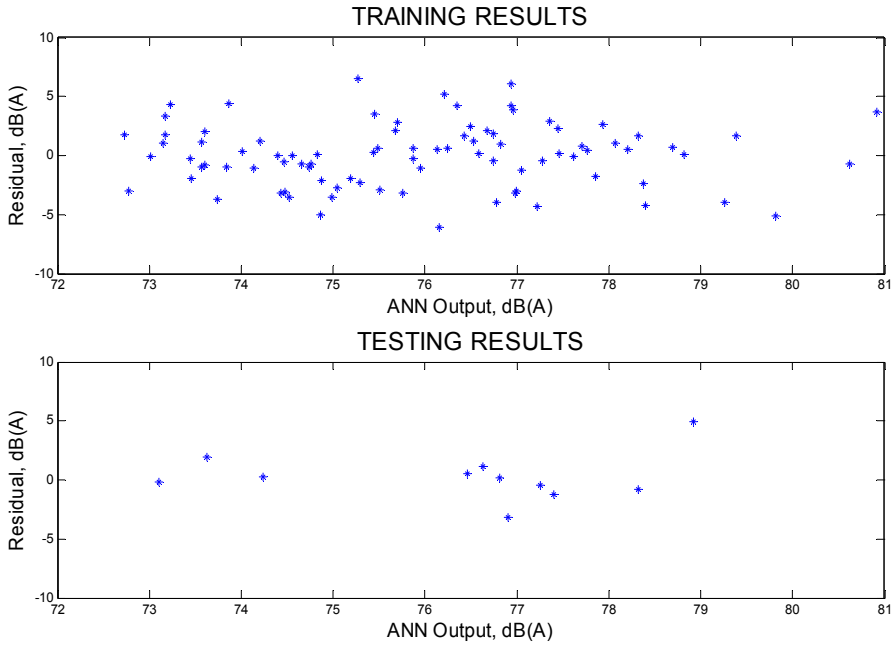

Figure **E.20**: Residual plots for ST-NOISE-R: Method-2 (RF5).

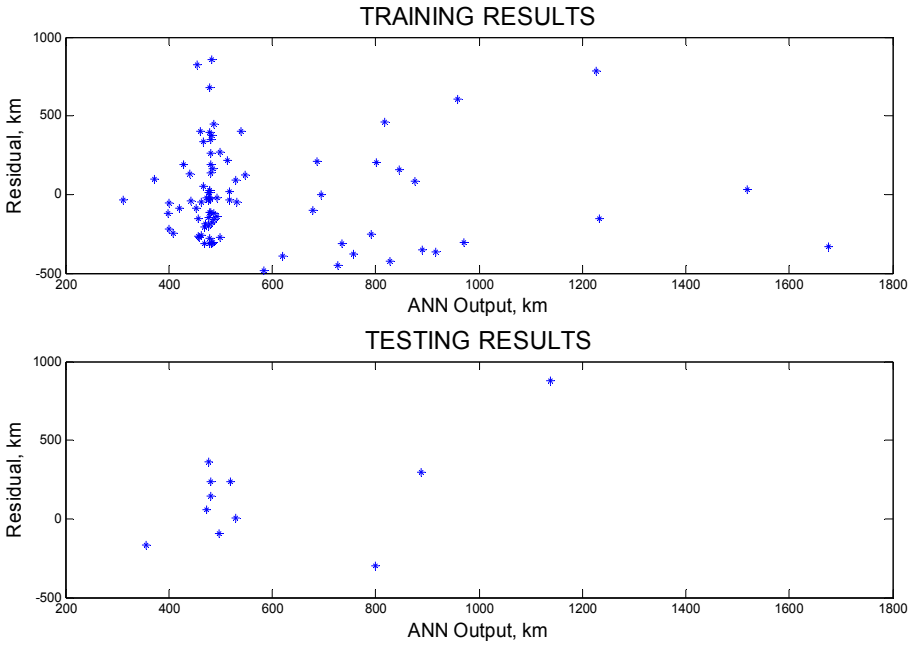

Figure **E.21**: Residual plots for PTI reliability: Method-1 (N2PFA).

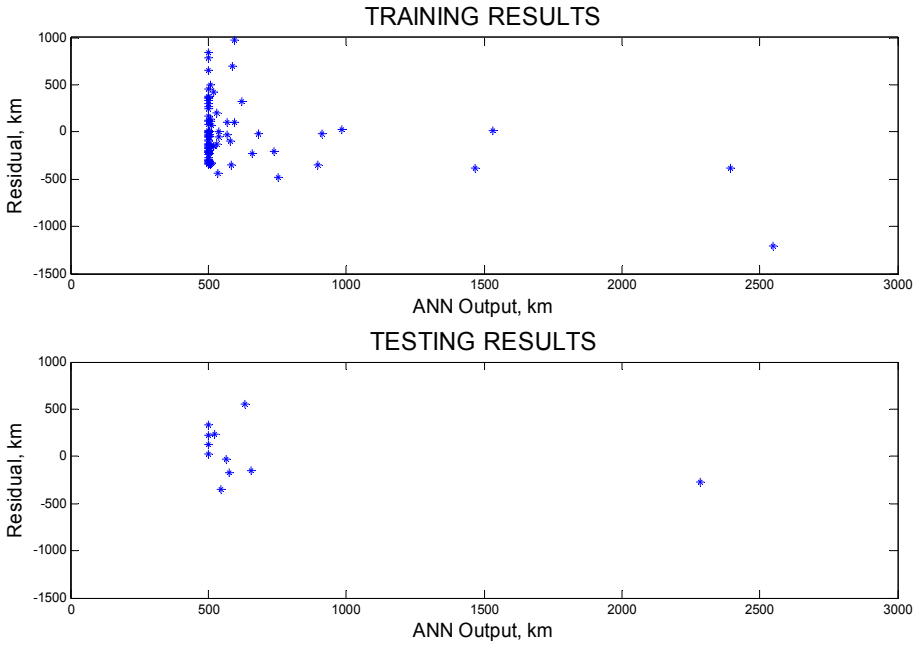

Figure **E.22**: Residual plots for PTI reliability: Method-2 (RF5).

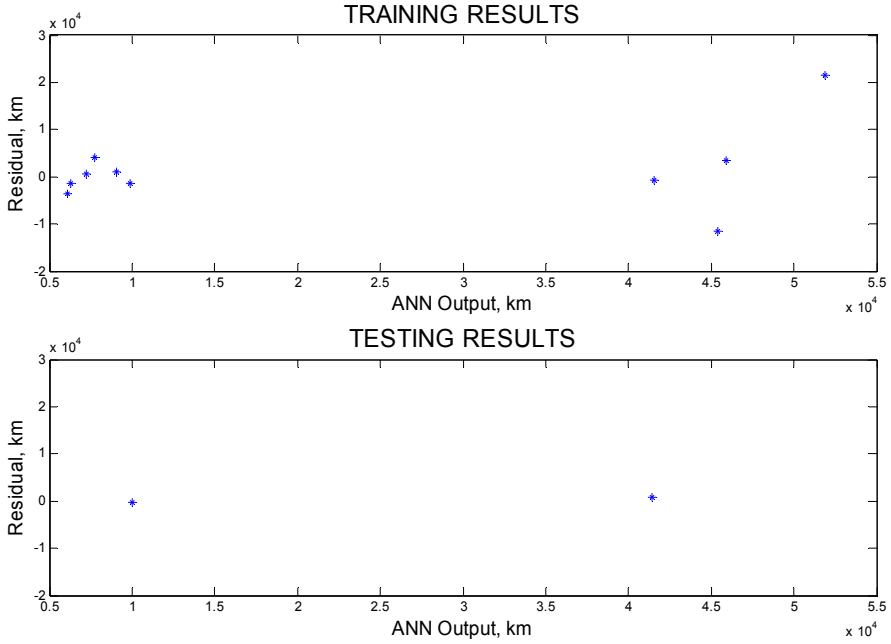

Figure **E.23**: Residual plots for NTD reliability: Method-1 (N2PFA).

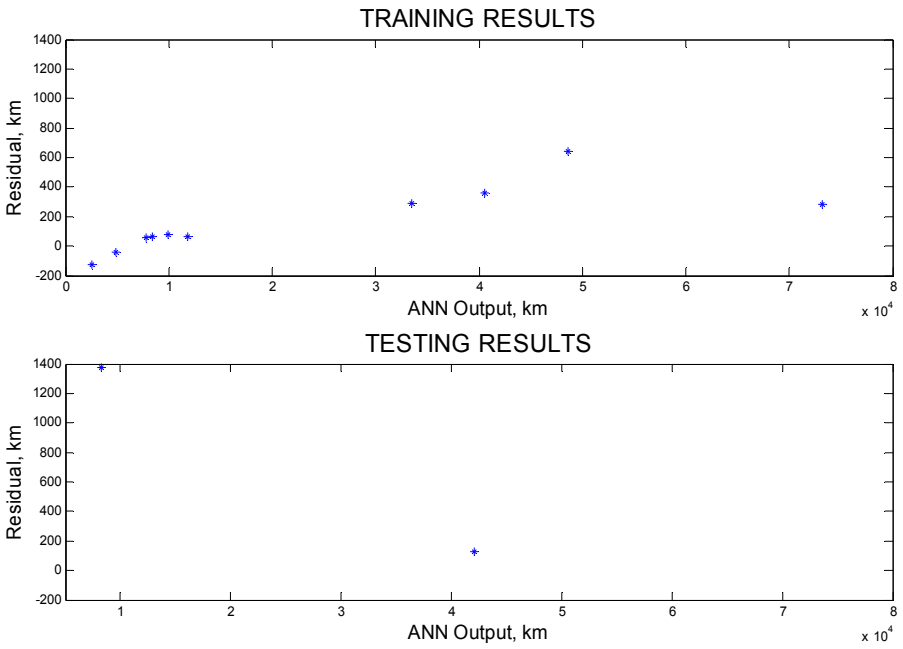

Figure **E.24**: Residual plots for NTD reliability: Method-2 (RF5).

Appendix F

Summary of the Forward Models Obtained Using Method-2

As explained in Chapter 4, the forward models developed using Method-2 (RF5) can be easily expressed in the form of equations. The equations obtained for the six models described in Sub-sections **5.1.1** - **5.1.6** are given below. It should be noted that the equations are in terms of normalized input variables (normalized by their respective means). The output variables are in terms of their original units as given in Chapter 3.

F.1 PTI Fuel Economy

$$CBD = 6.640 - 4.594 W^{-0.002} H^{0.280} RO^{0.002} GC^{-0.032} SLWT^{0.284} AR^{0.008} P^{0.059} \quad \textbf{F.1}$$

$$ART = 0.041 + 2.147 W^{-0.411} H^{-1.105} RO^{0.148} GC^{0.081} SLWT^{-0.504} AR^{0.043} P^{-0.286} \quad \textbf{F.2}$$

$$COM = 0.670 + 3.223 W^{-0.406} H^{-1.416} RO^{0.231} GC^{0.186} SLWT^{-0.473} AR^{-0.033} P^{-0.580} \quad \textbf{F.3}$$

F.2 NTD Fuel Economy

The following input variable substitutions have been used in Eq. **F.4** for an easy representation of the six-term model equation:

AVG-SP : a

MIL-PER-BUS : b

AVG-MIL : c

PTI-ART : d

$$NTD\_FE = 1.8842 - 0.0584\,a^{-0.445}b^{-0.528}c^{0.657}d^{-9.045} + 0.0014\,a^{1.278}b^{0.673}c^{-1.858}d^{-18.632} - 0.0062a^{-9.779}b^{6.166}c^{4.884}d^{18.270} + 9.4E-6\,a^{-7.547}b^{-0.083}c^{3.780}d^{-28.747} + 0.0003a^{-0.674}b^{5.273}c^{-0.418}d^{27.455} \quad \textbf{F.4}$$

F.3 Acceleration

$$ACC\_16 = 0.671 + 0.554\,H^{0.226}WB^{0.428}GC^{0.236}SLWT^{-1.622}AR^{0.596}P^{0.347}D^{-0.055} \quad \textbf{F.5}$$

$$ACC\_32 = 0.545 + 0.439\,H^{-0.14}WB^{0.393}GC^{0.225}SLWT^{-1.638}AR^{0.596}P^{0.512}D^{0.04} \quad \textbf{F.6}$$

$$ACC\_48 = 0.362 + 0.394\,H^{-0.704}WB^{0.245}GC^{0.219}SLWT^{-1.456}AR^{0.439}P^{0.793}D^{0.12} \quad \textbf{F.7}$$

$$ACC\_64 = 0.196 + 0.343\,H^{-1.138}WB^{0.124}GC^{0.271}SLWT^{-1.35}AR^{0.316}P^{1.098}D^{0.103} \quad \textbf{F.8}$$

F.4 Pass-by Noise

$$CON\_NOISE\_R = 79.470 - 3.496\,H^{-1.50}WB^{0.22}RO^{0.54}GC^{0.31}SLWT^{-0.57}AR^{-0.17}P^{-1.45}D^{2.03} \quad \textbf{F.9}$$

$$ST\_NOISE\_R = 72.223 + 3.331W^{0.70}WB^{-0.49}GC^{0.30}SLWT^{1.91}AR^{-0.50}P^{1.48}D^{-2.84} \quad \textbf{F.10}$$

F.5 PTI Reliability

$$PTI\_MDBF = 499.45 + 0.61 H^{25.31} WB^{-3.07} GC^{-2.28} SLWT^{-16.67} P^{11.82} D^{-16.61} DMIL^{3.57} OMIL^{2.20} \quad \text{F.11}$$

F.6 NTD Reliability

The following input variable substitutions have been used in Eq. F.12 for an easy representation of the five-term model equation:

AVG-SP : a

LHPB : b

PER-SP : c

AVG-MIL : d

PTI-MDBF : e

$$\begin{aligned} NTD\_MDBF = {} & 664.10 + 946.38 a^{0.547} b^{2.273} c^{1.145} d^{-4.175} e^{4.977} \\ & + 317.52 a^{-0.544} b^{3.30} c^{-0.05} d^{-0.008} e^{7.158} \\ & + 0.05 a^{5.53} b^{4.801} c^{-0.40} d^{-3.203} e^{-2.257} \\ & + 118.24 a^{-4.418} b^{-1.735} c^{1.82} d^{3.795} e^{-6.715} \end{aligned} \quad \text{F.12}$$

VITA

SARAVANAN MUTHIAH

Saravanan Muthiah was born in Nagercoil, Tamil Nadu (India) in August 1974. He received his B.E. (with distinction) in Mechanical Engineering in May 1995 from Delhi College of Engineering, India. After a brief stint in Larsen & Toubro (L&T) Limited, Saravanan joined Maruti Udyog Limited (India's largest automotive company) in October 1995. At Maruti, from 1995-2000, Saravanan organized whole vehicle type approval testing at national test agencies and supervised Maruti's 2nd Mass Emission Laboratory.

Saravanan came to The Pennsylvania State University (Penn State) in August 2000. He completed his M.S. in Mechanical Engineering in December 2001 and is currently pursuing his Ph.D. in Mechanical Engineering. Since August 2000, he has been a graduate research assistant in the Bus Testing Program at the Pennsylvania Transportation Institute (PTI) affiliated with Penn State. In June 2006, Saravanan received "The Scania Best Paper Award" at the 9th International Symposium on Heavy Vehicle Weights and Dimensions (9ISHVWD) for his paper titled "A Neural Network Based Model for Predicting Acceleration and Gradeability Performances of Transit Buses". Saravanan's areas of interest include modeling of dynamic systems, vehicle dynamics and control, vehicle exhaust emissions, effect of automotive regulations on vehicle design, artificial neural networks, CAD and data mining.